Synthesis of 8-*O*-Methylfusarubin, 8-*O*-Methylanhydrofusarubin, Fusarubin and Anhydrofusarubin

Pongsit Vijitphan

A Thesis Submitted in Partial Fulfillment of the Requirements for the Degree of Master of Science in Organic Chemistry

Prince of Songkla University

2019

Synthesis of 8-*O*-Methylfusarubin, 8-*O*-Methylanhydrofusarubin, Fusarubin and Anhydrofusarubin

Pongsit Vijitphan

A Thesis Submitted in Partial Fulfillment of the Requirements for the Degree of Master of Science in Organic Chemistry

Prince of Songkla University

2019

Thesis Title	Synthesis of 8-*O*-Methylfusarubin, 8-*O*-Methylanhydrofusarubin, Fusarubin and Anhydrofusarubin
Author	Mr. Pongsit Vijitphan
Major Program	Organic Chemistry

Major Advisor

……

(Asst. Prof. Dr. Kwanruthai Tadpetch)

Examining Committee :

…….....……..Chairperson

(Assoc. Prof. Dr. Darunee Soorukram)

…….Committee

(Asst. Prof. Dr. Kwanruthai Tadpetch)

…….Committee

(Prof. Dr. Vatcharin Rukachaisirikul)

…….Committee

(Asst. Prof. Dr. Juthanat Kaeobamrung)

…….Committee

(Asst. Prof. Dr. Chittreeya Tansakul)

The Graduate School, Prince of Songkla University, has approved this thesis as partial fulfillment of the requirements for the Master of Science Degree in Organic Chemistry.

……

(Prof. Dr. Damrongsak Faroongsarng)

Dean of Graduate School

This is to certify that the work here submitted is the result of the candidate's own investigations. Due acknowledgement has been made of any assistance received.

……...Signature

(Asst. Prof. Dr. Kwanruthai Tadpetch)

Major Advisor

……...Signature

(Mr. Pongsit Vijitphan)

Candidate

I hereby certify that this work has not been accepted in substance for any degree, and is not being currently submitted in candidature for any degree.

……Signature

(Mr. Pongsit Vijitphan)

Candidate

ชื่อวิทยานิพนธ์ การสังเคราะห์ 8-*O*-Methylfusarubin, 8-*O*-Methylanhydrofusarubin, Fusarubin และ Anhydrofusarubin

ผู้เขียน นายพงศ์สิทธิ์ วิจิตรพันธุ์

สาขาวิชา เคมีอินทรีย์

ปีการศึกษา 2561

บทคัดย่อ

pyranonaphthoquinones เป็นสารเมตาบอไลต์ทุติยภูมิในกลุ่ม naphthoquinones ซึ่งแยกได้จากแหล่งธรรมชาติที่หลากหลาย fusarubin (**1**) anhydrofusarubin (**2**) และ 8-*O*-methylfusarubin (**3**) เป็นสารผลิตภัณฑ์ธรรมชาติในกลุ่ม pyranonaphthoquinones ที่แยกได้จากเชื้อราชนิดต่างๆ ในปี ค.ศ. 2010 กลุ่มวิจัยของ Rukachaisirikul ได้รายงานการแยกรวมถึงฤทธิ์ทางชีวภาพของสาร **1** และ **2** ซึ่งแยกได้จากเชื้อราทะเล *Fusarium* spp. PSU-F14 และ PSU-F135 นอกจากนี้ยังสามารถแยกสาร **3** ได้จากเชื้อราหญ้าทะเล *Pestalotiopsis* sp. PSU-ES180 ซึ่งสารทั้งสามแสดงฤทธิ์ต้านเซลล์มะเร็งเต้านม MCF-7 ในระดับที่ดีมากด้วยค่า IC_{50} ในช่วง 0.9-9.8 μM เมื่อเทียบกับยา doxorubicin (IC_{50} = 2.18 μM) 8-*O*-methylanhydrofusarubin (**4**) เป็นอนุพันธ์ของ 8-*O*-methylfusarubin (**3**) ที่แยกได้เป็นครั้งแรกจากเชื้อรา *F. oxysporum* จากรากที่ติดเชื้อของต้นส้ม โดย Tatum และคณะในปีค.ศ. 1985 ในปัจจุบันยังไม่มีการรายงานฤทธิ์ทางชีวภาพของสาร **4** รวมถึงการสังเคราะห์ของสาร **1 3** และ **4** งานวิจัยนี้ศึกษาการสังเคราะห์สาร **1-4** รวมถึงการเตรียมสารให้เพียงพอเพื่อศึกษาฤทธิ์ต้านมะเร็งของสารทั้งสี่ต่อไป ผู้วิจัยใช้ปฏิกิริยา Diels-Alder เป็นปฏิกิริยาหลักในการสร้างวง naphthalene และปฏิกิริยา intramolecular acetalization เพื่อสร้างวง pyran ในการสังเคราะห์ **1-4** โดยใช้ naphthoquinone **8** เป็นสารตัวกลางซึ่งสามารถได้จาก pentaalkoxynaphthalene **6** โดยสามารถสังเคราะห์ naphthalene **6** ได้ใน 6 ขั้นตอนตามวิธีการสังเคราะห์ของ Green และคณะจากสารตั้งต้น 5-bromovanilin (**5**) ซึ่งเป็นสารที่มีจำหน่าย สำหรับ naphthoquinone **7** สามารถสังเคราะห์ได้ใน 3 ขั้นตอน ผ่านปฏิกิริยา Vilsmeier-Haack formylation ของ naphthalene **6** และปฏิกิริยาออกซิเดชันที่มีหมู่ hydroxymethylene เหนี่ยวนำโดยใช้ diacetoxyiodobenzene จากนั้นเตรียมสารตัวกลาง naphthoquinone **8** ผ่าน 2 ขั้นตอนด้วยปฏิกิริยา acetonylation โดยใช้ pyridinium ylide ของ **7** 8-*O*-methylfusarubin (**3**) สามารถสังเคราะห์ได้จากปฏิกิริยา acetalization โดยใช้กรดของ **8** นอกจากนี้ยังสามารถสังเคราะห์ **3** ได้ใน 3 ขั้นตอนจาก naphthoquinone **7** ผ่านปฏิกิริยา one-pot

acetalization ซึ่ง 8-*O*-methylanhydrofusarubin (**4**) สามารถเตรียมได้จาก **3** ผ่านปฏิกิริยา dehydration โดยใช้กรดเป็นตัวเร่งปฏิกิริยา สำหรับ fusarubin (**1**) และ anhydrofusarubin (**2**) สามารถสังเคราะห์จากสารตัวกลาง naphthoquinone **8** โดยการเปลี่ยนออกซิเดชันสเตทของวง naphthoquinone โดยเริ่มต้นจากปฏิกิริยา selective reduction ของสาร **8** และทำการป้องกันบนวง hydroquinone ด้วยหมู่ ethoxymethyl (EOM) ให้ ether **9** จากนั้นทำการกำจัดหมู่ป้องกัน benzyl (Bn) ตามด้วยปฏิกิริยาออกซิเดชันของ naphthol ได้เป็น naphthoquinone **10** ที่มีออกซิเดชันสเตทใหม่ผ่าน 2 ขั้นตอน สำหรับ fusarubin (**1**) สามารถสังเคราะห์ได้จากการกำจัดหมู่ป้องกันทั้งหมดและปฏิกิริยา acetalization ของสาร **10** ภายใต้สภาวะที่เป็นกรด สุดท้ายนำสาร **1** ทำปฏิกิริยา dehydration เพื่อให้ anhydrofusarubin (**2**) ในการสังเคราะห์สาร **1**-**4** ทำได้สำเร็จผ่านปฏิกิริยา 16 17 12 และ 13 ขั้นตอนจากสารตั้งต้น 5-bromovanillin ด้วยร้อยละผลิตภัณฑ์ทั้งหมดเป็น 3 2 13 และ 9 ตามลำดับ ซึ่งฤทธิ์ต้านมะเร็งของเซลล์มะเร็งเต้านม MCF-7 ของสารสังเคราะห์ทั้งสี่ได้ถูกทดสอบโดยเทคนิค REMA, MTT และการทดสอบเซลล์มะเร็งแบบสามมิติ จากผลการทดสอบพบว่าสารสังเคราะห์ **3** แสดงฤทธิ์ต้านเซลล์มะเร็ง MCF-7 ที่ดีที่สุดจากสารทดสอบทั้งสี่ตัว นอกจากนี้สาร **1**-**4** ยังแสดงฤทธิ์ต้านเซลล์มะเร็งที่ดีเมื่อทดสอบกับเซลล์มะเร็งจากมนุษย์ทั้งห้าชนิด (C33A HeLa SiHa HCT116 และ HepG2) ด้วยค่า IC_{50} ในช่วง 4.73 ถึง >22.5 μM

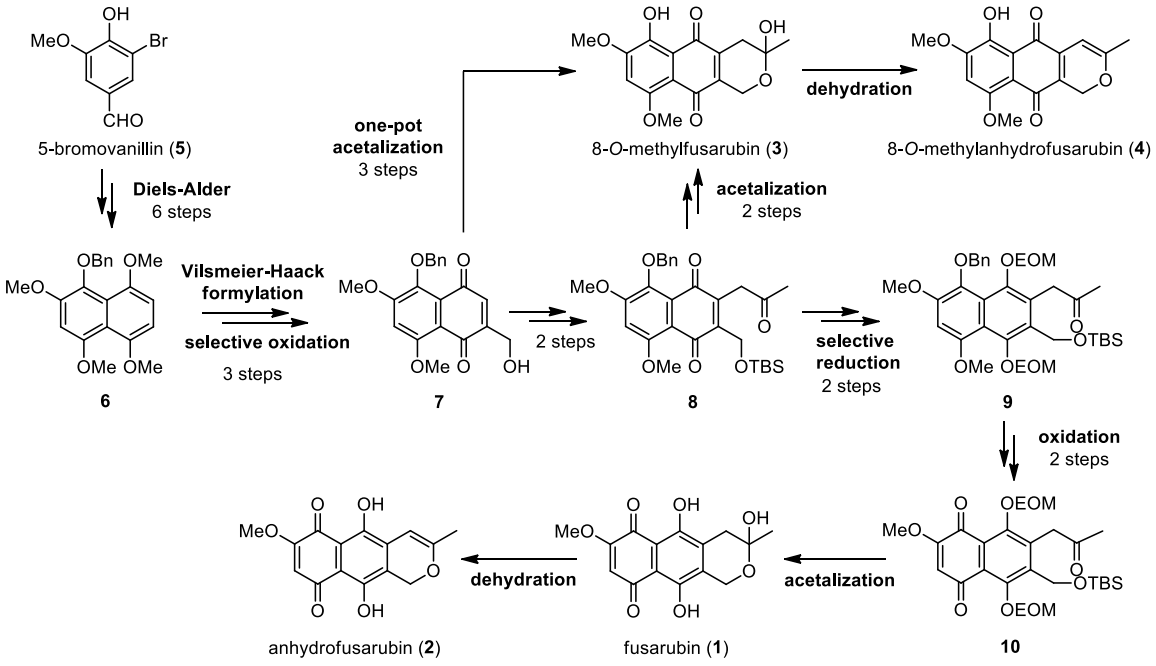

Thesis Title Synthesis of 8-*O*-Methylfusarubin, 8-*O*-Methylanhydrofusarubin, Fusarubin and Anhydrofusarubin

Author Mr. Pongsit Vijitphan

Major Program Organic Chemistry

Academic Year 2018

ABSTRACT

Pyranonaphthoquinones are a group of secondary metabolites in naphthoquinone family which were isolated from diverse natural sources. Fusarubin (**1**), anhydrofusarubin (**2**) and 8-*O*-methylfusarubin (**3**) are pyranonaphthoquinone natural products which were isolated from various strain of fungi. In 2010, Rukachaisirikul and co-workers reported the isolation and biological activity of **1** and **2** from sea-fan derived fungi *Fusarium* spp. PSU-F14 and PSU-F135. Additionally, compound **3** was isolated from a seagrass-derived fungus *Pestalotiopsis* sp. PSU-ES180. These three pyranonaphthoquinones exhibited good cytotoxic activity against human breast (MCF-7) cancer cells with IC_{50} ranges of 0.9 to 9.8 μM compared with doxorubicin standard drug (IC_{50} = 2.18 μM). 8-*O*-Methylanhydro fusarubin (**4**), an analogue of 8-*O*-methylfusarubin (**3**), was first isolated from *F. oxysporum* from roots of diseased citrus tree by the Tatum group in 1985. To date, the biological activity of **4** as well as the synthesis of **1**, **3** and **4** have not been reported. This work involves the syntheses of compounds **1**-**4** to provide sufficient materials for further study of their cytotoxic activities. Our synthetic approach relied on the key Diels-Alder reaction to construct naphthalene core and intramolecular acetalization to form pyran ring. The syntheses of **1**-**4** utilized the common naphthoquinone intermediate **8**, which could be elaborated from the known pentaalkoxynaphthalene **6**. Naphthalene **6** can be prepared in 6 steps starting from commercially available 5-bromovanillin (**5**) following a protocol reported by Green and co-workers. The naphthoquinone skeleton was generated via Vilsmeier-Haack formylation of naphthalene **6** and hydroxymethylene-directed selective oxidation using diacetoxyiodobenzene to provide the desired naphthoquinone **7** in 3 steps.

Acetonylation of **7** via pyridinium ylide furnished the key naphthoquinone intermediate **8** in 2 steps. The synthesis of 8-*O*-methylfusarubin (**3**) was completed via acid-promoted acetalization of acetonyl naphthoquinone **8**. Alternatively, compound **3** could be achieved in 3 steps from naphthoquinone **7** via one-pot acetalization. 8-*O*-Methylanhydrofusarubin (**4**) can be prepared from acid-catalyzed dehydration of **3**. The syntheses of **1** and **2** were accomplished via manipulation of the oxidation state of naphthoquinone precursor **8**. Selective quinone reduction of **8** and subsequent protection of the hydroquinone moiety with ethoxymethyl (EOM) protecting groups gave EOM ether **9**. Removal of benzyl (Bn) protecting group followed by naphthol oxidation generated new naphthoquinone core **10** in 2 steps. Fusarubin (**1**) was then synthesized via global deprotection and acetalization of **10** under acidic conditions. Lastly, dehydration of **1** furnished anhydrofusarubin (**2**). The syntheses of **1**-**4** were achieved in 16, 17, 12 and 13 steps from 5-bromovanillin with 3, 2, 13 and 9 overall yields, respectively. The cytotoxic activity against MCF-7 breast cancer cells of four synthetic compounds were evaluated using REMA, MTT and 3D cancer spheroid assays. Synthetic **3** displayed highest cytotoxicity against MCF-7 cells among the four compounds. Additionally, compounds **1**-**4** exhibited good cytotoxic activity against five human cancer (C33A, HeLa, SiHa, HCT116 and HepG2) cell lines with IC_{50} ranges of 4.73 – >22.5 μM.

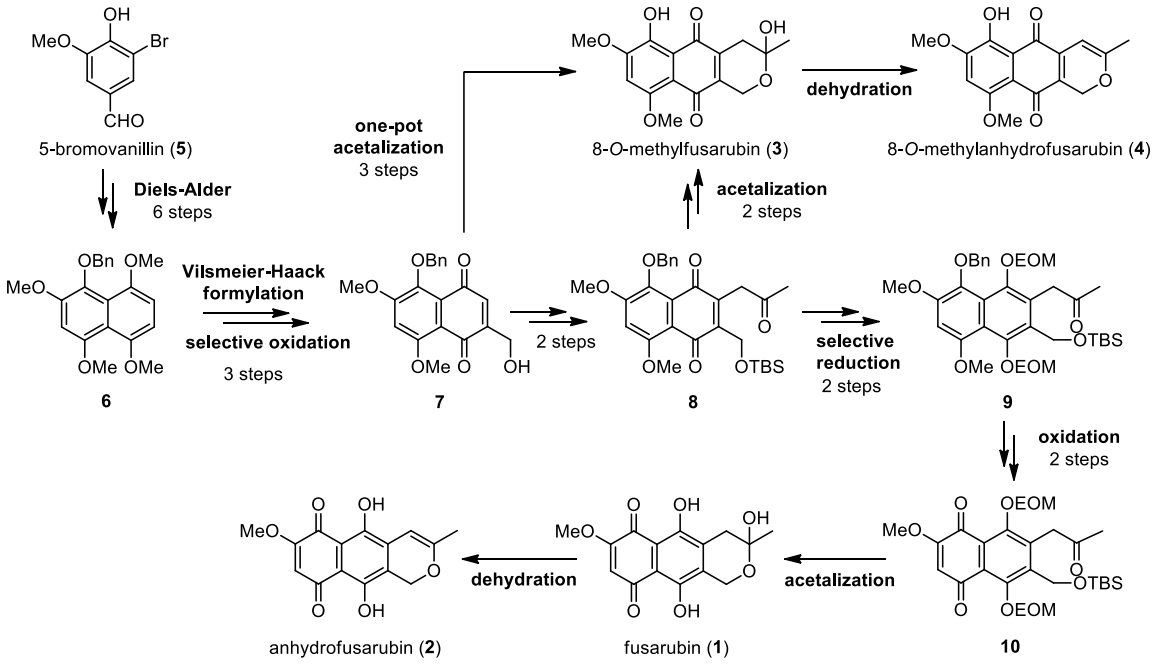

ACKNOWLEDGEMENT

First and foremost, I would like to express my deepest thanks to my advisor, Asst. Prof. Dr. Kwanruthai Tadpetch, for her great support, encouragement, expert guidance, motivation and suggestion. Her guidance is not only in the research work, but also everything in working life.

I would like to thank my dissertation committee members, Assoc. Prof. Dr. Darunee Soorukrum, Asst. Prof. Dr. Kwanruthai Tadpetch, Prof. Dr. Vatcharin Rukachaisirikul, Asst. Prof. Dr. Juthanat Kaeobamrung and Asst. Prof. Dr. Chittreeya Tansakul for taking the time to oversee my thesis and their helpful suggestion.

I also would like to thank Assoc. Prof. Dr. Chatchai Muanprasat for cytotoxic activity evaluation against MCF-7 cells via MTT and 3D cancer spheroid assays. I would like to thank Asst. Prof. Dr. Panata Iawsipo and Miss Jiraporn Panprasert for cytotoxic activity evaluation against five human cancer cells.

I am grateful to the Research Assistantship from Faculty of Science. Center of Excellence for Innovation in Chemistry (PERCH-CIC), NSTDA Chair Professor grant (the fourth Grant) and the Graduate School, Prince of Songkla University are appreciatively acknowledged for partial support.

Lastly, I would like to extend my appreciation to my family, my friends, Miss Supattra Kaewtaro and members of Ch416 laboratory for their love, encouragement and great support. I also thank them all for all their kindness and precious advice through my graduate career.

Pongsit Vijitphan

THE RELEVANCE OF THE RESEARCH WORK TO THAILAND

To date, natural products have been widely used for the source of new medicines and pharmaceutical drugs. Pyranonaphthoquinone natural products displayed broad range of biological activities e.g. antifungal antimalarial as well as anticancer activity. This work involves the syntheses of four related pyranonaphthoquinone natural products including fusarubin, anhydrofusarubin, 8-*O*-methylfusarubin and 8-*O*-methylanhydrofusarubin and highlights the first syntheses of fusarubin, 8-*O*-methylfusarubin and 8-*O*-methylanhydro-fusarubin. The *in vitro* cytotoxic activity of the four synthetic compounds against human breast cancer (MCF-7) cells and others five human cancer cells line (C33A, HeLa, SiHa, HCT116 and HepG2) were evaluated. 8-*O*-Methylfusarubin displayed potent cytotoxic activity against breast cancer (MFC-7) cells compared with standard drug doxorubicin and exhibited the highest cytotoxicity among the four compounds tested. Additionally, the four synthetic compounds showed good cytotoxic activity against five human cancer cells line with IC_{50} ranges of 4.73 – >22.5 μM. This research could potentially be further studied for the development of new anti-breast cancer drug discovery.

CONTENTS

CONTENTS (Continued)

LIST OF TABLES

LIST OF FIGURES

LIST OF FIGURES (Continued)

LIST OF FIGURES (Continued)

LIST OF SCHEMES

LIST OF SCHEMES (Continued)

LIST OF ABBREVIATIONS AND SYMBOLS

[α]	=	specific rotation
AcOH	=	acetic acid
br	=	broad (spectral)
ºC	=	degree Celsius
c	=	concentration
calcd	=	calculated
cat	=	catalytic
$CDCl_3$	=	deuterochloroform
cm^{-1}	=	wavenumbers(s)
m-CPBA	=	*meta*-chloroperoxybenzoic acid
δ	=	chemical shift in parts per million downfield from tetramethylsilane
d	=	doublet (spectral)
DMAP	=	4-(*N*,*N*-dimethylamino)pyridine
DMF	=	dimethylformamide
DMSO	=	dimethyl sulfoxide
DMSO-d_6	=	hexadeuterodimethyl sulfoxide
EOM	=	ethoxymethyl
equiv	=	equivalent
ESI	=	electrospray ionization
Et_2O	=	diethyl ether
EtOAc	=	ethyl acetate
FT	=	Fourier transform
g	=	gram(s)
h	=	hour(s)

LIST OF ABBREVIATIONS AND SYMBOLS (Continued)

H_2	=	hydrogen gas
HMBC	=	heteronuclear multiple bond correlation
HMQC	=	heteronuclear multiple quantum correlation
HRMS	=	high-resolution mass spectrometry
Hz	=	hertz
IC_{50}	=	half maximal inhibitory concentration
IR	=	infrared
J	=	coupling constant (in NMR spectrometry)
µ	=	micro
m	=	multiplet (spectral)
M	=	molar (moles per liter)
Me	=	methyl
MeCN	=	acetonitrile
MHz	=	megahertz
min	=	minute(s)
mL	=	milliliter
mmol	=	millimole
mol%	=	mole percent
mp	=	melting point
m/*z*	=	mass-to-charge ratio
NaH	=	sodium hydride
NBS	=	*N*-bromosuccinimide
NMR	=	nuclear magnetic resonance

LIST OF ABBREVIATIONS AND SYMBOLS (Continued)

nOe	=	nuclear Overhauser effect
Pd/C	=	palladium on carbon
ppm	=	part(s) per million
q	=	quartet (spectral)
R_f	=	retention factor (in chromatography)
rt	=	room temperature
s	=	singlet (spectral)
TBAF	=	tetrabutylammonium fluoride
TBS	=	*tert*-butyldimethylsilyl
THF	=	tetrahydrofuran
TLC	=	thin-layer chromatography
wt	=	weight

LIST OF PUBLICATION

Vijitphan, P.; Rukachaisirikul, V.; Muanprasat, C.; Iawsipo, P.; Panprasert, J.; Tadpetch, K. 2019. Unified synthesis and cytotoxic activity of 8-*O*-methylfusarubin and its analogues. Org. Biomol. Chem. 17, 7078–7087.

COPYRIGHT PERMISSION NOTICE

CHAPTER 1

INTRODUCTION

CHAPTER 1

INTRODUCTION

1.1 Introduction

Naphthoquinones are a group of secondary metabolites isolated from diverse natural sources e.g. plants, fungi and bacteria (Thomson, 1987, Tišler, 1989, Ramos-Peralta *et al.,* 2015). The basic skeleton of naphthoquinones consists of a naphthalene ring containing two carbonyl functional groups. Naphthoquinones can be defined as 1,4-naphthoquinones or 1,2-naphthoquinones based on the position of both carbonyls (**Figure 1**). 1,4-Naphthoquinones are the major group of naturally occuring naphthoquinones whereas 1,2-naphthoquinones are rarely found in natural sources (Thomson, 1992). There are many subgroups of these naphthoquinones e.g. naphthazarin derivatives, anthraquinone derivatives and naphthoquinones containing pyridine or pyran rings. A group of naphthoquinones bearing a pyran ring is called pyranonaphthoquinones. The core structure of this subgroup is naphtho[2,3-*c*]pyran-5,10-dione. Naphthoquinone metabolites have been reported to display good antibacterial, antifungul, antiparasitic and antiviral activities (Ramos-Peralta *et al.,* 2015). Some members of the pyranonaphtho-quinone family also contain a γ-lactone attached to a pyran moiety. Some of these pyranonaphthoquinones have been reported to exhibit potent biological activity against a broad range of microorganisms. Hence, these pyranonaphthoquinones are also called pyranonaphthoquinone antibiotics (Brimble *et al*., 1999). In addition, some members of these pyranonaphthoquinones were reported to exhibit potent activity against Gram-positive bacteria and displayed antifungal, antiplasmodial, antimalarial and anticancer activities (Sperry *et al*., 2008; Naysmith *et al*., 2017; Kumar *et al*., 2017). In this section,

the structures, biological activities and the synthetic strategies of selected examples of these bioactive pyranonaphthoquinones will be presented (**Figures 2**-**4**).

Figure 1. Core structures of 1,4 and 1,2-naphthoquinones and pyranonaphthoquinones

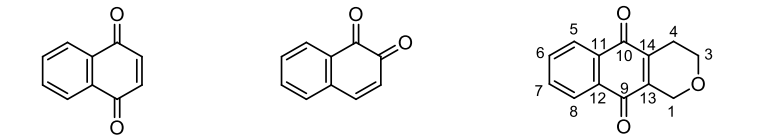

The selected examples of common pyranonaphthoquinones and pyrano-naphthoquinones containing methyl substituents on the pyran ring are demonstrated in **Figure 2**. Psychorubin (**1**) represented the simplest analogue of the pyranonaphthoquinone family. Compound **1** was first isolated from *Psychotria rubra* by Lee and co-workers in 1987. Psychorubin displayed good cytotoxicity against KB (oral cancer) cells with an ED_{50} value of 3.0 µg/mL. Pentalongin (**2**) was obtained via dehydration of **1** and was first isolated from natural source *Pentas longiflora* in 1991. In 2012, Yenesew and co-workers reported the isolation of **1** and **2** from dichloromethane/methanol extracts of *P. longiflora*. Psychorubin and pentalongin exhibited potent antiplasmodial activity against W2 chloroquine-resistant and D6 chloroquine-sensitive strains of *P. falciparum* with both IC_{50} value of < 1 µg/mL. Eleutherin (**3**) and isoeleutherin (**4**) were originally isolated from the tubers of *Eleutherin bulbosa* by the group of Ebnother in 1950 and 1951 (Schmid *et al*., 1950; Schmid *et al*., 1951), respectively. The structures of these compounds were confirmed by X-ray crystallography and ^{1}H NMR analysis decades later (Cameron *et al*., 1964; De Camargo *et al*., 1978). Compounds **3** and **4** displayed anti-proliferative activity with cytocidal effect against U251 and MCF-7 (glioma and breast cancer cells, respectively) with total growth inhibition (TGI) values of 2.6-13.8 µg/mL. Two eleutherin derivatives, 6-methoxyeleutherin (**5**) and 5-hydroxy-6-methoxyeleutherin (**6**) were discovered from hexane extracts of seed of *Karwinskia humboldtiana* by Daves, Jr. and co-workers in 1975. A yellow crystalline metabolite, thysanone (**7**) was originally isolated from a fungus *Thysanophora penicillolides* (Singh *et al*., 1991). Thysanone exhibited

potent activity against HRV-3C protease (Human rhinoviruses) with an IC_{50} value of 13 µg/mL. Herbarin (**8**) and its dehydrated analogue, dehydroherbarin (**9**), were discovered from black molds *Torula herbarum* by the research group of Narasimhachari in 1971. Compounds **8** and **9** displayed weak antibacterial and antifungal activities.

Figure 2. Selected examples of common pyranonaphthoquinones and pyranonaphthoquinones containing methyl substituents

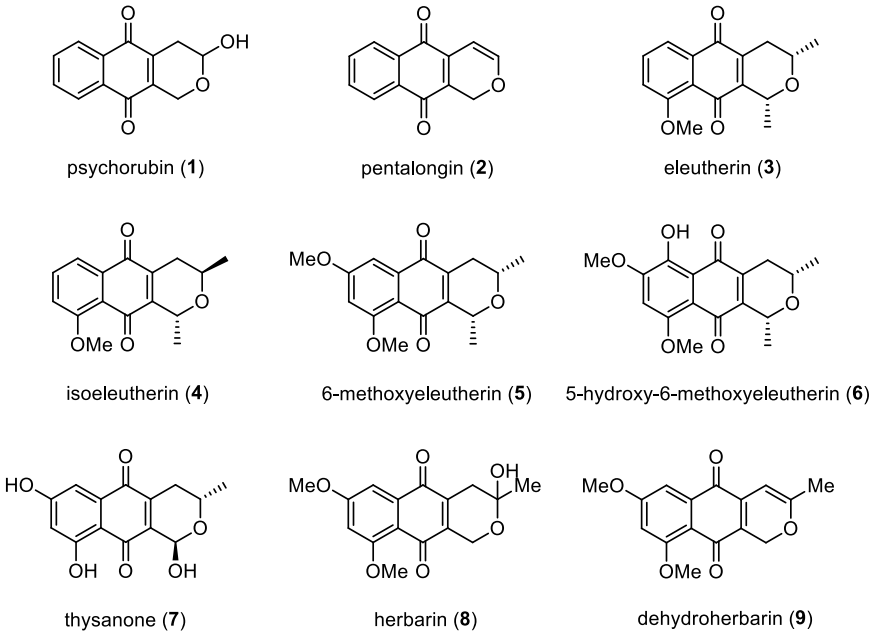

Another families of pyranonaphthoquinones which will be mentioned are the kalafungin and the frenolicin families (**Figure 3**). Compounds in these families contain carboxylic acid or γ-lactone moieties attached to a pyran ring at C-3 and C-4. A pyrano naphthoquinone containing a lactone, kalafungin (**10**), was first isolated from the broth extract of fermentation of *Streptomyces tanashiensis* strain Kala by Bergy in 1968. Kalafungin displayed *in vitro* antibacterial activity against broad spectrum of human pathogenic fungi and protozoa. Compound **10** also inhibited Gram-positive micro-organisms from 1.0 to 16.0 µg/mL and Gram-negative microorganisms with less potent activity (<100 to 250 µg/mL) (Johnson and Dietz, 1968). An analogue of **10**, tetrahydrokalafingin (**11**), was originally discovered from chloroform extracts from 24-

hour cultivation of a wild type strain of *Streptomyces tanashiensis* (Kakinuma *et al*., 1991). The frenolicin family is structurally nearly identical to the kalafungins. However, the frenolicins contain a propyl group at C-1 instead of a methyl group in the kalafungins. Frenolicin (**12**) and deoxyfrenolicin (**13**) were first isolated from a fermentation of *Streptomyces fradiae* by Van Meter *et al*. in 1966. Compound **12** displayed weak antibacterial activity, however the deoxy analogue **13** showed significant *in vitro* antifungal activity and *in vivo* activity against experimental ring worm infection in guinea pig (Ellestad *et al*., 1968). Ten years later, Omura and co-workers reported the isolation of **13** and frenolicin analogue, frenolicin B (**14**), from *Streptomyces Roseofulvus* strain AM-3867. Biological activities of **13** and **14** were also reported by the same research group. Compound **13** exhibited good antifungal activity against most of the fungi tested while **14** was inactive. In contrast, **14** displayed greater inhibition against mycoplasmas compared with **13**. For other frenolicin members, known compounds **12**-**14** and novel frenolicins D (**15**) and F (**16**) were isolated from *Streptomyces* sp. RM-4-15 by Thorson and co-workers in 2013. Compounds **12**, **13** and **14** exhibited moderate cytotoxic activity against A549 (human non-small-cell lung carcinoma) with IC_{50} values of 5.77, 1.07 and 0.28 µM while **15** and **16** were inactive (IC_{50} > 80 µM).

Figure 3. Examples of the kalafungin and the frenolicin families

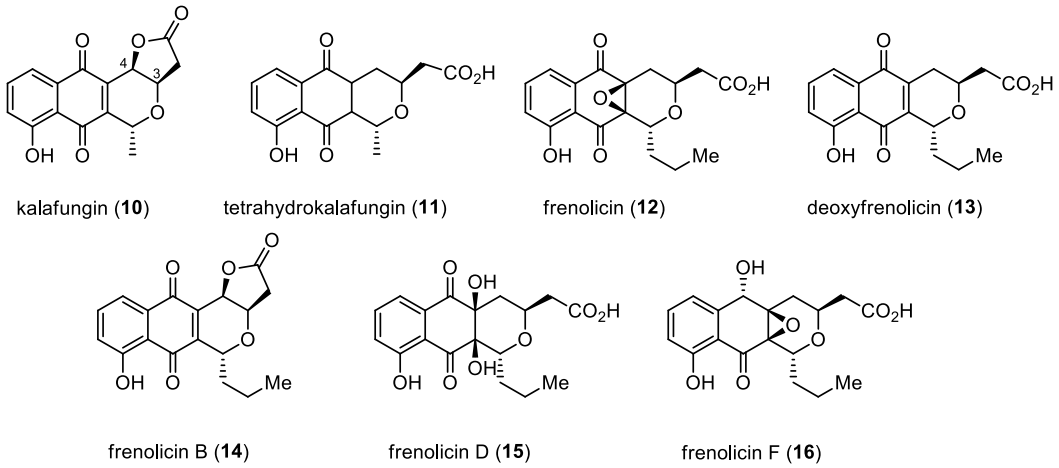

The last examples of pyranonaphthoquinone members are the fusarubin family (**Figure 4**). Members of the fusarubin family have a noticeable methoxy group at C-6 position. Fusarubin (**17**), a red pigment metabolite, was originally isolated from culture media of growing *Fusarium solani* and *Fusarium solani var. Martii*. by Ruelius and Gauhe in 1950. Compound **17** is also known as oxyjavanicin. The structure of fusarubin is different from most pyranonaphthoquinones by the position of 1,4-quinone moiety. In general, the pyran ring of most pyranonaphthoquinones is attached to the quinone ring. However, fusarubin has an aromatic ring attached to the pyran moiety instead of the quinone ring. Moreover, fusarubin has two chelating hydroxy groups which cause the compound to tautomerize easily (**Scheme 1**). Fusarubin can appear in 4 tautomeric forms. Tautomers **17i** and **17iv** are more stable than tautomers **17ii** and **17iii** because **17i** and **17iv** possess naphthoquinone moiety. Tautomer **17i** is the most stable tautomer due to the stabilizing effect of the methoxy group at C-6 to the *para*-quinone moiety (Moore *et al*., 1966, Chilton W. S., 1968). The dehydration analogue of fusarubin, anhydrofusarubin (**18**), was first discovered from *F. solani* by Baker and co-workers in 1981. Another two fusarubin analogues, 8-*O*-methylfusarubin (**19**) and 8-*O*-methylanhydrofusarubin (**20**), were discovered from another *Fusarium* species, *F. oxysporum* from roots of diseased citrus tree by the Tatum group in 1985. Most pyranonaphthoquinones isolated from *Fusarium* species exhibited good antibacterial activity. Fusarubin (**17**) and anhydrofusarubin (**18**) displayed potent antibacterial effect against *Staphylococcus aureus* with IC_{50} values of 16 and 2 µg/mL, respectively (Baker *et al*., 1990). Furthermore, compound **18** showed a significant activity against *Streptococcus pyogenes* with an IC_{50} value of 8 µg/mL while **19** displayed much weaker activity with a IC_{50} value of >128 µg/mL. Moreover, compound **19** exhibited weak antibacterial activity against *S. aureus* and *S. pyogenes* with both an IC_{50} value of >128 µg/mL.

Figure 4. Example metabolites of the fusarubin family

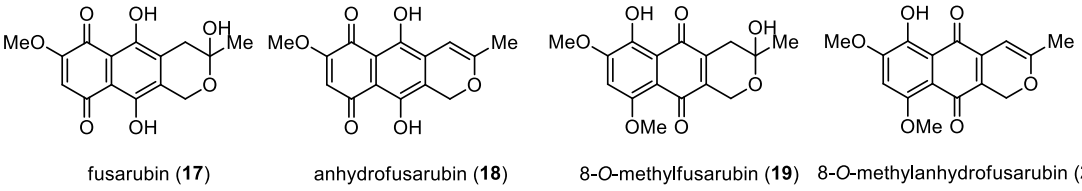

Scheme 1. The four tautomeric isomers of fusarubin (**17**)

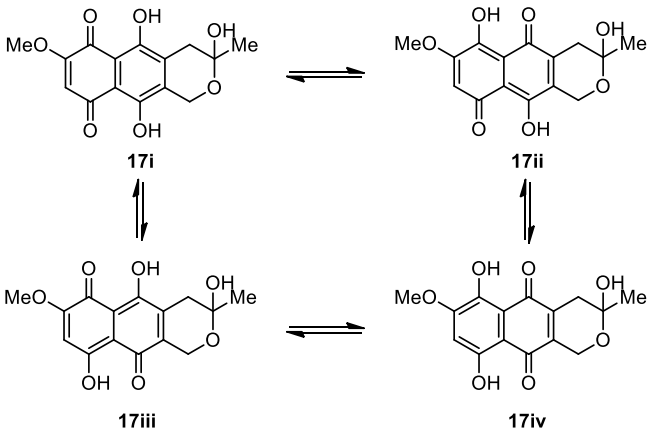

In 2010, Rukachaisirikul and co-workers reported the isolation of 5 new along with 18 known compounds of naphthoquinone and pyranonaphthoquinone families including fusarubin and anhydrofusarubin from sea-fan derived fungi *Fusarium* spp. PSU-F14 and PSU-F135 (**Figure 5**). Additionally, 8-*O*-methylfusarubin was isolated from a seagrass-derived fungus *Pestalotiopsis* sp. PSU-ES180. Isolated compounds **17**, **18** and **19** displayed highly potent cytotoxic activity against MCF-7 (human breast cancer) cells with IC_{50} values of 9.8, 0.9 and 1.06 µM, respectively. From this study, the cytotoxic activities of **18** and **19** were comparable to a standard drug doxorubicin (IC_{50} = 2.18 µM). Furthermore, compounds **17**-**19** exhibited insignificant harmful effect to Vero (African green monkey kidney fibroblast) cells with IC_{50} values of 79, 58 and 49 µM, respectively. To date, the syntheses of **17**, **19** and **20** have not yet been documented. With the excellent cytotoxic activity against MCF-7 breast cancer cells and their low toxicity against Vero cells, we became interested in synthesizing compounds **17**-**20**. These syntheses will

provide sufficient materials for further study on cytotoxic activities and potential development of new anticancer drug.

Figure 5. Cytotoxic activity against MCF-7 cells of fusarubin, anhydrofusarubin and 8-*O*-methylfusarubin isolated from *Fusarium* spp. PSU-F14, PSU-F135 and *Pestalotiopsis* sp. PSU-ES180 compared with a standard drug doxorubicin

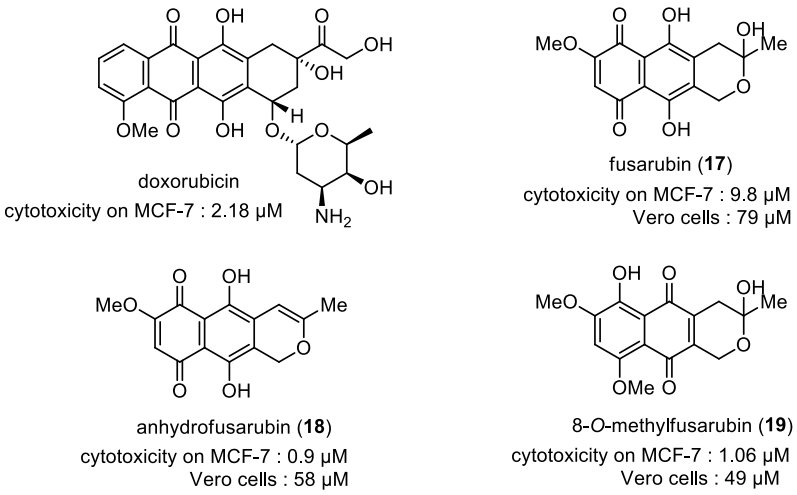

With impressive biological activities of pyranonaphthoquinone natural products, many research groups have reported the syntheses of these pyranonaphtho quinone members. However, the syntheses of **17**, **19** and **20** have not yet been reported, only the synthesis of **18** has been disclosed. Herein, this section will focus on literature precedents on the key strategies for syntheses of pyran moiety of pyranonaphthoquinone natural products. The first strategy is oxidative cyclization. The first total synthesis of anhydrofusarubin (**18**) was disclosed by Pillay *et al*. in 2012 via key Stobbe condensation and Wacker oxidation (**Scheme 2**). Stobbe condensation of 2,4,5-trimethoxybenzaldehyde (**21**) and subsequent ring closure provided naphthalene core **22** in 82% yield. Next, alcohol **24** was prepared from **22** in 7 linear steps. For the formation of pyran ring, Wacker oxidation of **24** using $PdCl_2$ and $CuCl_2 \cdot H_2O$ in the presence of gaseous oxygen provided the corresponding isochromene skeleton **25** in 49% yield over two steps. Compound **25** was then treated with AgO and 6M HNO_3 to generate naphthoquinone **26**. Lastly, demethylation of **26** using BCl_3 smoothly gave the desired product **18** in 65% yield.

Scheme 2. Total synthesis of anhydrofusarubin by Pillay *et al*.

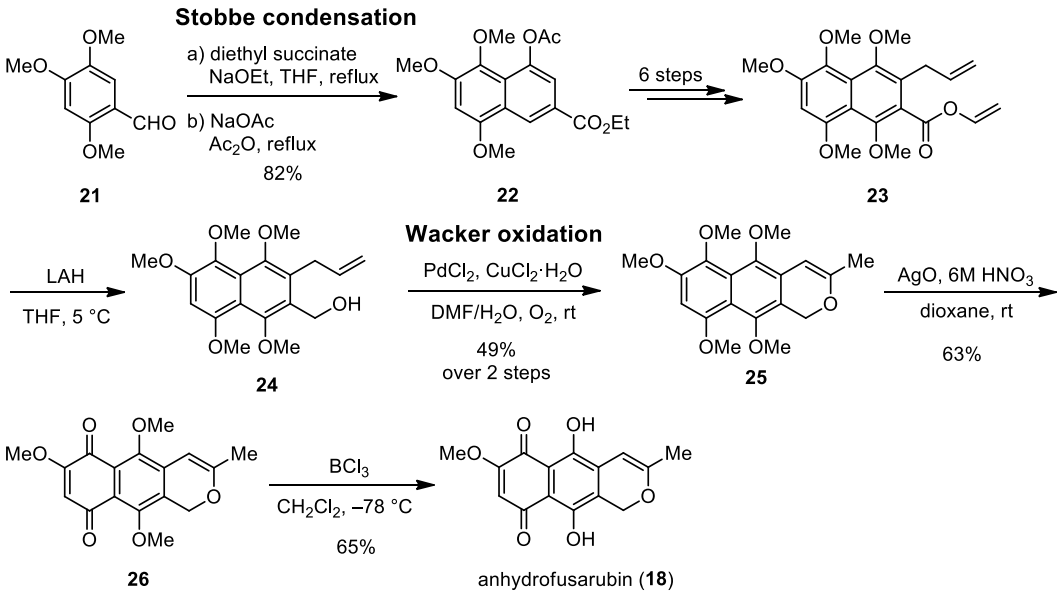

The next strategy for construction of the pyran moiety is oxa-Pictet-Spengler method. Oxa-Pictet-Spengler (OPS) reaction has been used as a common strategy to generate a pyran ring (Larghi *et al*., 2006). Generally, the OPS reaction only constructs the naphthopyran ring from an aromatic ring containing hydroxyethyl moiety and ketone or aldehyde precursor. This reaction requires a directing group on the aromatic moiety. In addition, the OPS reaction also requires Lewis or Brönsted acid catalyst and some weak promoters such as carboxylic acid. The proposed mechanism of OPS reaction is illustrated in **Scheme 3**. The advantages of OPS reaction are the construction of the corresponding pyran in a single step and the installation of any R^1 and R^2 groups by varying the ketone counterpart. However, the disadvantage of this method is the needs of *ortho*-directing groups on benzene or naphthalene moiety. In 2010, the Sawant group reported the syntheses of four deoxypyranonaphthoquinone analogues using OPS reaction as their key methodology. The syntheses of (+)-demethoxyeleutherin (**39**), (+)-demethoxyallo-eleutherin (**40**) are outlined in **Scheme 4a**. Firstly, the OPS reaction of chiral alcohol **34** with $CH_3CH(OEt)_2$ and $BF_3{\cdot}OEt_2$ generated the corresponding pyrans **35** and **36** in 21% and 65% yield, respectively. These naphthopyran intermediates were then treated with

CAN to provide 1,4-naphthoquinones **37** and **38**. To complete the syntheses, Diels–Alder reaction of **37** and **38** with 1-acetoxy-1,3-butadiene in toluene at room temperature smoothly gave (+)-**39** and (+)-**40** in 80% and 82% yield over two steps from **35** and **36**, respectively. The synthesis of another analogue, (+)-deoxythysanone (**44**), is shown in **Scheme 4b**. The same chiral alcohol **34** was treated with $MeOCH_2Cl$ and $ZnCl_2$ to give naphthopyran **41** in 21% yield. Compound **41** was then subjected to oxidation with CAN, followed by Diels–Alder cycloaddition using the same conditions previously mentioned to furnish the corresponding pyranonaphthoquinone **43**. Lastly, benzylic bromination of **43** followed by hydrolysis led to (+)-**44** in 77% yield over two steps. Later on, the complete synthesis of (+)-deoxynanomycin A methyl ester (**49**) was achieved in 8 steps via key intramolecular OPS reaction of acetal **45** (**Scheme 4c**). Treatment of **45** with $TiCl_4$ as a Lewis acid smoothly provided benzopyran **46** in 87% yield. Compound **46** was then converted to methyl ester **47** in 4 steps via key cyanation. Oxidation of **47** with CAN smoothly gave naphthoquinone **48** in 82% yield. Finally, **48** was subjected to the same conditions used for **37**, **38** and **42** to cleanly produce (+)-**49** in 78% yield over two steps.

Scheme 3. Proposed mechanism of the oxa-Pictet-Spengler reaction

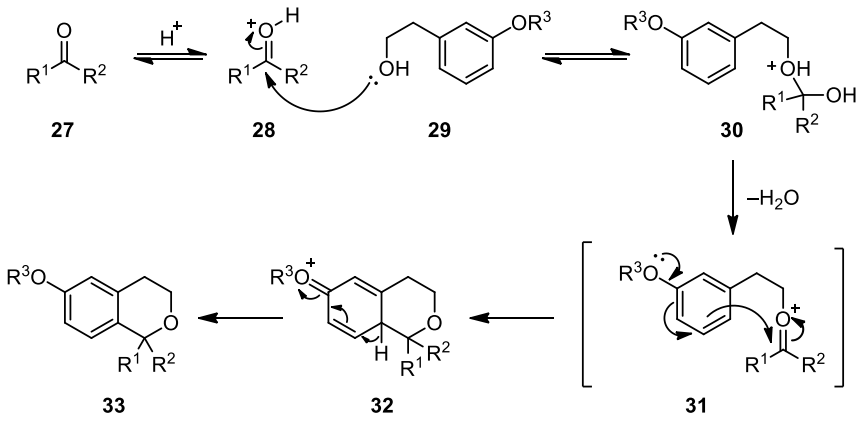

Scheme 4. The syntheses of a) (+)-demethoxyeleutherin (**39**) and (+)-demethoxyallo-eleutherin (**40**), b) (+)-deoxythysanone (**44**), c) (+)-deoxynanomycin A methyl ester (**49**) via key oxa-Pictet-Spengler reaction by Sawant *et al*.

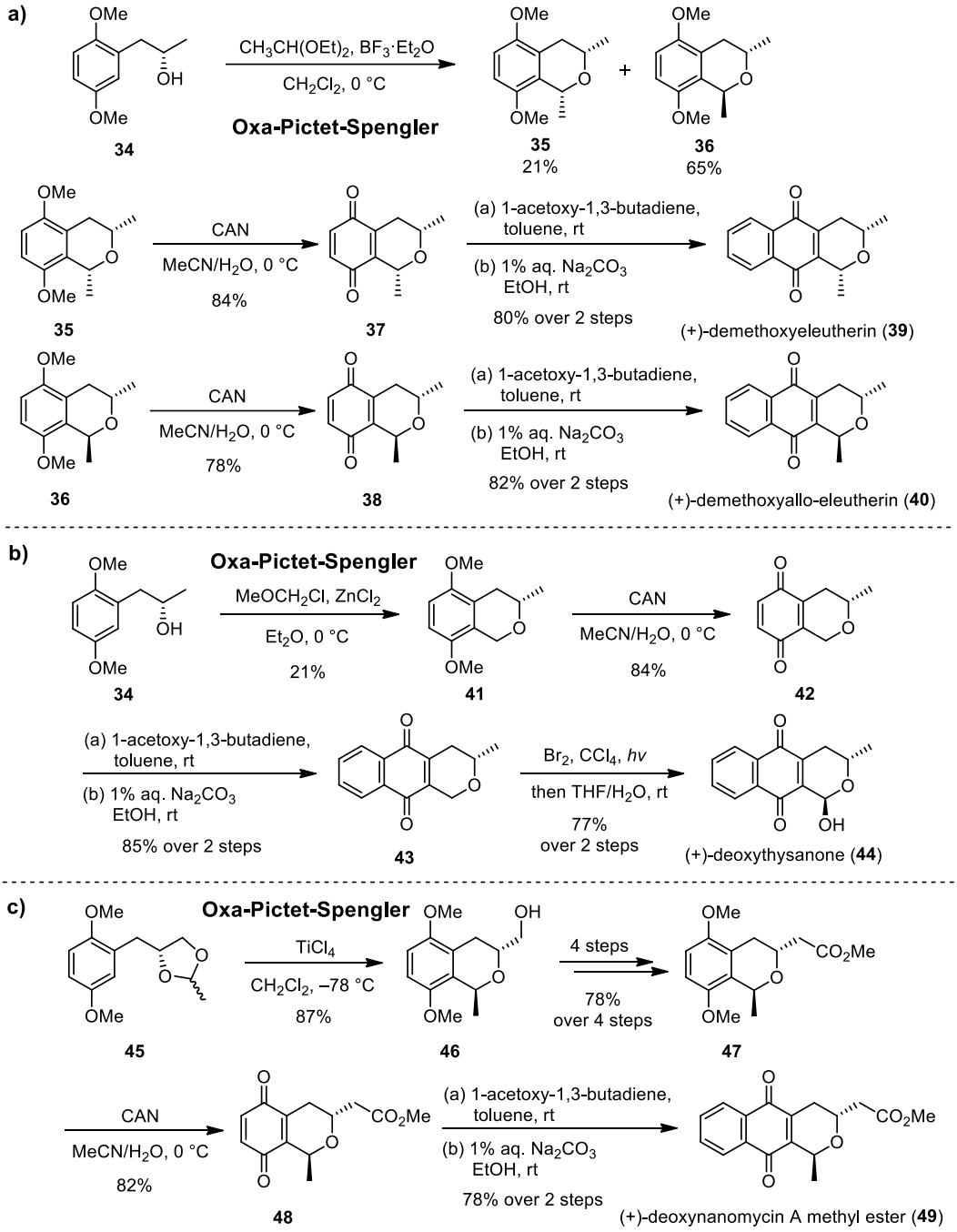

Michael type addition is one of the well-known methods to construct the pyran ring of pyranonapthoquinones. In 2004, the synthesis of pyranonaphthoquinone skeleton isochromene **56** was disclosed by Bianchi *et al*. via key Wittig-oxa-Michael strategy (**Scheme 5**). Firstly, compound **51** was prepared from glyoxylate **50** in 4 steps. Wittig olefination of **51** in refluxing MeCN provided α,β-unsaturated ester **52** which underwent oxa-Michael addition in the presence of KO*t*-Bu to give *anti* pyran product **53**. Subsequent deprotection of TBS group of **53** using TBAF furnished alcohol **54** in 68% yield over three steps. Finally, lactonization of **54** using Et_3N and subsequent oxidation with AgO led to isochromene core **56** in 80% and 55% yield, respectively.

Scheme 5. The synthesis of isochromene **56** by Bianchi *et al*.

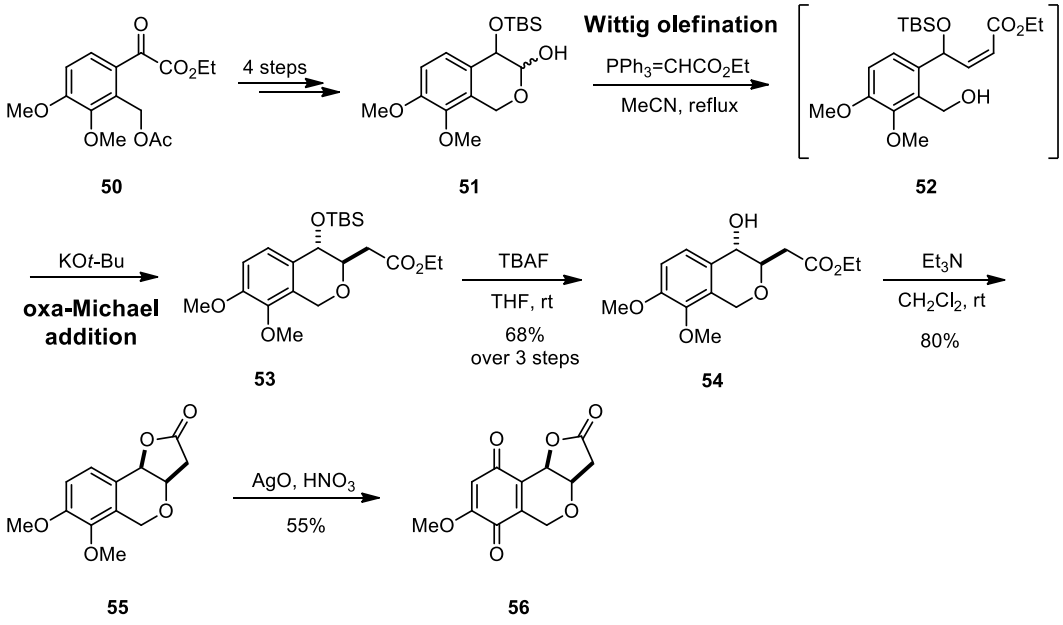

Another example of oxa-Michael addition for the synthesis of pyran moiety is highlighted in the syntheses of deoxydihydrokalafungin (**62**), *cis*-deoxy dihydrokalafungin (**65**) and deoxykalafungin (**64**) by Hume *et al*. in 2011 as outlined in **Scheme 6**. First, the CBS reduction of prochiral ketone **57** cleanly provided chiral alcohol **58** in 92% yield. Alcohol **58** was further elaborated to naphthalene **59** in 5 steps (**Scheme 6a**). To construct the pyran moiety, desilylation of silyl ether **59** using TBAF with

concomitant 1,4-addition afforded the corresponding diastereomeric naphthopyrans **60** and **61** in a 1.3:1 ratio and 84% combined yield. Compound **60** was then subjected to hydrolysis with LiOH, followed by oxidation with CAN to yield **62** and hydroquinone **63** in a 1:4 ratio (**Scheme 6b**). Hydroquinone **63** could be converted to **62** using $FeCl_3 \cdot 6H_2O$ or could be oxidized with salcomine and gaseous oxygen to furnish **64** in 39% yield. For the synthesis of **65**, hydrolysis of **61** with LiOH and subsequent oxidation with CAN smoothly gave the desired product **65** in 92% and 80% yield, respectively (**Scheme 6c**).

Scheme 6. The syntheses of deoxydihydrokalafungin (**62**), deoxykalafungin (**64**) and *cis*-deoxydihydrokalafungin (**65**) via key oxa-Michael reaction by Hume *et al*.

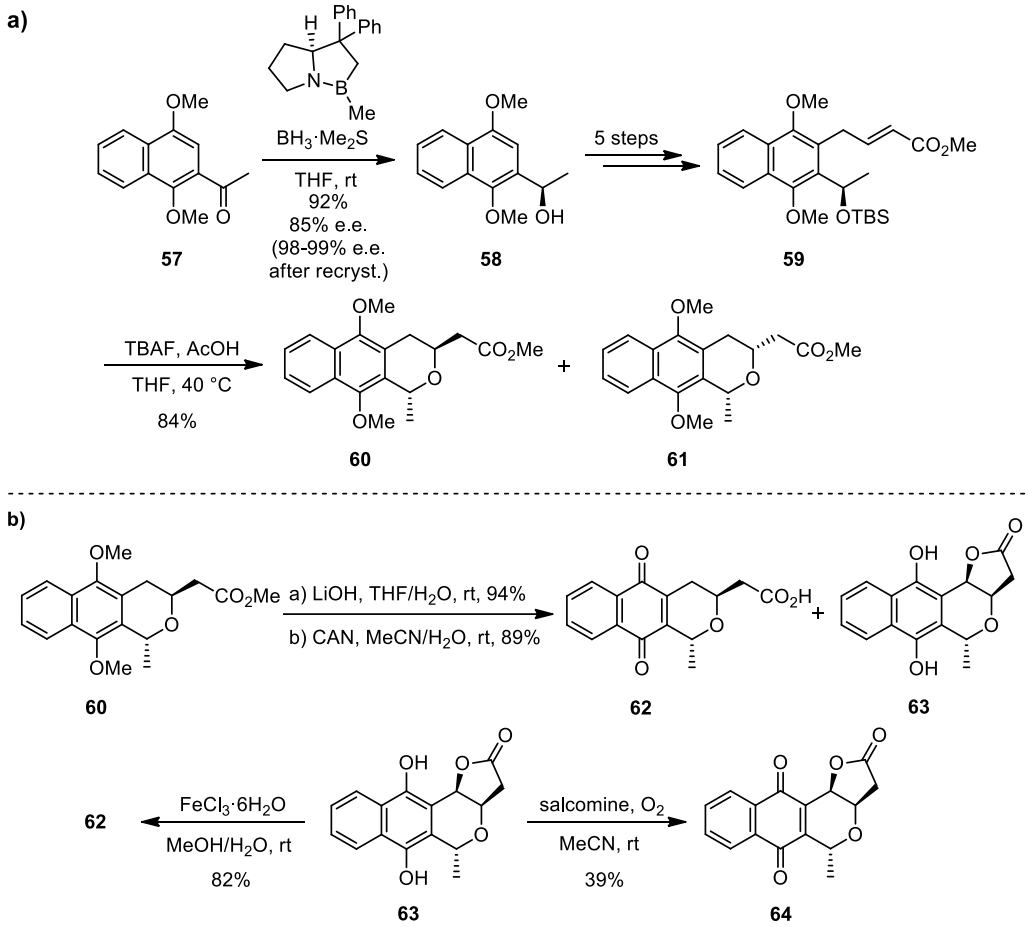

Scheme 6 (*cont.*). The syntheses of deoxydihydrokalafungin (**62**), deoxykalafungin (**64**) and *cis*-deoxydihydrokalafungin (**65**) via key oxa-Michael reaction by Hume *et al*.

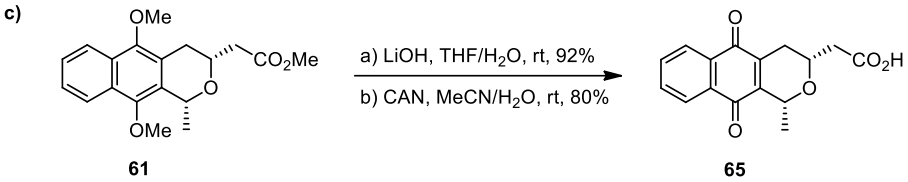

The next methodology for the construction of pyran is via lactonization. This strategy was showcased in the synthesis of an inhibitor of HRV 3C protease, (±)-9-deoxythysanone (**73**) by Jeong *et al*. in 2014 (**Scheme 7**). Firstly, dimethoxynaphthalene **66** was used as a starting material to construct naphthoquinone **67** in 6 steps. Alkylation of **67** with excess of 3-hydroxybutyric acid (**68**) via oxidative decarboxylation followed by lactonization furnished the corresponding lactone **69**. For the lactone reduction step to construct the pyran ring, the Jeong group discovered that conversion of naphthoquinone to hydroquinone prior to the reduction of lactone improved the product yield. Thus, **69** was treated with aqueous $Na_2S_2O_4$ to provide hydroquinone **70** in 60% yield over two steps. Lactone moiety of **70** was then reduced using $BH_3 \cdot Me_2S$, followed by air oxidation of an unstable hydroquinone *in situ* to deliver the corresponding pyranonaphthoquinone **71** in 48% yield. Cleavage of the isopropyl group with excess $AlCl_3$ smoothly furnished naphthoquinone **72** in excellent yield. Finally, benzylic bromination of **72**, followed by hydrolysis afforded (±)-**73** in 85% yield.

Scheme 7. The synthesis of (±)-9-deoxythysanone (**73**) via the reduction of the lactone by Jeong *et al*.

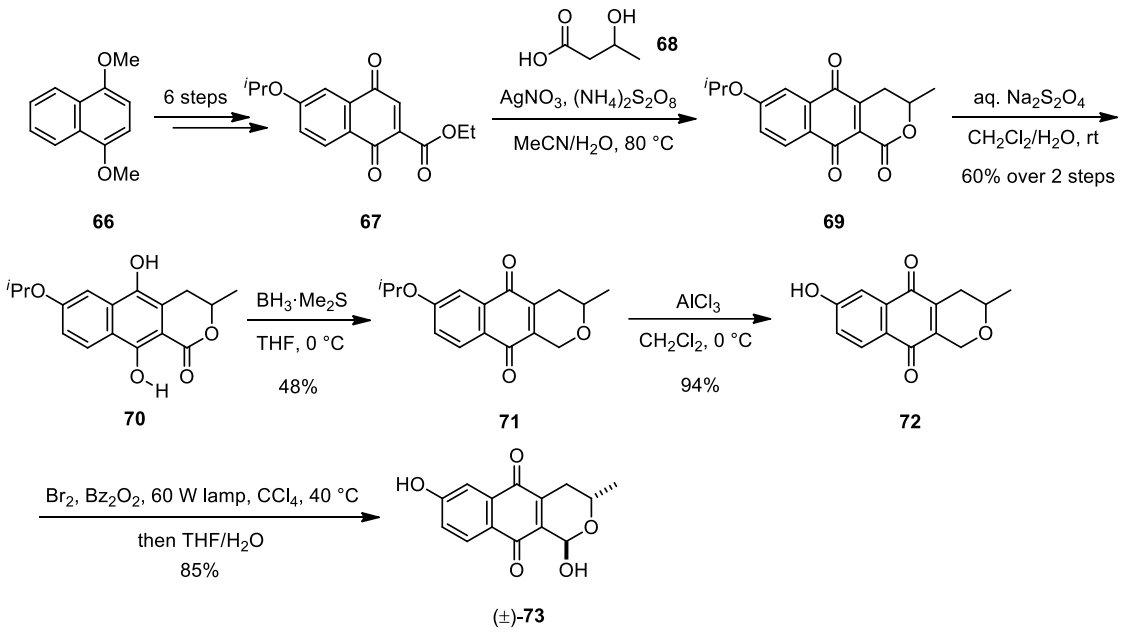

The last strategy to construct the pyran ring is via intramolecular acetalization of acetonyl and alcohol moieties. The acetonyl group is introduced via pyridinium ylide which can be generated from pyridinium salt in the presence of bases. The requirement of this strategy is that the acetonyl group can only be established at the quinone ring via Michael addition reaction. The syntheses of pyranonaphthoquinone analogues using pyridinium ylide to install acyl methyl groups on naphthoquinones were originally exposed by the Dean group (Aldersley *et al*., 1990). This method was later utilized in the synthesis of tetracyclic naphthoquinone from *Pentas longiflora,* isagarin (**79**) by the Kesteleyn group in 1999 (**Scheme 8**). Firstly, Wittig olefination of 1,4-dimethoxy benzaldehyde (**74**) furnished vinyl naphthalene **75** in 77% yield. Treatment of **75** with OsO_4 and base NMO, followed by oxidation with CAN cleanly provided naphthoquinone intermediate **77** in two steps. For acetalization step, pyridinium ylide was generated via treatment of acetyl methyl pyridinium chloride (**78**) with Et_3N and the acetonyl group was subsequently installed at naphthoquinone **77** to furnish acetonyl naphthoquinone

intermediate **77a**. Simultaneous acetalization of **77a** smoothly gave isagarin in 96% yield in one pot from **77**. In addition, the same research group reported the syntheses of pyranonaphthoquinone analogues using another pyridium salts with different R groups which provided compounds **80** and **81** in 97% and 91%, respectively.

Scheme 8. The syntheses of isagarin (**79**) and some pyranonaphthoquinone analogues via key acetalization from pyridinium ylide by Kesteleyn and co-workers.

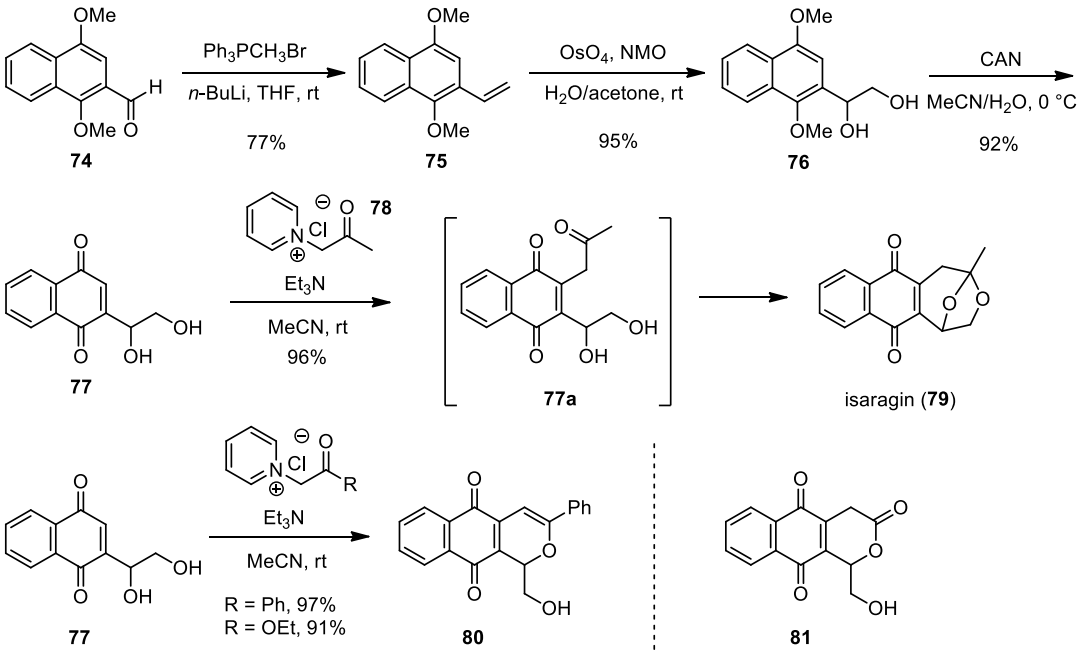

Another literature precedent of acetalization via pyridinium ylide strategy is illustrated in **Scheme 9**. The research group of Thi reported the syntheses of (dihydro)pyranonaphthoquinones and their epoxy analogues via key acetalization using *N*-acylpyridinium ylide to construct the pyran rings with various R groups. Naphthoic acid **82** was used as a starting material to prepare naphthoquinone intermediate **83** in 4 steps. After that, naphthoquinone **83** was treated with various pyridinium salts and Et_3N in MeCN in order to install the acyl methyl group with concomitant acetalization to furnish hemiacetal intermediate **84**. Compound **84** was subsequently subjected dehydration using catalytic TsOH in refluxing toluene to provide the corresponding dehydropyrano

naphthoquinone **85**. Lastly, epoxidation of **85** using hydrogen peroxide and Na_2CO_3 led to epoxynaphthoquinone analogues **86**. Moreover, the syntheses of six dihydronaphtho quinones and dihydronaphthoquinone epoxy analogues were then achieved in three steps from naphthoquinone **85**. Reduction of **85** using CF_3COOH in the presence of Et_3SiH provided the corresponding dihydronaphthoquinones **87**. Finally, nucleophilic epoxidation of **87** cleanly furnished epoxide analogues **88**.

Scheme 9. The syntheses of (dihydro)pyranonaphthoquinones **85**, **87** and their epoxy analogues **86** and **88** by Thi *et al*.

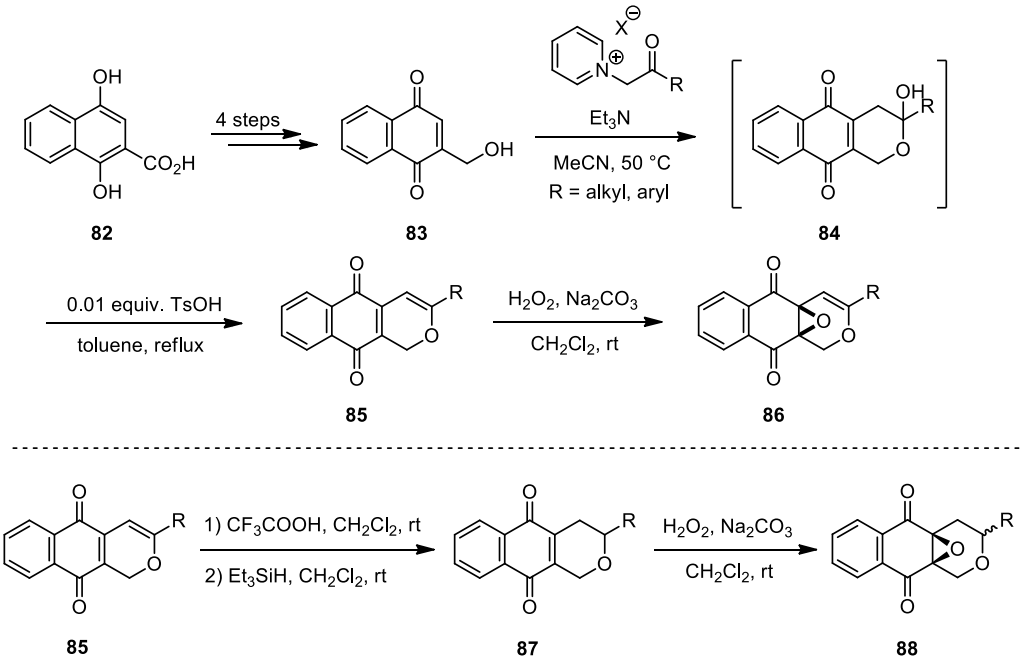

From all of the aforementioned synthetic approaches, we can categorize the major pathways for synthesizing the pyran moiety of pyranonaphthoquinones into 5 strategies including oxidative cyclization, oxa-Pictet-Spengler (OPS) reaction, oxa-Michael addition, lactonization and acetalization via the use of pyridinium ylide (**Figure 6**). In summary, oxidative cyclization, oxa-Michael addition and lactonization construct

the pyran ring via C3–O bond formation. These three reactions can be utilized with both hydroquinone and quinone precursors to construct the naphthopyran moiety. The OPS reaction can generate the pyran moiety via C–C bond formation at C-1 and C-13 from benzene or naphthalene starting material and the directing group is required for this cyclization. On the other hand, the acetalization reaction of acyl methyl groups and alcohol moiety requires the naphthoquinone precursor. Pyridinium ylides generated from pyridinium salts deliver the acyl methyl groups to be installed at the quinone moiety via Michael addition which would further construct the pyran ring upon intramolecular acetalization. Inspired by these reports, we envisioned that the pyran moiety in our target compounds **17**-**20** would be derived via intramolecular acetalization of acetonyl and alcohol moieties as a key step. The proposed syntheses of our target molecules is shown in **Scheme 10**. Structurally, compounds **19** and **20** possess the *para*-quinone ring attached to the pyran moiety which are suitable for utilizing acetalization to construct the pyran ring. Naphthoquinone **89** would be treated with pyridinium salt **78** to install the acetonyl group. Acetalization of **90** followed by removal of protecting group would lead to **19** which would undergo dehydration to furnish **20**. The syntheses of **17** and **18** would be modified from the synthesis protocols of **19** and **20**. Compounds **17** and **18** only differ from **19** and **20** by the position of the *para*-quinone moiety. Thus, we envisioned that compounds **17** and **18** would be synthesized using acetonyl naphthoquinone **90** as a common intermediate via manipulation of the oxidation state of the naphthoquinone ring. Selective reduction of **90** using $Na_2S_2O_4$ and subsequent protection of the corresponding hydroquinone would provide protected naphthalene **91**. Deprotection of the R^1 group of **91** followed by selective oxidation of the corresponding naphthol would furnish naphthoquinone intermediate **92**. Finally, acetalization and global deprotection of **92** would lead to **17**. Dehydration of **17** under the same conditions for **20** would ultimately provide compound **18**.

Figure 6. Synthetic strategies for construction of pyran ring of pyranonaphthoquiones

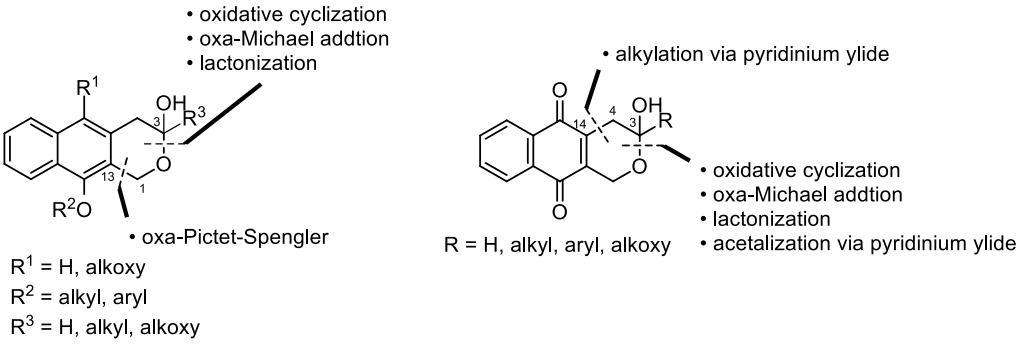

Scheme 10. Proposed syntheses of 8-*O*-methylfusarubin, fusarubin and their dehydration analogues via key acetalization to construct the pyran ring

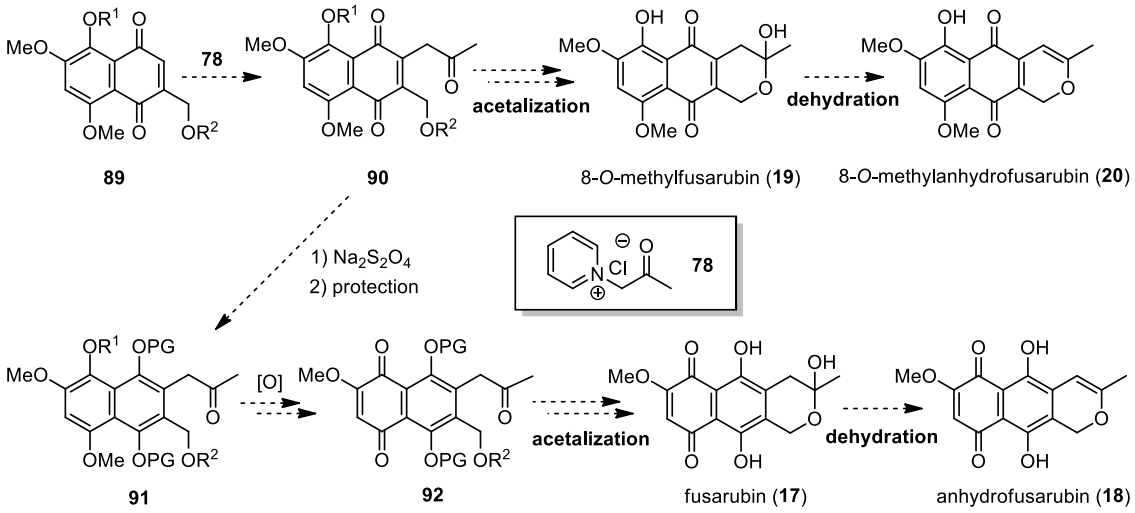

1.2 Objective

To synthesize fusarubin (**17**), anhydrofusarubin (**18**), 8-*O*-methylfusarubin (**19**) and 8-*O*-methylanhydrofusarubin (**20**) in order to provide sufficient materials for further study on cytotoxic activities and potential development of new anticancer drug.

CHAPTER 2

OPTIMIZATION TO CONSTRUCT NAPHTHOQUINONE CORE AND SYNTHESES OF 8-*O*-METHYLFUSARUBIN AND 8-*O*-METHYLANHYDROFUSARUBIN

CHAPTER 2

OPTIMIZATION TO CONSTRUCT NAPHTHOQUINONE CORE AND SYNTHESES OF 8-*O*-METHYLFUSARUBIN AND 8-*O*-METHYLANHYDROFUSARUBIN

2.1 Results and Discussion

2.1.1 Attempted synthesis of naphthoquinone core of 8-*O*-methylfusarubin

The retrosynthetic analysis of 8-*O*-methylfusarubin (**19**) and 8-*O*-methyl anhydrofusarubin (**20**) is illustrated in **Scheme 11**. Compound **20** was envisioned to be derived from **19** by the acid-promoted dehydration reaction. Our retrosynthetic approach toward **19** would form the pyran ring in the penultimate step. The pyran ring of **19** would be generated via acetalization of alcohol and acetonyl moieties of naphthoquinone **93**. The acetonyl group of **93** would be installed by the acetonylation reaction of naphthoquinone **94** using pyridinium ylide **78**. For the construction of naphthoquinone skeleton, naphthoquinone **94** would be obtained via the oxidation of the dimethoxy groups at C5 and C8 of naphthalene ring **95**. The protected hydroxymethylene moiety of naphthalene **95** would be elaborated from the reduction of the formyl group, which in turn would be installed via the Vilsmeier-Haack formylation of the known naphthalene **96**. The naphthalene precursor **96** would be prepared from 5-bromovanillin (**97**) in six steps via key Diels-Alder reaction following a protocol exposed by Green and co-workers in the synthesis of acetylated pentaalkoxynaphthalenes analogues.

Scheme 11. Retrosynthesis of 8-*O*-methylfusarubin (**19**) and 8-*O*-methylanhydro fusarubin (**20**)

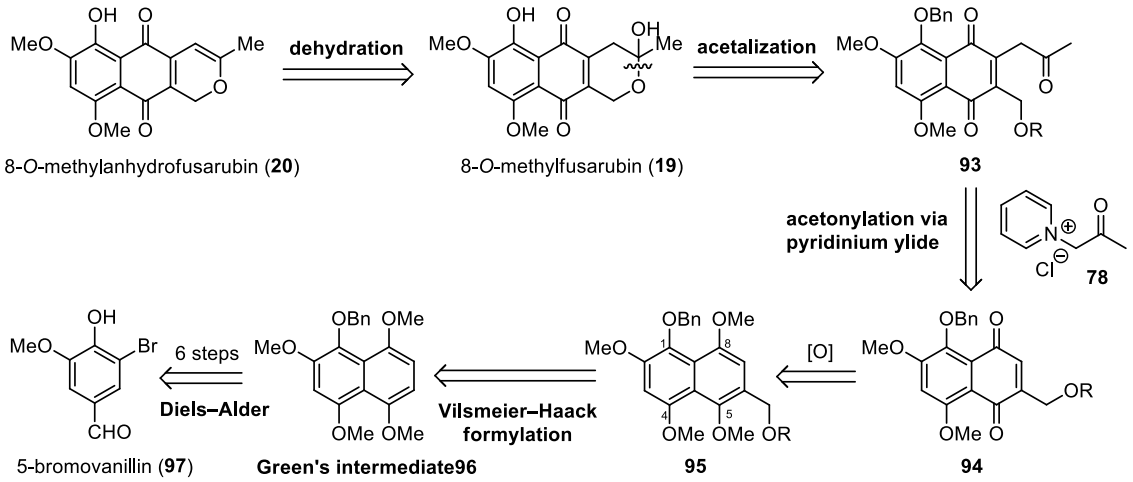

The Green group disclosed the synthesis of pentaalkoxynaphthalene **96** in six steps via key Diels-Alder reaction between dibromobenzene **101** and 2-methoxyfuran (**102**) (**Scheme 12**). Commercially available 5-bromovanillin (**97**) was used as a starting material to prepare dienophile precursor **101**. To generate the naphthalene skeleton, the benzyne intermediate generated by lithium-bromine exchange of **101** with *n*-BuLi was subjected to [4+2] cycloaddition reaction with **102** in THF at –78 °C to provide a mixture of naphthols **103** and **104** which were subsequently methylated to furnish naphthalene **96**. The overall yield of the synthesis of **96** by the Green group was reported in only 20% over six steps. Notably, some steps in Green's procedure used dimethylsulfate (Me_2SO_4) which is a highly toxic reagent and some of forceful conditions. Therefore, the modification of their protocol to synthesize our desired intermediate **96** was needed (**Scheme 13**). The modified synthesis of pentaalkoxynaphthalene **96** was started with protection of phenol group of 5-bromovanillin (**97**) with benzyl group in DMF at room temperature to furnish benzyl ether **98** in quantitative yield. Baeyer-Villiger oxidation of **98** followed by basic hydrolysis provided the corresponding phenol **99** in 86% yield. Phenol **99** was then treated with CH_3I and K_2CO_3 in refluxing acetone to give methoxybenzene **100** in excellent yield. Subsequent bromination of **100** using *N*-bromosuccinimide (NBS) and catalytic NH_4OAc

in MeCN smoothly furnished the corresponding dibromobenzene **101** in quantitative amount. The key Diels-Alder reaction of precursor **101** with 2-methoxyfuran (**102**) under reaction conditions reported by the Green group led to the inseparable naphthols **103** and **104** in only 48% combined yield. Thus, optimization of the key Diels-Alder reaction to construct **103** and **104** was needed.

Scheme 12. Synthesis of pentaalkoxynaphthalene **96** by Green and co-workers

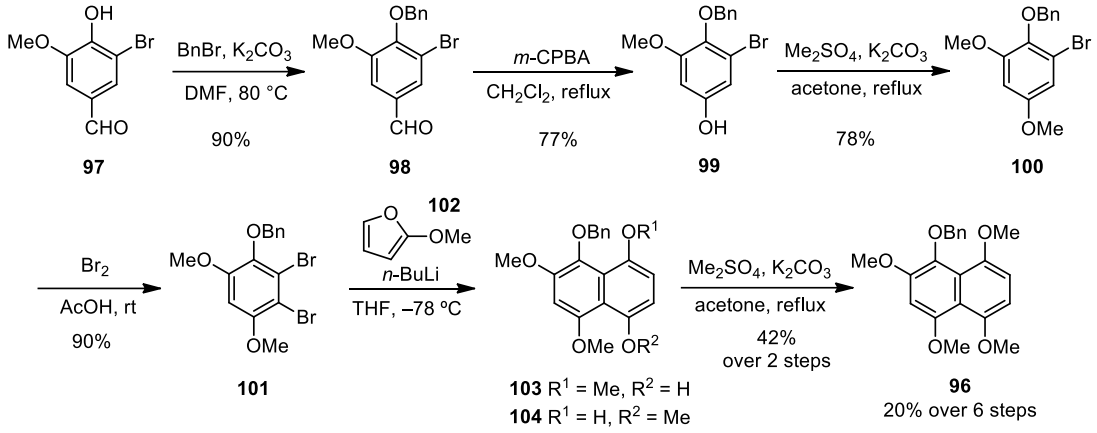

Scheme 13. Our synthesis of pentaalkoxynaphthalene **96** via modified Green's protocol

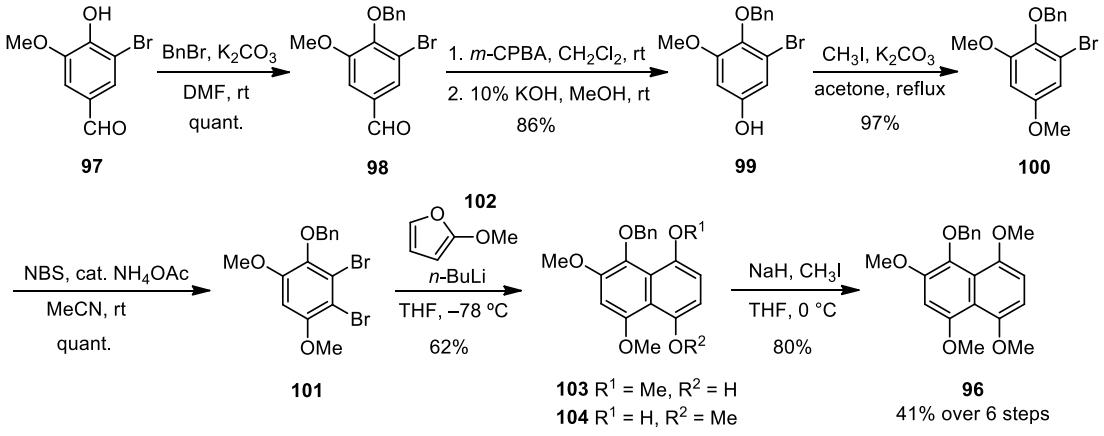

Screening of the Diels-Alder reaction conditions was investigated and shown in **Table 1**. From the previous literatures, the Diels-Alder reaction between benzyne precursor and furan analogues could be performed in various solvents e.g. ether, toluene and THF at –78 °C with variable equivalents of 2-methoxyfuran (**102**) and *n*-BuLi (Hart *et al*., 1980.; De Koning *et al*., 1988; De Koning *et al*., 1991; Buttery J. H. and Wege D., 1998; Giles *et al*., 2006). However, De Koning and co-workers reported the isolation of *n*-butyl naphthalene byproduct when using the excess amount of *n*-BuLi in this reaction. Hence, the effects of amounts of diene **102** and *n*-BuLi as well as the reaction concentration were studied. In entry 1, the same conditions reported by the Green group, using 1.15 equivalents of **102** and 1.2 equivalents for *n*-BuLi resulted in the formation of a mixture of naphthols **103** and **104** in 48% yield. We thus increased the amount of *n*-BuLi to 1.5 equivalents, however the yield of **103** and **104** was lower (33% yield, entry 2). Unsurprisingly, *n*-butyl naphthalene byproduct was observed in this reaction when using greater amount of *n*-BuLi which caused the lower yield. Hence, we increased the equivalents of **102** to be the same as *n*-BuLi but the result was also disappointing (30% yield, entry 3). From this result, we found that increasing the equivalents of *n*-BuLi was not necessary. Thus, the amount of *n*-BuLi was reduced to 1.0 equivalent which increased the yield of the desired naphthol products to 57% yield (entry 4). We next investigated the effect of reaction concentration in order to improve the yield of our desired naphthols. Increasing the reaction concentration from 0.3 to 0.4 molar with the same equivalents of diene and *n*-BuLi as entry 4 resulted in diminished yield of naphthols **103** and **104** from 57% to 31% yield (entry 5). The complex mixture between unidentified byproducts and some of unreacted starting material were observed which led to lower yield of naphthols **103** and **104**. After that, we tried to improve the yield of **103** and **104** by just decreasing the amount of diene **102**. Gratifyingly, treatment of **101** in 0.4M THF with 1.3 equivalents of **102** and 1.0 equivalent of *n*-BuLi furnished the mixture of naphthols **103** and **104** in the highest yield in 62% combined yield (entry 6). Hence, the conditions using 1.0 equivalent of **101** and *n*-BuLi and 1.3 equivalents of **102**, in 0.4M THF was used as the optimal conditions to construct the naphthalene core in our synthesis of naphthalene **96**. With the optimal Diels-Alder conditions in hand, the methylation of inseparable naphthols **103** and

104 to generate the desired naphthalene **96** was established. The mixture of **103** and **104** was then treated with NaH and CH_3I in THF at 0 °C to cleanly furnish the corresponding pentaalkoxynaphthalene **96** in 80% yield. In summary, the Green's procedure led to **96** in 20% yield over six steps while our modification with the optimal conditions in the Diels-Alder step furnished naphthalene **96** in 41% yield with the same number of steps.

Table 1. Optimization of Diels-Alder reaction between dibromobenzene **101** and 2-methoxyfuran (**102**)

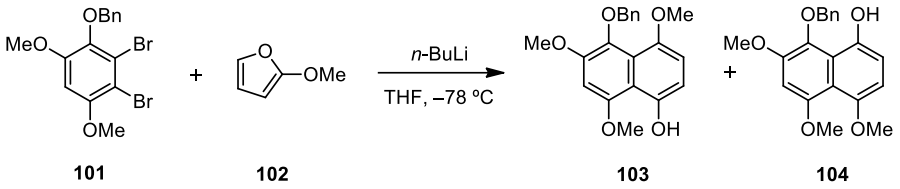

101 **102** **103** **104**

entry	reagents (equivalents)		concentration (molar)	% yield of **103** and **104**
	2-methoxyfuran	*n*-BuLi		
1	1.15	1.2	0.3	48
2	1.15	1.5	0.3	33
3	1.5	1.5	0.3	30
4	1.5	1.0	0.3	57
5	1.5	1.0	0.4	31
6	**1.3**	**1.0**	**0.4**	**62**

Having successfully synthesized the naphthalene skeleton **96** via key Diels-Alder reaction, we continued to focus on the preparation of naphthoquinone precursor **107** in order to install the acetonyl group for construction of the pyran ring. Our next task was to regioselectively introduce the formyl group at C6 position. The Kozlowski group has previously reported the regioselective formylation of pentamethoxynaphthalene ring system which is similar to our naphthalene core **96** (Lowell *et al*., 2007; Bandichhor *et al*., 2011, **Scheme 14a**). The Vilsmeier-Haack formylation of naphthalene **105** using $POCl_3$ and DMF furnished naphthaldehyde **106** with C6 formyl group which is the desired position in our synthesis. The Kozlowski group suggested that the methoxy group at C2

could be a good directing group as there are a few precedents for this type of formylation reactions (Terada *et al*., 1987; Tanoue *et al*., 1989). Hence, the Vilsmeier-Haack formylation was selected to install the formyl moiety of our intermediate. Gratifyingly, treatment of naphthalene **96** with oxalyl chloride in the presence of DMF cleanly provided desired naphthaldehyde **107** as an exclusive product in 86% yield (**Scheme 14b**). The position of the formyl group of **107** was then confirmed by HMBC and nOe correlations between aldehyde proton (δ 10.49) and C5 methoxy proton (δ 3.92). Subsequent reduction of **107** using $NaBH_4$ smoothly gave alcohol **108** in 99% yield. To construct the naphthoquinone core, there have been two literature precedents of the oxidation of polyalkoxynaphthalene system which is related to our naphthalene skeleton. In 1988, Tanoue and Terada disclosed the synthesis of 1,4-naphthoquinone derivatives via demethylation and oxidation of tetramethoxynaphthalene analogues using cerium(IV) ammonium nitrate (CAN) as an oxidizing agent (**Scheme 15a**). Naphthalene **109** contained the hydroxymethylene group ($-CH_2OH$) at C6 which was very similar to our precursor **108** except for the benzyl protecting group at C1 and the extra methoxy group at C2. Compound **109** was oxidized with CAN to generate naphthoquinones **110** and **111** in 75% and 13% yield, respectively. Presumably, the hydroxymethylene group acted as an electron donating group of tetramethoxynaphthalene ring which directed the formation of **108** as a major product. For the second literature, in 1991, the Clive group reported the syntheses of naphthoquinone analogues via regioselective oxidation of pentaalkoxynaphthalenes using CAN oxidation (**Scheme 15b**). Naphthalene precursor **105** had the methoxy group at C2 which was structurally similar to our naphthalene, however the hydroxymethylene group at C6 of **105** was absent. Oxidation of **105** with CAN gave naphthoquinone **113** exclusively in 68% yield. The regioselectivity in this oxidation was then explained by the Clive group that the left ring of **105** had more electron density from the methoxy group at C2 as an electron donating group which would induce the selective oxidation on the left-hand ring. Our naphthalene intermediate **108** possessed the two directing groups i.e. a methoxy group at C2 and a hydroxymethylene group at C6 which could lead to competition in the oxidation step. Unfortunately, treatment of **108** with CAN in MeCN at 0 °C resulted in exclusive formation of the undesired naphthoquinone **114** in 50% yield. Clearly from this result, the

methoxy group at C2 of **108** exhibited stronger electron donating ability over the hydroxymethylene group at C6 which led to selective oxidation on the left ring. Hence, another pathway to synthesize naphthoquinone **115** was necessitated.

Scheme 14. a) Regioselective formylation of naphthalene **105** by the Kozlowski group,
b) Synthesis of naphthalene precursor **108**

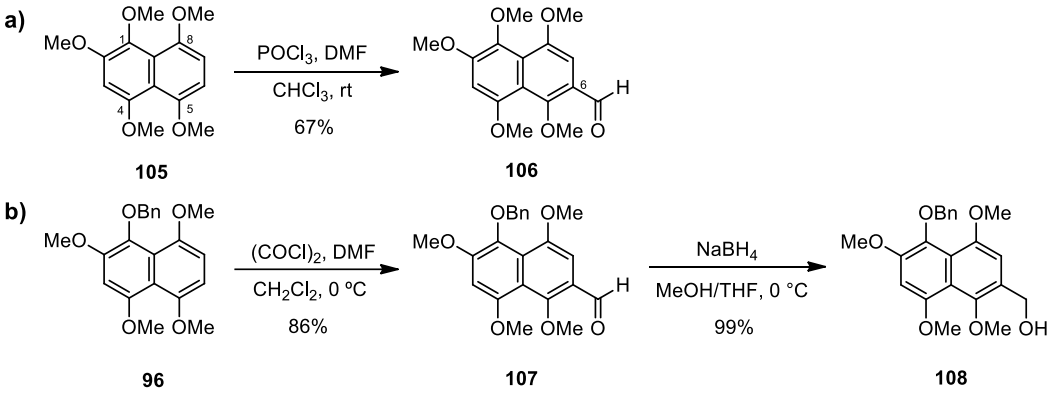

Scheme 15. Regioselective oxidation of polyalkoxynaphthalene mediated by CAN

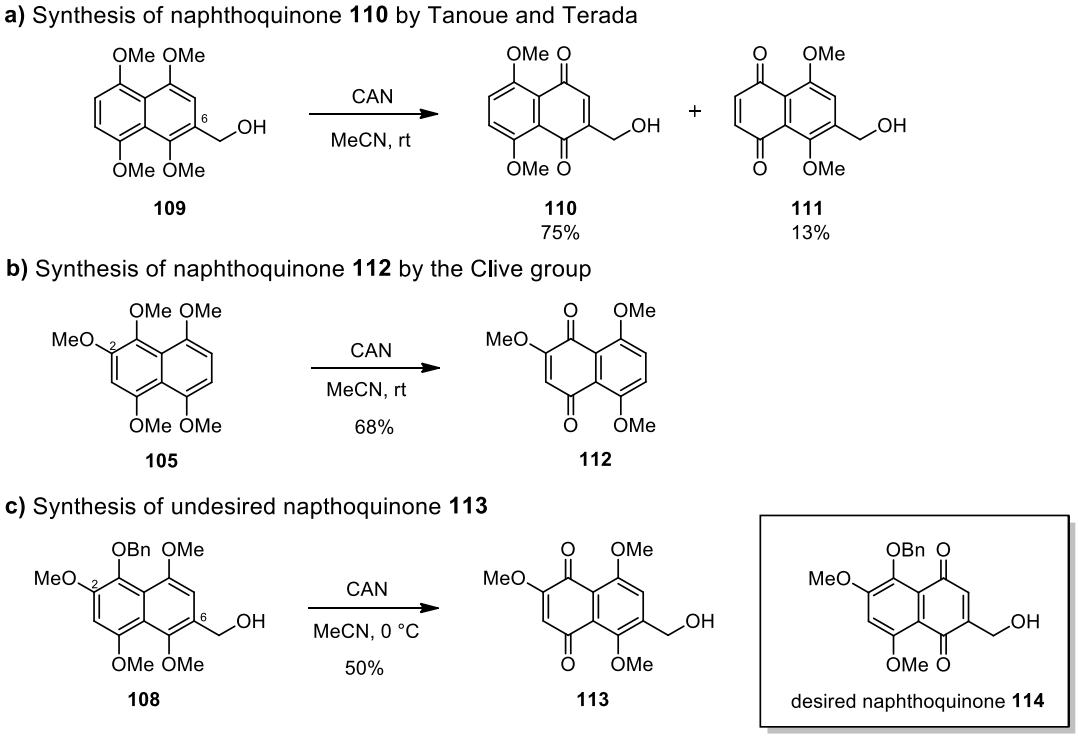

2.1.2 Completion of synthesis of 8-*O*-methylfusarubin (19) and 8-*O*-methylanhydrofusarubin (20)

Due to regioselectivity problem encountered in CAN oxidation of **108**, we turned our attention to naphthol precursors instead of methyl ether intermediate. The hydroquinone mono ether derivatives have been reported to be oxidized more easily compared with the *para*-dimethoxy naphthalenes for the construction of naphthoquinone cores (Jammula *et al*., 1991; Buttery J. H. and Wege D., 1998; Roush *et al*., 2004; Cui, *et al*., 2012). Moreover, the hydroxyl group could direct the regioselectivity of the formylation step at the requisite *ortho*-like position (at C6) due to the strong electron donating role of bare hydroxy moiety (Tanoue *et al*., 1989; Paruch *et al*., 2003). However, the drawback of this precursor was exposed by the Tanoue group that the formylation of naphthol intermediate could also generate the formate ester byproduct resulting from *O*-formylation. A mixture of naphthols **103** and **104** was then subjected to the previously described reaction conditions for Vilsmeier-Haack formylation to provide the desired naphthaldehyde **115** in 42% yield along with naphthyl formate byproduct **116** in 17% yield (**Scheme 16a**). The structure of naphthaldehyde **115** was confirmed by the nOe correlation between methoxy protons at C8 (δ 3.80) and aromatic proton at C7 (δ 7.02). In addition, the structure of formate **116** was further verified by subjecting to basic hydrolysis using 10% KOH to give naphthol **104** in 70% yield (**Scheme 16b**). The structure of **104** was confirmed by nOe correlations between hydroxy proton (δ 9.66) and benzylic protons of the benzyl group (δ 5.12). With the desired naphthaldehyde **115** with the correct position of the formyl group in hand, **115** was subjected to reduction with $NaBH_4$ to provide alcohol **117**. Unfortunately, compound **117** is very unstable and can easily decompose at room temperature in a few hours upon exposure to air. Due to the low stability of hydroxymethylene naphthalene **117**, this compound was immediately carried to the next step without chromatographic purification. To our delight, the key oxidation of **117** to construct naphthoquinone core was achieved via treatment with CAN in MeCN at 0 °C to smoothly furnish the desired naphthoquinone **114** in 94% over two steps.

Scheme 16. a) The synthesis of naphthoquinone **114** via Vilsmeier-Haack formylation of a mixture of naphthols **103** and **104**, b) Hydrolysis of naphthyl formate **116**

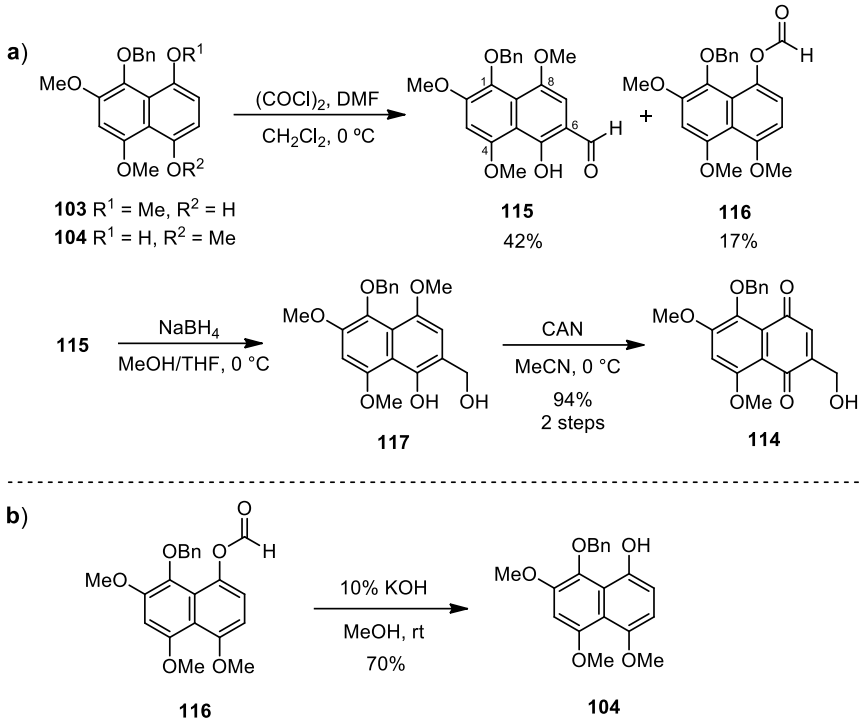

Although we could construct the desired naphthoquinone **114** via selective Vilsmeier-Haack formylation of inseparable naphthol isomers **103** and **104**, the limitation of this pathway is that only **103** was consumed to the target product. The other isomer **104** underwent *O*-formylation to generate the formate byproduct which lowered the yield in this formylation step (42% yield). To circumvent this problem, we decided to revisit the first pathway to construct the desired naphthoquinone **114** from naphthalene **108** by screening of other oxidizing agents. The silver reagent (AgO) and some of hypervalent iodines e.g. diacetoxyiodobenzene ($PhI(OAc)_2$) and (bis(trifluoroacetoxy)iodo)benzene (PIFA) were examined in this screening. The optimization data for oxidation of naphthalene **108** to construct naphthoquinone **114** are shown in **Table 2**. In entry 1, treatment of naphthalene **108** with silver(II) oxide (AgO) in the presence of 6M HNO_3 only provided the recovered starting material (de Koning *et al*., 1988; Pillay *et al*., 2012; Brimble *et al*., 2014). Hence, hypervalent iodine oxidizing agents were tested. Treatment

of precursor **108** with (bis(trifluoroacetoxy)iodo) benzene (PIFA) at 0 °C yielded the undesired naphthoquinone **113** as a major product in 52% yield along with the desired naphthoquinone **114** as a minor product in 25% yield (entry 2). Increasing the reaction temperature to ambient temperature still delivered naphthoquinone **113** as a major product in 42% yield but the amount of the desired naphthoquinone **114** was increased to 32% yield (entry 3). These results showed that PIFA preferentially oxidized on the more electron density ring (the left-hand ring) and gave **113** as a major product (Dohi and Kita, 2009; Zhdankin *et al*., 2016). Therefore, the less electron withdrawing iodobenzene species, $PhI(OAc)_2$ was investigated (Lamblin *et al*., 2012). To our delight, when compound **108** was subjected to oxidation with $PhI(OAc)_2$ at 0 °C, the desired naphthoquinone **114** was obtained as a major product in 58% yield along with **113** as a minor product in 34% yield (entry 4). Increasing the reaction temperature to ambient temperature led to higher yield (67%) of **114**, although **113** was still observed in 28% yield (entry 5). Notably from these two cases, elevating the reaction temperature improved the regioselectivity of this oxidation. Thus, the more robust conditions was selected. Gratifyingly, using $PhI(OAc)_2$ at elevated temperature of 50 °C could suppress the formation of undesired naphthoquinone **113** and gave the requisite naphthoquinone **114** exclusively in 75% yield (entry 6). This regioselective oxidation using $PhI(OAc)_2$ not only constructed **114** exclusively, but also shortened the reaction time from 30 minutes to 1 minute which could be noticeably observed by the color change of the reaction mixture from yellow to orange. The hydroxymethylene group was attributed as an excellent directing group in this regioselective $PhI(OAc)_2$-mediated oxidation of naphthalene **108**. To emphasize the importance of the hydroxymethlyene group in selective oxidation with $PhI(OAc)_2$, pentaalkoxynaphthalene **96** absent of hydroxymethylene moiety was subjected to oxidation under the conditions previously described in entry 6. As expected, the oxidation occurred on the more electron-rich (left-hand) ring of **96** to yield naphthoquinone **118** as a major product in 65% yield, whereas the product from oxidation of the less electron-rich (right-hand) ring, naphthoquinone **119**, was observed as a minor product in only 16% yield (**Scheme 17**). This observation suggested that the hydroxymethylene moiety could be a good directing group of pentaalkoxynaphthalene system and significantly directed the

regioselective oxidation for construction the naphthoquinone skeleton in $PhI(OAc)_2$-mediated oxidation at high temperature.

Table 2. Screening of oxidation conditions to construct naphthoquinone **114** from naphthalene **108**

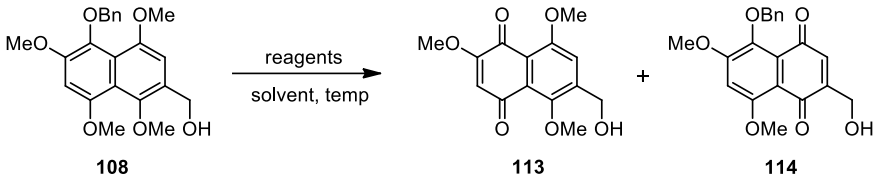

108 **113** **114**

entry	reagents	solvent (concentration)	temp	time	% yield	
					113	**114**
1	AgO, 6M HNO_3	1,4-dioxane (0.04M)	rt	overnight	no reaction	
2	$PhI(OCOCF_3)_2$	MeCN/H_2O (9:1, 0.1M)	0 °C	30 min	51%	25%
3	$PhI(OCOCF_3)_2$	MeCN/H_2O (9:1, 0.1M)	rt	30 min	42%	32%
4	$PhI(OAc)_2$	MeCN/H_2O (9:1, 0.1M)	0 °C	30 min	34%	58%
5	$PhI(OAc)_2$	MeCN/H_2O (9:1, 0.1M)	rt	30 min	28%	67%
6	**$PhI(OAc)_2$**	**MeCN/H_2O (9:1, 0.1M)**	**50 °C**	**1 min**	**–**	**75%**

Scheme 17. Oxidation of naphthalene **96** using $PhI(OAc)_2$ at 50 °C

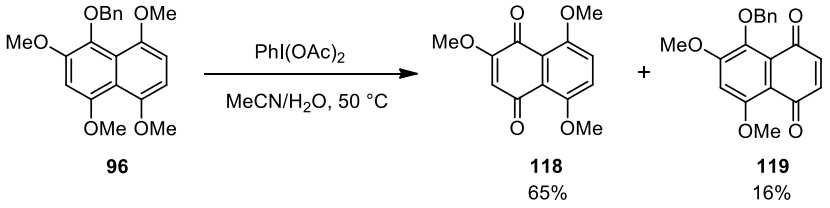

96 **118** 65% **119** 16%

The comparison between two synthetic routes to generate the naphthoquinone core **114** is shown in **Scheme 18**. Naphthoquinone **114** was first prepared from a mixture of naphthols **103** and **104** in 39% yield over three steps via CAN oxidation (pathway A). The drawback of this pathway was the low yield in the formylation step. Alternatively, the other synthetic route (pathway B) can construct **114** from naphthalene **108** in 51% yield over four steps via key selective oxidation using $PhI(OAc)_2$ at high temperature. Although, the number of steps of pathway B is greater than pathway A, pathway B provides a better overall yield of **114** than pathway A. Hence, the pathway B was selected for the syntheses of our target molecules.

Scheme 18. Comparison of the two synthetic routes for naphthoquinone **114**

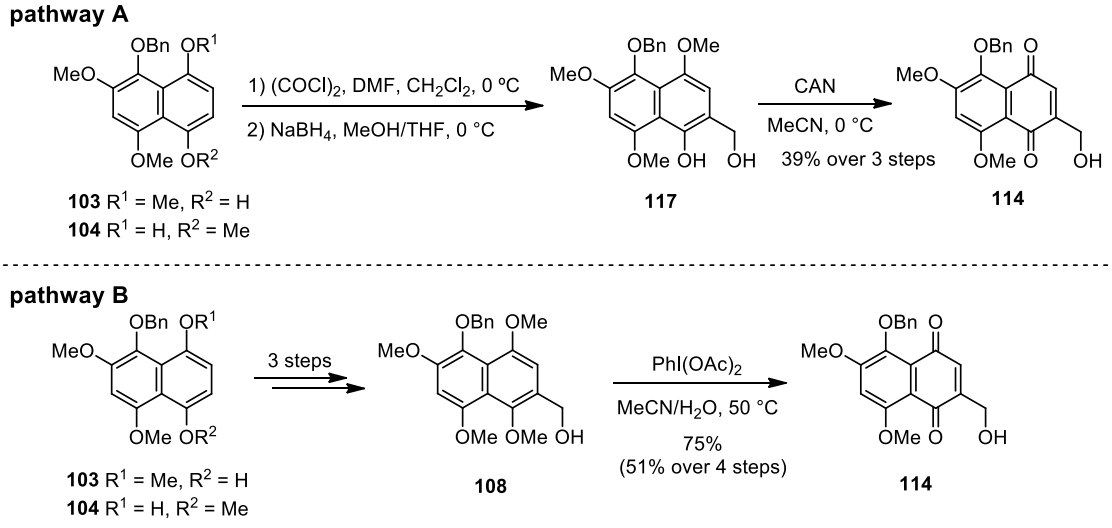

The completion of the syntheses of **19** and **20** is illustrated in **Scheme 19**. Our next task was to install the acetonyl group on the naphthoquinone core in order to construct of the pyran ring via acetalization. Previous works on the synthesis of pyranonaphthoquinone analogues have shown that the pyran ring could be established simultaneously in the acetonylation step and the reaction can proceed without the protection of hydroxymethylene moiety (Kesteleyn *et al*., 1999; Nguyen Van et al.; 2001; Thi *et al.*, 2015). Initially, naphthoquinone **114** was used in acetonylation reaction using **78** and Et_3N in MeCN. Unfortunately, acetonylation of **114** bearing free hydroxyl moiety led to the formation of complex mixture containing the desired pyran **122** which was evident from the ^1H NMR spectrum. Thus, naphthoquinone **114** containing a free hydroxymethylene group is not a suitable substrate for acetonylation under these conditions and the protection of hydroxymethylene group was needed. The protecting group of choice should be easily removed under acidic conditions because we desired to remove the protecting group and simultaneously construct the pyran ring in one step via acid-promoted intramolecular acetalization. Accordingly, the *tert*-butyldimethylsilyl group (TBS) was chosen. The hydroxymethylene moiety of naphthoquinone **114** was protected with TBS group to give silyl ether **120** in excellent yield. The protected naphthoquinone **120** was then treated with **78** in the presence of Et_3N in MeCN to furnish acetonylated naphthoquinone **121** in quantitative yield. To construct the pyran moiety, precursor **121** was treated with 1M HCl in MeCN to give the corresponding pyranonaphthoquinone **122** in 74% yield (Evans D. A. and Bender S. L., 1986; Min *et al*., 2007; Kuramochi K. and Tsubaki K., 2015). Alternatively, compound **122** could be synthesized via one-pot fashion by simply quenching the acetonylation reaction of naphthoquinone **120** with excess 1M HCl and prolonged stirring to yield **122** in 85% yield without the isolation of intermediate **121**. The only task remained was removal of the benzyl protecting group. Unfortunately, deprotection of benzyl group under typical hydrogenolysis conditions (Pd/C in alcohol solvent) resulted in the formation of pyran acetal instead of the hemiacetal counterpart. Presumably, slightly acidic Pd/C promoted the dehydration of pyran intermediate which was easily trapped with the alcohol nucleophile to give the acetal analogue. Therefore, the other Pd catalyst and polar aprotic solvent were chosen. Gratifyingly, hydrogenolysis of

122 with $Pd(OH)_2$ catalyst in ethyl acetate under the atmosphere of hydrogen afforded 8-*O*-methylfusarubin (**19**) as a red brick solid in 60% yield (Tatum *et al*., 1985; Studt *et al*., 2012). Finally, following the dehydration procedure disclosed by the Van Nguyen group, **19** was treated with catalytic TsOH in toluene at 105 °C to give 8-*O*-methylanhydro fusarubin **20** in 69% yield as black needles (Thi *et al*., 2015).

Scheme 19. Completion of the syntheses of 8-*O*-methylfusarubin (**19**) and 8-*O*-methyl anhydrofusarubin (**20**)

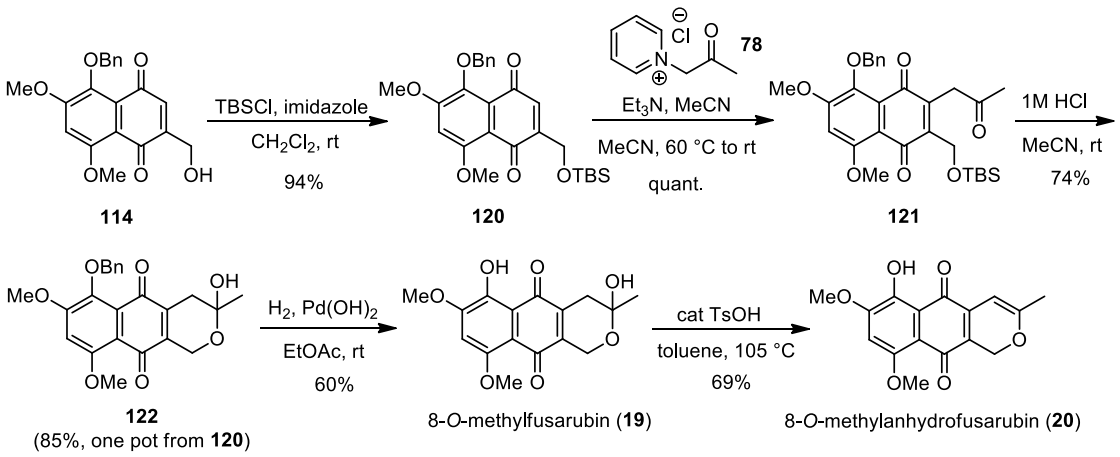

The ^1H and ^{13}C NMR spectroscopic data of synthetic 8-*O*-methylfusarubin (**19**) were in good agreement with those reported for the natural product **19** (**Table 3**, Studt *et al*., 2012). The specific rotation of synthetic **19** was observed to be +7.33 (*c* 0.03, acetone), suggesting that synthetic **19** was obtained as a scalemic mixture. Although, Masi *et al.* disclosed the specific rotation of natural product **19** isolated from grass weed-derived fungus *Rutstroemia capillus-albis* to be (*R*)-**19**, the specific rotation and absolute configuration of natural product **19** isolated from *Fusarium* species were not reported. The ^1H NMR spectroscopic data of synthetic 8-*O*-methylanhydrofusarubin (**20**) were in accordance with those reported for the natural product **20** (**Table 4**, Tatum *et al*., 1985). Nevertheless, the ^{13}C NMR data of natural product **20** were not disclosed by the isolation group. We also herein reported the ^{13}C NMR as well as HRMS data of synthetic **20**.

Table 3. Comparison of ^{1}H and ^{13}C NMR data for natural product and synthetic **19**

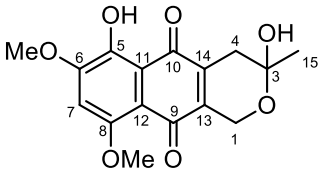

8-*O*-methylfusarubin (**19**)

Position	^{1}H NMR (δ and *J* in Hz)		^{13}C NMR (δ)	
	Natural (400 MHz) in DMSO-d_6	Synthetic (300 MHz) in DMSO-d_6	Natural (125 MHz) in DMSO-d_6	Synthetic (75 MHz) in DMSO-d_6
1	4.43, m	4.46, m	57.65	58.04
3	–	–	93.16	93.56
3-OH	6.04, s	6.05, s	–	–
4	2.54, d (18.6)	2.57, d (18.3)	31.73	32.10
	2.36, d (18.6)	2.37, d (18.3)		
5	–	–	147.53	147.90
5-OH	12.94, s	12.95, s	–	–
6	–	–	155.20	155.53
6-OMe	3.88, s	3.90, s	56.45	56.82
7	6.95, s	6.95, s	103.97	104.09
8	–	–	155.70	156.04
8-OMe	3.95, s	3.97, s	56.57	56.93
9	–	–	178.92	179.14
10	–	–	189.09	189.34
11	–	–	113.53	113.81
12	–	–	108.57	108.86
13	–	–	144.71	145.02
14	–	–	136.92	137.21
15	1.43, s	1.47, s	28.35	28.75

Table 4. Comparison of ^{1}H and ^{13}C NMR data for natural product and synthetic **20**

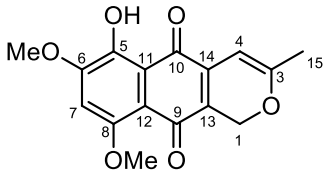

8-*O*-methylanhydrofusarubin (**20**)

Position	^{1}H NMR (δ and *J* in Hz)		^{13}C NMR (δ)
	Natural (270 MHz) in $CDCl_3$	Synthetic (300 MHz) in $CDCl_3$	Synthetic (75 MHz) in $CDCl_3$
1	5.15, s	5.12, s	63.45
3	–	–	163.43
4	5.83, s	5.85, s	92.99
5	–	–	148.70
5-OH	13.14, s	13.14, s	–
6	–	–	155.21
6-OMe	3.97, s	3.98, s	56.95
7	6.74, s	6.73, s	103.29
8	–	–	155.11
8-OMe	4.00, s	4.00, s	56.34
9	–	–	179.41
10	–	–	187.63
11	–	–	114.37
12	–	–	110.76
13	–	–	135.74
14	–	–	126.45
15	2.00, s	2.01, s	20.08

2.2 Conclusion

The total syntheses of 8-*O*-methylfusarubin (**19**) and 8-*O*-methylanhydro fusarubuin (**20**) were accomplished in 12 and 13 steps starting from commercially available 5-bromovanillin (**97**) with overall yields of 13% and 9%, respectively. The naphthalene core was prepared via key Diels-Alder reaction from modified protocol reported by the Green group. Selective Vilsmeier-Haack formylation of the naphthalene core to install the hydroxymethylene moiety, followed by hydroxymethylene group directed $PhI(OAc)_2$-mediated oxidation exclusively constructed the requisite naphthoquinone skeleton in good yield. The formation of pyran ring of **19** was established via acetonylation and subsequent acid-promoted acetalization to furnish the pyranonaphthoquinone core in one-pot fashion. Additionally, 8-*O*-methylanhydro fusarubuin (**20**) was prepared from **19** via dehydration using catalytic TsOH.

CHAPTER 3

COMPLETION OF SYNTHESES OF FUSARUBIN AND ANHYDROFUSARUBIN

CHAPTER 3

COMPLETION OF SYNTHESES OF FUSARUBIN AND ANHYDROFUSARUBIN

3.1 Results and Discussion

3.1.1 Attempted synthesis of fusarubin via TBS protection

Having successfully synthesized 8-*O*-methylfusarubin (**19**) and 8-*O*-methyl anhydrofusarubin (**20**), we next focused on the syntheses of fusarubin (**17**) and anhydrofusarubin (**18**) based on the syntheses of **19** and **20**. Structurally, the difference between **17** and **19** is the oxidation state of naphthoquinone rings. The pyran ring of **19** is attached to 1,4-quinone moiety, while the pyran ring of **17** is attached to the aromatic ring. According to their disparate position of naphthoquinone moiety, the syntheses of **17** and **18** were envisioned to be accomplished via manipulation of the oxidation state of an intermediate from the syntheses of **19** and **20**. The retrosynthetic analysis of **17** and **18** is shown in **Scheme 20**. Similar to the synthesis of **20**, anhydrofusarubin (**18**) would be achieved via dehydration of fusarubin (**17**). Fusarubin would be obtained via acetalization of protected naphthoquinone **123**. In the acetalization step, we planned to construct the pyran ring via global deprotection and *in situ* acid-promoted acetalization. Thus, the selected protecting group for naphthoquinone precursor **123** should be easily removed under acidic conditions. Naphthoquinone **123** would be generated via selective oxidation of naphthalene **124**, which would in turn be elaborated from naphthoquinone intermediate **121** via selective reduction of quinone ring using $Na_2S_2O_4$ as a reducing agent (Suhara *et al*., 2011; Nandi *et al*., 2012; Ito *et al*., 2013).

Scheme 20. Retrosynthesis of fusarubin (**17**) and anhydrofusarubin (**18**)

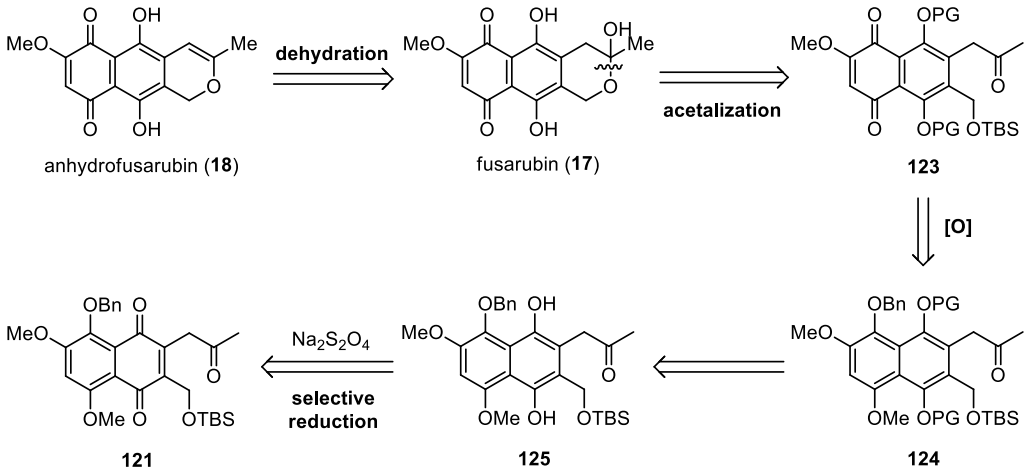

The attempted synthesis of fusarubin (**17**) is described in **Scheme 21**. In the previous chapter, we reported the procedure to synthesize naphthoquinone intermediate **121** from 5-bromovanillin (**97**) in 11 steps. To generate the new oxidation state of naphthoquinone core, the naphthoquinone moiety would be reduced back to hydroquinone ring in the protected form. The selective reduction of naphthoquinone skeleton **121** was then established by using $Na_2S_2O_4$ in THF to cleanly furnish the corresponding hydroquinone **125** (Sie *et al.*, 2018), which is prone to air oxidation at ambient temperature to return to 1,4-naphthoquinone precursor **121** (Miguel del Corral *et al.*; 2001; Kim, M. and Wiemer, D. F., 2004). Hence, hydroquinone **125** was carried to the next step without chromatographic purification. We initially chose TBS group as protecting groups of **125** in order to globally remove under acidic conditions in the penultimate step. Unfortunately, treatment of hydroquinone **125** with TBSOTf and 2,6-lutidine in CH_2Cl_2 at room temperature unexpectedly provided pyran TBS ether **126** in 94% yield over two steps (Couladouros *et al*., 2002). Nevertheless, the formation of TBS acetal of pyran in this step was inconsequential and should not affect the synthetic sequence planned. To switch the oxidation state of naphthoquinone core, the benzyl protecting group was removed via hydrogenolysis using H_2 gas and Pd/C as a catalyst to obtain unstable naphthol **127**. In this case, Pd on carbon worked well for deprotection of the benzyl group. Naphthol precursor

127 was then immediately oxidized with $PhI(OAc)_2$ in a 9:1 mixture of MeCN and H_2O at 0 °C to provide the requisite naphthoquinone **128** in 57% yield over two steps. At this stage, the naphthoquinone core with new oxidation state was established which was ready for completion of the syntheses of **17** and **18**. Unfortunately, we failed to remove the TBS protecting groups as well as to construct the pyran hemiacetal under various acidic conditions. Compound **128** was treated with a variety of Brønsted acids e.g. HCl, TsOH, AcOH, but only the decomposition of starting material and formation of complex mixture were observed. Desperately, we attempted to just remove the TBS protecting groups at first using TBAF. Unsuccessfully, only complex mixtures were observed in this reaction. Thus, another protecting group for hydroquinone **125** was sought.

Scheme 21. Synthesis of naphthoquinone **128** and attempts to remove TBS protecting group and form the pyran hemiacetal for the synthesis of **17**

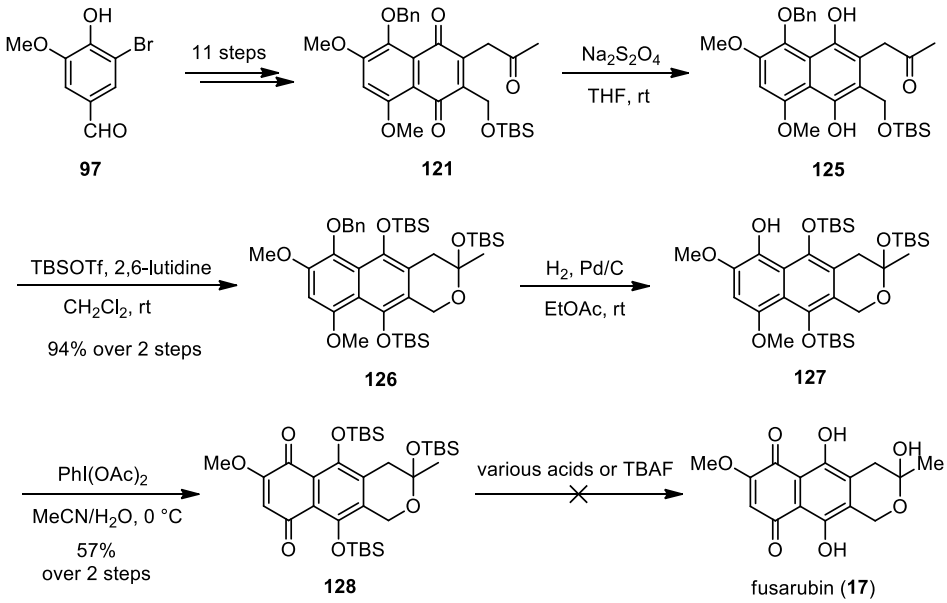

3.1.2 Completion of syntheses of fusarubin and anhydrofusarubin

To circumvent the problems with TBS deprotection and the formation of pyran ring, we decided to switch the hydroquinone protecting groups to ethoxymethyl (EOM) group. The alkoxymethyl protecting group of naphthols should be easily removed

under simple acidic conditions (Takuchi *et al*., 1988; White *et al*., 1999; Mazzini *et al*., 2004; Guerrero-Vásquez *et al*., 2014). The synthesis of naphthoquinone **131** is shown in **Scheme 22**. Treatment of naphthoquinone **121** with $Na_2S_2O_4$ in Et_2O provided the corresponding hydroquinone **125** in 87% yield (Suhara *et al*., 2011). In this selective reduction step, we found that using Et_2O as a solvent shortened the reaction time compared with THF. In the previous scheme, hydroquinone **125** was protected with TBS group without the purification of hydroquinone intermediate to avoid the air oxidation which yielded the silyl ether **126** in excellent yield (94% over two steps). However, for EOM protection, the quick chromatographic purification of hydroquinone **125** was required because employing the crude mixture of **125** directly in the protection step led to the low yield of **129** (22% yield over two steps). The hydroxyl moieties of **125** were protected with EOM group using NaH and EOMCl in DMF at 0 °C to give pentaalkoxynaphthalene **129** in 60% (53% yield over two steps from **121**) (Peng *et al*., 2015). To construct the naphthoquinone core, the benzyl protecting group of **129** was then removed under previously described conditions for hydrogenolysis to yield the desired naphthol **131** in 82% yield. Oxidation of naphthol **130** with $PhI(OAc)_2$ under the same conditions of **128** provided the requisite 1,4-naphthoquinone **131** as a major product in 50% yield along with a minor product, 1,2-naphthoquinone **132** in 15% yield. Naphthoquinone byproduct **132** was unstable and decomposed at ambient temperature upon exposure to air in a few days.

Scheme 22. The synthesis of naphthoquinone **131** via EOM protecting group

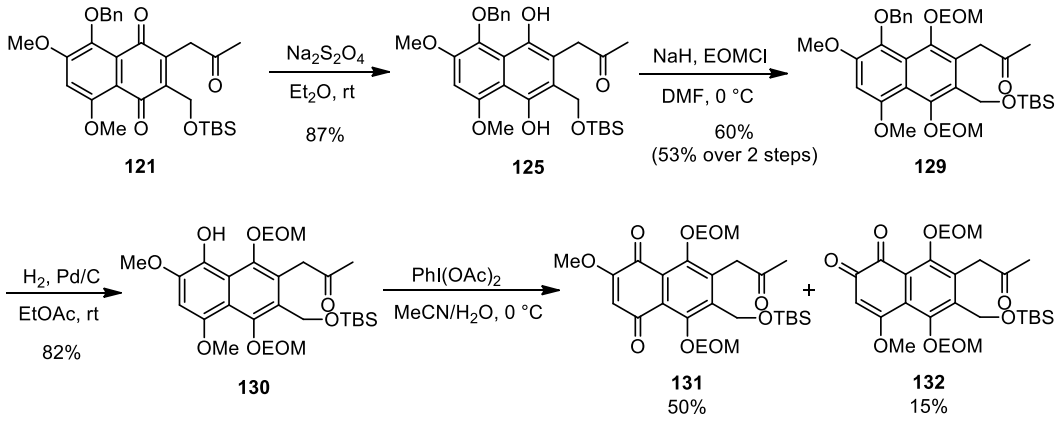

The completion of syntheses of fusarubin (**17**) and anhydrofusarubin (**18**) is illustrated in **Scheme 23**. Naphthoquinone **131** was treated with 1M HCl in MeCN to achieve the red pigment metabolite, fusarubin (**17**) in 54% along with some of its dehydrated analogue, anhydrofusarubin (**18**) in 22% yield. Alternatively, compound **17** could be converted to **18** by dehydration under previously described dehydration conditions to yield **18** in 73% yield.

Scheme 23. Completion of the syntheses of fusarubin (**17**) and anhydrofusarubin (**18**)

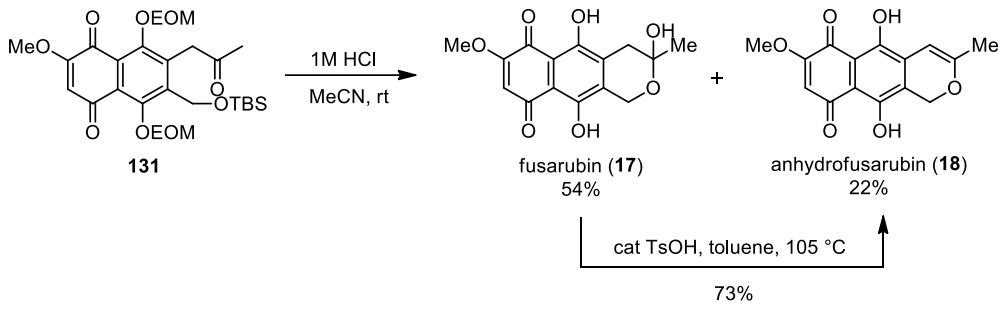

The ^{1}H and ^{13}C NMR spectroscopic and HRMS data of synthetic fusarubin (**17**) were in reasonable agreement with those reported for the natural product **17** (**Table 5**, Chowdury *et al*., 2017). Due to solubility problem of synthetic **17** in $CDCl_3$ which was obtained in 17.6 mg quantity, the NMR spectroscopic data of synthetic **17** were also collected in DMSO-d_6 solvent (**Table 6**). There has been no report of the specific rotation of natural product **17**. Nevertheless, we also reported the specific rotation of synthetic **17** in our work ($[\alpha]_D^{26}$ +4.35, *c* 0.036, acetone). Hence, synthetic **17** was suggested to be a scalemic mixture. The ^{1}H and ^{13}C NMR spectroscopic data of synthetic anhydrofusarubin (**18**) are shown in **Table 7** which were identical to those reported for the natural product **17** (Khan *et al*., 2016).

Table 5. Comparison of ^{1}H and ^{13}C NMR data for natural product and synthetic **17**

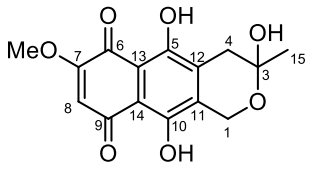

fusarubin (**17**)

Position	^{1}H NMR (δ and *J* in Hz)		^{13}C NMR (δ)	
	Natural (400 MHz) in $CDCl_3$	Synthetic (300 MHz) in $CDCl_3$	Natural (100 MHz) in $CDCl_3$	Synthetic (75 MHz) in $CDCl_3$
1	4.88, s	4.89, s	58.30	58.47
3	–	–	93.80	94.06
3-OH	2.25, brs	2.31, brs	–	–
4	2.70, brd (18.4)	2.71, d (18.0)	32.50	32.31
	3.02, d, (17.9)	3.03, d, (18.0)		
5	–	–	156.80	156.97
5-OH	12.93, s	12.94, s	–	–
6	–	–	178.30	178.43
7	–	–	160.40	160.65
7-OMe	3.93, s	3.94, s	56.70	56.69
8	6.17, s	6.19, s	109.60	109.64
9	–	–	184.90	184.64
10	–	–	160.60	160.65
10-OH	12.66, s	12.68, s	–	–
11	–	–	137.20	137.10
12	–	–	137.20	137.10
13	–	–	109.60	109.64
14	–	–	107.50	107.63
15	1.64, s	1.64, s	22.60	22.63

Table 6. ^{1}H and ^{13}C NMR data for synthetic **17** in DMSO-d_6

Position	^{1}H NMR (δ and *J* in Hz) 300 MHz in DMSO-d_6	^{13}C NMR (δ) 75 MHz in DMSO-d_6
1	4.62, s	57.74
3	–	93.44
3-OH	6.10, s	–
4	2.51, d (18.0)	33.20
	2.71, d, (18.0)	
5	–	156.68
5-OH	12.90, s	–
6	–	178.10
7	–	160.04
7-OMe	3.88, s	57.49
8	6.37, s	110.10
9	–	185.05
10	–	161.06
10-OH	12.43, s	–
11	–	133.67
12	–	137.21
13	–	110.10
14	–	107.45
15	1.46, s	28.88

Table 7. Comparison of ^{1}H and ^{13}C NMR data for natural product and synthetic **18**

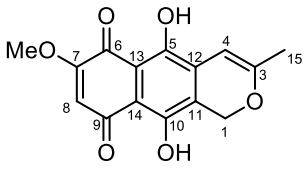

anhydrofusarubin (**18**)

Position	^{1}H NMR (δ and *J* in Hz)		^{13}C NMR (δ)	
	Natural (500 MHz) in $CDCl_3$	Synthetic (300 MHz) in $CDCl_3$	Natural (125 MHz) in $CDCl_3$	Synthetic (75 MHz) in $CDCl_3$
1	5.16, s	5.19, s	62.90	62.92
3	–	–	161.50	161.53
4	5.92, s	5.96, s	94.60	94.65
5	–	–	157.60	157.66
5-OH	12.57, s	12.61, s	–	–
6	–	–	177.80	177.85
7	–	–	159.90	159.95
7-OMe	3.88, s	3.92, s	56.60	56.67
8	6.11, s	6.14, s	109.90	109.91
9	–	–	182.90	182.93
10	–	–	157.60	157.62
10-OH	12.97, s	13.01, s	–	–
11	–	–	122.70	122.69
12	–	–	132.90	132.95
13	–	–	110.90	110.87
14	–	–	107.90	107.92
15	1.98, s	2.01, s	20.10	20.11

3.2 Cytotoxic activities

The *in vitro* cytotoxic activities against human breast cancer (MCF-7) cells and African green monkey kidney fibroblast (Vero) cells of four synthetic pyranonaphthoquinones **17**-**20** were evaluated using the resazurin microplate assay (REMA, **Table 8**) (O'Brien *et al*., 2000). Among the four compounds tested, 8-*O*-methylfusarubin (**19**) displayed potent cytotoxic activity against MCF-7 cells with the highest IC_{50} value of 1.01 μM, compared with standard drugs, doxorubicin and tamoxifen (IC_{50} values of 15.25 and 17.23 μM, respectively). Moreover, **19** showed very low cytotoxic activity against Vero cells (IC_{50} = 47.49 μM) compared with a positive control for Vero Cells, ellipticine (IC_{50} = 3.97 μM). In addition, compounds **17**, **18** and **20** exhibited good cytotoxic activity against MCF-7 cells with IC_{50} values of 3.19, 12.28 and 2.96 μM, respectively. However, synthetic anhydrofusarubin (**18**) displayed the lowest cytotoxic activity against MCF-7 cells among the four synthetic compounds tested which is in contrast to the cytotoxicity against MCF-7 reported for natural **18** (0.9 μM). Nevertheless, synthetic **18** also showed the lowest cytotoxic activity against Vero cells with an IC_{50} value of 77.54 μM. Overall from these results, synthetic **17**-**20** exhibited potent cytotoxic activities against MCF-7 cells more than standard drugs, doxorubicin and tamoxifen. In addition, compounds **17**-**20** also displayed low cytotoxicity against Vero cells compared with ellipticine.

Table 8. Cytotoxic activity of **17**-**20** against MCF-7 cancer and Vero cells using resazurin microplate assay (REMA)

compound	cytotoxicity, IC_{50} (μM)	
	MCF-7 cells	Vero cells
17	3.19	19.36
18	12.28	77.54
19	1.01	47.49
20	2.96	20.54
doxorubicin	15.25	–
tamoxifen	17.23	–
ellipticine	–	3.97

To further evaluate the cytotoxic activities of analogues **17**-**20**, these compounds were subjected to *in vitro* cytotoxic activity evaluation against MCF-7 cells using MTT colorimetric assay (**Table 9**). The results showed that compounds **17**-**20** exhibited the cytotoxic activity against MCF-7 cells with similar trend compared with REMA. Synthetic **19** displayed the most potent cytotoxic activity with an IC_{50} value of 2.85 μM, followed by compounds **20**, **17** and **18** (IC_{50} values of 8.63, 11.31 and 20.88 μM, respectively). Additionally, cytotoxicity against MCF-7 of compounds **17**-**20** were tested using 3D cancer spheroid assay (**Figure 7**). From these data, compound **19** still exhibited the highest efficiency against breast cancer cells in a long-term effect (day 3). In accordance with previous results, synthetic compounds **17**-**20** showed potent cytotoxic activity against MCF-7 cells compared with standard drug, doxorubicin. 8-*O*-Methylfusarubin (**19**) displayed the most potent cytotoxic activity against MCF-7 cells in this series of fusarubin analogues, which could be further studied in the development for anti-breast cancer drug discovery.

Table 9. Cytotoxic activity of synthetic compounds **17**-**20** against MCF-7 cancer cells using the MTT and 3D spheroid assays

compound	cytotoxicity, IC_{50} (μM)			
	MTT assay	3D cancer spheroid assay		
		day 1	day 2	day 3
17	11.31	18.70	12.50	13.14
18	20.88	57.09	39.67	31.46
19	2.85	4.44	1.83	2.29
20	8.63	25.49	16.42	5.79
doxorubicin	28.94	–	–	–

Figure 7. High-content imaging of synthetic **17**-**20** on 3D MCF-7 breast cancer spheroids

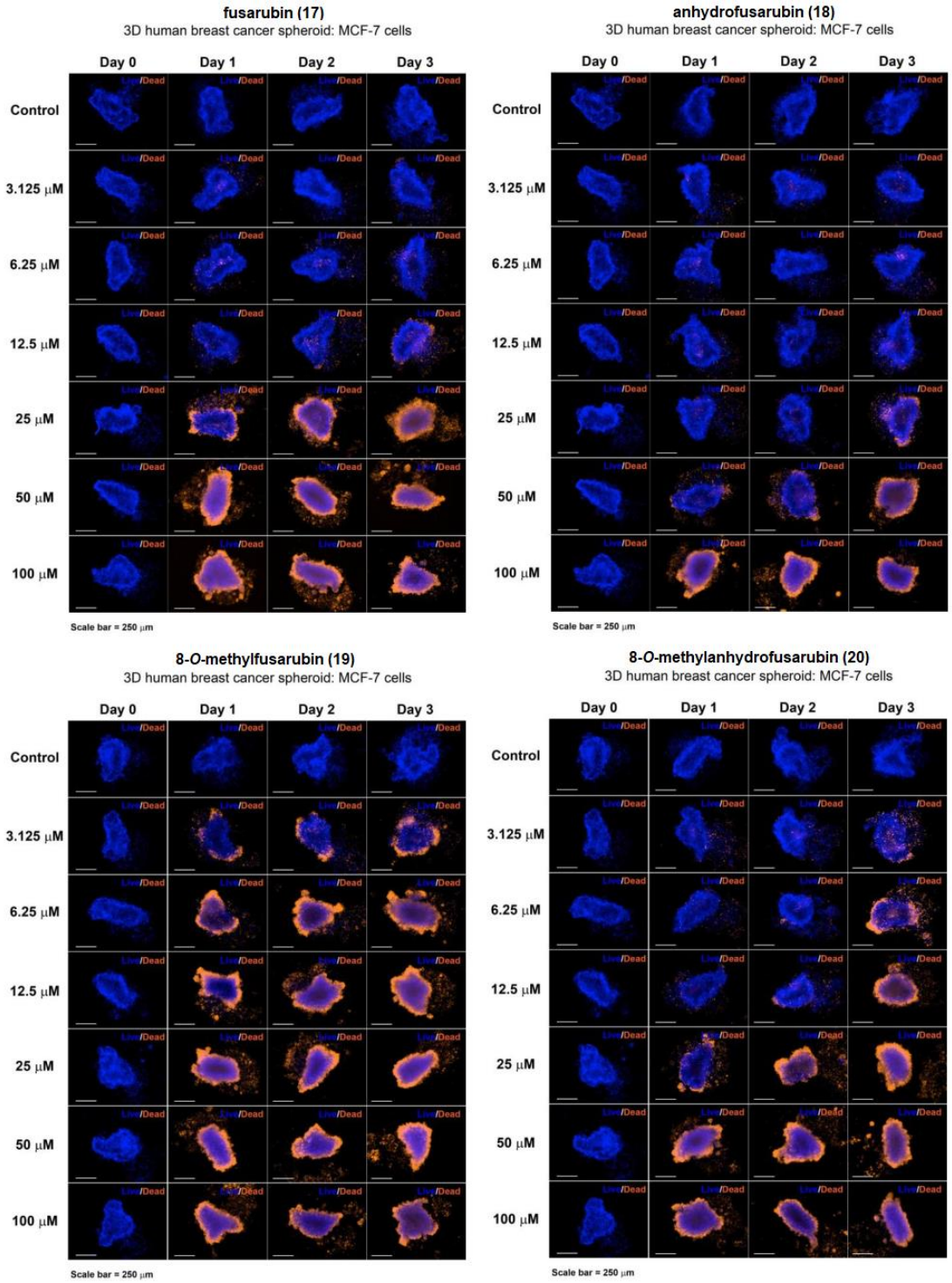

Additionally, compounds **17-20** were further evaluated for cytotoxic activities against other five human cancer cell lines including three cervical carcinoma (C33A, HeLa and SiHa), colorectal carcinoma (HCT116) and hepatoma (HepG2) cells as well as Vero cells by using MTT colorimetric assay (**Table 10**). Doxorubicin and cisplatin were used as positive controls in this MTT assay. Synthetic compounds **17-20** exhibited good antiproliferative effect against all tested cancer cell lines with IC_{50} in ranges of 4.73 up to >22.5 μM. However, the standard drug doxorubicin displayed more potent cytotoxic activities against five cancer cell lines compared with analogues **17-20**. Notable from this result, compounds **17-20** exhibited significant cytotoxic activity against colorectal carcinoma HCT116 (IC_{50} values of 4.73 to 6.08 μM) which could be further evaluated for development of anti-cancer drug from these pyranonaphthoquinone series.

Table 10. Cytotoxic activity of synthetic **17-20** against five human cancer cell lines and Vero cells.

cell lines	cytotoxicity, IC_{50} (μM)					
	17	**18**	**19**	**20**	doxorubicin	cisplatin
C33A	10.47±3.21	>22.5	7.3±1.08	13.15±0.35	0.14±0.03	7.44±0.77
HeLa	6.98±1.72	14.12±1.86	13.4 ±5.03	14.6±1.14	0.16±0.01	12.73±6.41
SiHa	6.05±1.74	14.75±3.36	19.8±0.54	6.87±0.33	0.185±0.02	15.33±4.28
HCT116	6.08±1.47	4.87±0.33	5.42±1.43	4.73±2.10	0.23±0.03	>25
HepG2	5.33±0.09	4.87±0.53	12.65±2.87	15.54±2.24	0.66±0.06	>25
Vero	9±0.67	17.92±5.46	17.83±4.73	13.63±2.21	>1	20.13±2.44

3.3 Conclusion

The total syntheses of fusarubin (**17**) and anhydrofusarubin (**18**) were achieved in 16 and 17 steps with overall yields of 3% and 2%, respectively, via the manipulation of oxidation state of the key intermediate from the syntheses of **19** and **20**. The same key Diels-Alder reaction and selective oxidation to construct naphthoquinone core as well as the formation of pyran ring via acetalization were also utilized in the syntheses of **17** and **18**. The oxidation state of the naphthoquinone intermediate could be switched via selective quinone reduction using $Na_2S_2O_4$ and protection of the hydroquinone moiety with acid-labile EOM groups. Subsequent deprotection of the benzyl group and oxidation with $PhI(OAc)_2$ generated the naphthoquinone nucleus with new oxidation state. Global deprotection and acetalization of naphthoquinone precursor under acidic conditions furnished fusarubin (**17**). Additionally, **18** can be prepared from **17** via acid-catalyzed dehydration. The evaluation of cytotoxic activity of synthetic compounds **17**-**20** by resazurin microplate assay (REMA) and MTT assay showed that **17**-**20** displayed potent cytotoxicity against human breast (MCF-7) cancer cells compared with doxorubicin standard drug. Among the four synthetic compounds tested, 8-*O*-methylfusarubin (**19**) displayed the highest cytotoxic activity against MCF-7 cancer cells. Moreover, from MTT assay, compounds **17**-**20** also exhibited good antiproliferative activity against five human cancer cell lines with IC_{50} ranges of 4.73 – >22.5 μM.

CHAPTER 4

EXPERIMENTAL

CHAPTER 4

EXPERIMENTAL

4.1 General Information

Unless otherwise stated, all reactions were performed under argon or nitrogen atmosphere in oven- or flamed-dried glassware. Solvents were used as received from suppliers or distilled prior to use using standard procedures. All other reagents were obtained from commercial sources and used without further purification. Column chromatography was performed on SiliaFlash® G60 Silica (60-200 μm, Silicycle). Thin-layer chromatography (TLC) was performed on SiliaPlate™R10011B-323 (Silicycle) or Silica gel 60 F_{254} (Merck). ^{1}H, ^{13}C and 2D NMR spectroscopic data were recorded on a 300 MHz Bruker FTNMR UltraShield spectrometer. ^{1}H NMR spectra are reported in ppm on the δ scale and referenced to the internal tetramethylsilane. The data are presented as follows: chemical shift, multiplicity (s = singlet, d = doublet, t = triplet, q = quartet, m = multiplet, br = broad), coupling constant(s) in hertz (Hz), and integration. Infrared (IR) spectra were recorded on a Perkin Elmer 783 FTS165 FT-IR spectrometer. The optical rotations were recorded on a JASCO P-2000 polarimeter. High-resolution mass spectra were obtained on a liquid chromatograph-mass spectrometer (Alliance 2690, LCT, Waters, Micromass). Melting points were measured using an ElectrothermalIA9200 digital melting point apparatus and are uncorrected.

4.2 Experimentals and Characterization Data

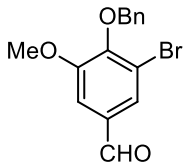

98

4-Benzyloxy-3-bromo-5-methoxybenzaldehyde (98). To a solution of 5-bromovanillin (**97**) (5.52 g, 23.9 mmol) in DMF (52 mL) were added K_2CO_3 (16.51 g, 119.5 mmol, 5.0 equiv) and BnBr (3.1 mL, 26.3 mmol, 1.1 equiv). The reaction mixture was stirred at rt overnight before H_2O (150 mL) was added. The aqueous phase was extracted with EtOAc (5x50 mL). The combined organic layers were washed with water (5x50 mL) and brine, dried over anhydrous Na_2SO_4 and concentrated *in vacuo*. Purification of the crude residue by column chromatography (hexanes–40% EtOAc/hexanes) yielded **98** (7.67 g, quantitative yield) as a white solid: R_f = 0.50 (20% EtOAc/hexanes); mp 52.0–55.0 °C; ^{1}H NMR (300 MHz, $CDCl_3$) δ 9.84 (s, 1H), 7.65 (d, *J* = 1.5 Hz, 1H), 7.54–7.51 (m, 2H), 7.41–7.31 (m, 4H), 5.16 (s, 2H), 3.94 (s, 3H); ^{13}C NMR (75 MHz, $CDCl_3$) δ 189.89, 154.26, 150.49, 136.54, 133.11, 128.68, 128.53, 128.43, 128.39, 118.40, 110.19, 74.97, 56.24; IR (thin film) 3065, 2940, 2845, 1697, 1278, 1139, 1044 cm^{-1}; HRMS (ESI) *m/z* calcd for $C_{15}H_{13}BrNaO_3$ $(M + Na)^+$ 342.9940, found 342.9941. The ^{1}H and ^{13}C spectral data of **98** matched those previously described (Giles *et al*., 2006).

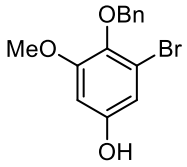

99

4-Benzyloxy-3-bromo-5-methoxyphenol (99). To a solution of 4-benzyloxy-3-bromo-5-methoxybenzaldehyde (**98**) (2.57 g, 8.0 mmol) in CH_2Cl_2 (16 mL) was added *m*-CPBA (70%, 2.37 g, 9.6 mmol, 1.2 equiv). The reaction mixture was stirred at rt overnight before EtOAc (50 mL) was added. The organic layer was washed with saturated aqueous $NaHCO_3$ (2x50 mL), brine, dried over anhydrous Na_2SO_4 and concentrated *in vacuo*. The crude

residue was diluted with MeOH (16 mL), followed by addition of a solution of 10% KOH in H_2O (5.0 mL). The reaction mixture was stirred further at rt for 15 min before 50 mL of EtOAc was added. The organic layer was washed with brine (2x50 mL) and dried over anhydrous Na_2SO_4, filtered and concentrated *in vacuo*. Purification of the crude residue by column chromatography (10–20% EtOAc/hexanes) yielded **99** (2.14 g, 86%) as a colorless oil: R_f = 0.56 (40% EtOAc/hexanes); ^{1}H NMR (300 MHz, $CDCl_3$) δ 7.55–7.52 (m, 2H), 7.40–7.29 (m, 3H), 6.58 (d, *J* = 2.7 Hz, 1H), 6.38 (d, *J* = 2.7 Hz, 1H), 5.36 (brs, 1H), 4.94 (s, 2H), 3.79 (s, 3H); ^{13}C NMR (75 MHz, $CDCl_3$) δ 154.20, 153.18, 138.54, 136.74, 128.89, 128.44, 128.38, 117.84, 110.93, 100.36, 75.45, 56.02; IR (thin film) 3367, 2942, 1584, 1472, 1215, 1042 cm^{-1}; HRMS (ESI) *m/z* calcd for $C_{14}H_{13}BrNaO_3$ $(M + Na)^+$ 330.9940, found 330.9939. The ^{1}H and ^{13}C spectral data of **99** matched those previously described (Giles *et al*., 2006).

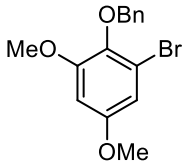

100

2-Benzyloxy-3,5-dimethoxybromobenzene (100). To a solution of 4-benzyloxy-3-bromo-5-methoxyphenol (**99**) (2.35 g, 7.6 mmol) in acetone (15 mL) were added K_2CO_3 (3.15 g, 22.8 mmol, 3.0 equiv) and iodomethane (950 µL, 15.2 mmol, 2.0 equiv). The reaction mixture was heated at reflux overnight. The white suspension was cooled to rt before H_2O (70 mL) was added and extracted with EtOAc (3x50 mL). The combined organic layers were washed with brine, dried over anhydrous Na_2SO_4 and concentrated *in vacuo*. Purification of the crude residue by column chromatography (20% EtOAc/hexanes) yielded **100** (2.37 g, 97%) as a yellow oil: R_f = 0.60 (20% EtOAc/hexanes); ^{1}H NMR (300 MHz, $CDCl_3$) δ 7.55–7.52 (m, 2H), 7.39–7.28 (m, 3H), 6.64 (d, *J* = 3.0 Hz, 1H), 6.44 (d, *J* = 3.0 Hz, 1H), 4.94 (s, 2H), 3.79 (s, 3H), 3.73 (s, 3H); ^{13}C NMR (75 MHz, $CDCl_3$) δ 156.57, 154.34, 139.60, 137.35, 128.52, 128.32, 128.04, 117.97, 107.99, 100.04, 74.91, 56.06, 55.76; IR (thin film) 2939, 1599, 1571, 1487, 1211, 1149, 1037 cm^{-1}; HRMS (ESI)

m/z calcd for $C_{15}H_{15}BrNaO_3$ $(M + Na)^+$ 345.0097, found 345.0095. The ^1H and ^{13}C spectral data of **100** matched those previously described (Giles *et al*., 2006).

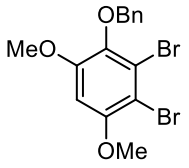

101

1,2-Dibromo-3-benzyloxy-4,6-dimethoxybenzene (101). To a solution of 2-benzyloxy-3,5-dimethoxybromobenzene (**100**) (3.95 g, 12.2 mmol) in MeCN (40 mL) were added NH_4OAc (95.3 mg, 1.2 mmol, 0.1 equiv) and *N*-bromosuccinimide (2.29 g, 12.9 mmol, 1.05 equiv). The reaction mixture was stirred at rt for 1.5 h before being concentrated *in vacuo*. The crude residue was added H_2O (100 mL) and extracted with EtOAc (3x50 mL). The combined organic layers were washed with brine, dried over anhydrous Na_2SO_4 and concentrated *in vacuo*. Purification of the crude residue by column chromatography (20–60% EtOAc/hexanes) yielded **101** (4.89 g, quantitative yield) as a yellow solid: R_f = 0.39 (20% EtOAc/hexanes); mp 104.8–106.0 °C; ^1H NMR (300 MHz, $CDCl_3$) δ 7.53–7.51 (m, 2H), 7.39–7.28 (m, 3H), 6.49 (s, 1H), 4.92 (s, 2H), 3.83 (s, 6H); ^{13}C NMR (75 MHz, $CDCl_3$) δ 153.79, 153.22, 140.48, 137.00, 128.51, 128.37, 128.17, 122.62, 105.51, 97.35, 74.93, 56.98, 56.46; IR (thin film) 2938, 1560, 1458, 1367, 1220, 1035 cm^{-1}; HRMS (ESI) *m/z* calcd for $C_{15}H_{14}Br_2NaO_3$ $(M + Na)^+$ 422.9202, found 422.9199. The ^1H and ^{13}C spectral data of **101** matched those previously described (Giles *et al*., 2006).

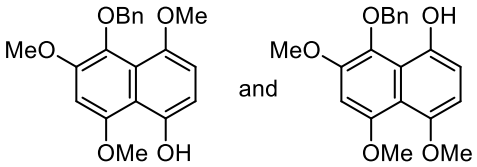

103 **104**

Naphthols 103 and 104. To a solution of dibromobenzene **101** (2.0 g, 5.0 mmol) and 2-methoxyfuran (**102**) (600 µL, 6.5 mmol, 1.3 equiv) in dry THF (12.5 mL) at –78 °C was added dropwise of *n*-BuLi (*ca*. 1.0 M solution in hexanes, 5.0 mL, 5.0 mmol, 1.0 equiv). The reaction mixture was stirred at –78 °C for 3.5 h before being warmed to rt and some

of H_2O was then added. The aqueous phase was extracted with EtOAc (4x30 mL). The combined organic layers were washed with brine, dried over anhydrous Na_2SO_4 and concentrated *in vacuo*. Purification of the crude residue by column chromatography (10–30% EtOAc/hexanes) yielded an inseparable mixture of **103** and **104** (1.04 g, 62%) as a brown solid: R_f = 0.46 (40% EtOAc/hexanes); mp 106.6–108.0 °C; ^{1}H NMR (300 MHz, $CDCl_3$) δ 9.69 (s, 1H), 9.14 (s, 1.3H), 7.56 (d, *J* = 7.2 Hz, 2.8H), 7.51–7.48 (m, 2H), 7.39–7.26 (m, 7H), 6.79–6.72 (m, 2.4H), 6.66–6.62 (m, 3.4H), 6.58 (s, 1.4H), 5.08 (s, 2H), 4.91 (s, 2.8H), 3.92–3.86 (m, 14.4H), 3.81 (s, 3.2H), 3.74 (s, 4.2H); ^{13}C NMR (75 MHz, $CDCl_3$) δ 154.88, 152.98, 149.97, 149.93, 148.88, 148.55, 147.82, 147.47, 138.57, 137.63, 135.92, 135.46, 129.07, 128.84, 128.77, 128.37, 128.28, 127.63, 123.71, 120.52, 114.97, 112.68, 110.97, 110.65, 107.95, 107.53, 97.42, 96.58, 76.94, 76.17, 57.80, 57.65, 57.59, 57.20, 56.89, 56.50; IR (thin film) 3393, 2936, 1609, 1361, 1064, 1040 cm^{-1}; HRMS (ESI) *m/z* calcd for $C_{20}H_{20}NaO_5$ $(M + Na)^+$ 363.1203, found 363.1202.

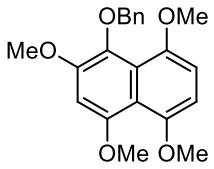

96

1-Benzyloxy-2,4,5,8-tetramethoxynaphthalene (96). To a solution of mixture of naphthols **103** and **104** (3.44 g, 10.1 mmol) in THF (34 mL) at 0 °C was added NaH (60% in mineral oil, 1.02 g, 25.6 mmol, 2.5 equiv). The dark suspension was stirred at 0 °C for 1 h before iodomethane (3.2 mL, 51.4 mmol, 5.0 equiv) was added. The reaction mixture was stirred from 0 °C to rt overnight before being re-cooled to 0 °C then 60 mL of H_2O was added. The aqueous phase was extracted with EtOAc (3x50 mL). The combined organic layers were washed with brine, dried over anhydrous Na_2SO_4 and concentrated *in vacuo*. Purification of the crude residue by column chromatography (10–30% EtOAc/hexanes) yielded naphthalene **96** (2.88 g, 80%) as a brown solid: R_f = 0.49 (40% EtOAc/hexanes); mp 112.6–113.5 °C; ^{1}H NMR (300 MHz, $CDCl_3$) δ 7.56–7.41 (m, 2H), 7.41–7.28 (m, 3H), 6.77 (d, *J* = 9.0 Hz, 1H), 6.75 (s, 1H), 6.64 (d, *J* = 9.0 Hz, 1H), 4.95 (s, 2H), 3.93 (s, 6H), 3.87 (s, 3H), 3.78 (s, 3H); ^{13}C NMR (75 MHz, $CDCl_3$) δ 154.14, 151.54,

150.55, 150.16, 138.66, 137.05, 128.28, 128.21, 127.51, 124.46, 115.68, 108.74, 105.33, 99.19, 76.12, 57.54, 57.54, 57.41, 57.36; IR (thin film) 2935, 2837, 1598, 1358, 1259, 1070 cm^{-1}; HRMS (ESI) *m/z* calcd for $C_{21}H_{22}NaO_5$ $(M + Na)^+$ 377.1359, found 377.1359. The ^1H and ^{13}C spectral data of **96** matched those previously described (Giles *et al*., 2006).

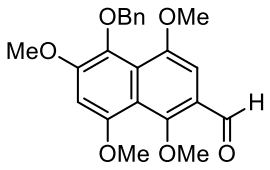

107

Naphthaldehyde 107. *N*,*N*-dimethylformamide (230 µL, 2.9 mmol) was added dropwise into a solution of oxalyl chloride (250 µL, 2.9 mmol) in CH_2Cl_2 (4 mL) at 0 °C. After 30 min, a solution of naphthalene **96** (690.0 mg, 2.0 mmol) in CH_2Cl_2 (6 mL) was added and the reaction mixture was stirred from 0 °C to rt overnight. The brown reaction mixture was then slowly quenched with saturated aqueous $NaHCO_3$ (20 mL) to give a yellow solution, diluted with H_2O (30 mL) and extracted with EtOAc (4x30 mL). The combined organic layers were washed with brine, dried over anhydrous Na_2SO_4 and concentrated *in vacuo*. Purification of the crude residue by column chromatography (20–30% EtOAc/hexanes) yielded naphthaldehyde **107** (638.0 mg, 86%) as a yellow solid: R_f = 0.38 (40% EtOAc/hexanes); mp 131.3–134.1 °C; ^1H NMR (300 MHz, $CDCl_3$) δ 10.49 (s, 1H), 7.57–7.54 (m, 2H), 7.43–7.33 (m, 3H), 7.13 (s, 1H), 6.81 (s, 1H), 4.94 (s, 2H), 4.06 (s, 3H), 4.00 (s, 3H), 3.92 (s, 3H), 3.88 (s, 3H); ^{13}C NMR (75 MHz, $CDCl_3$) δ 189.73, 157.94, 154.82, 153.87, 152.54, 138.28, 137.37, 128.28, 128.07, 127.66, 127.66, 123.88, 116.21, 101.29, 97.84, 76.12, 65.46, 56.98, 56.80, 56.30; IR (thin film) 2934, 1668, 1593, 1362, 1069 cm^{-1}; HRMS (ESI) *m/z* calcd for $C_{22}H_{22}NaO_6$ $(M + Na)^+$ 405.1309, found 405.1308.

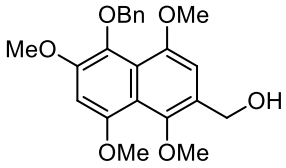

108

Naphthyl alcohol 108. To a solution of naphthaldehyde **107** (2.51 g, 6.6 mmol) in MeOH/THF (1:1, 28 mL) at 0 °C was added a single portion of $NaBH_4$ (495.0 mg, 13.1 mmol, 2.0 equiv). The reaction mixture was stirred further for 30 min at 0 °C before quenched with 10 mL of saturated aqueous NH_4Cl. The white suspension was added 50 mL of H_2O and extracted with EtOAc (3x40 mL). The combined organic layers were washed with brine, dried over anhydrous Na_2SO_4 and concentrated *in vacuo* to yield alcohol **108** (2.50 g, 99% yield) as a pale yellow solid: R_f = 0.38 (60% EtOAc/hexanes); mp 142.0–143.4 °C; ^{1}H NMR (300 MHz, $CDCl_3$) δ 7.56 (d, *J* = 7.5 Hz, 2H), 7.41–7.28 (m, 3H), 6.84 (s, 1H), 6.73 (s, 1H), 4.91 (s, 2H), 4.78 (s, 2H), 3.95 (s, 3H), 3.92 (s, 3H), 3.77 (s, 3H), 3.73 (s, 3H), 2.88 (brs, 1H); ^{13}C NMR (75 MHz, $CDCl_3$) δ 152.94, 152.27, 150.24, 147.39, 138.56, 137.29, 128.38, 128.24, 128.21, 127.56, 123.74, 117.48, 107.81, 98.66, 76.13, 62.59, 60.79, 57.60, 56.75, 56.58; IR (thin film) 3447, 2931, 2838, 1522, 1356, 1069 cm^{-1}; HRMS (ESI) *m/z* calcd for $C_{22}H_{24}NaO_6$ $(M + Na)^+$ 407.1465, found 407.1464.

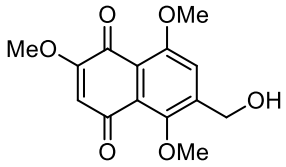

113

Naphthoquinone 113. To a solution of naphthalene **108** (131.5 mg, 0.34 mmol) in MeCN (3.6 mL) at 0 °C was added dropwise a solution of cerium ammonium nitrate (377.1 mg in 1:1 of MeCN/H_2O 4.6 mL, 0.68 mmol, 2.0 equiv). The reaction mixture was stirred for 30 min before 30 mL of H_2O was added and extracted with EtOAc (5x10 mL). The combined organic layers were washed with brine, dried over anhydrous Na_2SO_4 and concentrated *in vacuo*. Purification of the crude residue by column chromatography (100% EtOAc) yielded naphthoquinone **113** (47.4 mg, 50%) as an orange solid: R_f = 0.39 (100% EtOAc); mp 218.8–219.3 °C; ^{1}H NMR (300 MHz, DMSO-d_6) δ 7.48 (s, 1H), 6.03 (s, 1H), 5.44 (s, 1H),

4.60 (s, 2H), 3.84 (s, 3H), 3.74 (s, 3H), 3.63 (s, 3H); ^{13}C NMR (75 MHz, DMSO-d_6) δ 184.37, 178.18, 159.88, 156.66, 150.00, 147.52, 124.57, 118.02, 117.07, 109.90, 61.46, 58.38, 56.72, 56.72; IR (thin film) 3489, 2914, 2848, 1651, 1589, 1067 cm^{-1}; HRMS (ESI) *m/z* calcd for $C_{14}H_{14}NaO_6$ $(M + Na)^+$ 304.0683, found 304.0685.

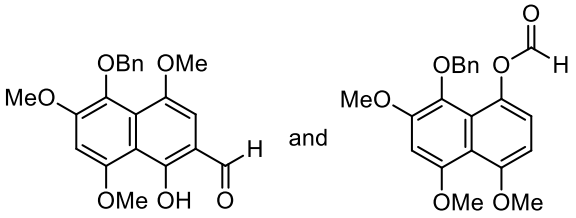

115 **116**

N,*N*-dimethylformamide (310 µL, 4.0 mmol) was added dropwise into a solution of oxalyl chloride (340 µL, 4.0mmol) in CH_2Cl_2 (4 mL) at 0 °C. After 35 min, a solution of naphthols **103** and **104** (677.1 mg, 2.0 mmol) in CH_2Cl_2 (6 mL) was added and the reaction mixture was stirred from 0 °C to rt overnight. The brown reaction mixture was then slowly quenched with saturated aqueous $NaHCO_3$ (30 mL) to give a yellow solution, diluted with H_2O (30 mL) and extracted with EtOAc (4x30 mL). The combined organic layers were washed with brine, dried over anhydrous Na_2SO_4 and concentrated *in vacuo*. Purification of the crude residue by column chromatography (15–30% EtOAc/hexanes) yielded naphthaldehyde **115** (305.1 mg, 42%) as a yellow solid and naphthyl formate **116** (122.5 mg, 17%) as a brown solid.

Naphthaldehyde 115. R_f = 0.30 (40% EtOAc/hexanes); mp 118.5–120.0 °C; ^{1}H NMR (300 MHz, $CDCl_3$) δ 10.47 (brs, 1H), 10.40 (s, 1H), 7.55–7.52 (m, 2H), 7.42–7.29 (m, 3H), 7.02 (s, 1H), 6.67 (s, 1H), 4.90 (s, 2H), 4.04 (s, 3H), 3.94 (s, 3H), 3.80 (s, 3H); ^{13}C NMR (75 MHz, $CDCl_3$) δ 189.45, 156.75, 155.29, 153.98, 148.54, 138.14, 137.73, 128.28, 128.16, 127.71, 127.42, 115.15, 111.67, 103.28, 96.39, 76.13, 56.92, 56.88, 56.64; IR (thin film) 3320, 2943, 2846, 1605, 1367, 1199 cm^{-1}; HRMS (ESI) *m/z* calcd for $C_{21}H_{20}NaO_6$ $(M + Na)^+$ 391.1152, found 391.1151.

Naphthyl formate 116. R_f = 0.45 (40% EtOAc/hexanes); mp 112.8–113.5 °C; ^{1}H NMR (300 MHz, $CDCl_3$) δ 7.96 (s, 1H), 7.55–7.54 (m, 2H), 7.40–7.28 (m, 3H), 7.00 (d, *J*= 8.4 Hz, 1H), 6.71 (s, 1H), 6.62 (d, *J*= 8.4 Hz, 1H), 4.91 (s, 2H), 3.90 (s, 9H); ^{13}C NMR (75

MHz, $CDCl_3$) δ 160.43, 156.07, 154.92, 150.86, 137.81, 137.45, 134.59, 128.62, 128.36, 127.94, 124.69, 120.81, 114.76, 103.33, 98.24, 76.05, 57.44, 56.77, 56.64; IR (thin film) 2940, 1742, 1601, 1359, 1249, 1118 cm^{-1}; HRMS (ESI) *m/z* calcd for $C_{21}H_{20}NaO_6$ $(M + Na)^+$ 391.1152, found 391.1152.

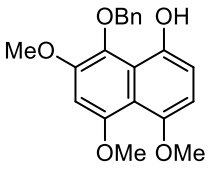

104

Naphthol 104. To a solution of naphthyl formate **116** (60.3 mg, 0.16 mmol) in MeOH (0.5 mL) was added dropwise a solution of 10% KOH in H_2O (100 µL). The reaction mixture was stirred at rt for 30 min before being diluted with EtOAc (20 mL), washed with brine (2x10mL), dried over anhydrous Na_2SO_4 and concentrated *in vacuo*. Purification of the crude residue by column chromatography (20% EtOAc/hexanes) yielded naphthol **104** (39.1 mg, 70%) as a brown solid: R_f = 0.46 (40% EtOAc/hexanes); mp 100.8–102.8 °C; ^1H NMR (300 MHz, $CDCl_3$) δ 9.66 (s, 1H), 7.54–7.51 (m, 2H), 7.43–7.34 (m, 3H), 6.75 (d, *J* = 8.4 Hz, 1H), 6.68 (s, 1H), 6.68 (d, *J* = 8.4 Hz, 1H), 5.12 (s, 2H), 4.01 (s, 3H), 3.95 (s, 3H), 3.87 (s, 3H); ^{13}C NMR (75 MHz, $CDCl_3$) δ 154.85, 149.91, 147.79, 147.46, 135.87, 135.58, 129.06, 128.82, 128.75, 120.52, 115.03, 110.65, 107.60, 97.57, 77.12, 57.68, 57.27, 56.99; IR (thin film) 3321, 2917, 2848, 1607, 1251, 1038 cm^{-1}; HRMS (ESI) *m/z* calcd for $C_{20}H_{20}NaO_5$ $(M + Na)^+$ 363.1203, found 363.1203.

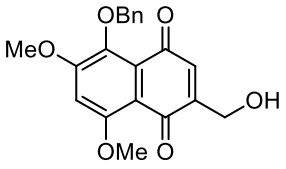

114

Naphthoquinone 114. From naphthaldehyde **115**: To a solution of naphthaldehyde **115** (303.2 mg, 0.8 mmol) in MeOH/THF (1:1, 3.6 mL) at 0 °C was added a single portion of $NaBH_4$ (68.8 mg, 1.6 mmol). The reaction mixture was stirred further for 30 min then quenched with saturated aqueous NH_4Cl (10 mL). The white suspension was added H_2O

(30 mL) and extracted with EtOAc (3x10 mL). The combined organic layer were washed with brine, dried over anhydrous Na_2SO_4 and concentrated *in vacuo* to yield naphthyl alcohol **117** (310.0 mg, quantitative yield) as a pale brown solid. Naphthyl alcohol **117** (310.0 mg, 0.8 mmol) was diluted with MeCN (9 mL) and was then cooled to 0 °C. The yellow solution was added dropwise CAN solution (924.5 mg in 5.5 mL of 1:1 MeCN/H_2O). The reaction mixture was stirred further for 30 min before H_2O (40 mL) was added. The aqueous phase was extracted with EtOAc (4x10 mL). The combined organic layers were washed with brine, dried over anhydrous Na_2SO_4 and concentrated *in vacuo*. Purification of the crude residue by column chromatography (80% EtOAc/hexanes) yielded naphthoquinone **114** (291.6 mg, 94% over 2 steps) as an orange solid.

From naphthalene **108**: A solution of naphthalene **108** (921.7 mg, 2.4 mmol) in MeCN/H_2O (9:1, 24 mL) was heated at 50 °C before a single portion of $PhI(OAc)_2$ (801.3 mg, 2.4 mmol, 1.0 equiv) was added. After 1 min, the reaction mixture then turned to an orange solution. The reaction flask was immediately removed from oil bath before 50 mL of H_2O was added and then extracted with EtOAc (4x30 mL). The combined organic layers were washed with brine, dried over anhydrous Na_2SO_4 and concentrated *in vacuo*. Purification of the crude residue by column chromatography (60–90% EtOAc/hexanes) yielded naphthoquinone **114** (612.0 mg, 75%) as an orange solid: R_f = 0.45 (100% EtOAc); mp 151.6–153.0 °C; ^{1}H NMR (300 MHz, $CDCl_3$) δ 7.61–7.59 (m, 2H), 7.42–7.30 (m, 3H), 6.76 (s, 1H), 6.71 (s, 1H), 4.97 (s, 2H), 4.56 (s, 2H), 3.98 (s, 3H), 3.94 (s, 3H), 2.76 (brs, 1H); ^{13}C NMR (75 MHz, $CDCl_3$) δ 184.90, 183.81, 160.25, 158.39, 149.57, 141.87, 137.08, 132.80, 128.80, 128.33, 128.15, 126.87, 112.95, 100.94, 75.21, 60.08, 56.53, 56.23; IR (thin film) 3458, 2943, 1648, 1458, 1353, 1217 cm^{-1}; HRMS (ESI) *m/z* calcd for $C_{20}H_{18}NaO_6$ $(M + Na)^+$ 377.0996, found 377.0993.

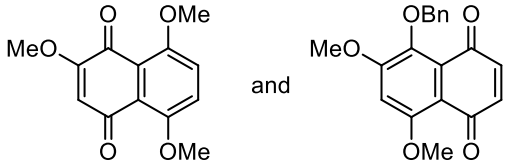

118 **119**

A solution of naphthalene **96** (29.6 mg, 0.08 mmol) in MeCN/H_2O (9:1, 1 mL) was heated at 50 °C before a single portion of $PhI(OAc)_2$ (36.4 mg, 0.08 mmol, 1.0 equiv) was added. After 1 min, the reaction flask was removed from an oil bath before 10 mL of H_2O was added and extracted with EtOAc (3x5 mL). The combined organic layers were washed with brine, dried over anhydrous Na_2SO_4 and concentrated *in vacuo*. Purification of the crude residue by column chromatography (40–60% EtOAc/hexanes) yielded naphthoquinone **118** (13.4 mg, 65%) and naphthoquinone **119** (4.3 mg, 16%).

Naphthoquinone 118: orange solid; R_f = 0.50 (40% acetone/hexanes); mp 169.0–171.0 °C; ^{1}H NMR (300 MHz, $CDCl_3$) δ 7.34 (d, *J* = 9.0 Hz, 1H), 7.28 (d, *J* = 9.0 Hz, 1H), 6.02 (s, 1H), 3.96 (s, 6H), 3.84 (s, 3H); ^{13}C NMR (75 MHz, $CDCl_3$) δ 184.80, 179.40, 159.32, 154.38, 153.39, 121.34, 120.88, 120.39, 119.69, 110.03, 57.02, 56.92, 56.24; IR (thin film) 2925, 2849, 1641, 1267, 1243, 1022 cm^{-1}. ^{1}H and ^{13}C NMR spectral data of **118** matched those previous report (Brötz *et al*., 2014).

Naphthoquinone 119: orange solid; R_f = 0.45 (50% acetone/hexanes); mp 147.0–149.5 °C; ^{1}H NMR (300 MHz, $CDCl_3$) δ 7.62–7.60 (m, 2H), 7.42–7.31 (m, 3H), 6.76 (s, 1H), 6.74 (s, 2H), 5.00 (s, 2H), 4.00 (s, 3H), 3.96 (s, 3H); ^{13}C NMR (75 MHz, $CDCl_3$) δ 185.07, 183.41, 160.04, 158.20, 142.03, 139.64, 137.59, 137.11, 128.76, 128.35, 128.13, 126.89, 113.11, 101.28, 75.26, 56.71, 56.25; IR (thin film) 2931, 1650, 1352, 1258, 1220, 1036 cm^{-1}; HRMS (ESI) *m/z* calcd for $C_{19}H_{16}NaO_5$ $(M + Na)^+$ 347.0895, found 347.0887.

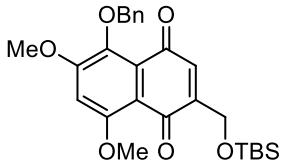

120

Silyl ether 120. To a solution of alcohol **114** (1.43 g, 4.0 mmol) in CH_2Cl_2 (20 mL) were added imidazole (551.2 mg, 8.1 mmol, 2.0 equiv) and TBSCl (917.7 mg, 6.1 mmol, 1.5 equiv). The reaction mixture was stirred at rt overnight before H_2O (60 mL) was added and extracted with EtOAc (4x30 mL). The combined organic layers were washed with brine, dried over anhydrous Na_2SO_4 and concentrated *in vacuo*. Purification of the crude residue by column chromatography (10–80% EtOAc/hexanes) yielded silyl ether **120** (1.78 g, 94%) as an orange solid: R_f = 0.56 (60% EtOAc/hexanes); mp145.5–147.5 °C; ^{1}H NMR (300 MHz, $CDCl_3$) δ 7.62–7.59 (m, 2H), 7.41–7.28 (m, 3H), 6.84 (d, *J* = 1.5 Hz, 1H), 6.71 (s, 1H), 4.99 (s, 2H), 4.64 (s, 2H), 3.96 (s, 3H), 3.93 (s, 3H), 0.94 (s, 9H), 0.10 (s, 6H); ^{13}C NMR (75 MHz, $CDCl_3$) δ 185.12, 183.48, 160.15, 158.27, 150.75, 141.96, 137.18, 132.22, 128.76, 128.32, 128.08, 127.09, 113.28, 100.93, 75.19, 59.58, 56.59, 56.22, 25.88, 18.32, –5.45; IR (thin film) 2930, 1653, 1217, 1103, 1046 cm^{-1}; HRMS (ESI) *m/z* calcd for $C_{26}H_{32}NaO_6Si$ $(M + Na)^+$ 491.1860, found 491.1858.

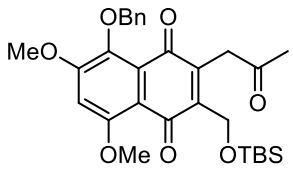

121

Acetonylnaphthoquinone 121. A suspension of naphthoquinone **120** (1.78 g, 3.8 mmol) and acetylmethylpyridinium chloride (**78**) (732.7 mg, 4.3 mmol, 1.1 equiv) in MeCN (65 mL) was heated at 60 °C for 30 min. The reaction mixture was then cooled to rt before a solution of Et_3N (585 µL in 6 mL of MeCN, 4.2 mmol, 1.1 equiv) was added. The reaction mixture was stirred at rt overnight before H_2O (80 mL) was added and extracted with EtOAc (4x30 mL). The combined organic layers were washed with brine, dried over anhydrous Na_2SO_4 and concentrated *in vacuo* to yield acetonylnaphthoquinone **121** (1.99 g, quantitative yield) as an orange solid: R_f = 0.59 (60% EtOAc/hexanes); mp 97.6–98.3

°C; ^{1}H NMR (300 MHz, $CDCl_3$) δ 7.56 (d, *J* = 6.9 Hz, 2H), 7.38–7.27 (m, 3H), 6.72 (s, 1H), 4.95 (s, 2H), 4.68 (s, 2H), 3.95 (s, 5H), 3.89 (s, 3H), 2.27 (s, 3H), 0.89 (s, 9H), 0.09 (s, 6H); ^{13}C NMR (75 MHz, $CDCl_3$) δ 203.97, 184.93, 182.28, 159.57, 157.80, 145.43, 141.88, 141.78, 137.30, 128.67, 128.21, 127.96, 126.93, 113.27, 101.49, 75.31, 57.38, 56.70, 56.18, 41.12, 30.08, 25.90, 18.31, –5.39; IR (thin film) 2930, 1653, 1350, 1246, 1215, 1080 cm^{-1}; HRMS (ESI) *m/z* calcd for $C_{29}H_{36}NaO_7Si$ $(M + Na)^+$ 547.2123, found 547.2123.

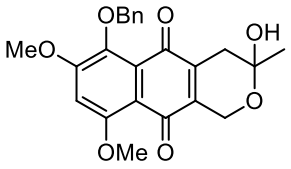

122

Pyranonaphthoquinone 122. From acetonylnaphthoquinone **121**: To a solution of acetonyl naphthoquinone **121** (40.1 mg, 0.08 mmol) in MeCN (2 mL) was added a solution of 1M HCl (0.7 mL). The reaction mixture was stirred at rt for 1 h before 20 mL of H_2O was added and extracted with EtOAc (3x10 mL). The combined organic layers were washed with brine, dried over anhydrous Na_2SO_4 and concentrated *in vacuo*. Purification of the crude residue by column chromatography (60–80% EtOAc/hexanes) yielded **122** (23.2 mg, 74%) as an orange solid.

From naphthoquinone **120**: A solution of naphthoquinone **120** (154.6 mg, 0.3 mmol) and acetylmethylpyridinium chloride (62.9 mg, 0.4mmol, 1.1 equiv) in MeCN (8 mL) was heated at 60 °C for 30 min. The reaction mixture was then cooled to rt and a solution of Et_3N (55 µL in 0.6 mL of MeCN, 0.4 mmol, 1.1 equiv) was added. The reaction mixture was left stirred at rt overnight. A solution of 1M HCl (4 mL) was then slowly added and the reaction mixture was stirred further for 1 h before H_2O (40 mL) was added. The aqueous phase was extracted with EtOAc (3x15 mL) and the combined organic layers were washed with brine, dried over anhydrous Na_2SO_4 and concentrated *in vacuo*. Purification of the crude residue by column chromatography (60–80% EtOAc/hexanes) yielded **122** (114.6 mg, 85%) as an orange solid: R_f = 0.47 (100% EtOAc); mp 164.5–166.2 °C; ^{1}H NMR (300 MHz $CDCl_3$) δ 7.58–7.56 (m, 2H), 7.40–7.30 (m, 3H), 6.57 (s, 1H), 4.88 (m, 2H), 4.63 (s, 2H), 3.91 (s, 5H), 3.84 (s, 3H), 2.79 (d, *J* = 18.6 Hz, 1H), 2.48 (d, *J* = 18.6

Hz, 1H), 1.56 (s, 3H); ^{13}C NMR (75 MHz, $CDCl_3$) δ 183.08, 181.49, 159.95, 158.11, 141.96, 141.56, 138.42, 137.11, 128.93, 128.26, 128.12, 126.31, 112.16, 101.07, 94.23, 74.97, 57.98, 56.40, 56.06, 32.24, 28.72; IR (thin film) 3446, 2940, 1653, 1354, 1263, 1017 cm^{-1}; HRMS (ESI) *m/z* calcd for $C_{23}H_{22}NaO_7$ $(M + Na)^+$ 433.1258, found 433.1256.

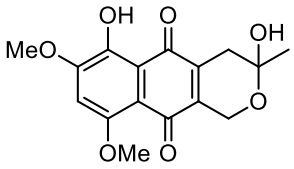

8-*O*-methylfusarubin (**19**)

8-*O*-methylfusarubin (19). To a solution of benzyl ether **122** (114.6 mg, 0.3 mmol) in EtOAc (6 mL) was added $Pd(OH)_2$ (9.6 mg, 0.02 mmol, 0.05 equiv). The reaction mixture was stirred at rt under H_2 atmosphere for 30 min before being filtered through a pad of Celite, washed with EtOAc and concentrated *in vacuo*. Purification of the crude residue by column chromatography (80% EtOAc/hexanes) yielded 8-*O*-methylfusarubin (**19**) (54.0 mg, 60%) as a red solid: R_f = 0.37 (100% EtOAc); mp 138.6–140.7 °C; ^{1}H NMR (300 MHz, DMSO-d_6) δ 12.89 (s, 1H), 6.90 (s, 1H), 5.99 (s, 1H), 4.40–4.32 (m, 2H), 3.92 (s, 3H), 3.85 (s, 3H), 2.51 (d, *J* = 18.3 Hz, 1H), 2.31 (d, *J* = 18.3 Hz, 1H), 1.41 (s, 3H); ^{13}C NMR (75 MHz, DMSO-d_6) δ 189.34, 179.14, 156.04, 155.54, 147.90, 145.02, 137.21, 113.82, 108.86, 104.10, 93.56, 58.50, 56.93, 56.82, 32.11, 28.76; IR (thin film) 3221, 2917, 2849, 1618, 1468, 1266 cm^{-1}; HRMS (ESI) *m/z* calcd for $C_{16}H_{16}NaO_7$ $(M + Na)^+$ 343.0794, found 343.0793.

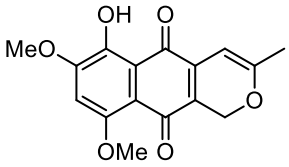

8-*O*-methylanhydrofusarubin (**20**)

8-*O*-methylanhydrofusarubin (20). To a solution of 8-*O*-methylfusarubin (**19**) (35.9 mg, 0.1 mmol) in toluene (55 mL) was added TsOH (1.0 mg, 0.05 equiv). The reaction mixture was heated at 105 °C for 30 min before being cooled to rt and 100 mL of H_2O was added. The aqueous phase was extracted with EtOAc (4x30 mL). The combined organic layers

were washed with brine, dried over anhydrous Na_2SO_4 and concentrated *in vacuo*. Purification of the crude residue by column chromatography (60%–80% EtOAc/hexanes) yielded 8-*O*-methylanhydrofusarubin (**20**) (23.4 mg, 69%) as black needles: R_f = 0.40 (100% EtOAc); mp 144.0–146.0 °C; ^{1}H NMR (300 MHz, $CDCl_3$) δ 13.14 (s, 1H), 6.73 (s, 1H), 5.85 (s, 1H), 5.12 (s, 2H), 4.00 (s, 3H), 3.98 (s, 3H), 2.01 (s, 3H) ; ^{13}C NMR (75 MHz, $CDCl_3$) δ187.63, 179.41, 163.43, 155.21, 155.11, 148.70, 135.74, 126.45, 114.37, 110.76, 103.29, 92.99, 63.45, 56.95, 56.34, 20.08; IR (thin film) 2923, 1582, 1470, 1433, 1380 cm^{-1}; HRMS (ESI) *m/z* calcd for $C_{16}H_{14}NaO_6$ $(M + Na)^+$ 325.0683, found 325.0680.

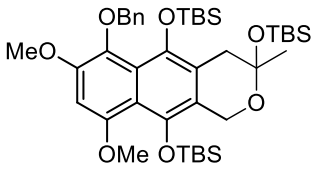

126

Pyran silyl ether 126. To a solution of naphthoquinone **121** (202.9 mg, 0.39 mmol) in THF (2.0 mL) was added three portions of $Na_2S_2O_4$ solution (675 mg in H_2O 3.2 mL) at a one-hour interval. The reaction mixture was vigorously stirred at rt for 1 h before 20 mL of H_2O was added. The aqueous phase was extracted with EtOAc (3x10 mL). The combined organic layers were washed with brine, dried over anhydrous Na_2SO_4 and concentrated *in vacuo*. The crude residue was diluted with CH_2Cl_2 (1.5 mL) before 2,6-lutidine (450 µL, 3.9 mmol, 10 equiv) was added. The brown reaction mixture was subsequently added TBSOTf (445µL, 1.93 mmol, 5 equiv) and the reaction mixture was left stirred at rt overnight. The yellow solution was added 10 mL of H_2O and extracted with EtOAc (3x5 mL). The combined organic layers were washed with 1–2% aqueous HCl (2x10 mL), brine, dried over anhydrous Na_2SO_4 and concentrated *in vacuo*. Purification of the crude residue by column chromatography (10–20% EtOAc/hexanes) yielded pyran silyl ether **126** (273.5 mg, 94%, over 2 steps) as a yellow oil; R_f = 0.41 (10% EtOAc/hexanes); ^{1}H NMR (300 MHz, $CDCl_3$) δ 7.69–7.67 (m, 2H), 7.44–7.32 (m, 3H), 6.59 (s, 1H), 5.13 (d, *J* = 9.0 Hz, 1H), 4.98 (d, *J* = 9.0 Hz, 1H), 4.91 (d, *J* = 12.0 Hz, 1H), 4.83 (d, *J* = 12.0 Hz, 1H), 3.94 (s, 3H), 3.88 (s, 3H), 3.39 (s, 2H), 1.82 (s, 3H), 1.16 (s, 9H), 0.98 (s, 9H), 0.84 (s, 9H), 0.16 (s, 6H), 0.09–0.00 (m, 9H), –0.18 (s, 3H); ^{13}C NMR (75 MHz, $CDCl_3$)

δ 154.13, 149.05, 146.60, 141.72, 138.56, 134.91, 128.87, 127.96, 127.49, 123.08, 122.33, 119.12, 116.42, 110.07, 96.60, 76.41, 58.89, 57.10, 55.73, 44.73, 29.04, 26.24, 26.07, 25.75, 18.53, 18.30, 17.69, –3.49, –3.84, –4.34, –4.49, –5.24, –5.27; IR (thin film) 2930, 2857, 1584, 1350, 1253, 1068 cm^{-1}; HRMS (ESI) *m/z* calcd for $C_{41}H_{66}NaO_7Si_3$ $(M + Na)^+$ 777.4014, found 777.4018.

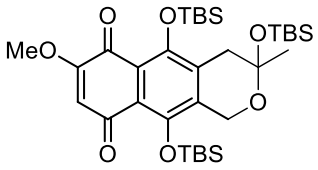

128

Naphthoquinone 128. To a solution of benzyl ether **126** (51.1 mg, 0.07 mmol) in EtOAc (1.5 mL) was added Pd/C (8.0 mg, 4 μmol, 0.05 equiv). The reaction mixture was stirred at rt under H_2 atmosphere for 4 h before being filtered through a pad of Celite, washed with EtOAc and concentrated *in vacuo*. Purification of the crude residue by column chromatography (5–10% EtOAc/hexanes) yielded naphthol precursor **127** (43.0 mg, 96%) as a yellow oil. Naphthol precursor (43.0 mg, 0.06 mmol) was diluted in MeCN/H_2O (9:1, 0.7 mL) and was then cooled to 0 °C. The yellow solution was added a portion of $PhI(OAc)_2$ (21.8 mg, 0.06mmol, 1.0 equiv). The reaction mixture was stirred further for 20 min before being diluted with H_2O (10 mL) and extracted with EtOAc (3x5 mL). The combined organic layers were washed with brine, dried over anhydrous Na_2SO_4 and concentrated *in vacuo*. Purification of the crude residue by column chromatography (20% EtOAc/hexanes) yielded naphthoquinone **128** (24.8 mg, 57% over 2 steps) as an orange gum; R_f = 0.34 (30% EtOAc/hexanes); ^1H NMR (300 MHz, $CDCl_3$) δ 5.86 (s, 1H), 4.75–4.65 (m, 2H), 3.86 (s, 3H), 3.30 (d, *J* = 18.0 Hz, 1H), 3.17 (d, *J* = 18.0 Hz, 1H), 1.75 (s, 3H), 1.04 (s, 9H), 0.88 (s, 9H), 0.77 (s, 9H), 0.25 (s, 3H), 0.06 (s, 6H), 0.00 (s, 3H), –0.01 (s, 3H), –0.11 (s, 3H); ^{13}C NMR (75 MHz, $CDCl_3$) δ 179.29, 178.21, 171.60, 156.73, 145.37, 139.57, 135.71, 118.95, 113.13, 111.83, 102.83, 59.13, 56.13, 43.83, 28.49, 25.83, 25.78, 25.52, 18.38, 18.19, 17.61, –3.45, –3.80, –4.46, –4.63, –5.43, –5.47; IR (thin film) 2955, 2858, 1605, 1383, 1254, 1004 cm^{-1}; HRMS (ESI) *m/z* calcd for $C_{33}H_{56}NaO_7Si_3$ $(M + Na)^+$ 671.3232, found 671.3229.

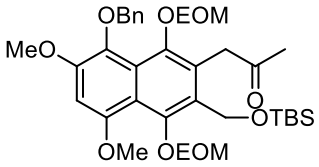

129

EOM ether 129. To a solution of naphthoquinone **121** (101.2 mg, 0.2 mmol) in Et_2O (5 mL) was added 5 mL of a solution of 10% $Na_2S_2O_4$ in H_2O. The reaction mixture was vigorously stirred at rt for 4 h before 20 mL of H_2O was added and extracted with EtOAc (3x10 mL). The combined organic layers were washed with brine, dried over anhydrous Na_2SO_4 and concentrated *in vacuo*. Purification of the crude residue by column chromatography (20–40% EtOAc/hexanes) yielded the corresponding hydroquinone **125** (88.8 mg, 87%) as a brown oil. The resultant hydroquinone (88.8 mg, 0.17mmol) was diluted with DMF (3.5 mL) and then cooled to 0 °C. The brown solution were added NaH (60% in mineral oil, 19.1 mg, 0.4 mmol, 2.5 equiv) and chloroethyl methyl ether (50 µL, 0.5 mmol, 3 equiv).The reaction mixture was stirred from 0 °C to rt for 2 h then being re-cooled to 0 °C before 10 mL of H_2O was added and extracted with EtOAc (4x10mL). The combined organic layers were washed with water (20 mL) then brine, dried over anhydrous Na_2SO_4 and concentrated *in vacuo*. Purification of the crude residue by column chromatography (5–20% EtOAc/hexanes) yielded EOM ether **129** (65.3 mg, 60%, 53% over 2 steps) as a yellow oil: R_f = 0.67 (40% EtOAc/hexanes); ^{1}H NMR (300 MHz, $CDCl_3$) δ 7.54–7.53 (m, 2H), 7.40–7.30 (m, 3H), 6.71 (s, 1H), 5.03 (s, 2H), 4.93 (s, 4H), 4.80 (s, 2H), 4.21 (s, 2H), 3.96 (s, 3H), 3.95 (s, 3H), 3.84 (q, *J* = 6.9 Hz, 2H), 3.57 (d, *J* = 7.2 Hz, 2H), 2.20 (s, 3H), 1.27 (t, *J* = 6.9 Hz, 3H), 1.12 (t, *J* = 7.2 Hz, 3H), 0.91 (s, 9H), 0.11 (s, 6H); ^{13}C NMR (75 MHz, $CDCl_3$) δ 206.35, 152.69, 149.34, 146.62, 146.29, 136.68, 134.21, 128.16, 127.49, 127.43, 127.25, 126.93, 124.22, 115.87, 99.20, 99.15, 96.60, 75.74, 64.84, 64.45, 56.96, 55.98, 55.88, 42.04, 28.48, 24.97, 17.33, 14.31, 1416, –6.37; IR (thin film) 2930, 2857, 1713, 1605, 1350, 1059 cm^{-1}; HRMS (ESI) *m/z* calcd for $C_{35}H_{50}NaO_9Si$ $(M + Na)^+$ 665.3116, found 665.3116.

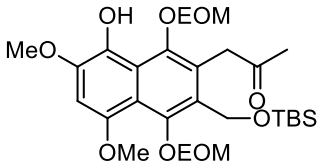

130

Naphthol 130. To a solution of benzyl ether **129** (95.7 mg, 0.15 mmol) in EtOAc (3 mL) was added Pd/C (16.3 mg, 7 μmol, 0.05 equiv). The reaction mixture was stirred at rt under H_2 atmosphere for 3.5 h before being filtered through a pad of Celite, washed with EtOAc and concentrated *in vacuo*. Purification of the crude residue by column chromatography (20–30% EtOAc/hexanes) yielded naphthol **130** (67.8 mg, 82%) as a yellow oil: R_f = 0.45 (40% EtOAc/hexanes); ^{1}H NMR (300 MHz, $CDCl_3$) δ 8.88 (s, 1H), 6.78 (s, 1H), 5.03 (s, 2H), 5.00 (s, 2H), 4.87 (s, 2H), 4.16 (s, 2H), 3.97 (s, 3H), 3.88 (s, 3H), 3.79 (q, *J* = 6.9 Hz, 4H), 2.21 (s, 3H), 1.24 (t, *J* = 6.9 Hz, 3H), 1.23 (t, *J* = 6.9 Hz, 3H), 0.87 (s, 9H), 0.07 (s, 6H); ^{13}C NMR (75 MHz, $CDCl_3$) δ 206.73, 149.35, 147.75, 147.02, 143.27, 135.48, 128.36, 126.11, 120.01, 116.32, 100.68, 100.68, 100.13, 66.95, 65.92, 58.01, 57.96, 57.19, 42.56, 29.52, 25.92, 18.26, 15.29, 15.20, –5.35; IR (thin film) 3369, 2930, 1718, 1350, 1160, 1057 cm^{-1}; HRMS (ESI) *m/z* calcd for $C_{28}H_{44}NaO_9Si$ $(M + Na)^+$ 575.2647, found 575.2645.

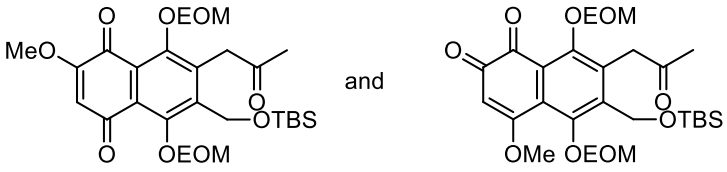

131 **132**

To a solution of naphthol **130** (68.0 mg, 0.12 mmol) in MeCN/H_2O (9:1, 1 mL) at 0 °C was added $PhI(OAc)_2$ (42.0 mg, 0.12 mmol, 1.0 equiv). The reaction mixture was stirred further for 5 min before being diluted with H_2O (10 mL) and extracted with EtOAc (3x10 mL). The combined organic layers were washed with brine, dried over anhydrous Na_2SO_4 and concentrated *in vacuo*. Purification of the crude residue by column chromatography (20–50% EtOAc/hexanes) yielded *para*-naphthoquinone **131** (33.0 mg, 50%) as an orange oil and *ortho*-naphthoquinone **132** (9.6 mg, 15%) as a red oil.

***para*-Naphthoquinone 131.** R_f = 0.57 (60% EtOAc/hexanes); ^{1}H NMR (300 MHz, $CDCl_3$) δ 6.00 (s, 1H), 5.08 (s, 2H), 5.07 (s, 2H), 4.81 (s, 2H), 4.18 (s, 2H), 3.84–3.74 (m, 7H), 2.19 (s, 3H), 1.23 (t, *J* = 7.2 Hz, 3H), 1.22 (t, *J* = 6.9 Hz, 3H), 0.86 (s, 9H), 0.05 (s, 6H); ^{13}C NMR (75 MHz, $CDCl_3$) δ 204.56, 183.96, 179.17, 159.36, 153.72, 151.49, 143.59, 139.41, 123.70, 123.28, 110.29, 100.78, 100.59, 66.01, 65.92, 57.48, 56.36, 42.78, 29.71, 25.85, 18.28, 15.16, 15.16, –5.45; IR (thin film) 2931, 2857, 1721, 1630, 1557, 1257 cm^{-1}; HRMS (ESI) *m/z* calcd for $C_{27}H_{40}NaO_9Si$ $(M + Na)^+$ 559.2334, found 559.2334.

***ortho*-Naphthoquinone 132.** R_f = 0.38 (60% EtOAc/hexanes),^{1}H NMR (300 MHz, $CDCl_3$) δ 5.96 (s, 1H), 5.10 (s, 2H), 5.00 (s, 2H), 4.79 (s, 2H), 4.18 (s, 2H), 4.00 (s, 3H), 3.75–3.58 (m, 4H), 2.24 (s, 3H), 1.27 (t, *J* = 6.9 Hz, 6H), 0.91 (s, 9H), 0.11 (s, 6H); ^{13}C NMR (75 MHz, $CDCl_3$) δ204.53, 179.52, 179.52, 170.46, 156.10, 150.11, 144.36, 137.42, 123.61, 122.81, 102.74, 100.70, 100.70, 66.30, 65.99, 57.72, 56.97, 42.36, 29.70, 25.84, 18.27, 15.19, 15.14, –5.47; IR (thin film) 2930, 2857, 1721, 1635, 1594, 1160 cm^{-1}; HRMS (ESI) *m/z* calcd for $C_{27}H_{40}NaO_9Si$ $(M + Na)^+$ 559.2334, found 559.2329.

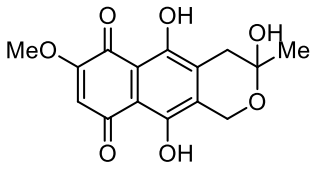

fusarubin (**17**)

Fusarubin (17). To a solution of naphthoquinone **131** (56.8 mg, 0.1mmol) in MeCN (2.5 mL) was added a solution of 1M HCl (0.7 mL). The reaction mixture was stirred for 3.5 h before 30 mL of H_2O was added and extracted with EtOAc (4x10 mL). The combined organic layers were washed with brine, dried over anhydrous Na_2SO_4 and concentrated *in vacuo*. Purification of the crude residue by column chromatography (20–40% EtOAc/hexanes) yielded fusarubin (**17**) (17.6 mg, 54%) as a red solid and anhydrofusarubin (**18**) (6.4 mg, 22%) as purple needles : R_f = 0.43 (50% EtOAc/hexanes); mp193.7–195.0 °C; ^{1}H NMR (300 MHz, $CDCl_3$) δ 12.94 (s, 1H), 12.68 (s, 1H), 6.19 (s, 1H), 4.89, (s, 2H), 3.94 (s, 3H), 3.03 (d, *J* = 18.0 Hz, 1H), 2.71 (d, *J* = 18.0 Hz, 1H), 2.31 (brs, 1H), 1.64 (s, 3H); ^{13}C NMR (75 MHz, $CDCl_3$) δ 184.64, 178.43, 160.65, 160.65, 156.97, 137.10, 137.10, 109.64, 109.64, 107.63, 94.06, 58.47, 56.68, 32.31, 22.63; ^{1}H

NMR (300 MHz, DMSO-d_6) δ 12.90 (s, 1H), 12.43 (s, 1H), 6.37 (s, 1H), 6.10, (s, 1H), 4.62 (s, 2H), 3.88 (s, 3H), 2.71 (d, J = 18.0 Hz, 1H), 2.51 (d, J = 18.0 Hz, 1H), 1.46 (s, 3H); ^{13}C NMR (75 MHz, DMSO-d_6) δ 185.05, 178.10, 161.06, 160.04, 156.68, 137.21, 133.67, 110.10, 109.74, 107.45, 93.44, 57.74, 57.49, 33.20, 28.88; IR (thin film) 3357, 2927, 1592, 1418, 1215, 1149 cm^{-1}; HRMS (ESI) *m/z* calcd for $C_{15}H_{14}NaO_7$ $(M + Na)^+$ 329.0632, found 329.0629.

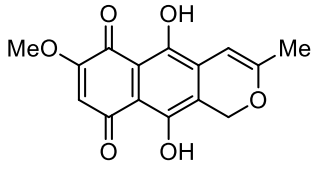

anhydrofusarubin (**18**)

Anhydrofusarubin (18). To a solution of fusarubin (**17**) (20 mg, 0.1mmol) in toluene (33 mL) was added catalytic amount of TsOH. The reaction mixture was heated at 105 °C for 1 h before being cooled to rt and 70 mL of H_2O was added. The aqueous phase was extracted with EtOAc (3x20 mL). The combined organic layers were washed with brine, dried over anhydrous Na_2SO_4 and concentrated *in vacuo*. Purification of the crude residue by column chromatography (20% EtOAc/hexanes) yielded anhydrofusarubin (**18**) (14.0 mg, 73%) as purple needles: R_f = 0.65 (50% EtOAc/hexanes); mp 193.0–194.5 °C; ^{1}H NMR (300 MHz, $CDCl_3$) δ 13.01 (s, 1H), 12.61 (s, 1H), 6.14 (s, 1H), 5.96 (s, 1H), 5.19 (s, 2H), 3.92 (s, 3H), 2.01 (s, 3H); ^{13}C NMR (75 MHz, $CDCl_3$) δ 182.93, 177.85, 161.53, 159.95, 157.66, 157.62, 132.95, 122.69, 110.87, 109.91, 107.92, 94.65, 62.92, 56.67, 20.11; IR (thin film) 2922, 1603, 1393, 1257, 1150, 1046 cm^{-1}; HRMS (ESI) *m/z* calcd for $C_{15}H_{12}NaO_6$ $(M + Na)^+$ 311.0520, found 311.0520.

CYTOTOXIC ASSAYS

REMA assay against MCF-7 cells

Cytotoxicity assay against human breast adenocarcinoma (MCF-7) cells (ATCC HTB-22) was evaluated at the National Center for Genetic Engineering and Biotechnology (BIOTEC), Thailand using the resazurin microplate assay (REMA) reported by O'Brien and co-workers. Doxorubicin and tamoxifen were used as positive controls. Cytotoxicity assay against African green monkey kidney fibroblast (Vero) cells was also tested at BIOTEC using REMA assay via a protocol disclosed by Hunt *et al*. Ellipticine was used as a standard compound for cytotoxicity against Vero cells.

MTT assay against MCF-7 cells

Cytotoxicity assay against human breast adenocarcinoma (MCF-7) was tested at Excellent Center for Drug Discovery (ECDD), Mahidol University, Thailand. Human breast cancer MCF-7 cells were seeded at 1 x 10^4 cells per well on 96-well plates and cultured for 24 h in DMEM (Dulbecco's Modified Eagle Medium) high glucose supplemented with 10% FBS and 1% penicillin/streptomycin at 37 °C and 5% CO_2 atmosphere. Then, compounds were screened by high throughput liquid handling system and were added into cell plates at indicated concentrations and incubated for 24 h at 37 °C and 5% CO_2 atmosphere. After 24 h of incubation, the culture media was removed and replaced with serum-free media containing MTT. After 3 h incubation, the media was removed and DMSO was added before measuring MTT absorbance at 570 nm by Multi-Mode Microplate Reader (ENVISION, Perkin Elmer). Doxorubicin was used as a positive control.

MTT assay against C33A, HeLa, SiHa, HCT116, HepG2 and Vero cells

Cervical carcinoma SiHa, HeLa, and C33A cell lines were obtained from the American Type Culture Collection (ATCC, USA). Hepatoma HepG2 and colorectal carcinoma HCT116 cell lines were kindly provided by Prof. Dr. Mathurose Ponglikitmongkol (Mahidol University, Thailand) and the noncancer Vero cell line was kindly provided by Dr. Sittirak Roytrakul (The National Center for Genetic Engineering

and Biotechnology, Thailand). All cell lines were maintained in Dulbecco's modified Eagle's (DMEM) medium supplemented with fetal bovine serum (10 %), penicillin (100 U/mL), and streptomycin (100 μg/mL) at 37 °C in a humidified atmosphere containing CO_2 (5%). All culture reagents were purchased from ThermoFisher Scientific (Gibco®, USA). Log-phase cells were seeded onto a 96-well culture plate (Costar®, Corning Incorporated, USA) at a density of 2.5 or 5×10^3 cells/well, and incubated overnight. After that, the cells were exposed to various concentrations of the compounds [0–200 μM; 0.2 % (v/v) DMSO]. After 72 h of incubation, cell viability was determined by an MTT [3-(4,5-dimethylthiazol-2-yl)-2,5-diphenyltetrazolium bromide; Applichem, Germany] assay as described previously (Wanichwatanadecha *et al*., 2012) Each experiment was carried out in triplicate. Dataare expressed in terms of % cell viability and IC50 values (the concentration needed for 50 % cell growth inhibition) relative to untreated cells [0.2 % (v/v) DMSO] (mean ± standard deviation). Cisplatin and doxorubicin (Pfizer, Australia) were used as positive controls.

3D cancer spheroid models: protocol description

3D cancer spheroid models were performed at Excellent Center for Drug Discovery (ECDD), Mahidol University, Thailand. Human breast cancer MCF-7 cells were seeded at 2×10^4 cells per well on ULA 96-well plates and cultured by DMEM (Dulbecco's Modified Eagle Medium) high glucose supplemented with 10% FBS and 1% penicillin/streptomycin. Cells were incubated in an atmosphere of 37 °C and 5% CO_2 for 3 days in order to form 3D spheroid. After 3 days of incubation, compounds were screened using high throughput liquid handing system. Compounds at indicated concentrations were added and incubated for 24 h, 48 h or 72 h at 37 °C and 5% CO_2. Detection of live cells by Hoechst 33342 staining and dead cells by Ethidium homodimer in 3D breast spheroid was performed by Operetta (Perkin Elmer). The analysis process was performed by high-content imaging analysis software (Columbus, Perkin Elmer).

REFERENCES

Baker, R. A.; Tatum, J. H.; Nemec, S. Jr. 1990. Antimicrobial activity of naphthoquinones from Fusaria. Mycopathologia, 111, 9–15.

Bandichhor, R.; Lowell, A. N.; Kozlowski, M. C. 2011. Alternative spiroketalization methods toward purpuromycin: A hemiketal conjugate addition strategy and use of an electron-rich isocoumarin precursor. J. Org. Chem. 76, 6475–6487.

Bianchi, D. A.; Sutich, E. G.; Kaufman, T. S. 2004. Synthesis and antibiotic activity of the tricyclic furo[3,2-*c*] isochromen-2-trione unit of the pyranonaphthoquinones. Bioorg. Med. Chem. Lett. 14, 757–760.

Brimble, M. A.; Duncalf, L. J.; Nairn, M. R. 1999. Pyranonaphthoquinone antibiotics–isolation, structure and biological activity. Nat. Prod. Rep. 16, 267–281.

Brötz, E.; Herrmann, J.; Wiese, J.; Zinceker, H.; Maier, A.; Kelter, G.; Imhoff, J. F.; Müller, R.; Paululat, T. 2014. Synthesis and cytotoxic activity of a small naphthoquinone library: first synthesis of juglonbutin. Eur. J. Org. Chem. 5318–5330.

Buttery, J. H.; Wege, D. 1998. Some transformations of adducts of 3,6-dimethoxy-4,5-methylenedioxy-1,2-didehydrobenzene and furans. An approach to the 5,8-dimethoxy-6,7-methylenedioxynaphtho[2,3-c]furan-4,9-dione ring system of ventilone A. Aust. J. Chem. 51, 409–420.

Chilton, W. S. 1968. Isolation and structure of norjavanicin. J. Org. Chem. 33, 4299–4300.

Chowdhury, N. S.; Sohrab, Md. H.; Rana, Md. S.; Hasan, C. M.; Jamshidi, S.; Rahman, K. M. 2017. Cytotoxic naphthoquinone and azaanthraquinone derivatives from an endophytic *Fusarium solani*. J. Nat. Prod. 80, 1173–1177.

Clive, D. L. J.; Middleton, D. S. 1991. Regioselective oxidation of polyalkoxy naphthalenes: formation of naphthoquinones by ammonium cerium(IV) nitrate oxidation of methoxymethyl ethers. Isr. J. Chem. 31, 211–213.

Cui, J.-h.; Zhou, W.; Li, S.-s. 2012. A convenient and efficient synthesis of 2-acetyl-5,8-dimethoxy-1,4-naphthoquinone. J. Chem. Res. 264–265.

De Koning, C. B.; Giles, R. G. F.; Engelhardt, L. M.; White, A. H. 1988. Convenient syntheses of the naturally occurring benzo[*b*]xanthen-12-one bikaverin. *X* - Ray crystallographic confirmation of the product regiochemistry. J. Chem. Soc., Perkin Trans 1. 3209–3216.

De Koning, C. B.; Giles, R. G. F.; Green, I. R. 1991. Naphthoquinones. Conformation of the structures of ventiloquinones E, G and J by synthesis. J. Chem. Soc., Perkin Trans 1. 2743–2748.

Dohi, T.; Kita, Y. 2009. Hypervalent iodine reagents as a new entrance to organocatalysts. Chem. Commun. 2073–2085.

Evan, D. A.; Bender, S. L. 1986. Total synthesis of ionophore antibiotic X-206. Studies relevant to stereoselective synthesis of the C(17)-C(26) synthon. Tetrahedron Lett. 27, 799–802.

Giles, R. G. F.; Green, I. R.; van Eeden, N. 2006. Products of an acetylation protocol on two pentaalkoxynaphthalenes. Synth. Commun. 36, 1695–1706.

Guerrero-Vásquez, G. A.; Chinchilla, N.; Molinillo, J. M. G.; Macías, F. A. 2014. Synthesis of bioactive speciosins G and P from *Hexagonia speciosa*. J. Nat. Prod. 77, 2029–2036.

Hart, H.; Lai, C.-y.; Nwokogu, G.; Sbamouilian, S.; Teuerstein, A.; Zlotogorski, C. 1980. Bisannelation of arenes with bisaryne equivalents. J. Am. Chem. Soc. 102, 6649–6651.

Hume, P. A.; Sperry, J.; Brimble, M. A. 2011. Enantioselective synthesis of pyranonaphthoquinone antibiotics using a CBS reduction/cross-metathesis/oxa-Michael strategy. Org. Biomol. Chem. 9, 5423–5430.

Hunt, L.; Jordan, M.; De Jesus, M.; Wurm, F. M. 1999. GFP-expressing mammalian cells for fast, sensitive, noninvasive cell growth assessment in a kinetic mode. Biotechnol. Bioeng. 65, 201–205.

Ito, T.; Ikemoto, T.; Yamano, T.; Mizuno, Y.; Tomimatsu, K. 2003. Practical synthesis of (*R*)-(+)-6-(1,4-dimethoxy-3-methyl-2-naphthyl)-6-(4-hydroxyphenyl)hexanoic acid: a key intermediate for a therapeutic drug for neurodegenerative diseases. Tetrahedron Asymmetry. 14, 3525–3531.

Jammula, S. R.; Pepalla, S. B.; Telikepalli, H.; Jagannadha Rao, K. V.; Thomson, R H. 1991. An acetonnaphthone and an isofuranonaphtho-quinone from *Ventilago goughii*. Phytochemistry. 30. 2427–2429.

Kesteleyn, B.; Van Puyvelde, L.; De Kimpe, N. 1999. Synthesis of isagarin, a new type of tetracyclic naphthoquinone from *Pentas longiflora*. J. Org. Chem. 64, 438–440.

Khan, Md. I. H.; Sohrab, Md. H.; Rony, S. R.; Tareq, F. S.; Hasan, C. M.; Mazid, Md. A. 2016. Cytotoxic and antibacterial naphthoquinones from an endophytic fungus, *Cladosporium* sp. Toxicol. Rep. 3, 861–865.

Kim, M.; Wiemer, D. F. 2005. Syntheis of aromatic phosphates via cycloaddition of phosphate dienes. Tetrahedron Lett. 46, 7583–7587.

Kumar, K. P.; Javvaji, K.; Poornachandra, Y.; Allanki, A. D.; Misra, S. 2017. Antimicrobial, anti-plasmodial and cytotoxicity properties of bioactive compounds from *Fusarium* sp. USNPF102. J. Microbiol. Res. 7, 23–30.

Lamblin, M.; Sallustrau, A.; Commandeur, C.; Cresteil, T.; Felpin, F.-X.; Dessolin, J. 2012. Synthesis and biological evaluation of hydrophilic embelin derivatives. Tetrahedron. 68, 4655–4663.

Larghi, E. L.; Kaufman, T. S. 2006. The oxa-Pictet–Spengler cyclization: synthesis of isochromans and related pyran-type heterocycles. Synthesis. 2, 187–220.

Lowell, A. N.; Fennie, M. W.; Kozlowski, M. C. 2008. A concise synthesis of naphthalene portion of purpuromycin. J. Org. Chem. 73, 1911–1918.

Masi, M.; Meyer, S.; Górecki, M.; Pescitelli, G.; Clement, S.; Cimmino, A.; Evidente, A. 2018. Phytotoxic activity of metabolites isolated from *Rutstroemia sp.n.*, the causal agent of bleach blonde syndrome on cheatgrass (*Bromus tectorum*). Molecules. 23, 1734/1–1734/12.

Moore, R.E.; Scheuer, P. J. 1966. Nuclear magnetic resonance spectra of substituted naphthoquinones. Influence of substituents on tautomerism, anisotropy, and stereochemistry in the naphthazarin system. J. Org. Chem. 81, 3272–3283.

Naysmith, B. J.; Hume, P. A.; Sperry, J.; Brimble; M. A. 2017. Pyranonaphthoquinones – isolation, biology: an update. Nat. Prod. Rep. 34, 25–61.

Nguyen Van, T.; Kesteleyn, B.; De Kimpe, N. 2001. Synthesis of 1,3-disubstituted naphtho[2,3-*c*]pyran-5,10-diones. Tetrahedron. 57, 4213–4219.

O'Brien, J.; Wilson, I.; Orton, T.; Pognan, F. 2000. Investigation of Alamar Blue (resazurin) fluorescent dye for the assessment of mammalian cell cytotoxicity. Eur. J. Biochem. 267, 5421–5426.

Padwal, J.; Lewis, W.; Moody, C. J. 2011. Synthesis of balsaminone a, a naturally occurring pentacyclic dinaphthofuran quinone. J. Org. Chem. 76, 8082–8087.

Paruch, K.; Vyklicky, L.; Wang, D. Z.; Katz, T. J.; Incarvito, C.; Zakharov, L.; Rheingold, A. L. 2003. Functionalizations of [6]- and [7]helicenes at their most sterically hindered positions. J. Org. Chem. 68, 8539–8544.

Peng, C.-Y. Shen, J.-Y.; Chen, Y.-T.; Wu, P.-J.; Hung, W.-Y.; Hu, W.-P.; Chou, P.-T. 2015. Optiacally triggered stepwise double-proton transfer in an intramolecular proton relay: a case study of 1,8-dihydroxy-2-naphthaldehyde. J. Am. Chem. Soc. 137, 14349–14357.

Pillay, A.; Rousseau, A. L.; Fernandes, M. A.; de Koning, C. B. 2012. The synthesis of the pyranonaphthoquinonesdehydroherbarin and anhydrofusarubin using Wacker oxidation methodology as a key step and other unexpected oxidation reactions with ceric ammonium nitrate and salcomine. Org. Biomol. Chem. 10, 7809–7819.

Ramos-Peralta, L.; López-López, L. I.; Silva-Belmares, S. Y.; Zugasti-Cruz, A.; Rodríguez-Herrera, R.; Aguilar-González, C. N. In *The battle against microbial pathogens: basic science, technological advances and educational programs*, ed. Méndez-Vilas A., Formatex Research Center: Spain, vol. 1, 2015, December 2015, pp. 542–550.

Roush, W. R.; Neitz, R. J. 2004. Studies on the Synthesis of Landomycin A. Synthesis of the originally assigned structure of aglycone, landomycinone, and revision of structure. J. Org. Chem. 69, 4906–4912.

Ruelius, V. H. W.; Gauhe, A. 1950. Über Fusarubin, einen naphthochinonfarbstoff aus Fusarien. Justus Liebigs Ann Chem. 569, 38–59.

Sawant, R. T.; Jadhav, S. G.; Waghmode, S. B. 2010. Intra- and intermolecular oxa-Pictet–Spengler cyclization strategy for the enantioselective synthesis of deoxy analogues of (+)-nanomycin A methyl ester, (+)-eleutherin, (+)-allo, eleutherin, and (+)-thysanone. Eur. J. Org. Chem. 23, 4442–4449.

Sperry, J.; Bachu, P.; Brimble, M. A. 2008. Pyranonaphthoquinones–isolation, biological activity and synthesis. Nat. Prod. Rep. 25, 376–400.

Studt, L.; Wiemann, P.; Kleigrewe, K.; Humpfand, H.; Tudzynski, B. 2012. Biosynthesis of fusarubins accounts for pigmentation of *Fusarium fujikuroi* perithecia. Appl Environ. Microbiol. 78, 4468–4480.

Suhara, Y.; Watanabe, M.; Motoyoshi, S.; Nakagawa, K. Wada, A. Takeda, K.; Takahashi, K. Tokiwa, H.; Okano, T. 2011. Synthesis of new vitamin K analogues as steroid and xenobiotic receptor (SXR) agonists: insights into the biological role of the side chain part of vitamin K. J. Med. Chem. 54, 4918–4922.

Taguchi, T.; Suda, Y.; Hosoda, A.; Kobayashi, Y. 1988. Preparation of 2-trifluoromethylvitamin K analogs. Tetrahedron Lett. 29, 5765–5766.

Tanoue, Y.; Terada, A. 1988. The 2- or 6-(α-hydroxyalkyl- and α-oxoalkyl)-5,8-dimethoxy-1,4-naphthoquinones from the oxidative demethylation of 2-(α-hydroxyalkyl- and α-oxoalkyl)-1,4,5,8-tetramethoxynaphthalenes with cerium(iv) ammonium nitrate, and the further demethylations to naphthazarins. Bull. Chem. Soc. Jpn. 61, 2039–2045.

Tanoue, Y.; Terada, A.; Matsumoto, Y. 1989. A synthetic route of 1,4,8-trimethoxy-2-naphthalenecarbaldehyde via Duff formylation of 4,8-dimethoxy-1-naphthol. Bull. Chem. Soc. Jpn. 62, 2736–2738.

Tatum, J. H.; Baker, R. A. 1983. Naphthoquinones produced by *Fusarium solani* isolated from citrus. Phytochemistry. 22, 543–547.

Tatum, J. H.; Baker, R. A.; Berry, R. E. 1985. Naphthoquinones produced by *Fusarium oxysporum* isolated from citrus. Phytochemistry. 24, 457–459.

Terada, A.; Tanoue, Y.; Hatada, A.; Sakamoto, H. 1987. Synthesis of shikalkin (±shikonin) and related compounds. Bull. Chem. Soc. Jpn. 60, 205–213.

Thi, T. A. D.; Thi, T. H. V.; Phuong, H. T.; Nguyen, T. H.; The, C. P.; Duc, C. V.; Depetter, Y.; D'hooghe, M.; Nguyen, T. V. 2015. Synthesis and anticancer properties of new (dihydro)pyranonaphthoquinones and their epoxy analogs. Bioorg. Med. Chem. Lett. 25, 3355–3358.

Thomson, R. H. in *The total synthesis of natural products*, ed. ApSimon, J., John Wiley & Sons, Inc.: New York, vol. 8, 1992, pp. 311–531.

Tisler, M. 1989. Heterocyclic quinones. Adv. Heterocycl. Chem. 45, 37–150.

Trisuwan, K.; Khamthong, N.; Rukachaisirukul, V.; Phongpaichit, S.; Preedanon, S.; Sakayaroj, J. 2010. Anthraquinone, cyclopentanone, and naphthoquinone derivatives from the sea fan-derived fungi *Fusarium* spp. PSU-F14 and PSU-F135. J. Nat. Prod. 73, 1507–1511.

Wanichwatanadecha, P.; Sirisrimangkorn, S.; Kaewprag, J.; Ponglikitmongkol, M. 2012. Transactivation activity of human papillomavirus type 16 E6*I onaldo-keto reductase genes enhances chemoresistance in cervical cancer cells. J. Gen. Virol. 93, 1081–1092.

White, J. D.; Hrnciar, P.; Stappenbeck, F. 1999. Asymmetric total synthesis of (+)-codeine via intramolecular carbenoid insertion. J. Org. Chem. 64, 7871–7884.

Yoshimura, A.; Zhdankin, V. V. 2016. Advances in synthetic applications of hypervalent iodine compounds. Chem. Rev. 116, 3328–3435.

Young Jeong, J. Sperry, J. Taylor, J. A.; Brimble, M. A. 2014. Synthesis and evaluation of 9-deoxy analogues of (–)-thysanone, an inhibitor, of HRV 3C protease. J. Med. Chem. 87, 220–227.

APPENDIX

Organic & Biomolecular Chemistry

PAPER

Cite this: *Org. Biomol. Chem.*, 2019, **17**, 7078

Unified synthesis and cytotoxic activity of 8-*O*-methylfusarubin and its analogues†

Pongsit Vijitphan,[a] Vatcharin Rukachaisirikul,[a] Chatchai Muanprasat,[b,c] Panata Iawsipo,[d,e] Jiraporn Panprasert[d,e] and Kwanruthai Tadpetch *[a]

Received 26th May 2019,
Accepted 4th July 2019

DOI: 10.1039/c9ob01221d

rsc.li/obc

A simple and unified synthesis of four related pyranonaphthoquinone natural products, *e.g.* 8-*O*-methylfusarubin, 8-*O*-methylanhydrofusarubin, fusarubin and anhydrofusarubin, is reported. The key synthetic features include the precedented Diels–Alder cycloaddition to assemble the naphthalene skeleton, selective formylation and acetonylation and intramolecular acetalization to construct the pyran ring. Manipulation of the oxidation state of the naphthoquinone core was performed to construct the two analogues, fusarubin and anhydrofusarubin. This work also highlights an unprecedented directing effect of the hydroxymethylene group in the selective hypervalent iodine-mediated quinone oxidation. The four synthetic compounds were evaluated for their *in vitro* cytotoxic activities against six human cancer cells. 8-*O*-Methylfusarubin was the most potent analogue and displayed excellent cytotoxic activity against MCF-7 breast cancer cells with an IC_{50} value of 1.01 μM with no cytotoxic effect on noncancerous Vero cells, which could potentially be a promising lead compound for anti-breast cancer drug discovery.

Introduction

Naphthoquinones are secondary metabolites isolated from various natural sources such as plants, fungi, algae and bacteria.[1] The core structure of naphthoquinones consists of a naphthalene ring containing two carbonyl groups at 1,4 or 1,2 positions which can be named 1,4-naphthoquinones and 1,2-naphthoquinones, respectively (Fig. 1). Pyranonaphthoquinones are subgroups of naphthoquinones containing a pyran ring attached to naphthoquinones. The basic skeleton of pyranonaphthoquinones is naphtho[2,3-*c*]pyran-5,10-dione (Fig. 1).[2] This group of metabolites has been reported to exhibit diverse biological activities particularly antimicrobial activity against a broad range of microbial and fungal species *e.g. Staphylococcus aureus*, *Escherichia coli* and *Candida rugosa*.[3] Furthermore, some pyranonaphthoquinones were shown to exhibit antiplasmodial, antimalarial and anticancer activities.[4]

In 2010, our research group reported the isolation of new anthraquinone and naphthoquinone derivatives along with known fusarubin[5] (**1**) and anhydrofusarubin[6] (**2**) from sea fan-derived fungi, *Fusarium* spp. PSU-F14 and PSU-F135.[7] Concurrently, our group also isolated a known related pyranonaphthoquinone, 8-*O*-methylfusarubin[8] (**3**), from a seagrass-derived fungus *Pestalotiopsis* sp. PSU-ES180 (Fig. 2).[9] The isolated compounds **1**, **2** and **3** were examined for selected biological activities and were found to exhibit excellent *in vitro* cytotoxic activities against MCF-7 human breast cancer cells with IC_{50} values of 9.8, 1.06, 0.9 μM, respectively. Notably, the cytotoxic activities of compounds **2** and **3** were superior to that of the standard drug doxorubicin (IC_{50} = 2.18 μM). In addition, compounds **1**, **2** and **3** displayed very low cytotoxic effects against noncancerous African green monkey kidney (Vero) cells with IC_{50} values of 79, 49 and 58 μM, respectively. This finding has renewed the interest in the anticancer activity of this class of naphthoquinones. Owing to the promising cyto-

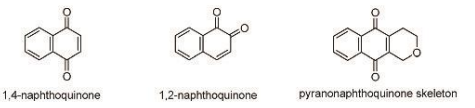

Fig. 1 The core structures of 1,4- and 1,2-naphthoquinones and pyranonaphthoquinones.

[a]*Department of Chemistry and Center of Excellence for Innovation in Chemistry, Faculty of Science, Prince of Songkla University, Hat Yai, Songkhla 90112, Thailand. E-mail: kwanruthai.t@psu.ac.th; Fax: +66 74 558841; Tel: +66 74 288437*
[b]*Department of Physiology, Faculty of Science, Mahidol University, Bangkok 10400, Thailand*
[c]*Excellent Center for Drug Discovery, Faculty of Science, Mahidol University, Bangkok 10400, Thailand*
[d]*Department of Biochemistry and Center of Excellence for Innovation in Chemistry, Faculty of Science, Burapha University, Chonburi 20131, Thailand*
[e]*Unit of Bioactive Natural Compounds for Healthcare Products Development, Faculty of Science, Burapha University, Chonburi 20131, Thailand*

†Electronic supplementary information (ESI) available. See DOI: 10.1039/c9ob01221d

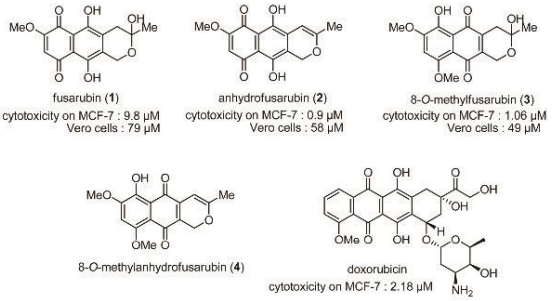

Fig. 2 Structures of fusarubin (**1**), anhydrofusarubin (**2**), 8-*O*-methylfusarubin (**3**) and 8-*O*-methylanhydrofusarubin (**4**) and cytotoxic activities against the MCF-7 cells of natural compounds **1–3** compared with doxorubicin.

toxic activities of these pyranonaphthoquinones and as part of our ongoing program for anticancer drug discovery, we have been focusing on a synthetic course of compounds in this class. Herein, we report a unified synthetic approach to pyranonaphthoquinone natural products **1–3** as well as a related analogue, 8-*O*-methylanhydrofusarubin[10] (**4**), and the cytotoxic activities against six human cancer cell lines of the synthetic compounds.

To our surprise, there has been no report on the synthesis of fusarubin and 8-*O*-methylfusarubin whereas only one synthesis of anhydrofusarubin has been reported so far. In 2012, de Koning and co-workers disclosed the first total synthesis of **2** using Stobbe condensation to construct the naphthalene core and Wacker oxidation to assemble the isochromene ring as the key strategy.[11] Their synthetic approach led to **2** in 11 steps with an overall yield of 5%.

Results and discussion

Structurally, fusarubin (**1**) and 8-*O*-methylfusarubin (**3**) differ only by the position of the 1,4-quinone moiety of the naphthoquinone core. From this inherent structural similarity, it was envisioned that compounds **1** and **3** could be synthesized by the same synthetic approach *via* the manipulation of the oxidation state of the naphthoquinone core. We would begin with the syntheses of **3** and its dehydrated analogue **4**, the retrosynthetic analysis of which is shown in Scheme 1. 8-*O*-Methylanhydrofusarubin (**4**) would be derived from **3** *via* dehydration. The dihydropyran hemiacetal moiety of **3** was envisaged to be constructed from acetonylnaphthoquinone **5** *via* intramolecular acetalization. The acetalization precursor **5** would then be obtained from the acetonylation of the corresponding naphthoquinone prepared from a selective oxidation of naphthol derivative **6**. The hydroxymethylene moiety of **6** would be installed *via* Vilsmeier–Haack formylation/reduction of the known pentaalkoxynaphthalene intermediate **7**, which in turn could be prepared from 5-bromovanillin following a protocol reported by Green and co-workers.[12]

The Vilsmeier–Haack formylation precursor, pentaalkoxynaphthalene **7**, was prepared following a procedure reported by Green and co-workers with slight modifications (Scheme 2). Starting with the commercially available 5-bromovanillin (**8**), dibromobenzene **9** was obtained in 4 steps in 83% yield.[13] The key Diels–Alder cycloaddition between the benzyne intermediate generated from **9** and 2-methoxyfuran (**10**) in THF at

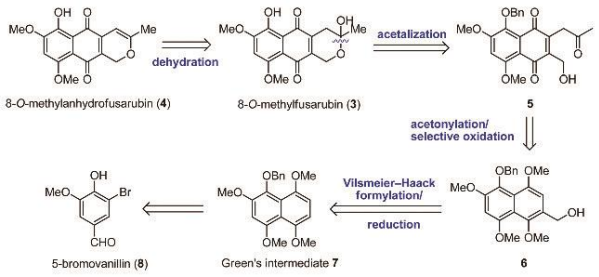

Scheme 1 Retrosynthetic analysis of 8-*O*-methylfusarubin (**3**) and 8-*O*-methylanhydrofusarubin (**4**).

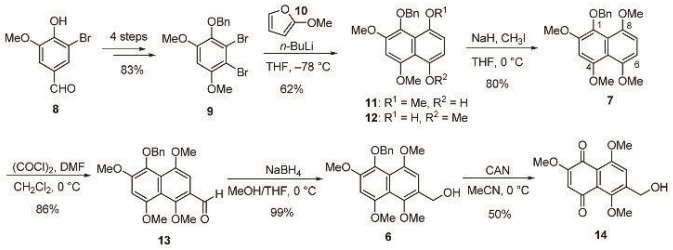

Scheme 2 Synthesis of pentaalkoxynaphthalene **6**.

−78 °C afforded naphthols **11** and **12** in 62% combined yield as an inseparable mixture. The subsequent treatment of a mixture of **11** and **12** with NaH and CH_3I at 0 °C provided the desired naphthalene intermediate **7** in good yield.[14] Our modified synthesis led to an improved yield of 42% of **7** over 6 steps. Our next task was to selectively install the formyl group at C-6 using the formylation reaction. Kozlowski *et al.* have previously reported the Vilsmeier–Haack formylation of a very similar pentamethoxynaphthalene analogue of **7** which yielded the formylated product at C-6.[15] As expected, the subjection of **7** to Vilsmeier–Haack formylation using oxalyl chloride and DMF resulted in the formation of naphthaldehyde **13** exclusively in 86% yield.[16] The position of the newly formed formyl group was confirmed by an nOe correlation between aldehyde proton (δ 10.49) and C-5 methoxy proton (δ 3.92) signals as well as HMBC correlations.[17] Subsequent $NaBH_4$ reduction of **13** smoothly provided the targeted naphthyl alcohol **6** in a quantitative yield. The next challenge was to selectively oxidize the right-hand ring of **6** to naphthoquinone. Electronically, the left-hand ring of **6** would be more likely to be oxidized due to an extra electron-donating methoxy group. Precedents of the regioselective oxidation of this type of substrate mediated by cerium ammonium nitrate (CAN) have revealed the exclusive oxidation of the left ring.[18] Unsurprisingly, the treatment of **6** with CAN in acetonitrile at 0 °C gave only the undesired product naphthoquinone **14** in 50% yield, which prompted us to revise this step of the synthesis.

To overcome the electronic bias in the oxidation step, we shifted our attention to using a hydroquinone mono-ether as an oxidation precursor in order to achieve the selective oxidation of the right-hand ring of **6**. It is well documented that the oxidation of hydroquinone mono-ethers to 1,4-quinones is a very facile process.[18b,19] In addition, the free hydroxyl group of the hydroquinone mono-ether would be a good directing group to induce the incoming formyl group at the requisite *ortho*-like position.[20] Thus, to prove this, we subjected a mixture of naphthols **11** and **12** to the aforementioned formylation conditions (Scheme 3a). Gratifyingly, the desired naphthaldehyde **15** resulting from *C*-formylation was obtained

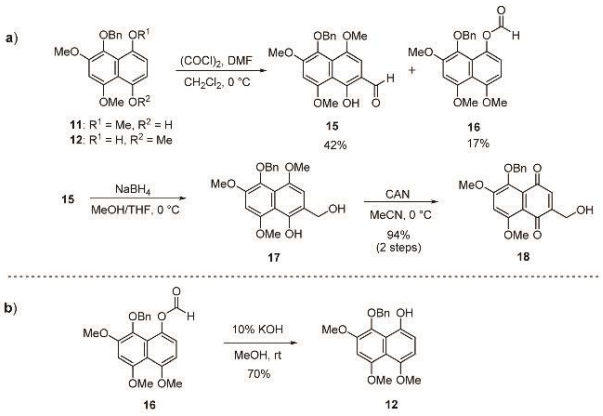

Scheme 3 (a) Synthesis of naphthoquinone **18** and (b) basic hydrolysis of formate ester **16**.

in 42% yield along with the *O*-formylation product, naphthyl formate **16**, in 17% yield. The position of the formyl group of **15** was confirmed by an nOe correlation between the methoxy protons (δ 3.80) and an aromatic proton (δ 7.02) on the right ring. Moreover, the structure of formate **16** was verified by subjection to hydrolysis using 10% KOH to give the naphthol regioisomer **12** in 70% yield (Scheme 3b). The structure of **12** was confirmed by an nOe enhancement of the hydroxy proton (δ 9.66) after irradiation of the benzylic protons (δ 5.12) of the Bn group. With the requisite naphthaldehyde **15** in hand, we continued with $NaBH_4$ reduction to obtain the corresponding naphthyl alcohol **17**. Unfortunately, compound **17** is very unstable and can easily decompose in a few hours upon exposure to air. Due to the low stability of alcohol **17**, this compound was immediately taken to the next step without chromatographic purification. To our delight, the treatment of naphthol **17** with CAN in MeCN at 0 °C smoothly furnished the desired naphthoquinone **18** in 94% yield over two steps.

Although we were successful in the selective oxidation to secure the appropriate oxidation state of the naphthoquinone intermediate, the drawback of this route was the use of a mixture of naphthols **11** and **12** as formylation precursors and only **11** was consumed to form the targeted product. The other precursor **12** underwent *O*-formylation to generate the naphthyl formate byproduct, which lowered the total yield of this step. To avoid this limitation, we decided to revisit the first pathway to convert pentaalkoxynaphthalene **6** to the desired naphthoquinone **18** by the screening of other oxidizing agents for quinone oxidation (Table 1). Using silver(II) oxide in the presence of 6 M nitric acid in dioxane at room temperature[11,21] led to no reaction and the starting compound was recovered (entry 1). Changing the oxidizing agents to hypervalent iodines gave more satisfactory results. Treating **6** with (bis(trifluoroacetoxy)iodo)benzene ($PhI(OCOCF_3)_2$) in a 9 : 1 mixture of MeCN and water at 0 °C for 30 minutes yielded the undesired naphthoquinone **14** as a major product in 51% yield and the desired naphthoquinone **18** as a minor product in only 25% yield (entry 2). Increasing the reaction temperature to room temperature slightly improved the yield of **18** to 32% while the undesired **14** was still a major product (entry 3). The more electron-withdrawing ligands of $PhI(OCOCF_3)_2$ might be attributed to the oxidation of the more electron-rich left ring of naphthalene **6**.[22] Therefore, the less reactive hypervalent iodine reagent with the less electron-withdrawing ability ligand, diacetoxyiodobenzene ($PhI(OAc)_2$), was investigated. Subjection of **6** to $PhI(OAc)_2$ under the same solvent mixture at 0 °C for 30 minutes yielded the desired naphthoquinone **18** as a major product in 58% yield along with **14** in 34% (entry 4). Elevating the reaction temperature to room temperature further enhanced the yield of **18** to 67% (entry 5). Thus, we further increased the reaction temperature to 50 °C under the same conditions for 1 min, following which the reaction could be judged complete by the color change from light yellow to dark orange, and found that the requisite naphthoquinone **18** was formed as a sole product in 75% (entry 6). The excellent regioselectivity was attributed to the hydroxymethylene moiety as a directing group in this $PhI(OAc)_2$-mediated oxidation at elevated temperature. To emphasize the importance of the hydroxymethylene directing group in this selective oxidation, pentaalkoxynapthalene **7** without the hydroxymethylene group was subjected to the same conditions of entry 6 (Scheme 4). It was discovered that oxidation occurred preferentially on the more electron-rich left ring of **7** to give **19** as a major product in 65% yield, whereas naphthoquinone regioisomer **20** resulting from the oxidation of the less electron-rich right-hand ring was obtained as a minor product in only 16% yield. This control experiment strongly suggested that the hydroxymethylene could be exploited as a directing group in hypervalent iodine-mediated quinone oxidation.

Having established the optimized synthetic sequence to construct the key naphthoquinone core **18**, we proceeded to complete the syntheses of the natural products **3** and **4** (Scheme 5). Although the acetonylation of **18** could be performed directly in the presence of free alcohol functionality, the yield and purity of the corresponding product were quite low. Hence, protection of the free alcohol was required. The protecting group of choice was the *tert*-butyldimethylsilyl (TBS) group since it could be removed under acidic conditions

Table 1 Screening of oxidation conditions to construct naphthoquinone **18** from naphthalene **6**

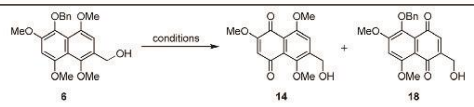

6 14 18

Entry	Reagents	Solvent (concentration)	Temp.	Time	Yield (%) 14	18
1	AgO, 6 M HNO_3	1,4-Dioxane (0.04 M)	rt	Overnight	No reaction	
2	$PhI(OCOCF_3)_2$	MeCN/H_2O (9 : 1, 0.1 M)	0 °C	30 min	51	25
3	$PhI(OCOCF_3)_2$	MeCN/H_2O (9 : 1, 0.1 M)	rt	30 min	42	32
4	$PhI(OAc)_2$	MeCN/H_2O (9 : 1, 0.1 M)	0 °C	30 min	34	58
5	$PhI(OAc)_2$	MeCN/H_2O (9 : 1, 0.1 M)	rt	30 min	28	67
6	$PhI(OAc)_2$	MeCN/H_2O (9 : 1, 0.1 M)	50 °C	1 min	—	75

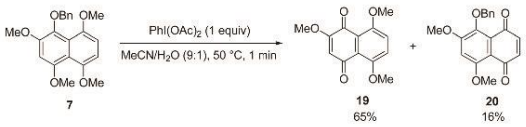

Scheme 4 PhI(OAc)$_2$-mediated oxidation of pentaalkoxynaphthalene **7** at 50 °C.

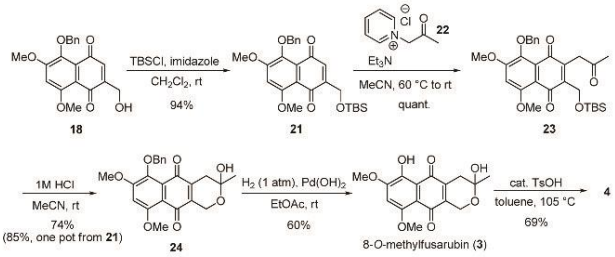

Scheme 5 Completion of the synthesis of 8-*O*-methylfusarubin (**3**) and 8-*O*-methylanhydrofusarubin (**4**).

which would also induce the intramolecular hemiacetal formation. Therefore, alcohol **18** was protected as silyl ether **21** using TBSCl and imidazole. The introduction of the acetonyl group was accomplished using acetylmethylpyridinium chloride (**22**) in the presence of Et_3N in MeCN to give acetonylnaphthoquinone **23** in a quantitative yield.[23] The treatment of **23** with 1 M hydrochloric acid in MeCN at room temperature resulted in the simultaneous removal of the TBS protecting group and intramolecular acetalization to smoothly furnish pyranonaphthoquinone **24** in 74% yield. Alternatively, **24** could be synthesized in a remarkable 85% yield *via* a one-pot fashion from **21** by simply quenching the acetonylation reaction with excess HCl and prolonged stirring without the isolation of **23**. Subsequent hydrogenolytic deprotection of the benzyl group using catalytic $Pd(OH)_2$ in ethyl acetate afforded the natural product **3** in 60% yield. It should be noted that hydrogenolysis using a typical Pd/C catalyst in an alcoholic solvent led to the formation of an unwanted pyran acetal product, which could not be hydrolyzed back to the corresponding pyran hemiacetal. Finally, following a procedure reported by Nguyen *et al.*,[24] compound **3** was subjected to dehydration using catalytic TsOH in toluene at 105 °C to give **4** in 69% yield. The ^{1}H and ^{13}C NMR spectroscopic data of synthetic **3** were in excellent agreement with those previously reported for the natural product.[25] The specific rotation of **3** was observed as $[\alpha]_D^{26}$ = +7.33 (*c* 0.03, acetone), suggesting that synthetic **3** was obtained as a scalemic mixture. Thus, no attempts were made to identify the absolute configuration of synthetic **3**. Although there is one literature precedent by Evidente *et al.* on the determination of the absolute configuration of natural **3** isolated from a grass weed-derived fungus *Rutstroemia capillus-albis*,[26] the specific rotation and absolute configuration of **3** isolated from other natural sources particularly *Fusarium* species were not reported. For compound **4**, only the ^{1}H NMR data were reported in the literature.[9] The ^{1}H NMR data of synthetic **4** were identical to those of natural **4**. We further confirmed the identity of synthetic **4** by ^{13}C and 2D NMR as well as HRMS data.

As previously mentioned, the other two targets fusarubin (**1**) and anhydrofusarubin (**2**) differ from **3** and **4** only by the position of the 1,4-quinone moiety of the naphthoquinone core. Therefore, we envisioned to synthesize **1** and **2** by exploiting the same strategy and utilizing the common intermediate from the syntheses of **3** and **4** *via* the manipulation of the oxidation state of the naphthoquinone nucleus. The retrosynthetic analysis of **1** and **2** is shown in Scheme 6. Anhydrofusarubin (**2**) would again be obtained from the dehydration of fusarubin (**1**), which in turn would be assembled by the intramolecular acetalization of **25**. Naphthoquinone **25** would be accessible from the selective oxidation of naphthol **26**. Naphthol **26** would then be derived from the selective quinone reduction/protection of naphthoquinone intermediate **23**. The appropriate protecting group should be easily and globally removed under acidic conditions which would be used in the acetalization step as well.

We initially chose the TBS group as a protecting group of hydroquinone for the purpose of global deprotection. The syntheses of **1** and **2** commenced with the selective reduction of the quinone moiety of **23** using $Na_2S_2O_4$ in THF at room temperature to furnish the corresponding hydroquinone,[27] which was carried on to the next step without chromatographic purification due to its facile autoxidation upon exposure to air (Scheme 7). The treatment of the hydroquinone with TBSOTf in the presence of 2,6-lutidine in CH_2Cl_2 unexpectedly pro-

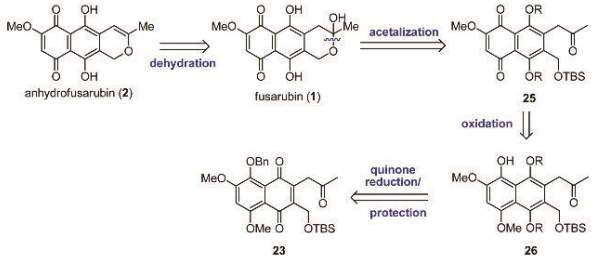

Scheme 6 Retrosynthetic analysis of fusarubin (**1**) and anhydrofusarubin (**2**).

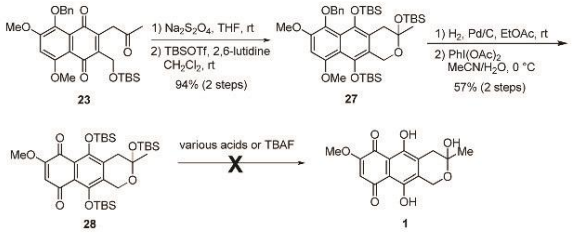

Scheme 7 Attempted synthesis of fusarubin (**1**) *via* TBS protection.

vided pyran TBS ether **27** in 94% yield over two steps. The next task was to selectively oxidize the left-hand ring of **27**. This involved the hydrogenolytic removal of the benzyl protecting group using a Pd/C catalyst to deliver the corresponding unstable naphthol, which was immediately subjected to subsequent oxidation with $PhI(OAc)_2$ under previously described conditions to afford pyranonaphthoquinone **28** in a moderate yield (57% over 2 steps). Compound **28** was then treated with various Brønsted acids *e.g.* HCl, TsOH and AcOH or TBAF in order to mediate global deprotection and concomitant formation of the pyran hemiacetal. Disappointingly, only the decomposition of the starting material or the formation of complex mixtures was observed. Thus, an alternative hydroquinone protecting group was sought.

To circumvent the problems encountered with the TBS protecting group, we decided to switch to the ethoxymethyl (EOM) group which should also be easily removed under acidic conditions.[28] The revised synthesis is described in Scheme 8. The selective reduction of naphthoquinone **23** using $Na_2S_2O_4$ in diethyl ether provided the corresponding hydroquinone in 87% yield. We discovered that using Et_2O as a solvent in this step shortened the reaction time and led to a higher yield of

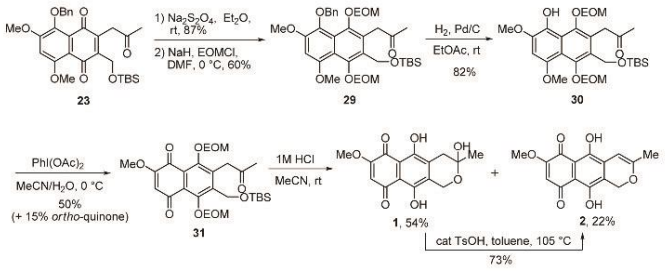

Scheme 8 Completion of the synthesis of fusarubin (**1**) and anhydrofusarubin (**2**).

the hydroquinone product.[29] In addition, despite its facile air oxidation, quick chromatographic purification of the resultant hydroquinone was required because employing the crude hydroquinone directly in the EOM protection step gave a low yield of **29** (22% over two steps). Therefore, after extensive experimentation, subjecting the purified hydroquinone to EOM protection using NaH and EOMCl in DMF at 0 °C delivered the requisite EOM ether **29** in 60% yield (53% over two steps).[30] The benzyl group was then removed under previously described conditions for hydrogenolysis in Scheme 7 to furnish naphthol **30** in 82% yield. The subsequent oxidation of **30** with $PhI(OAc)_2$ under the aforementioned conditions provided the requisite *para*-naphthoquinone **31** in 50% yield along with the *ortho*-naphthoquinone byproduct in 15% yield. However, the *ortho*-quinone byproduct is relatively unstable and decomposes at ambient temperature in a few days. With the requisite naphthoquinone **31** readily available, the final global deprotection of **31** using 1 M HCl in MeCN and concomitant pyran hemiacetal formation was performed to deliver fusarubin (**1**) in 54% yield along with the dehydrated derivative, anhydrofusarubin (**2**), in 22% yield. Compound **1** could be further converted to **2** in 73% yield by treating with catalytic TsOH in toluene at 105 °C. The ^1H and ^{13}C NMR spectroscopic data in the $CDCl_3$ solvent of synthetic **1** and **2** are identical to those reported in the literature.[11,31] However, due to the very low solubility of **1** in $CDCl_3$, we also report herein the ^1H and ^{13}C NMR spectroscopic data of **1** in the DMSO-d_6 solvent. The specific rotation of **1** was observed to be $[\alpha]_D^{26}$ = +4.35 (*c* 0.036, acetone), suggesting that synthetic **1** was also obtained as a scalemic mixture.

The four synthetic naphthoquinones **1–4** were evaluated for their *in vitro* cytotoxic activities against the MCF-7 breast cancer cells as well as against noncancerous Vero cells by a colorimetric method using the resazurin microplate assay (REMA, Table 2). Among the compounds tested, 8-*O*-methylfusarubin (**3**) showed the most potent cytotoxic activity against MCF-7 cells with an IC_{50} value of 1.01 μM and no cytotoxic effect to Vero cells (IC_{50} = 47.49 μM). This observation was consistent with the reported data for the natural product (Fig. 2). Synthetic **1** and **4** showed comparably potent cytotoxic effects against MCF-7 cells with IC_{50} values of 3.19 μM and 2.96 μM, respectively. It is worth noting that the cytotoxicity of synthetic fusarubin (**1**) is greater compared to the reported data of natural **1**. In addition, contrary to the observed cytotoxicity of natural anhydrofusarubin (**2**) (IC_{50} = 0.9 μM), we found that synthetic **2** displayed the least potent cytotoxic effect against MCF-7 cells with an IC_{50} value of 12.28 μM. Nevertheless, these four synthetic analogues exhibited more potent cytotoxic activities compared to those of the standard drugs, doxorubicin and tamoxifen.

To further verify the results of cytotoxic activity against MCF-7 cancer cells using REMA, synthetic compounds **1–4** were subjected to *in vitro* cytotoxic activity evaluation against MCF-7 cancer cells using MTT colorimetric assay (Table 3). We observed a similar trend in the potency of compounds **1–4** against MCF-7 cells compared to REMA *i.e.* compound **3** displayed the most potent cytotoxicity with an IC_{50} value of 2.85 μM. Importantly, compounds **1–4** were tested for MCF-7 cancer cell viability in 3D cancer spheroid models *via* the detection of live and dead cells using a high-content imaging system (Fig. 3). In this assay, compound **3** still showed the highest potency in a long-term effect (day 3). These data suggested that 8-*O*-methylfusarubin (**3**) is the most potent analogue of this series of pyranonaphthoquinones against MCF-7 breast cancer cells and could be a very promising lead compound for anti-breast cancer drug discovery.

Additionally, synthetic analogues **1–4** were further assessed for cytotoxic activities by MTT assay against five other human cancer cell lines including three cervical carcinoma cells (C33A, HeLa and SiHa), one colorectal carcinoma cell (HCT116), and one hepatoma (HepG2) cell as well as noncancerous Vero cells (Table 4). The four synthetic compounds showed an antiproliferative effect against the five cancer cell lines tested with IC_{50} ranges of 4.73–>22.5 μM albeit in a lower extent compared to the standard drug doxorubicin. Notably, compounds **1–4** exhibited significant and comparable cytotoxic effects against the HCT116 colorectal carcinoma cells (IC_{50} = 4.73–6.08 μM) suggesting that the naphthoquinone core might play an important role in this inhibitory effect. Nevertheless, in this MTT assay, synthetic compounds **1–4** displayed a less pronounced selectivity on cancer cells over Vero cells compared to REMA. This might be attributed to the sensitivity of the different cancer and Vero cells to the compounds tested and to the different assays used.

Table 2 Cytotoxic activities of synthetic compounds **1–4** against MCF-7 cancer and Vero cells using the resazurin microplate assay

	Cytotoxicity, IC_{50} (μM)	
Compound	MCF-7 cells	Vero cells
1	3.19	19.36
2	12.28	77.54
3	1.01	47.49
4	2.96	20.54
Doxorubicin	15.25	—
Tamoxifen	17.23	—
Ellipticine	—	3.97

Table 3 Cytotoxic activities of synthetic compounds **1–4** against MCF-7 cancer cells using the MTT and 3D spheroid assays

	Cytotoxicity, IC_{50} (μM)			
		3D cancer spheroid assay		
Compound	MTT assay	Day 1	Day 2	Day 3
1	11.31	18.70	12.50	13.14
2	20.88	57.09	39.67	31.46
3	2.85	4.44	1.83	2.29
4	8.63	25.49	16.42	5.79
Doxorubicin	28.94	—	—	—

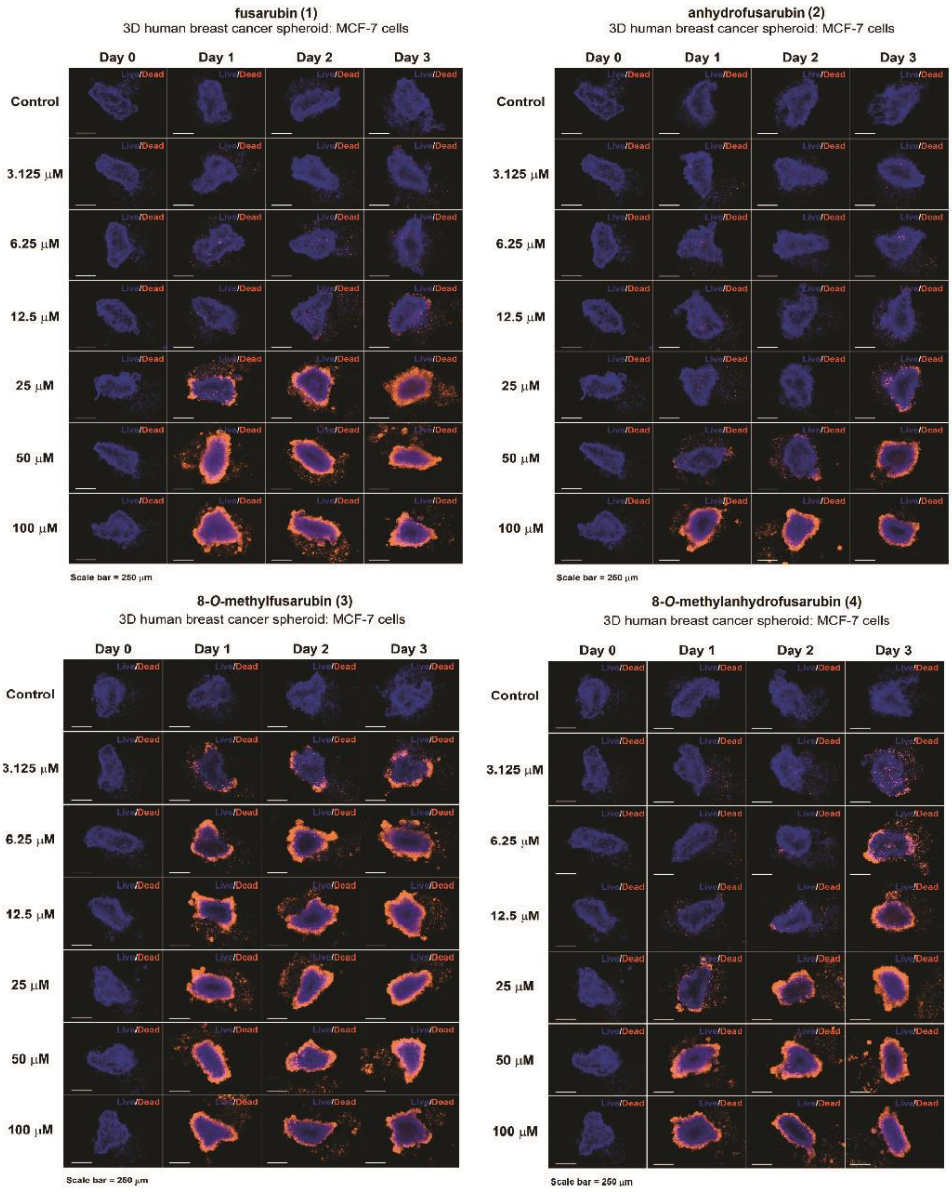

Fig. 3 High-content imaging of synthetic **1–4** on 3D MCF-7 breast cancer spheroids.

Table 4 Cytotoxic activities of synthetic **1–4** against five human cancer cell lines and Vero cells

	Cytotoxicity, IC_{50} (μM)					
Cell lines	**1**	**2**	**3**	**4**	Doxorubicin	Cisplatin
C33A	10.47 ± 3.21	>22.5	7.3 ± 1.08	13.15 ± 0.35	0.14 ± 0.03	7.44 ± 0.77
HeLa	6.98 ± 1.72	14.12 ± 1.86	13.4 ± 5.03	14.6 ± 1.14	0.16 ± 0.01	12.73 ± 6.41
SiHa	6.05 ± 1.74	14.75 ± 3.36	19.8 ± 0.54	6.87 ± 0.33	0.185 ± 0.02	15.33 ± 4.28
HCT116	6.08 ± 1.47	4.87 ± 0.33	5.42 ± 1.43	4.73 ± 2.10	0.23 ± 0.03	>25
HepG2	5.33 ± 0.09	4.87 ± 0.53	12.65 ± 2.87	15.54 ± 2.24	0.66 ± 0.06	>25
Vero	9 ± 0.67	17.92 ± 5.46	17.83 ± 4.73	13.63 ± 2.21	>1	20.13 ± 2.44

Conclusion

We herein report a simple and unified synthesis of four related pyranonaphthoquinone natural products **1–4**. We relied on the precedented Diels–Alder cycloaddition to assemble the naphthalene core. The selective installation of the formyl and acetonyl groups was used to install the three carbons of the pyran rings, which were in turn constructed by intramolecular acetalization. Our work also highlighted an unprecedented directing effect of the hydroxymethylene group in the selective hypervalent iodine-mediated quinone oxidation. Employing this strategy, 8-*O*-methylfusarubin (**3**) and 8-*O*-methylanhydrofusarubin (**4**) have been synthesized from Green's intermediate **7** in 5 and 6 steps in 41% and 28% overall yields, respectively. By the manipulation of the oxidation state of the naphthoquinone nuclei from the syntheses of **3** and **4**, fusarubin (**1**) and anhydrofusarubin (**2**) could be synthesized from **7** in 8 steps with 9% and 4% overall yields, respectively. The four synthetic compounds were evaluated for their cytotoxic activities against six human cancer cells using the resazurin microplate and MTT assays. 8-*O*-Methylfusarubin (**3**) was the most potent analogue and displayed excellent cytotoxic activity against MCF-7 breast cancer cells with an IC_{50} value of 1.01 μM with no cytotoxic effect on noncancerous Vero cells as determined by REMA. The four synthetic compounds also showed an antiproliferative effect against other five cancer cell lines tested with IC_{50} ranges of 4.73– >22.5 μM as determined by MTT assay.

Conflicts of interest

There are no conflicts of interest to declare.

Acknowledgements

This work was supported by The NSTDA Chair Professor grant (the Fourth Grant) of the Crown Property Bureau and the National Science and Technology Development Agency to Professor V. Rukachaisirikul. P. V. thanks the Faculty of Science Research Fund, Prince of Songkla University for research assistantship (Contract No. 1-2559-02-004). The Graduate School, Prince of Songkla University, and the Center of Excellence for Innovation in Chemistry (PERCH-CIC), Ministry of Higher Education, Science, Research and Innovation, are gratefully acknowledged for partial support.

Notes and references

1 (*a*) L. Ramos-Peralta, L. I. López-López, S. Y. Silva-Belmares, A. Zugasti-Cruz, R. Rodríguez-Herrera and C. N. Aguilar-González, in *The Battle Against Microbial Pathogens: Basic Science, Technological Advances and Educational Programs*, ed. A. Méndez-Vilas, Formatex Research Center, Spain, 2015, vol. 1, pp. 542–550; (*b*) Y. Kumagai, Y. Shinkai, T. Miura and A. K. Cho, *Annu. Rev. Pharmacol. Toxicol.*, 2012, **52**, 221–247.

2 M. A. Brimble, L. J. Duncalf and M. R. Nairn, *Nat. Prod. Rep.*, 1999, **16**, 267–281.

3 R. A. Baker, J. H. Tatum and S. Nemec Jr., *Mycopathologia*, 1990, **111**, 9–15.

4 (*a*) J. Sperry, P. Bachu and M. A. Brimble, *Nat. Prod. Rep.*, 2008, **25**, 376–400; (*b*) B. J. Naysmith, P. A. Hume, J. Sperry and M. A. Brimble, *Nat. Prod. Rep.*, 2017, **34**, 25–61; (*c*) K. P. Kumar, K. Javvaji, Y. Poornachandra, A. D. Allanki and S. Misra, *J. Microbiol. Res.*, 2017, **7**, 23–30.

5 V. H. W. Ruelius and A. Gauhe, *Justus Liebigs Ann. Chem.*, 1950, **569**, 38–59.

6 J. H. Tatum and R. A. Baker, *Phytochemistry*, 1983, **22**, 543–547.

7 K. Trisuwan, N. Khamthong, V. Rukachaisirikul, S. Phongpaichit, S. Preedanon and J. Sakayaroj, *J. Nat. Prod.*, 2010, **73**, 1507–1511.

8 P. S. Steyn, P. S. Wessels and W. F. O. Marasas, *Tetrahedron*, 1979, **35**, 1551–1555.

9 Unpublished results.

10 J. H. Tatum, R. A. Baker and R. E. Berry, *Phytochemistry*, 1985, **24**, 457–459.

11 A. Pillay, A. L. Rousseau, M. A. Fernandes and C. B. de Koning, *Org. Biomol. Chem.*, 2012, **10**, 7809–7819.

12 R. G. F. Giles, I. R. Green and N. van Eeden, *Synth. Commun.*, 2006, **36**, 1695–1706.

13 See the ESI for detailed experimental data.†

14 A. Toy, T. A. Scahill and A. Yamashita, *J. Org. Chem.*, 1989, **54**, 3625–3634.

15 A. N. Lowell, M. W. Fennie and M. C. Kozlowski, *J. Org. Chem.*, 2008, **73**, 1911–1918.

16 A. Thiraporn, V. Rukachaisirikul, P. Iawsipo, T. Somwang and K. Tadpetch, *Eur. J. Org. Chem.*, 2017, 7133–7147.

17 Assignment of the methoxy groups at C-2 (δ 4.05) and C-4 (δ 4.00) was based on nOe enhancements by irradiations of the aromatic methine proton at H-3 (δ 6.81). Assignment of the methoxy group at C-8 (δ 3.88) was based on nOe enhancement by irradiation of the aromatic methine proton at H-7 (δ 7.13).

18 (*a*) S. Kotha, V. R. Aswar and A. Manchoju, *Tetrahedron*, 2016, **72**, 2306–2315; (*b*) R. G. F. Giles, I. R. Green and N. van Eeden, *Synthesis*, 2004, 1601–1608.

19 (*a*) J.-h. Cui, W. Zhou and S.-s. Li, *J. Chem. Res.*, 2012, 264–265; (*b*) W. R. Roush and R. J. Neitz, *J. Org. Chem.*, 2004, **69**, 4906–4912; (*c*) C.-j. Sie, V. Patteti, Y.-R. Yang and K.-K. T. Mong, *Chem. Commun.*, 2018, **54**, 1885–1888.

20 (*a*) G. Jones and S. P. Stanforth, in *Organic Reactions*, ed. L. A. Paquette, John Wiley & Sons, Inc., 1997, vol. 49, pp. 1–330; (*b*) Y. Tanoue, A. Terada and Y. Matsumoto, *Bull. Chem. Soc. Jpn.*, 1989, **62**, 2736–2738; (*c*) J. Lin, W. Zhang, N. Jiang, Z. Niu, K. Bao, L. Zhang, D. Liu, C. Pan and X. Yao, *J. Nat. Prod.*, 2008, **71**, 1938–1941; (*d*) D. Maes, S. Vervisch, S. Debenedetti, C. Davio, S. Mangelinckx, N. Giubellina and N. De Kimpe, *Tetrahedron*, 2005, **61**, 2505–2511.

21 (*a*) C. B. de Koning, R. G. F. Giles, L. M. Engelhardt and A. H. White, *J. Chem. Soc., Perkin Trans. 1*, 1988, 3209–3216; (*b*) C.-L. Lee, K. Nakagawa-Goto, D. Yu, Y.-N. Liu, K. F. Bastow, S. L. Morris-Natschke, F.-R. Chang, Y.-C. Wu and K.-H. Lee, *Bioorg. Med. Chem. Lett.*, 2008, **18**, 4275–4277; (*c*) M. A. Brimble, N. P. S. Hassan, B. J. Naysmith and J. Sperry, *J. Org. Chem.*, 2014, **79**, 7169–7178; (*d*) J. E. Y. Sumani, K. J. Ngwira, A. Lemmerer and C. B. de Koning, *Eur. J. Org. Chem.*, 2019, 1145–1153.

22 (*a*) V. V. Zhdankin, *ARKIVOC*, 2009, 1–62; (*b*) A. Yoshimura and V. V. Zhdankin, *Chem. Rev.*, 2016, **116**, 3328–3435; (*c*) T. Dohi and Y. Kita, *Chem. Commun.*, 2009, 2073–2085.

23 B. Kesteleyn, L. Van Puyvelde and N. De Kimpe, *J. Org. Chem.*, 1999, **64**, 438–440.

24 T. A. D. Thi, T. H. V. Thi, H. T. Phuong, T. H. Nguyen, C. P. The, C. V. Duc, Y. Depetter, M. D'hooghe and T. V. Nguyen, *Bioorg. Med. Chem. Lett.*, 2015, **25**, 3355–3358.

25 L. Studt, P. Wiemann, K. Kleigewe, H.-U. Humpf and B. Tudzynski, *Appl. Environ. Microbiol.*, 2012, **78**, 4468–4480.

26 M. Masi, S. Meyer, M. Górecki, G. Pescitelli, S. Clement, A. Cimmino and A. Evidente, *Molecules*, 2018, **23**, 1734.

27 J. Padwal, W. Lewis and C. J. Moody, *J. Org. Chem.*, 2011, **76**, 8082–8087.

28 (*a*) X. Cai, K. Ng, H. Panesar, S.-J. Moon, M. Paredes, K. Ishida, C. Hertweck and T. G. Minehan, *Org. Lett.*, 2014, **16**, 2962–2965; (*b*) N. V. S. Mudiganti, S. Claessens, P. Habonimana and N. De Kimpe, *J. Org. Chem.*, 2008, **73**, 3867–3874; (*c*) T. Taguchi, Y. Suda, A. Hosoda and Y. Kobayashi, *Tetrahedron Lett.*, 1988, **29**, 5765–5766; (*d*) G. A. Guerrero-Vásquez, N. Chinchilla, J. M. G. Molinillo and F. A. Macías, *J. Nat. Prod.*, 2014, **77**, 2029–2036.

29 Y. Suhara, M. Watanabe, S. Motoyoshi, K. Nakagawa, A. Wada, K. Takeda, K. Takahashi, H. Tokiwa and T. Okano, *J. Med. Chem.*, 2011, **54**, 4918–4922.

30 C.-Y. Peng, J.-Y. Shen, Y.-T. Chen, P.-J. Wu, W.-Y. Hung, W.-P. Hu and P.-T. Chou, *J. Am. Chem. Soc.*, 2015, **137**, 14349–14357.

31 N. S. Chowdhury, Md. H. Sohrab, Md. S. Rana, C. M. Hasan, S. Jamshidi and K. M. Rahman, *J. Nat. Prod.*, 2017, **80**, 1173–1177.

^{1}H and ^{13}C NMR Spectra

Figure 8 ^{1}H NMR (300 MHz, $CDCl_3$) spectrum of compound **98**

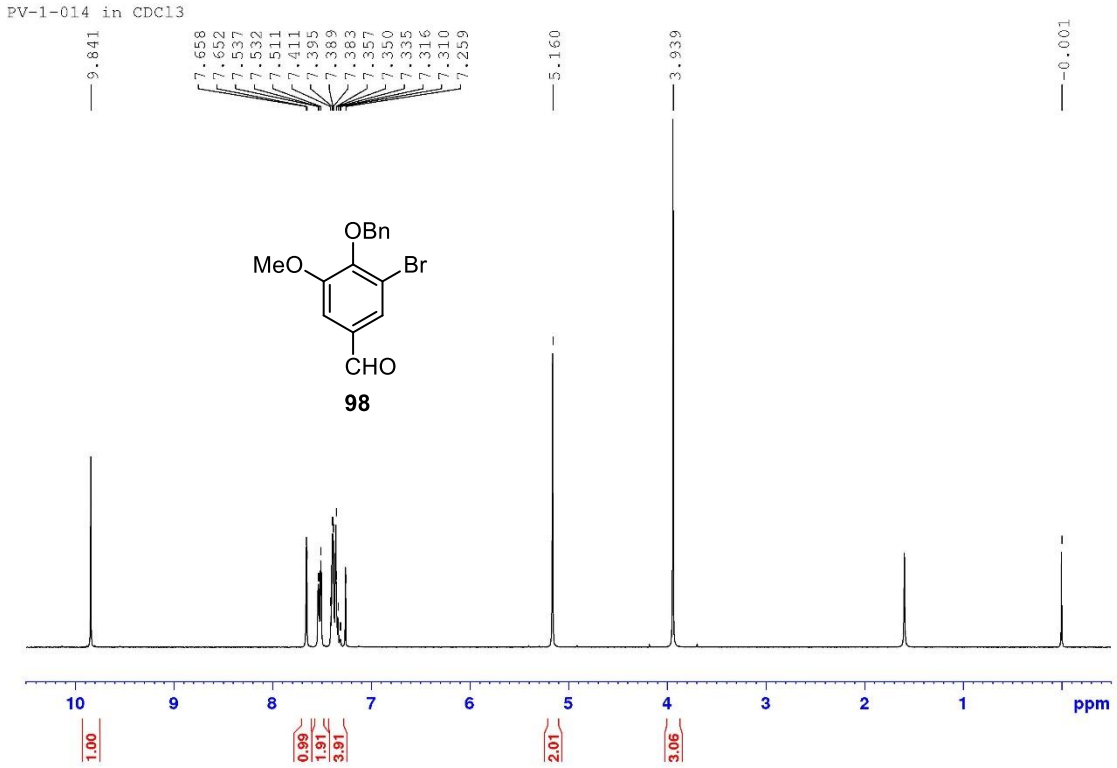

Figure 9 ^{13}C NMR (75 MHz, $CDCl_3$) spectrum of compound **98**

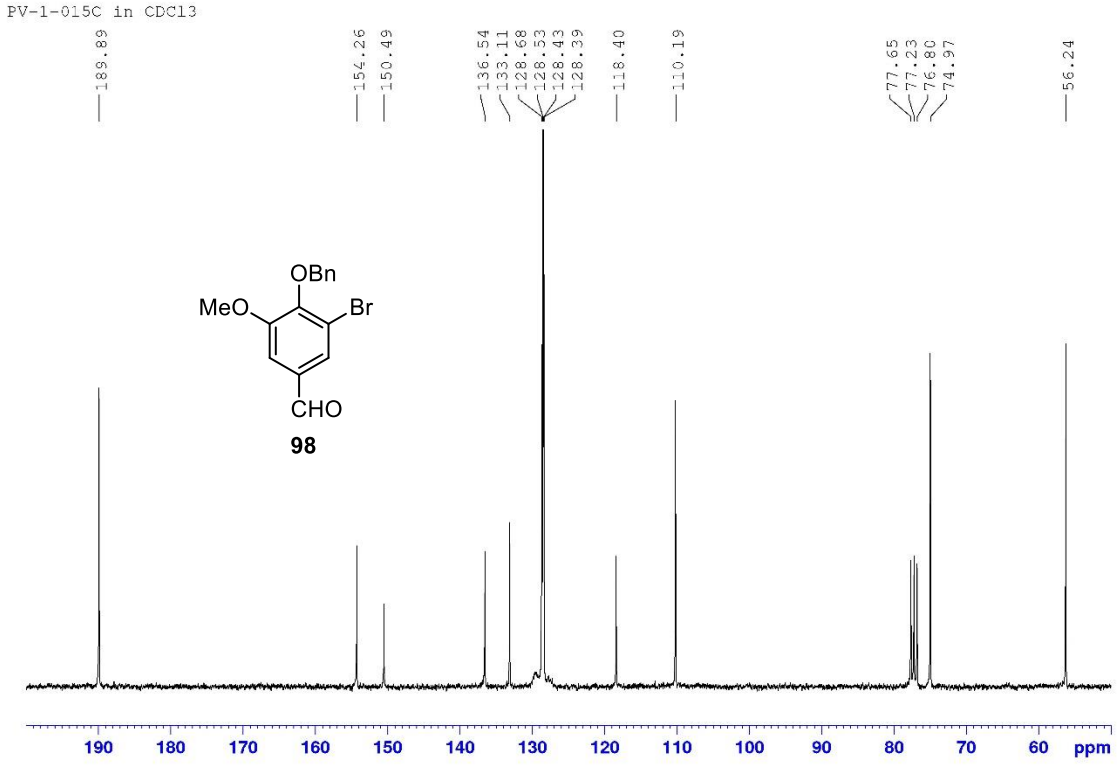

Figure 10 ^{1}H NMR (300 MHz, $CDCl_3$) spectrum of compound **99**

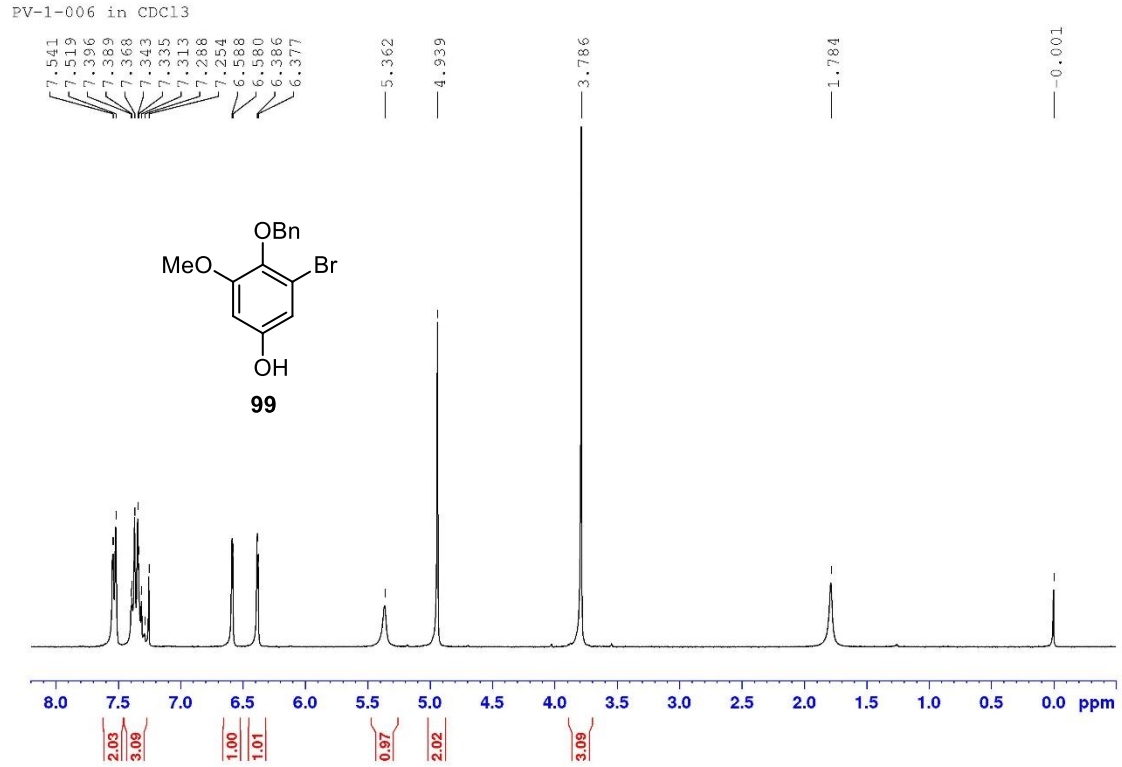

Figure 11 ^{13}C NMR (75 MHz, $CDCl_3$) spectrum of compound **99**

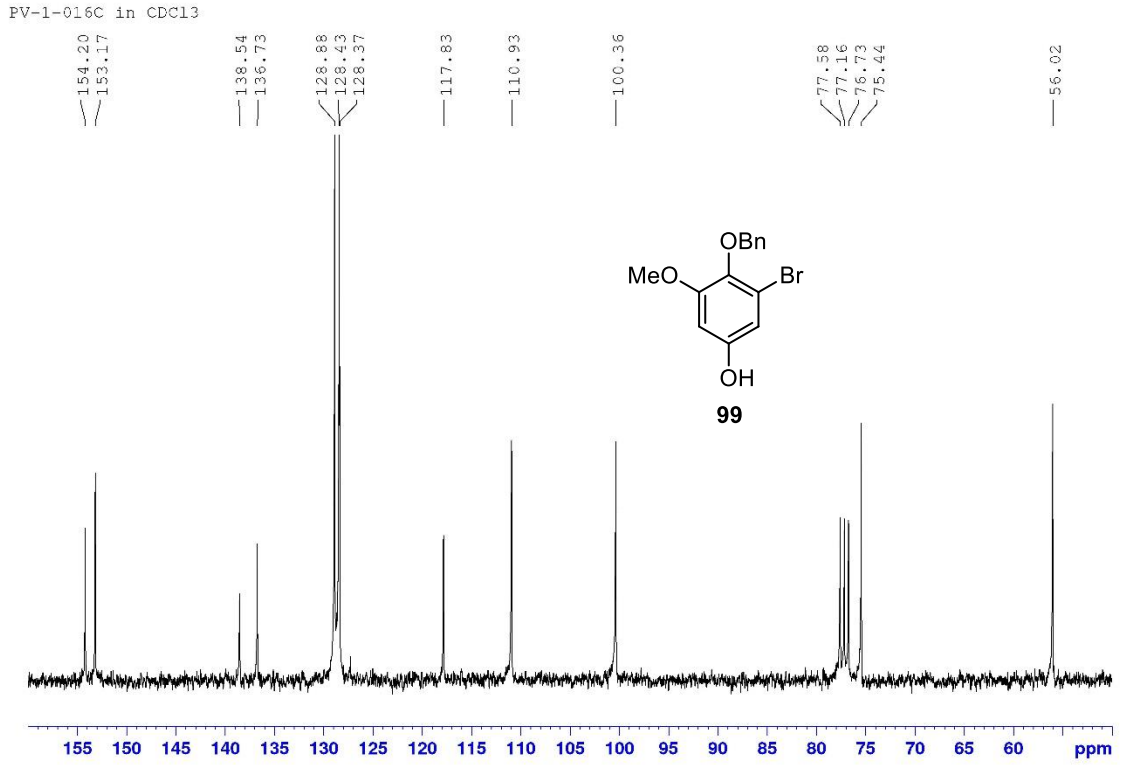

Figure 12 ^{1}H NMR (300 MHz, $CDCl_3$) spectrum of compound **100**

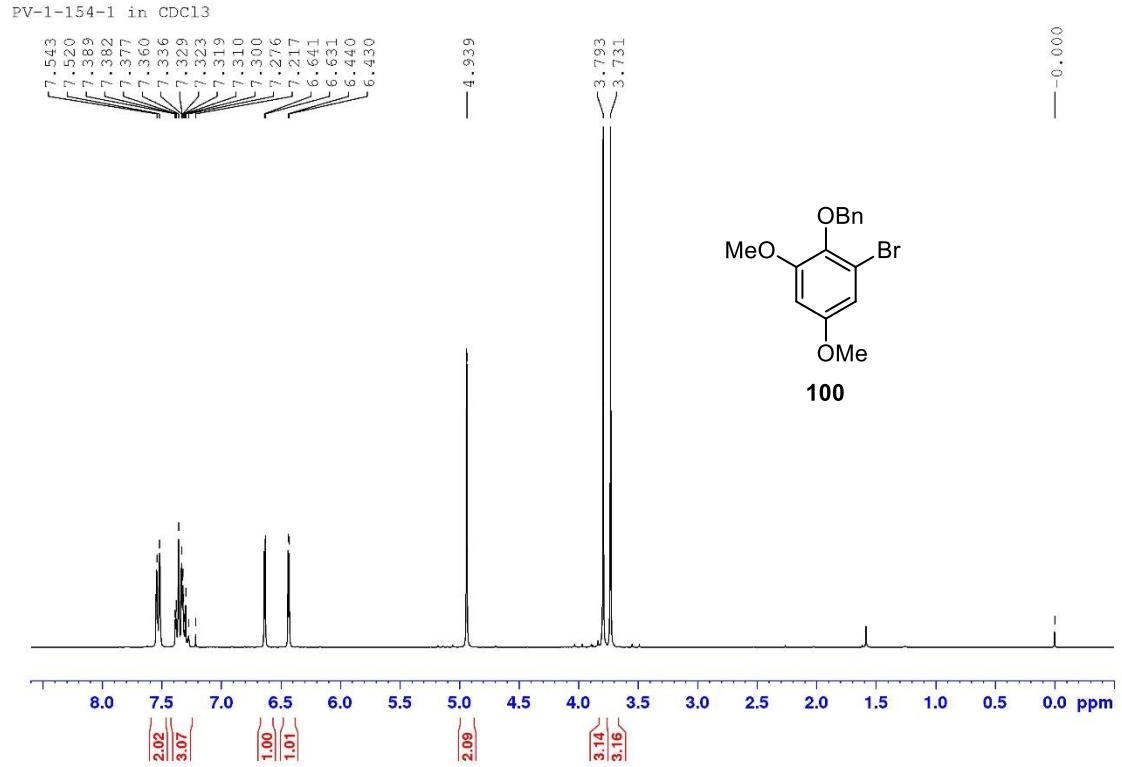

Figure 13 ^{13}C NMR (75 MHz, $CDCl_3$) spectrum of compound **100**

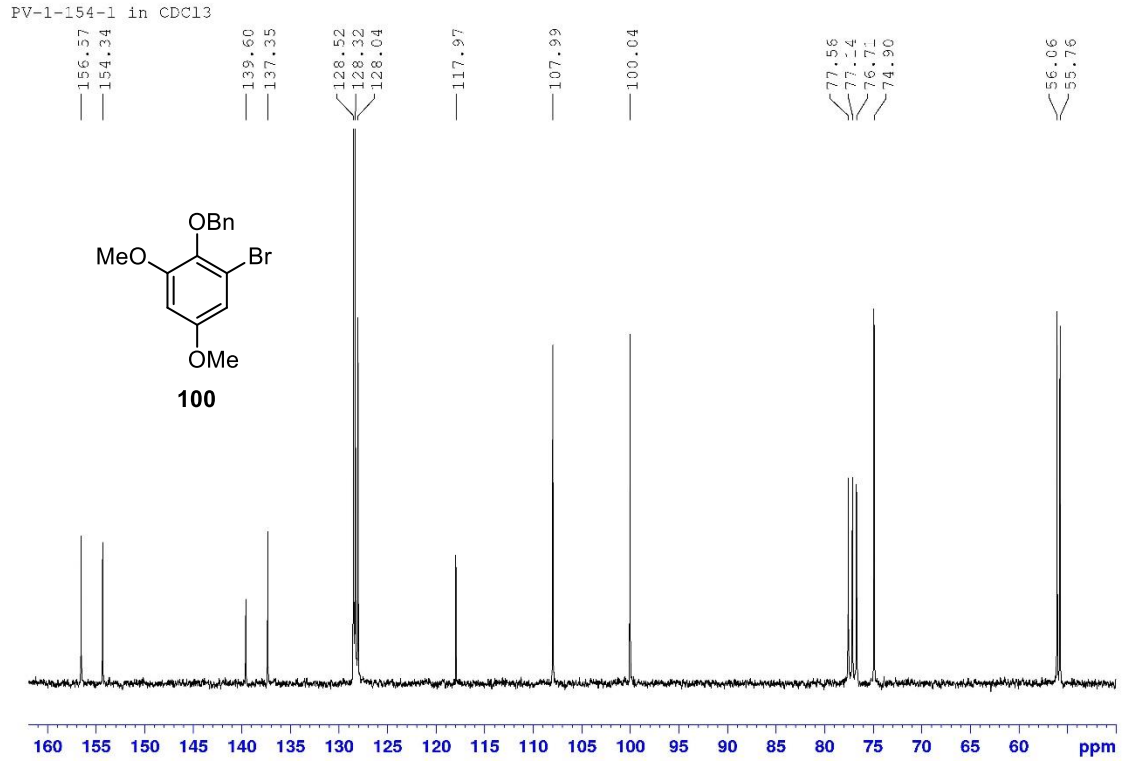

Figure 14 ^{1}H NMR (300 MHz, $CDCl_3$) spectrum of compound **101**

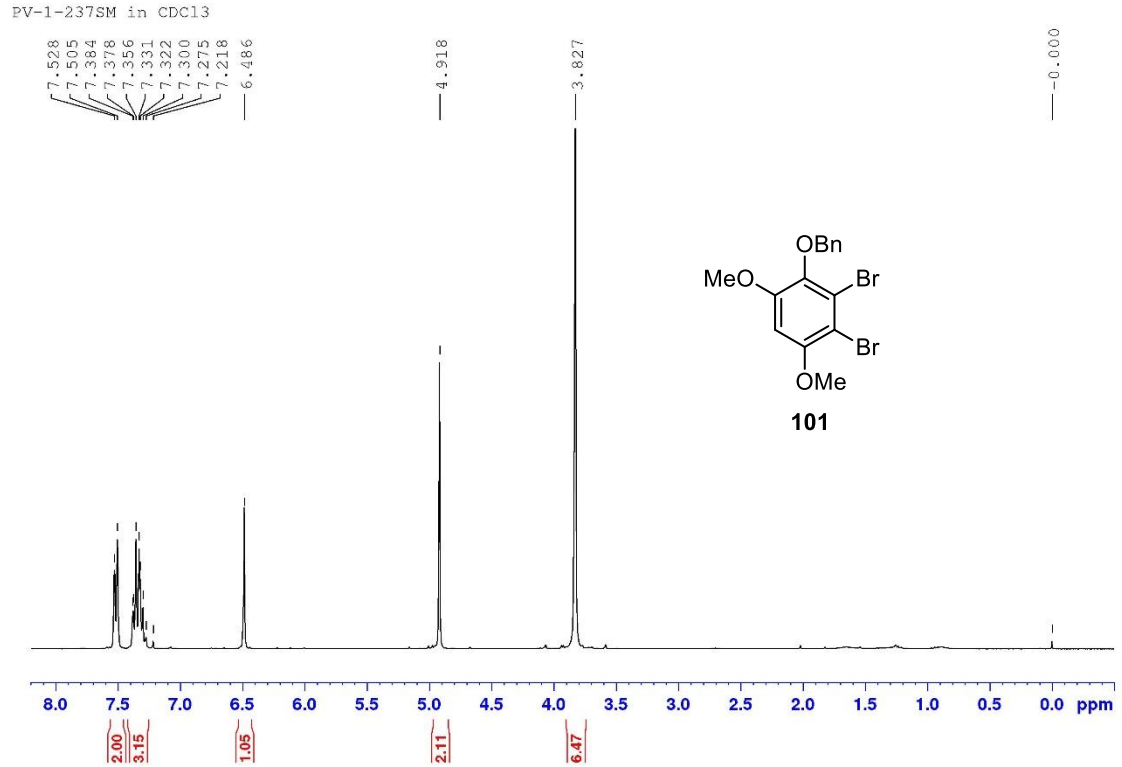

Figure 15 ^{13}C NMR (75 MHz, $CDCl_3$) spectrum of compound **101**

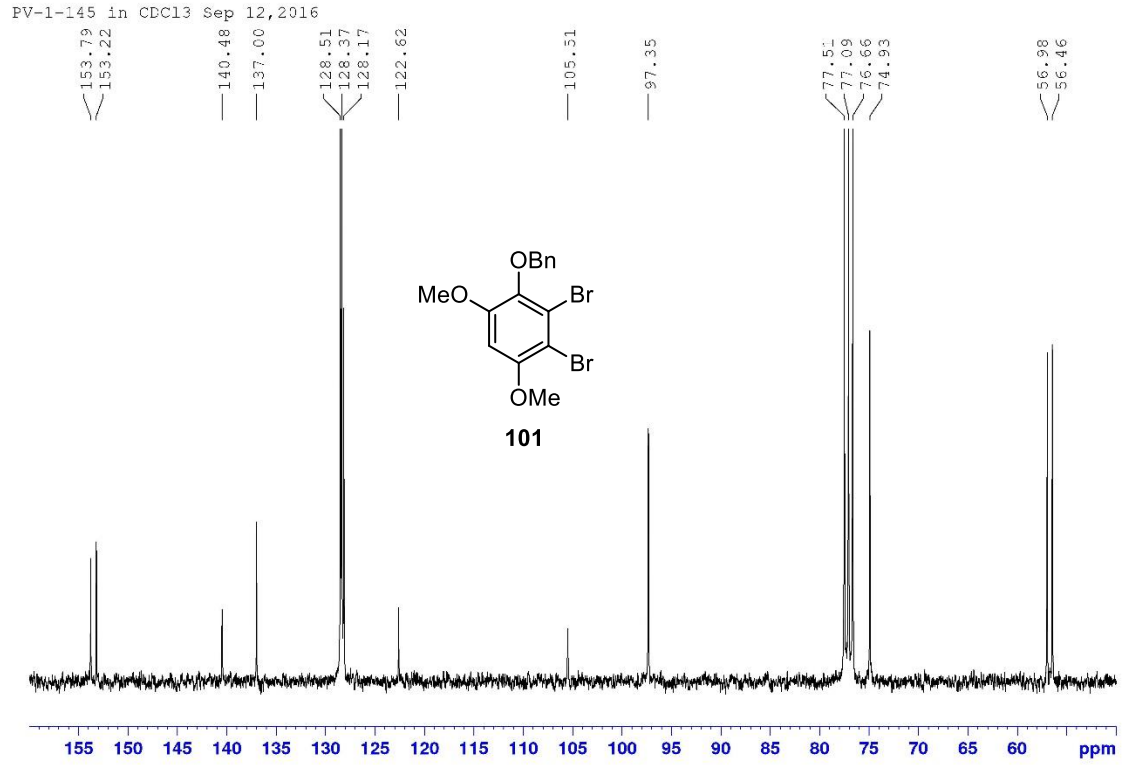

Figure 16 ^{1}H NMR (300 MHz, $CDCl_3$) spectrum of compounds **103** and **104**

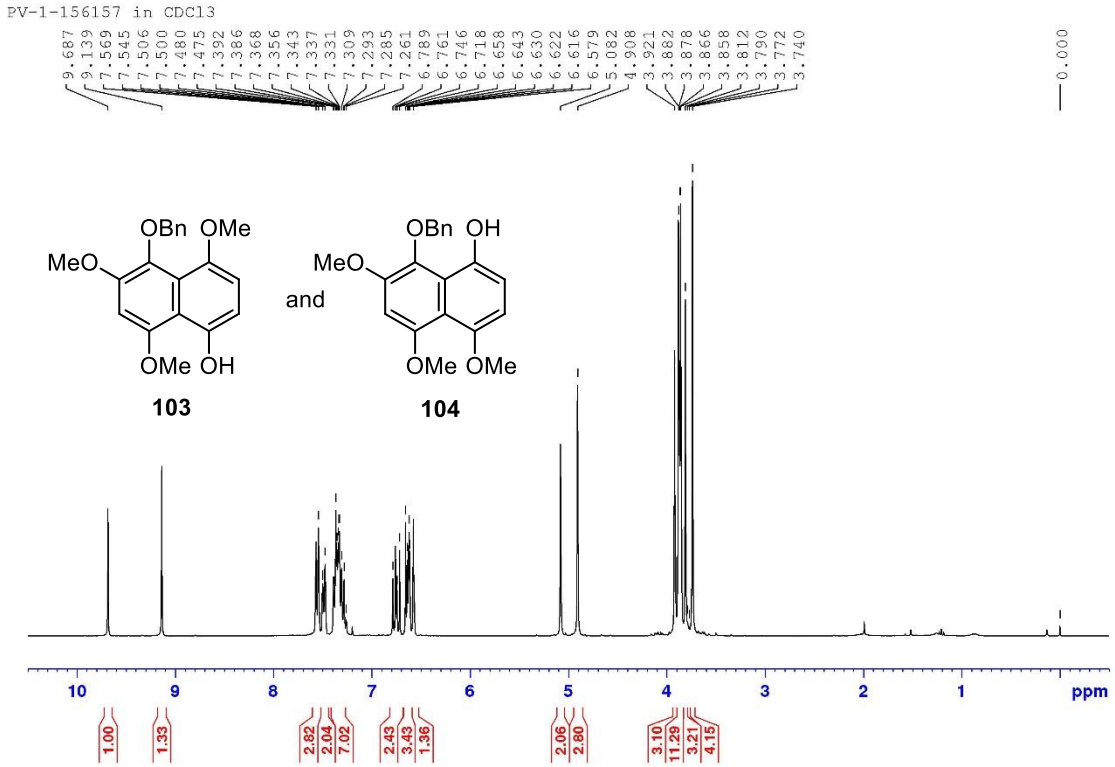

Figure 17 ^{13}C NMR (75 MHz, $CDCl_3$) spectrum of compounds **103** and **104**

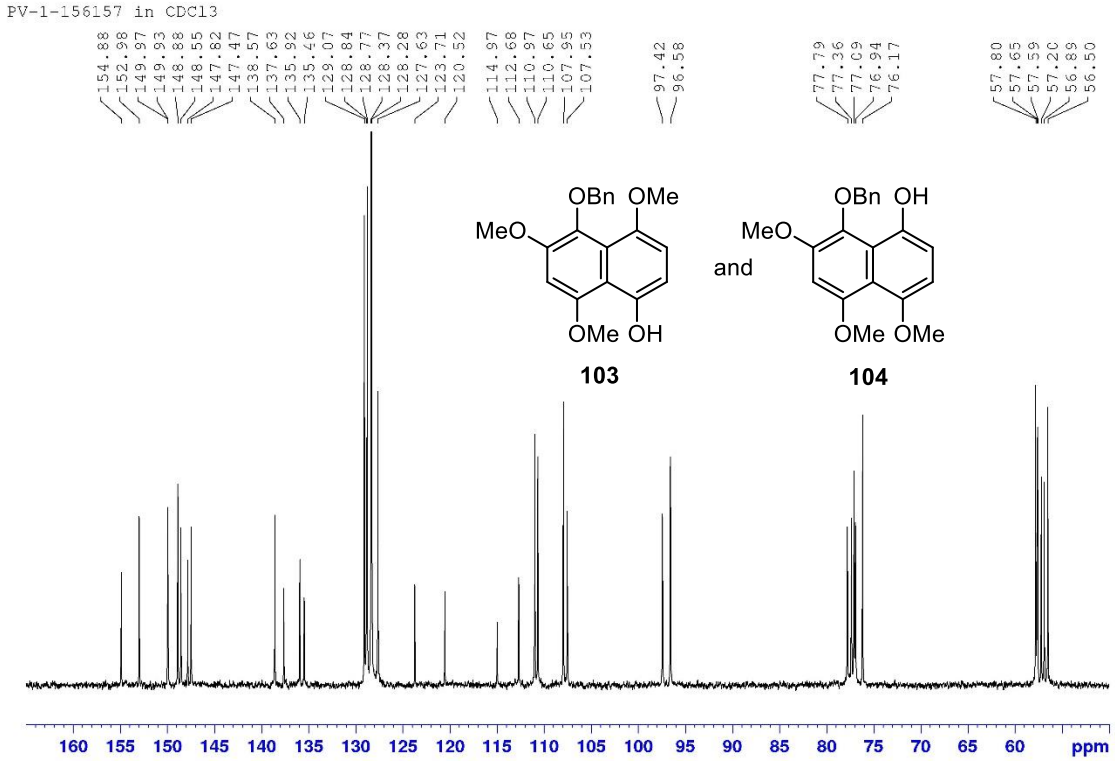

Figure 18 ^{1}H NMR (300 MHz, $CDCl_3$) spectrum of compound **96**

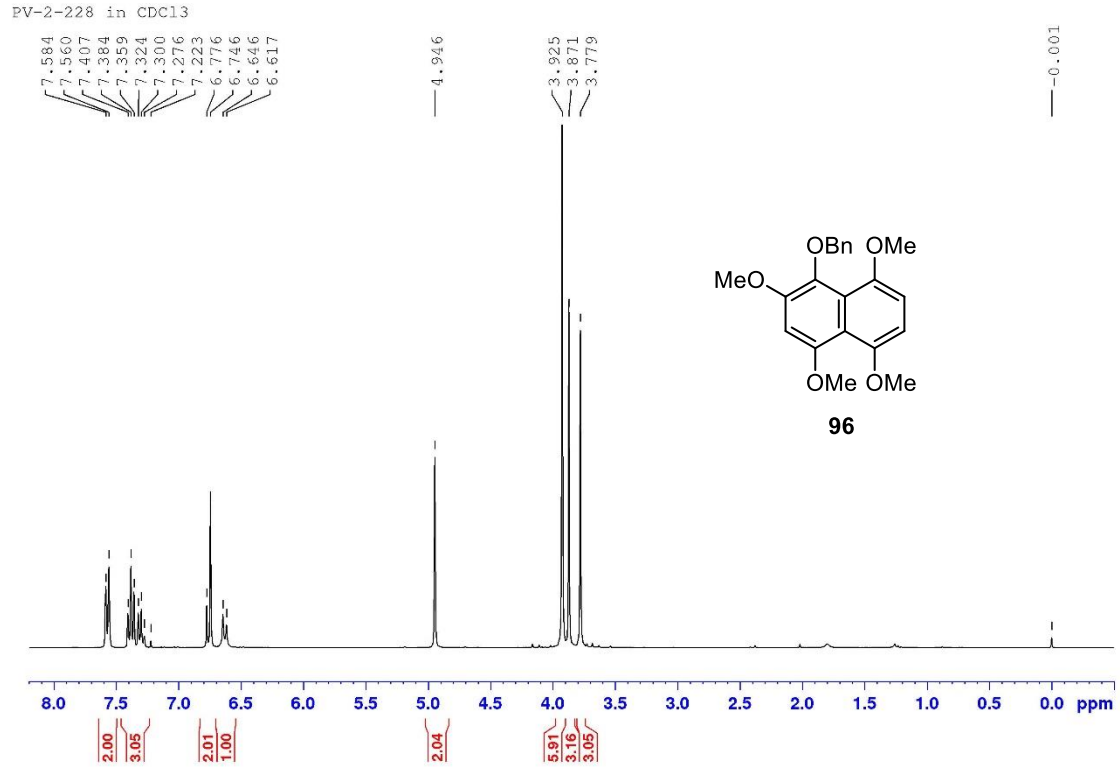

Figure 19 ^{13}C NMR (75 MHz, $CDCl_3$) spectrum of compound **96**

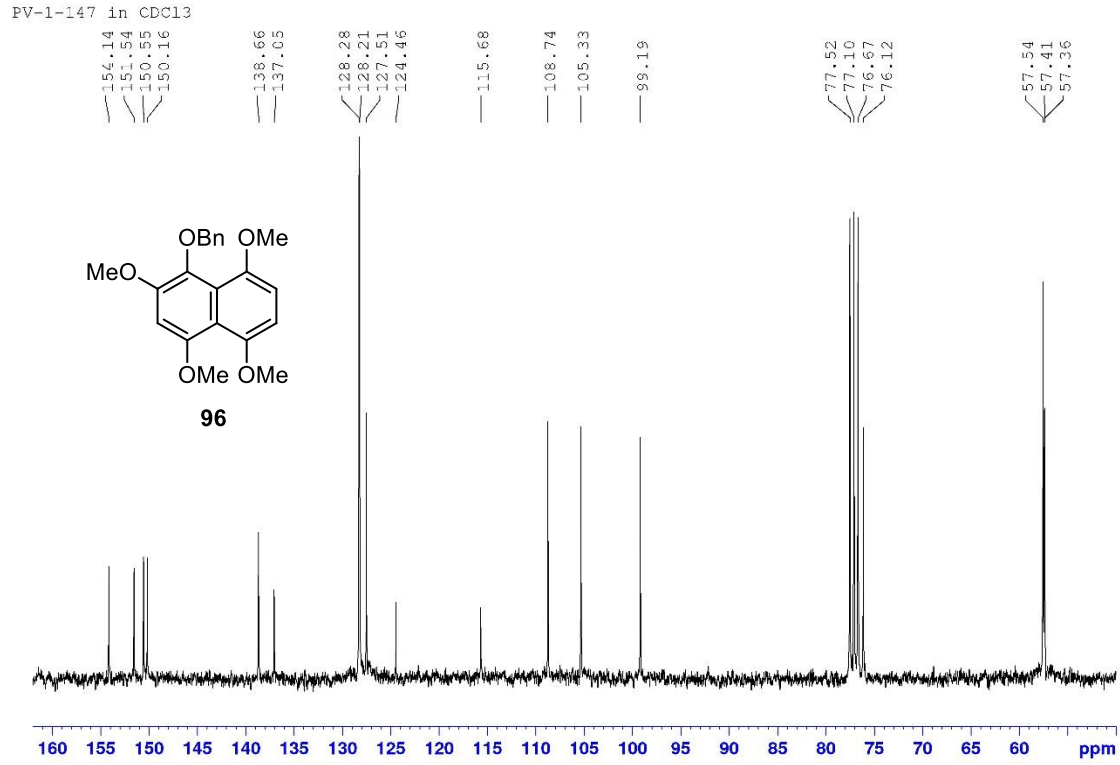

Figure 20 ^{1}H NMR (300 MHz, $CDCl_3$) spectrum of compound **107**

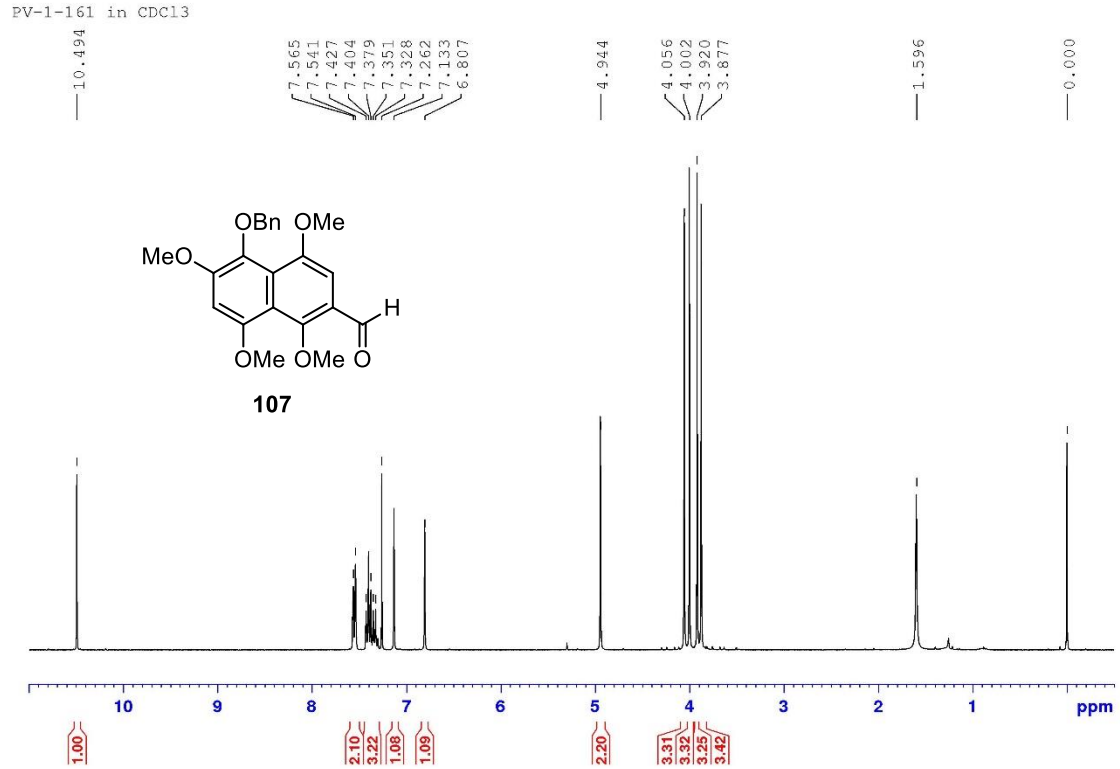

Figure 21 ^{13}C NMR (75 MHz, $CDCl_3$) spectrum of compound **107**

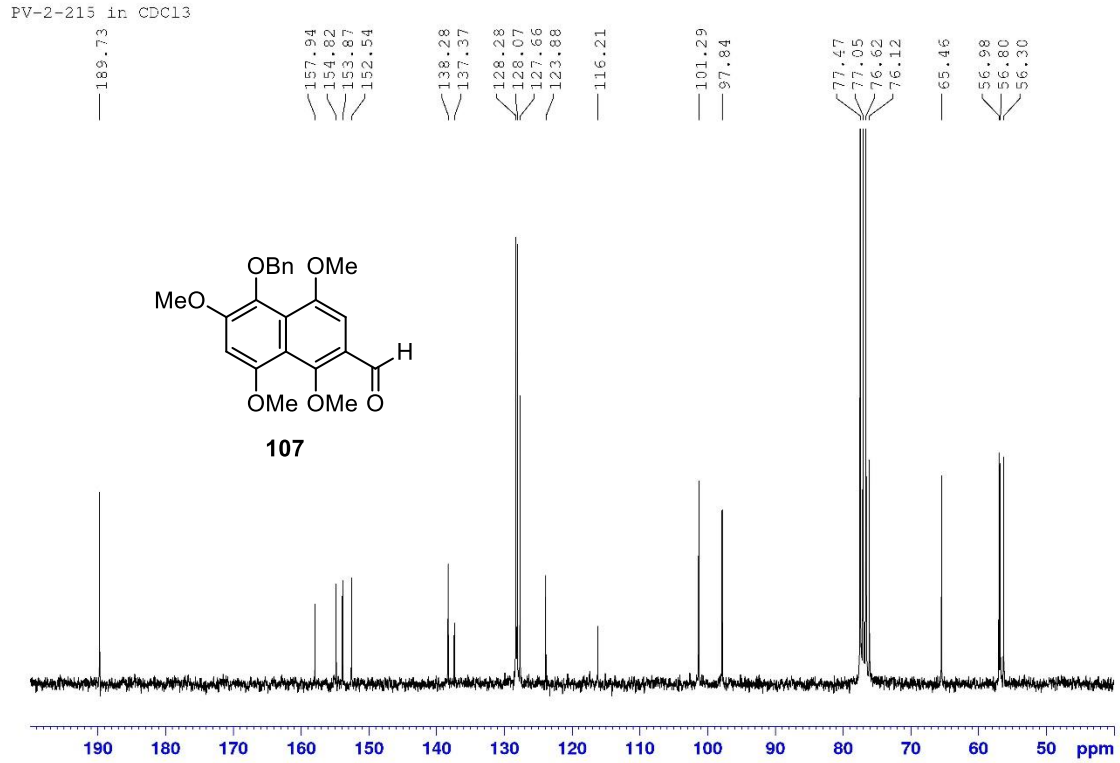

Figure 22 ^{1}H NMR (300 MHz, $CDCl_3$) spectrum of compound **108**

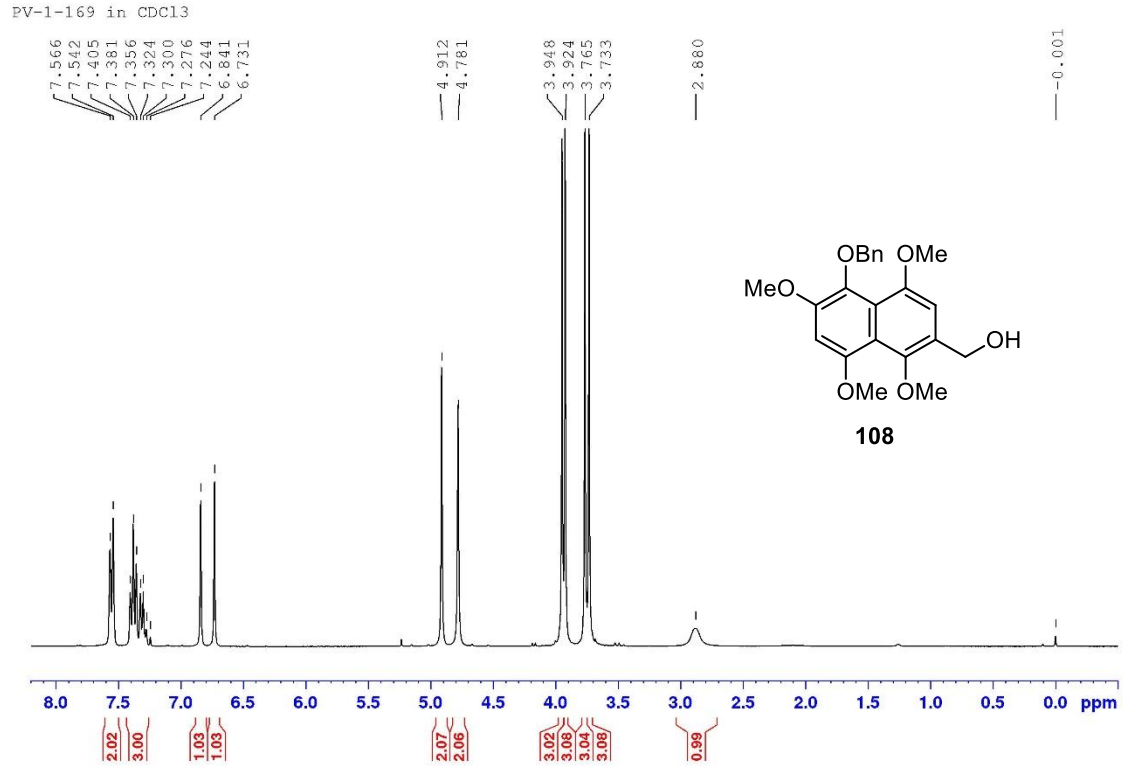

Figure 23 ^{13}C NMR (75 MHz, $CDCl_3$) spectrum of compound **108**

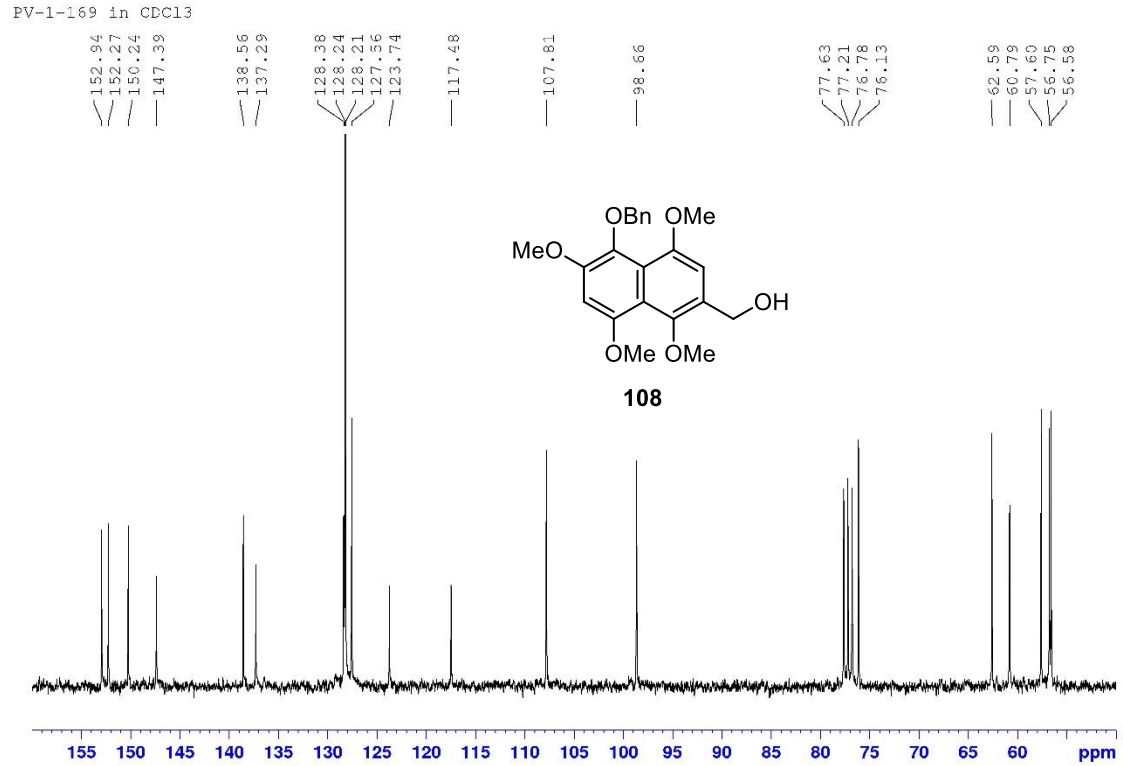

Figure 24 ^{1}H NMR (300 MHz, DMSO-d_6) spectrum of compound **113**

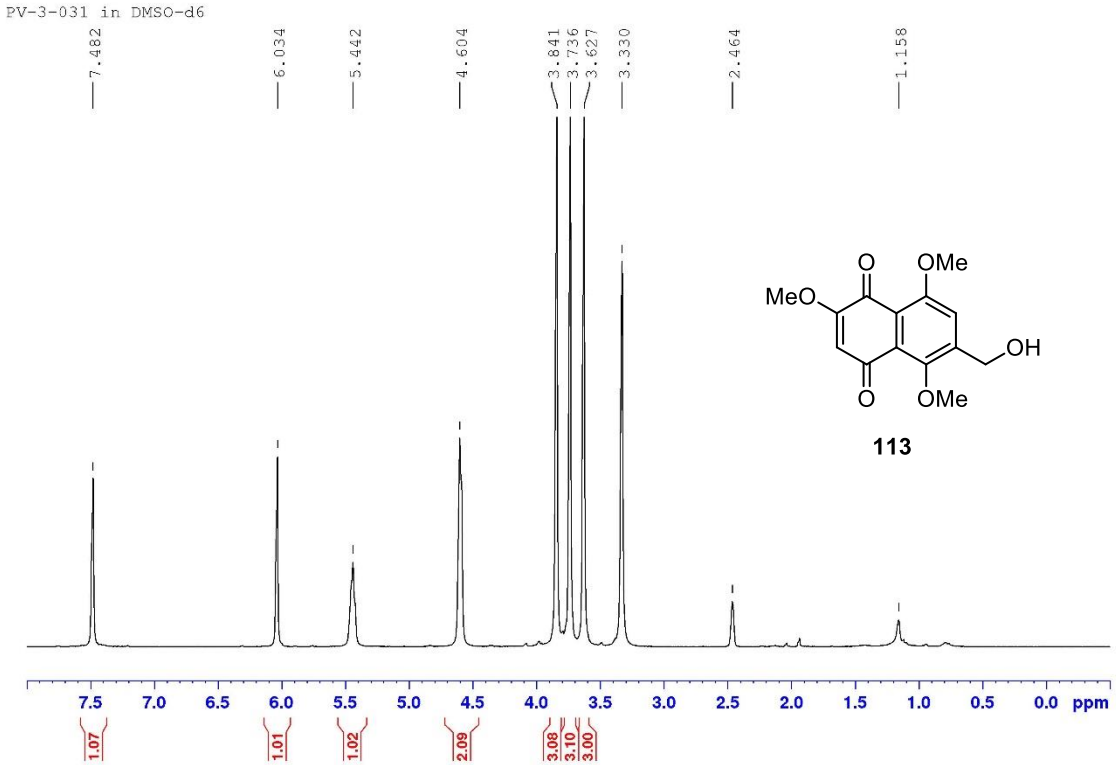

Figure 25 ^{13}C NMR (75 MHz, DMSO-d_6) spectrum of compound **113**

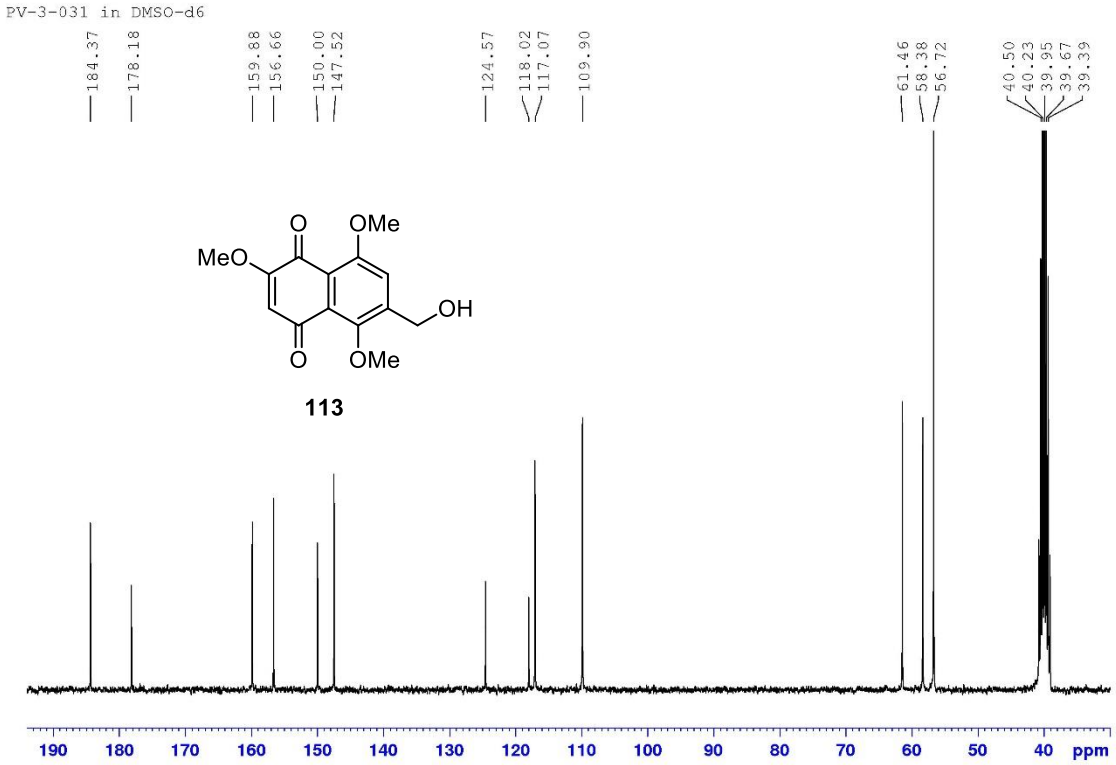

Figure 26 ^{1}H NMR (300 MHz, $CDCl_3$) spectrum of compound **115**

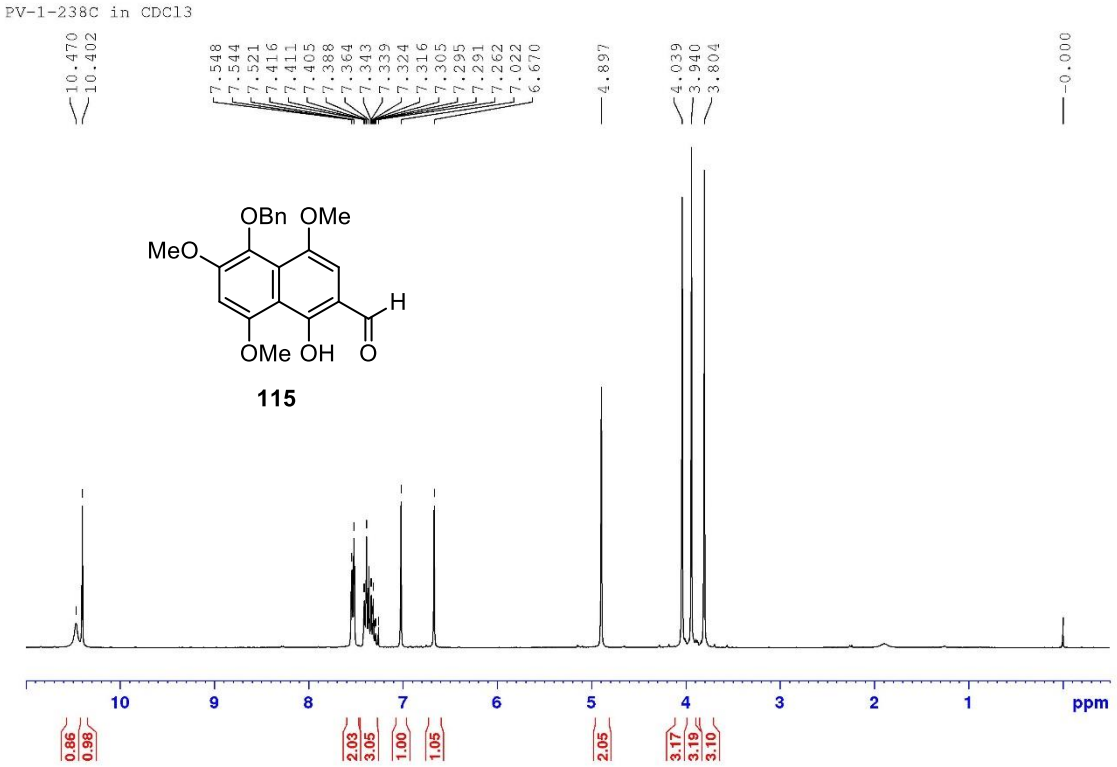

Figure 27 ^{13}C NMR (75 MHz, $CDCl_3$) spectrum of compound **115**

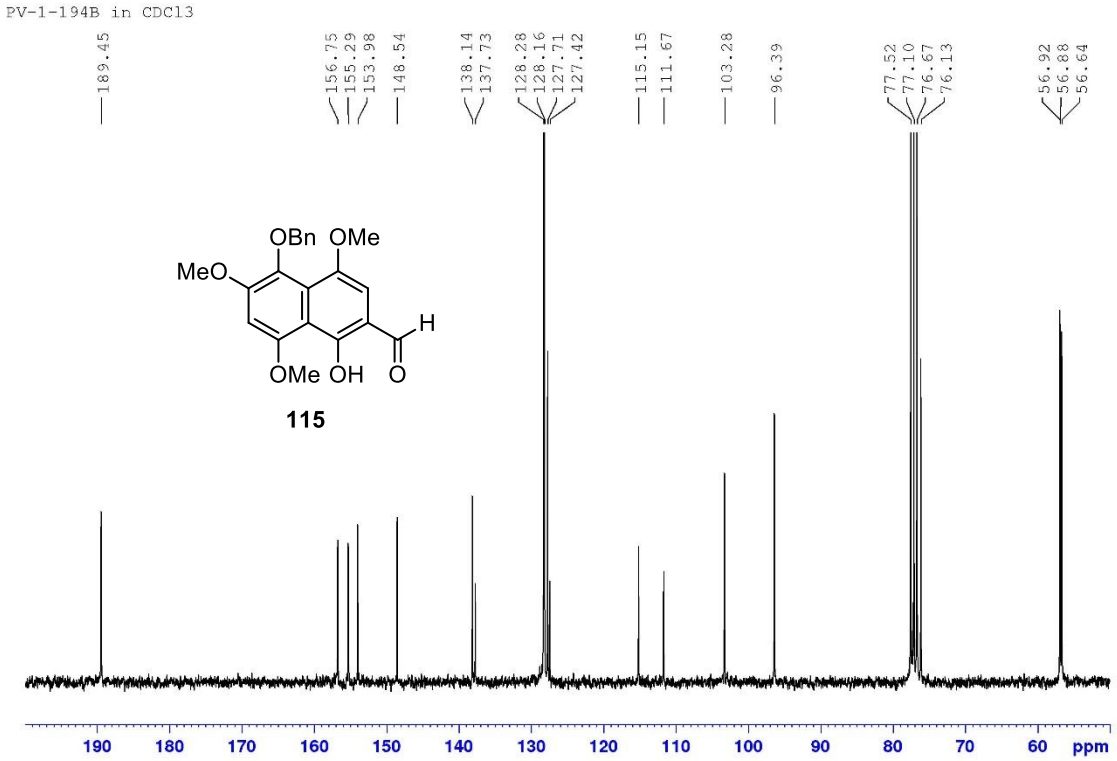

Figure 28 ^{1}H NMR (300 MHz, $CDCl_3$) spectrum of compound **116**

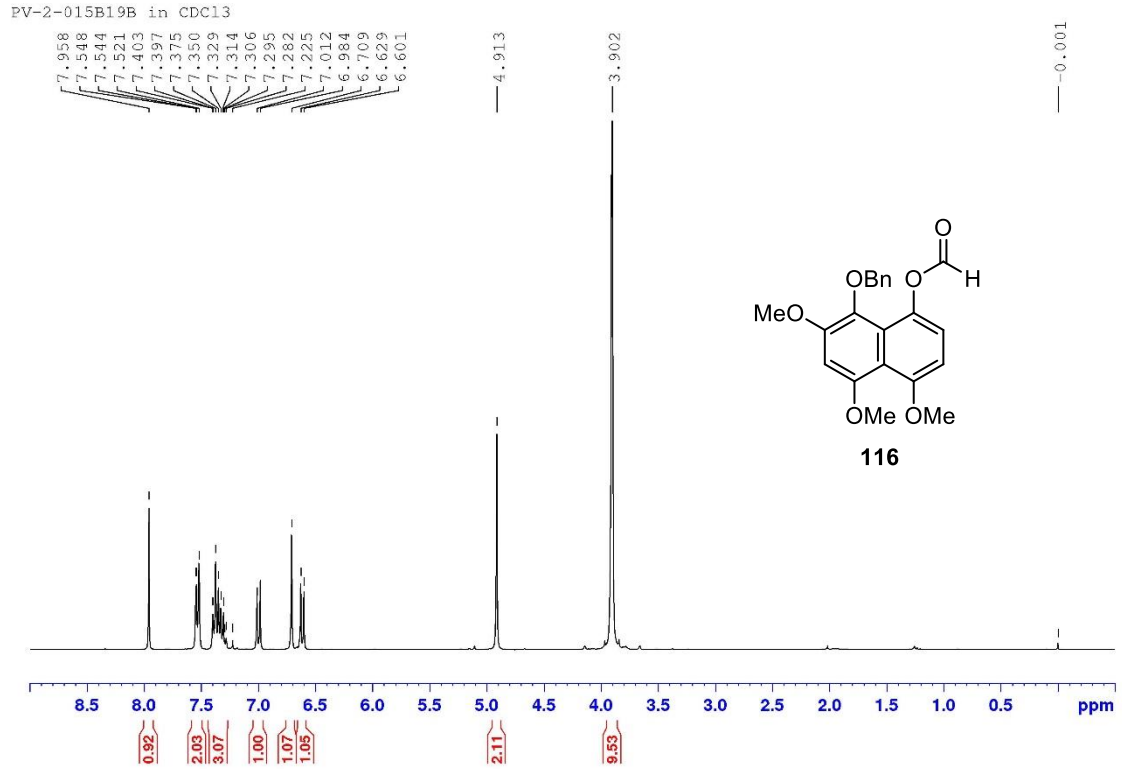

Figure 29 ^{13}C NMR (75 MHz, $CDCl_3$) spectrum of compound **116**

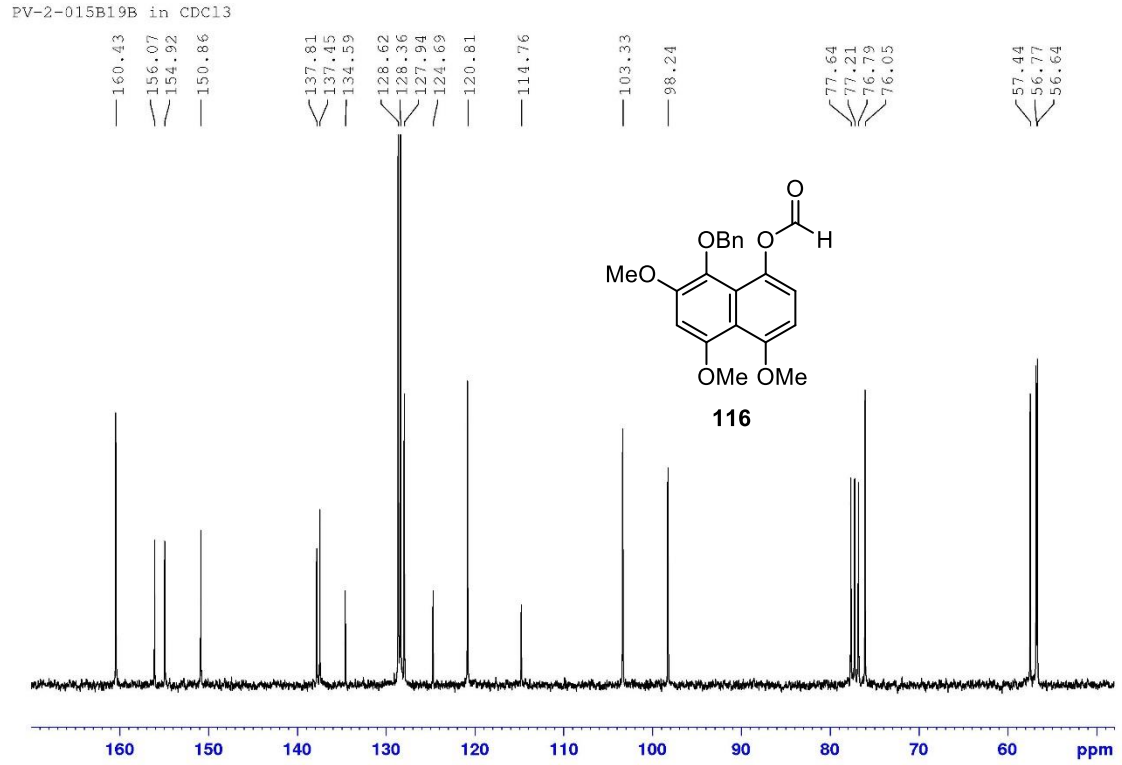

Figure 30 ^{1}H NMR (300 MHz, $CDCl_3$) spectrum of compound **104**

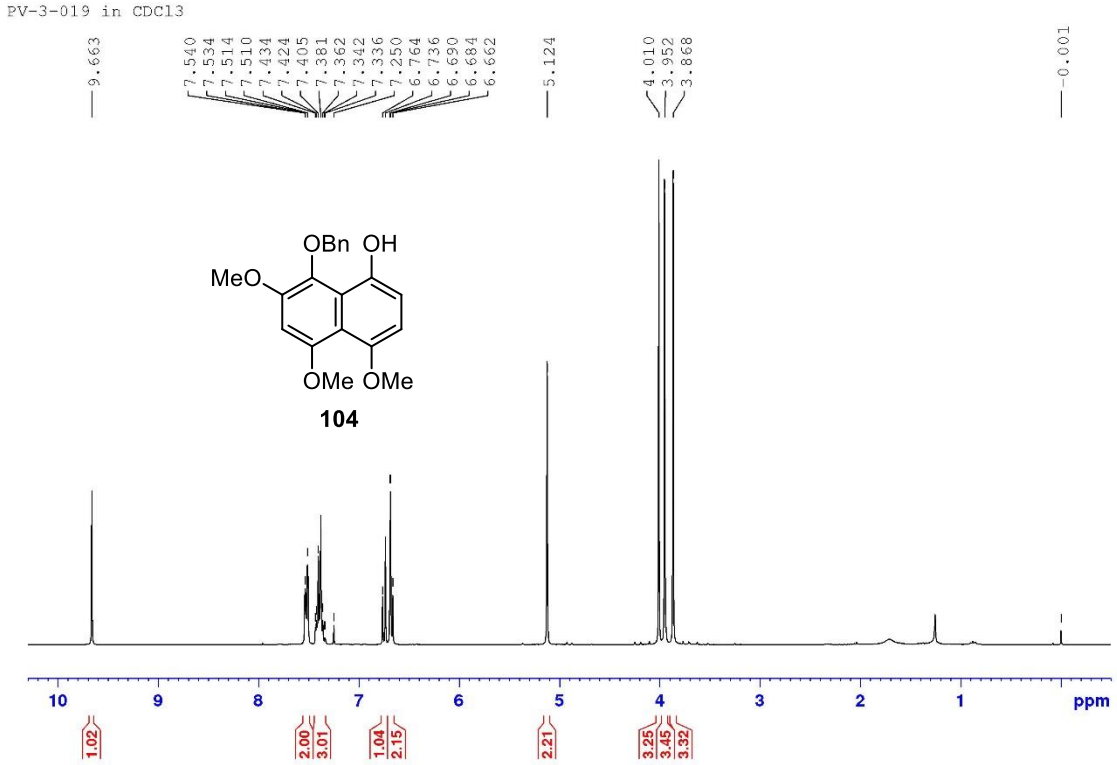

Figure 31 ^{13}C NMR (75 MHz, $CDCl_3$) spectrum of compound **104**

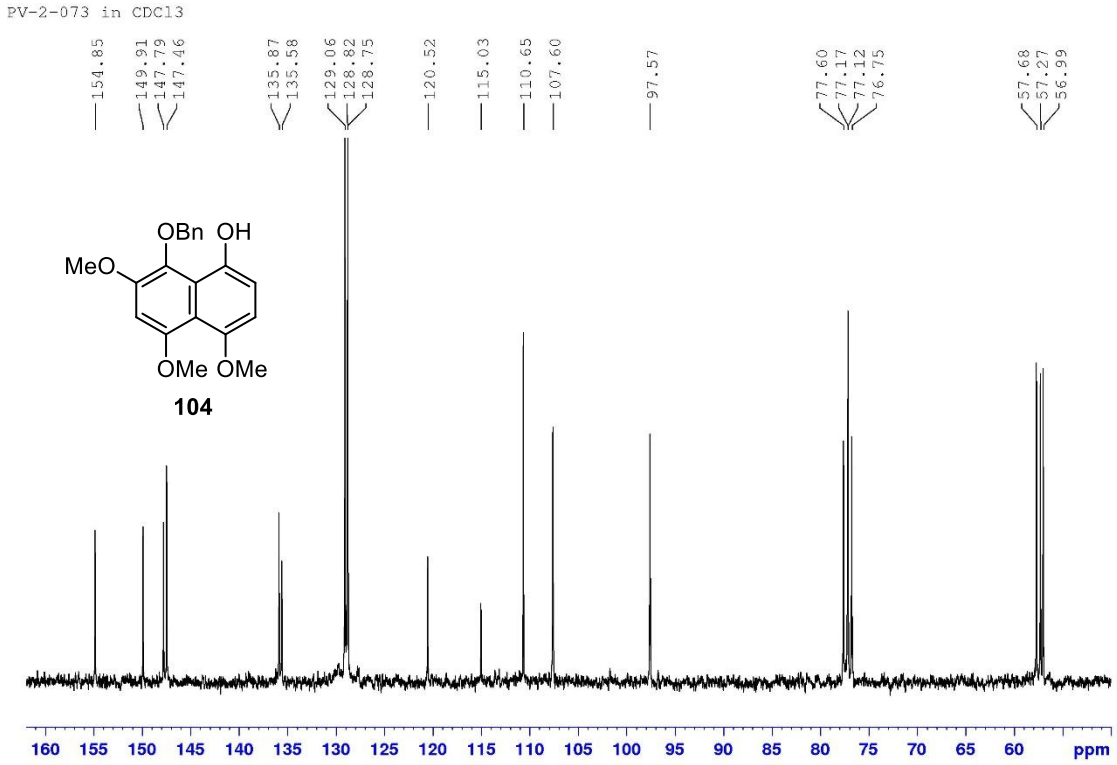

Figure 32 ^{1}H NMR (300 MHz, $CDCl_3$) spectrum of compound **114**

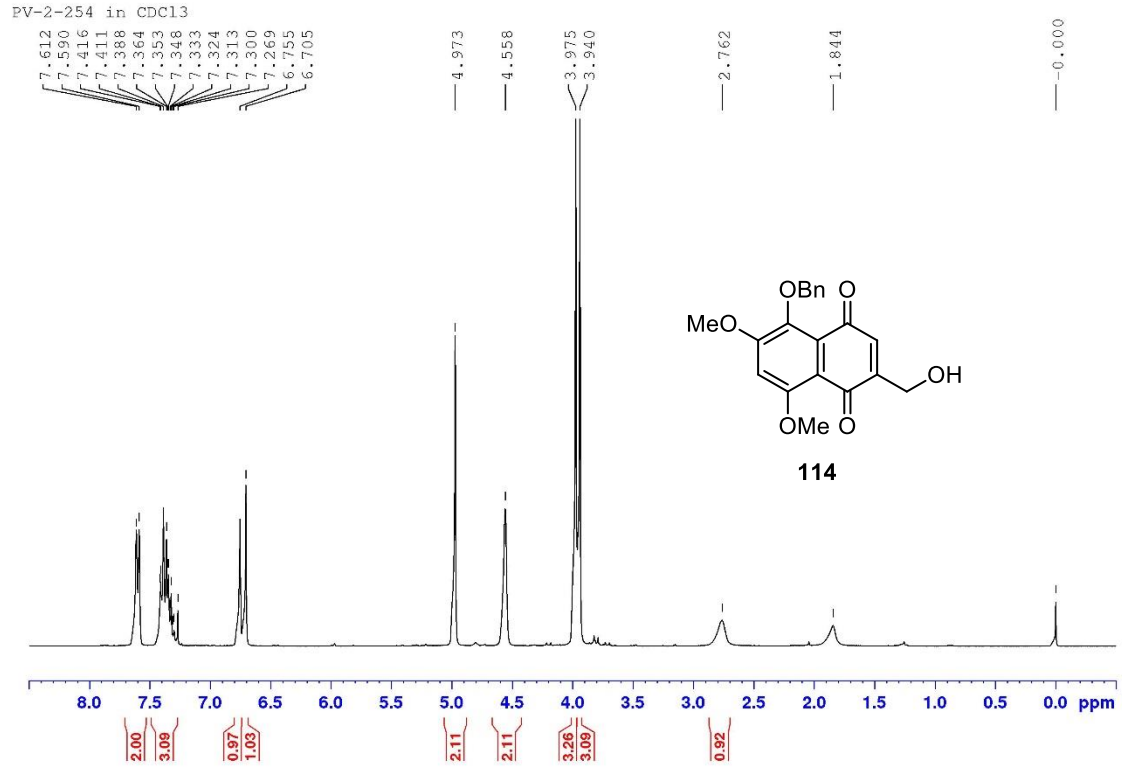

Figure 33 ^{13}C NMR (75 MHz, $CDCl_3$) spectrum of compound **114**

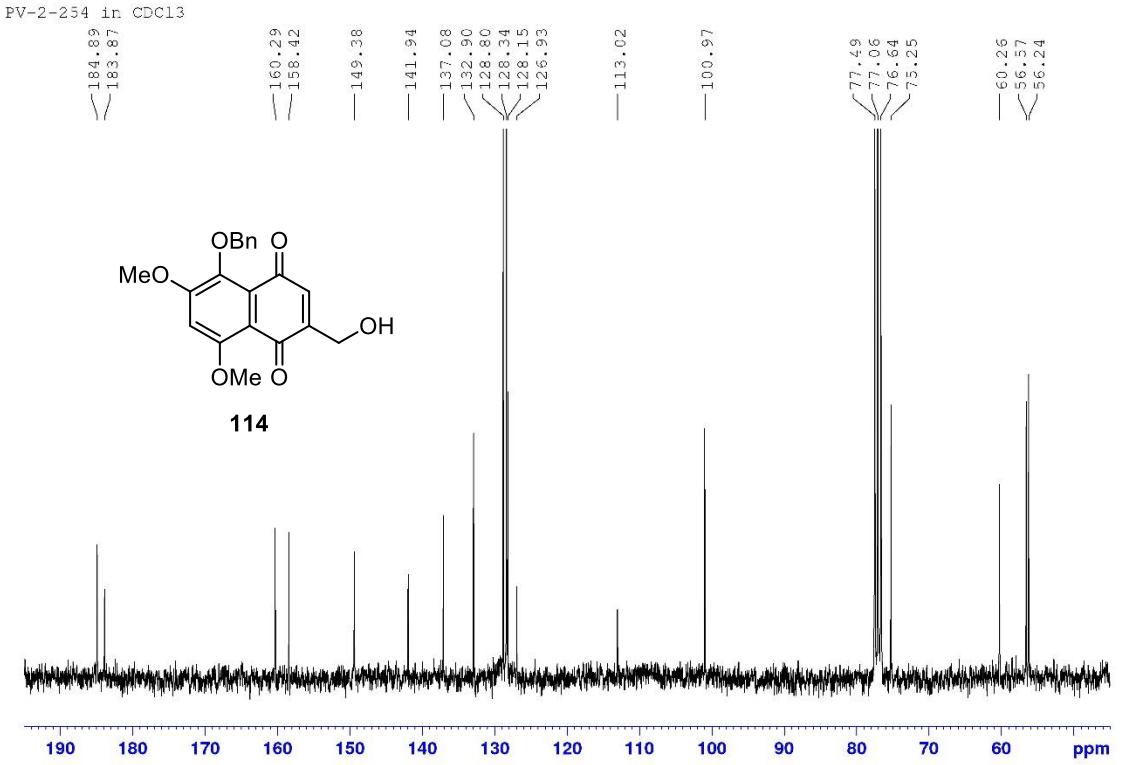

Figure 34 ^{1}H NMR (300 MHz, $CDCl_3$) spectrum of compound **118**

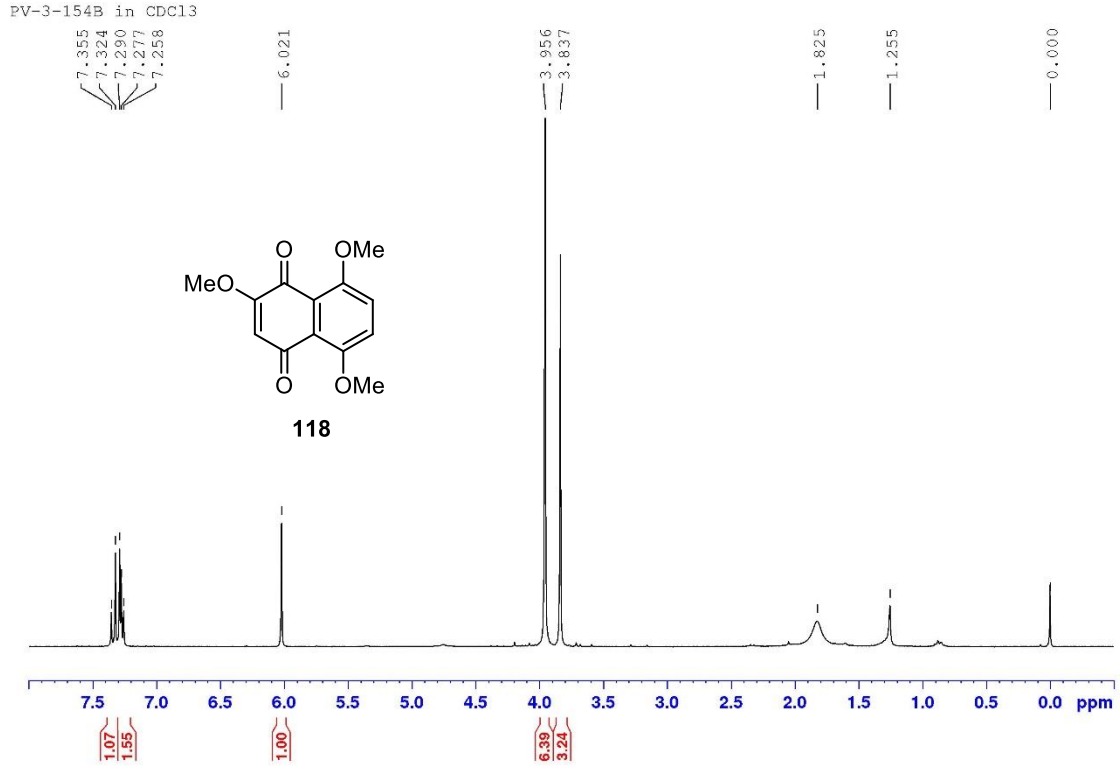

Figure 35 ^{13}C NMR (75 MHz, $CDCl_3$) spectrum of compound **118**

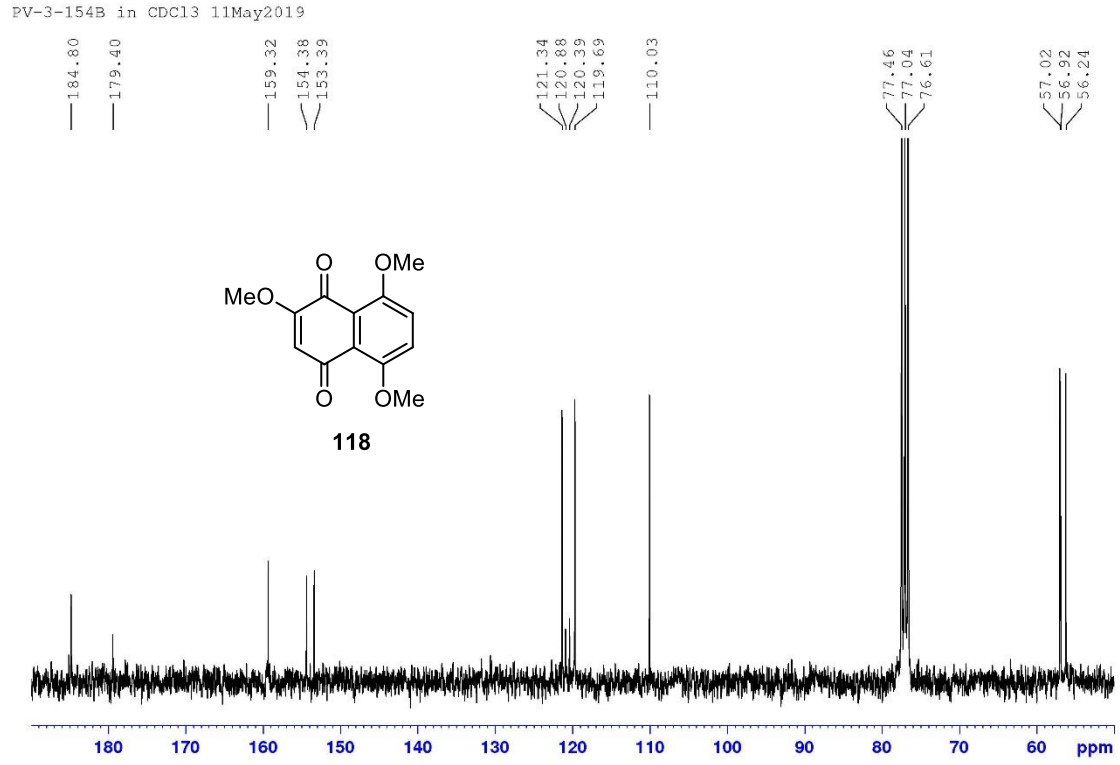

Figure 36 ^{1}H NMR (300 MHz, $CDCl_3$) spectrum of compound **119**

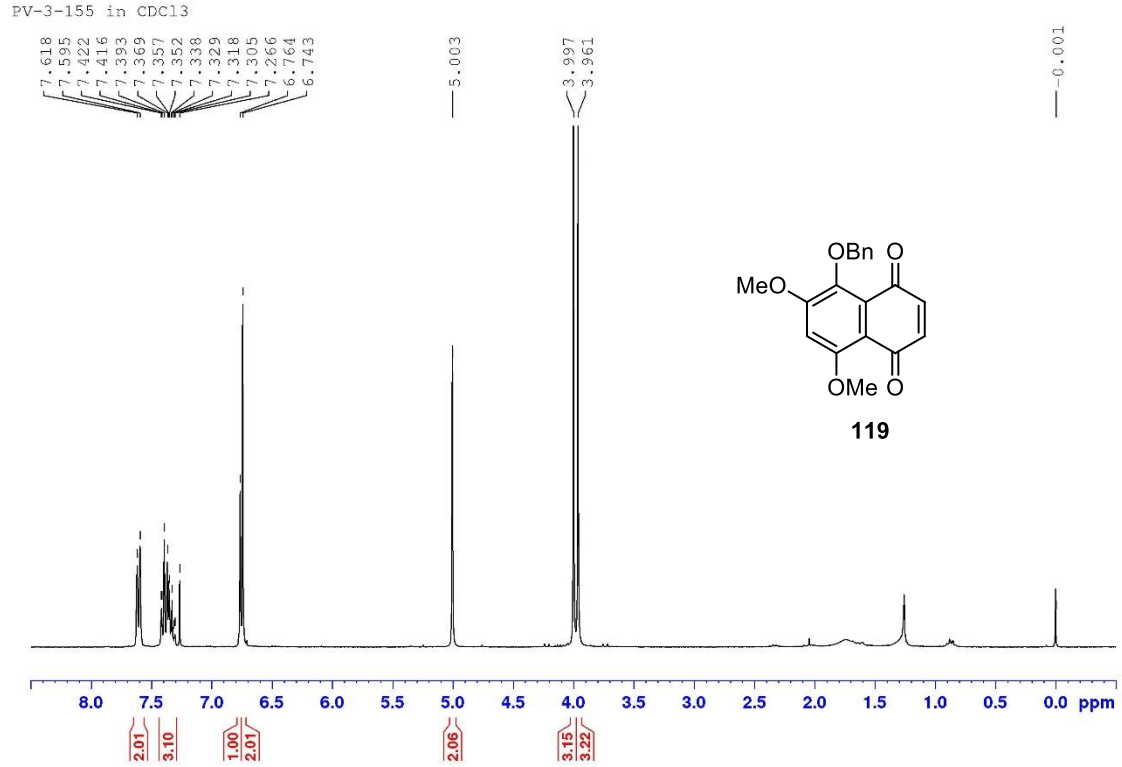

Figure 37 ^{13}C NMR (75 MHz, $CDCl_3$) spectrum of compound **119**

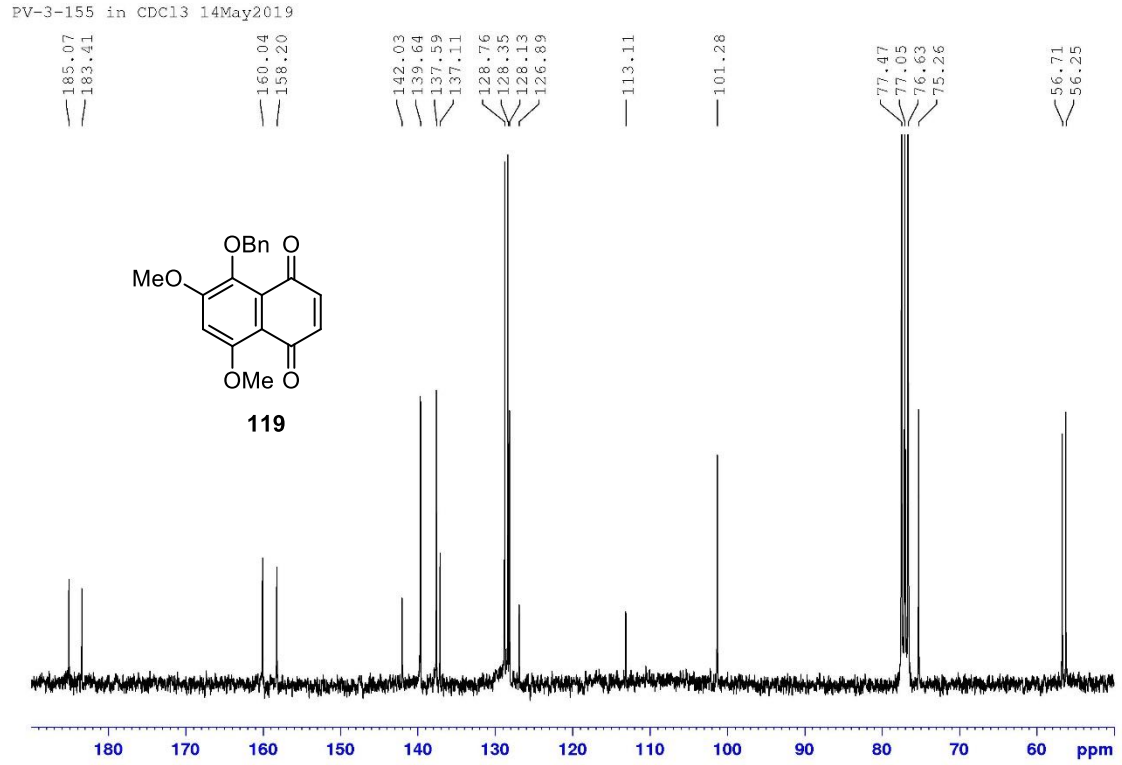

Figure 38 ^{1}H NMR (300 MHz, $CDCl_3$) spectrum of compound **120**

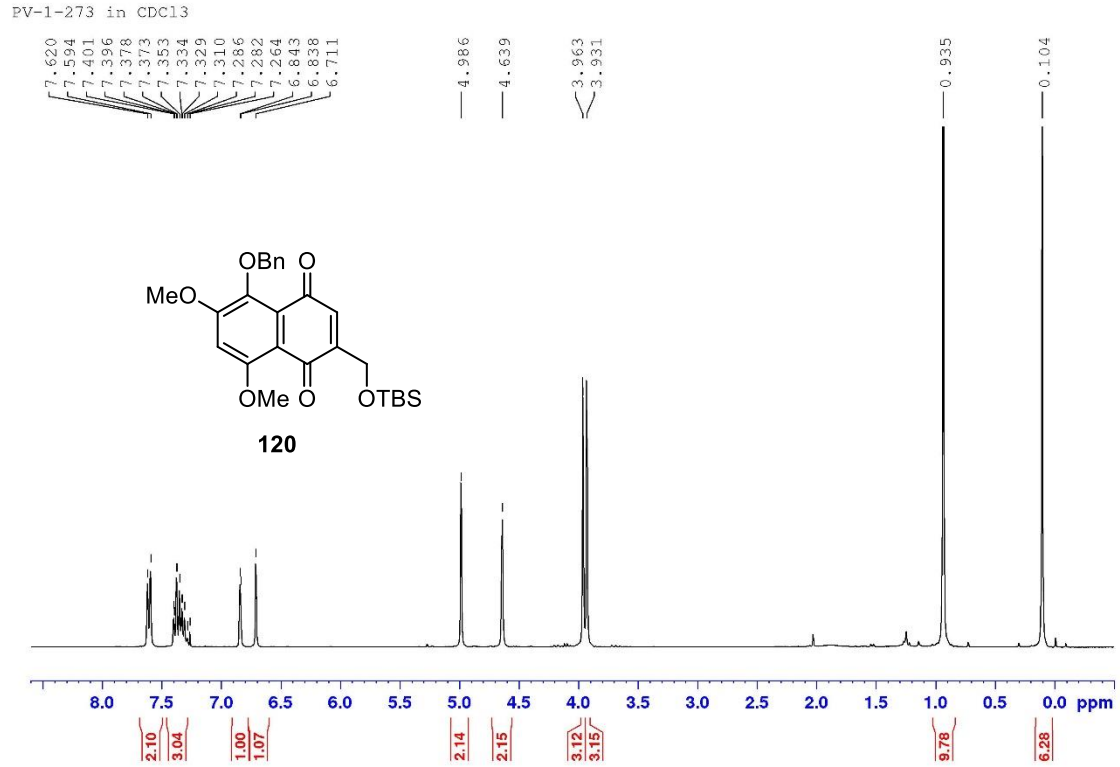

Figure 39 ^{13}C NMR (75 MHz, $CDCl_3$) spectrum of compound **120**

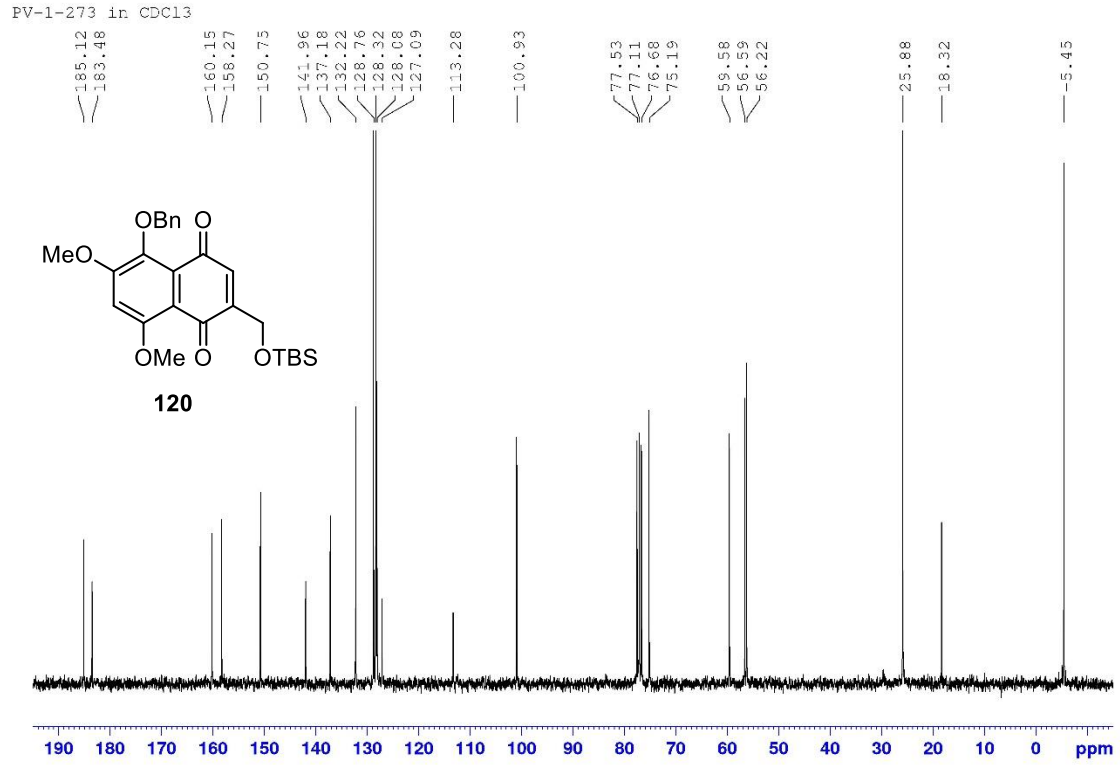

Figure 40 ^{1}H NMR (300 MHz, $CDCl_3$) spectrum of compound **121**

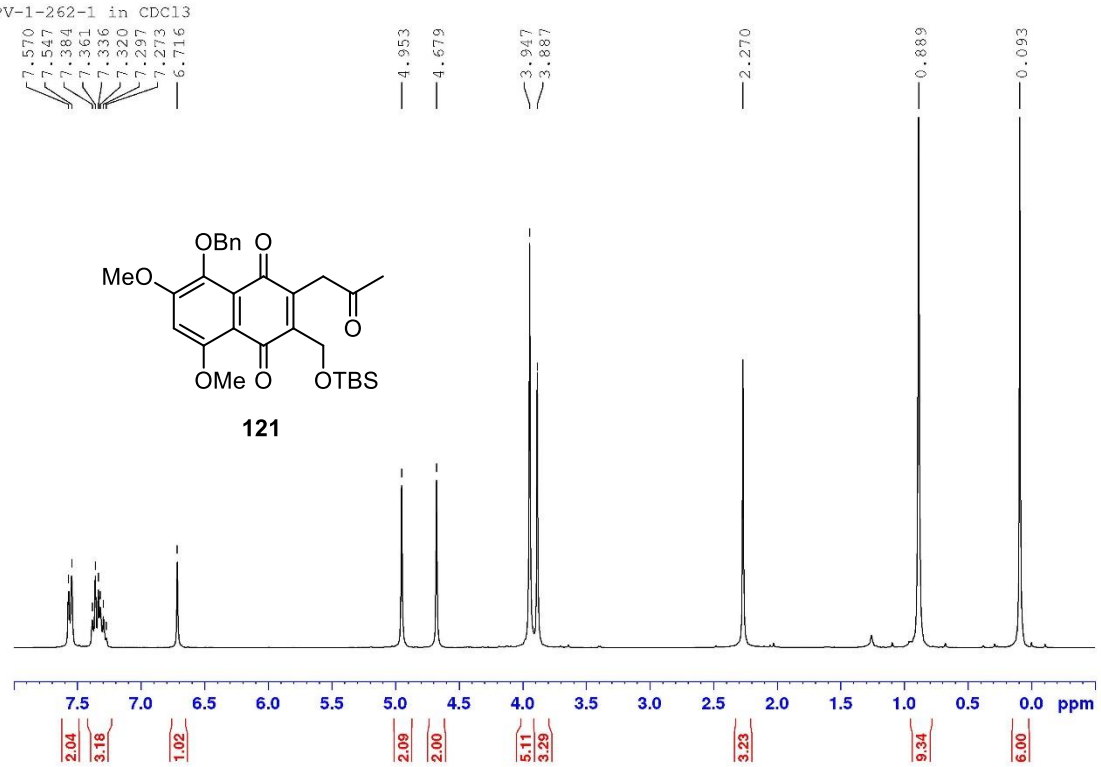

Figure 41 ^{13}C NMR (75 MHz, $CDCl_3$) spectrum of compound **121**

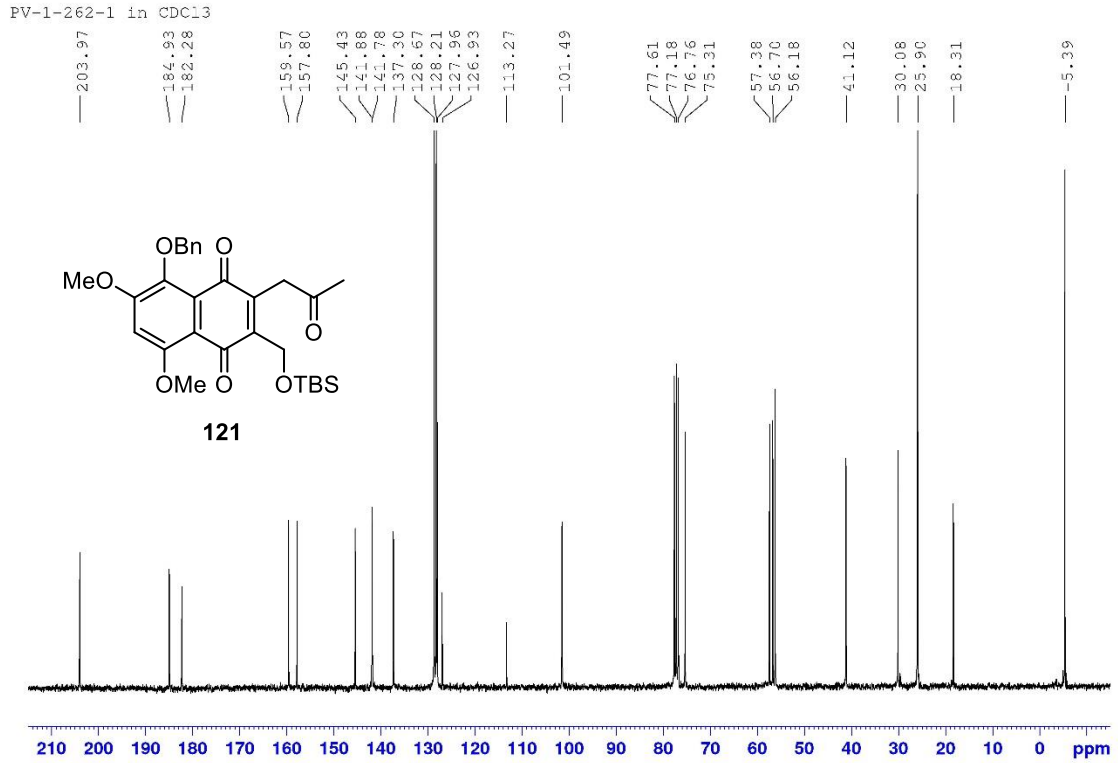

Figure 42 ^{1}H NMR (300 MHz, $CDCl_3$) spectrum of compound **122**

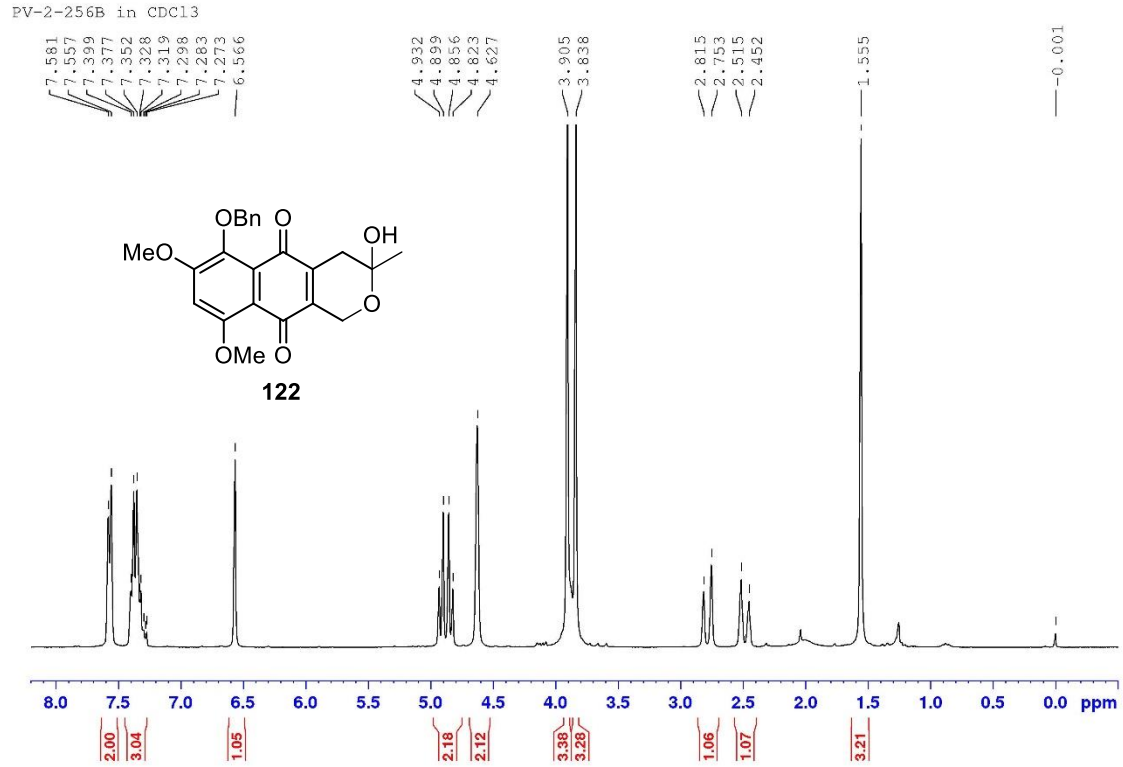

Figure 43 ^{13}C NMR (75 MHz, $CDCl_3$) spectrum of compound **122**

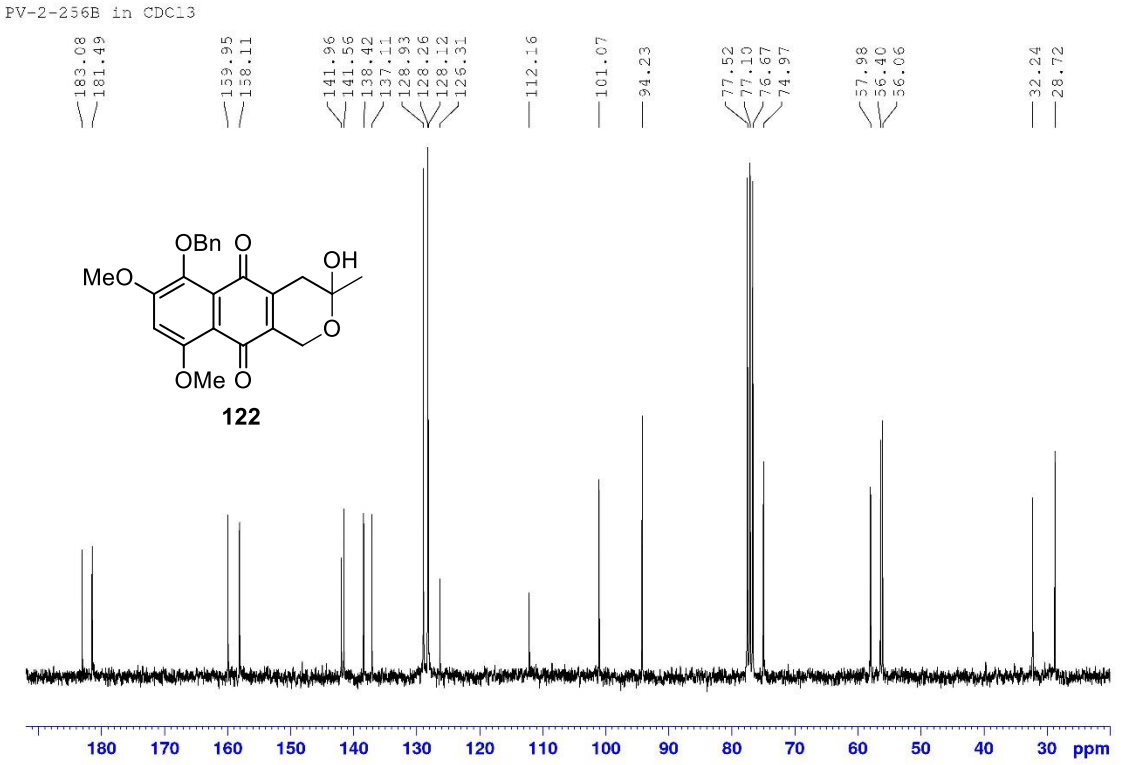

Figure 44 ^{1}H NMR (300 MHz, DMSO-d_6) spectrum of 8-*O*-methylfusarubin (**19**)

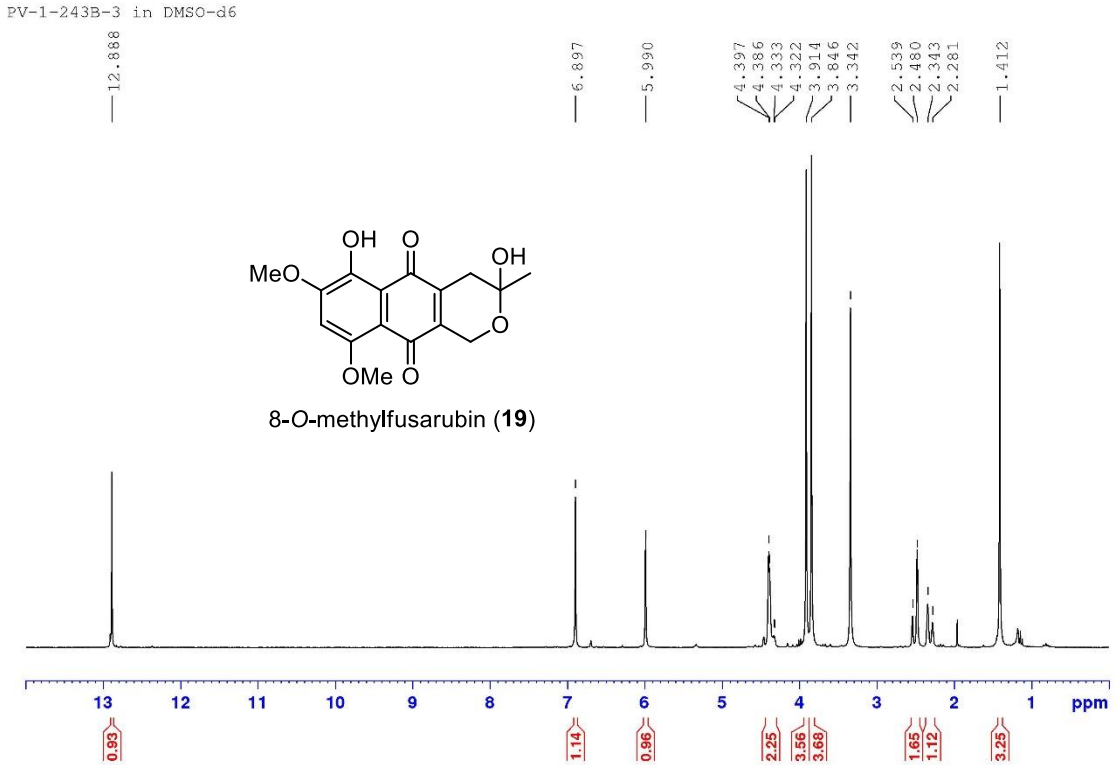

Figure 45 ^{13}C NMR (75 MHz, DMSO-d_6) spectrum of 8-*O*-methylfusarubin (**19**)

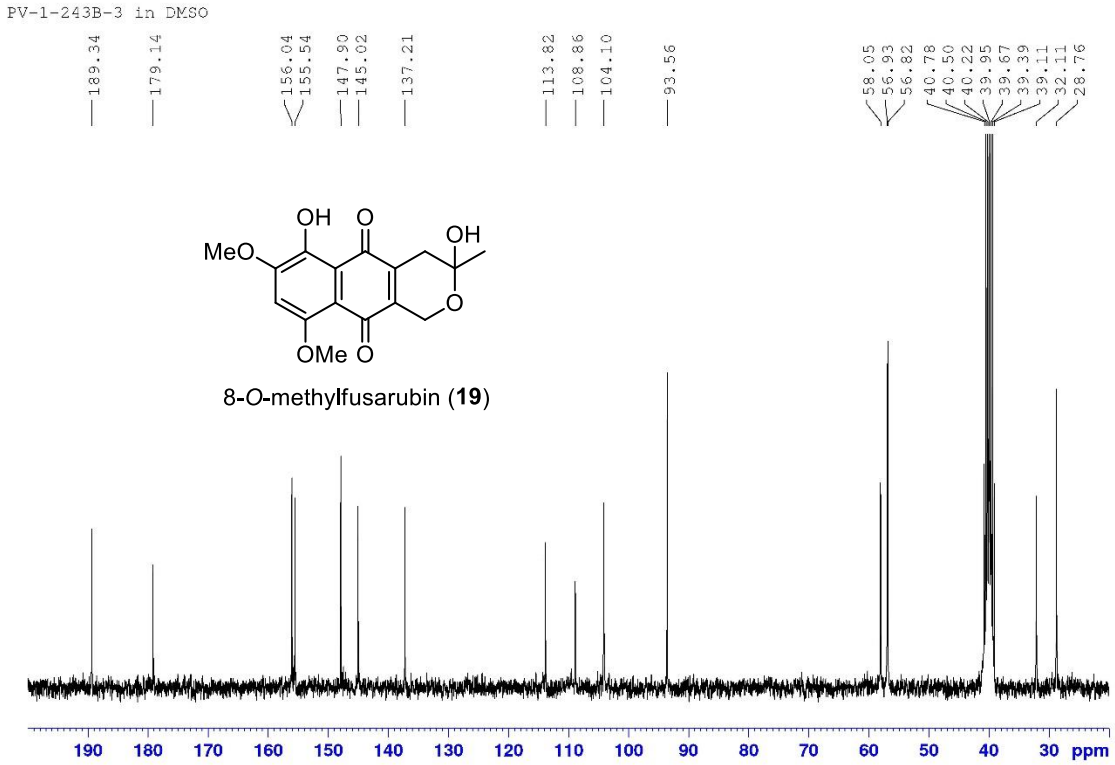

Figure 46 ^{1}H NMR (300 MHz, $CDCl_3$) spectrum 8-*O*-methylanhydrofusarubin (**20**)

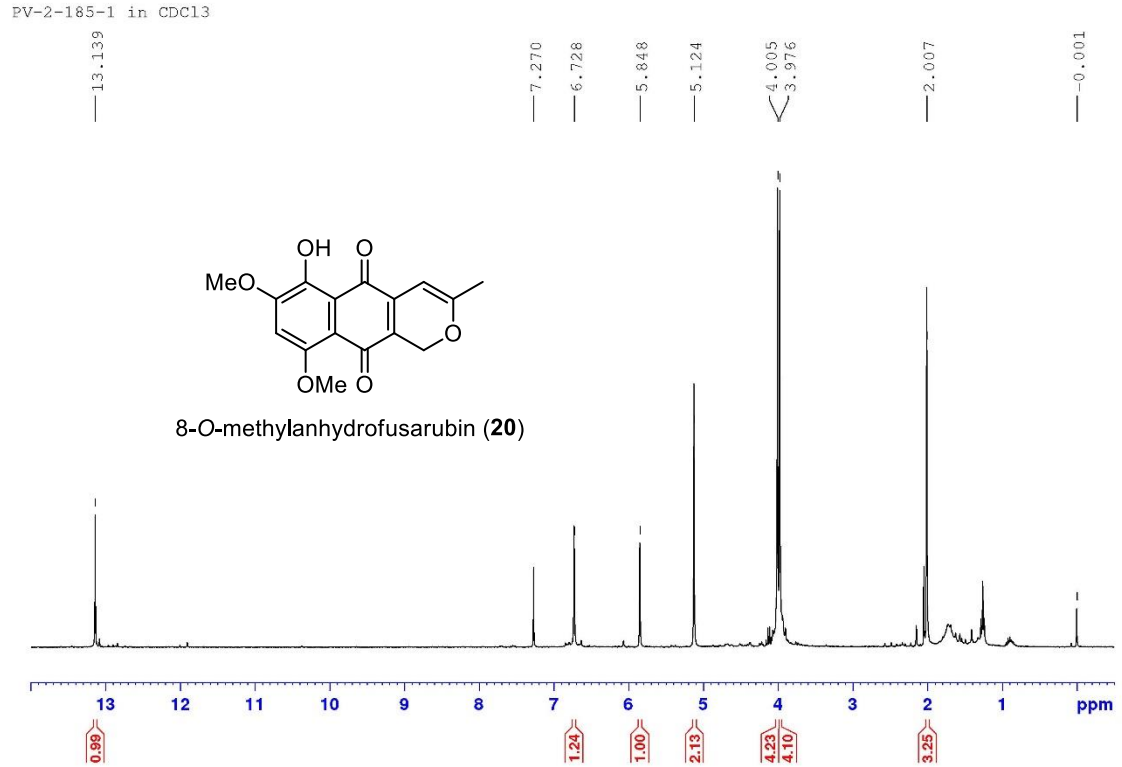

Figure 47 ^{13}C NMR (75 MHz, $CDCl_3$) spectrum of 8-*O*-methylanhydrofusarubin (**20**)

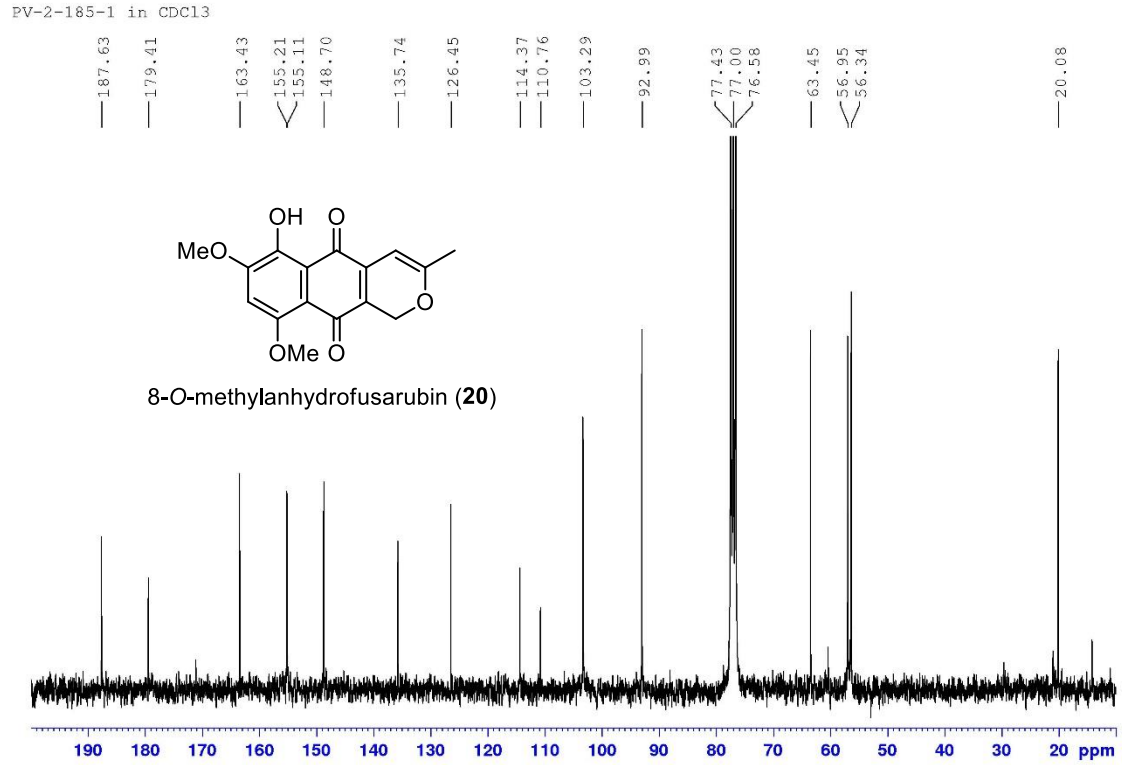

Figure 48 ^{1}H NMR (300 MHz, $CDCl_3$) spectrum of compound **126**

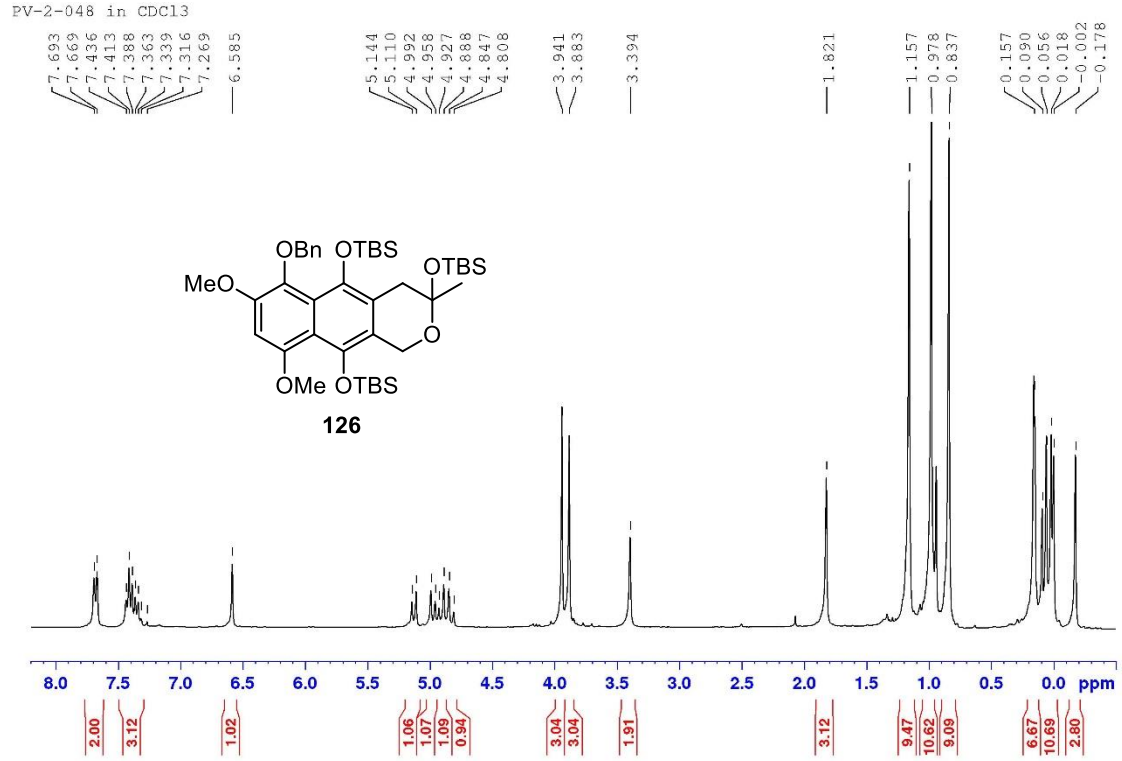

Figure 49 ^{13}C NMR (75 MHz, $CDCl_3$) spectrum of compound **126**

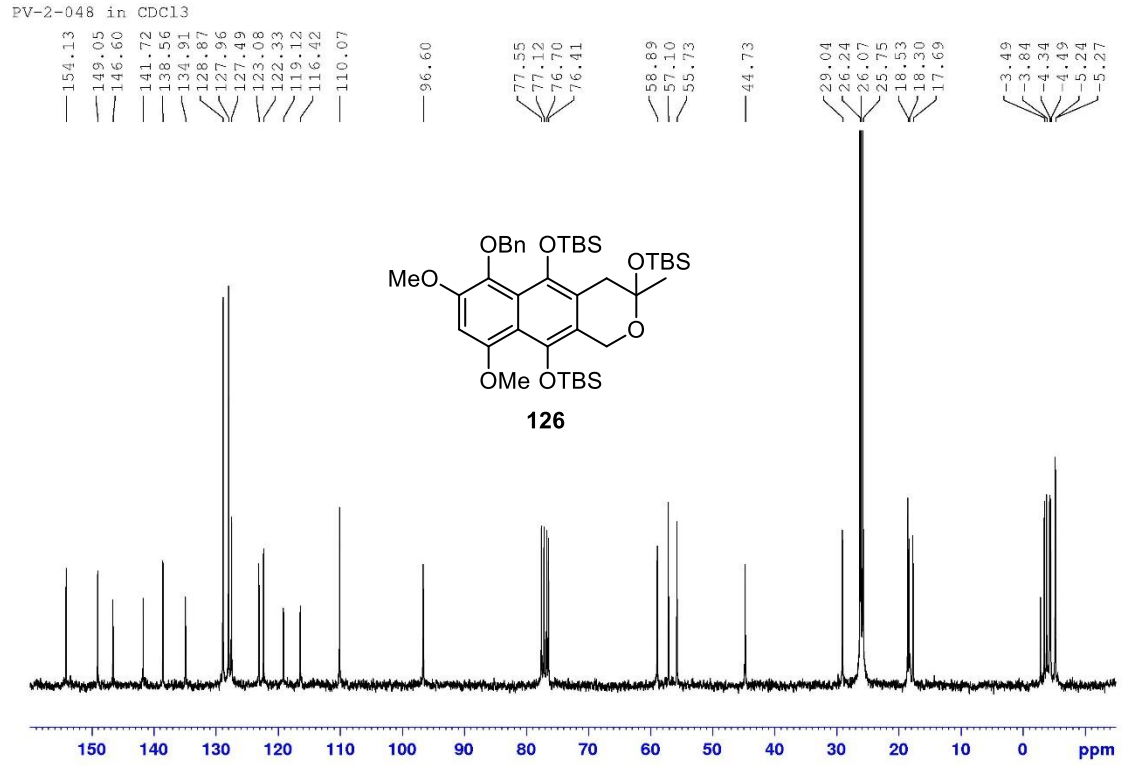

Figure 50 ^{1}H NMR (300 MHz, $CDCl_3$) spectrum of compound **128**

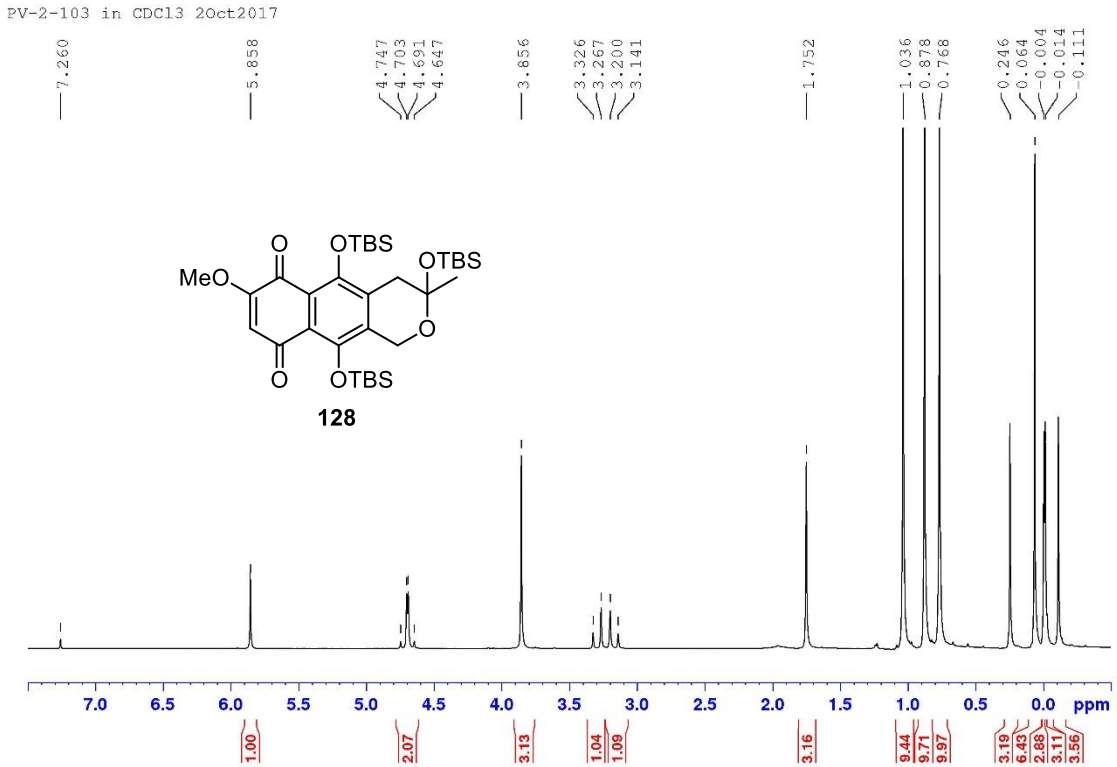

Figure 51 ^{13}C NMR (75 MHz, $CDCl_3$) spectrum of compound **128**

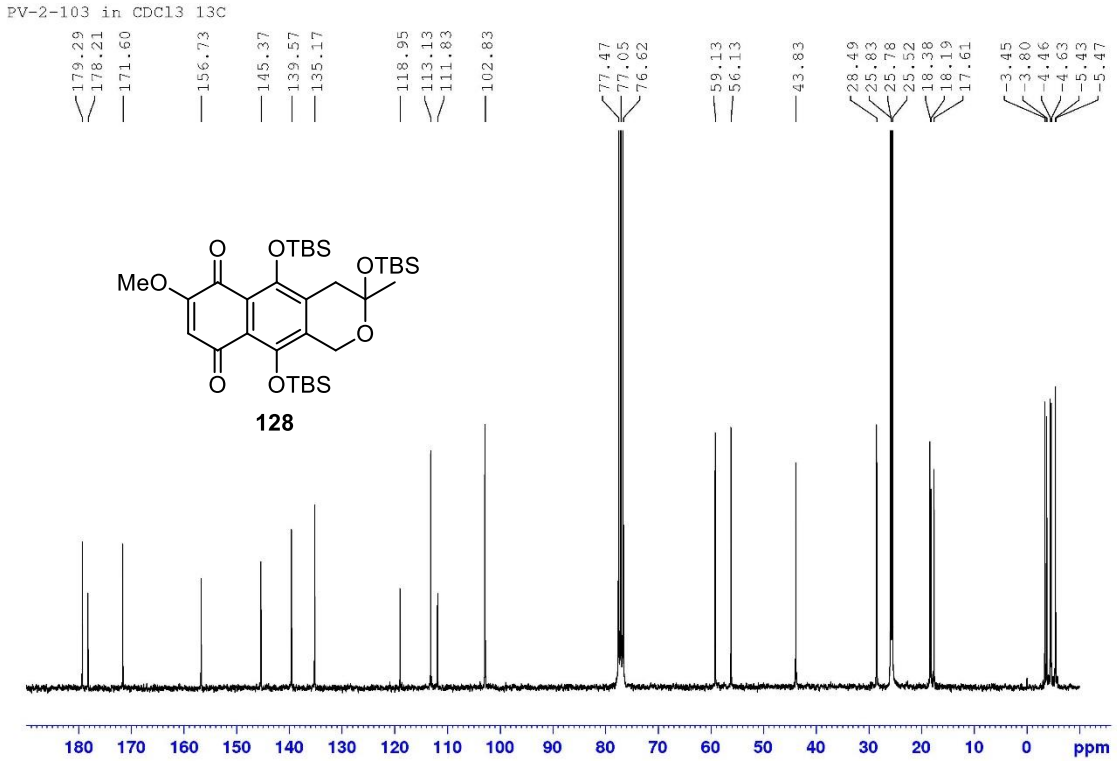

Figure 52 ^{1}H NMR (300 MHz, $CDCl_3$) spectrum of compound **129**

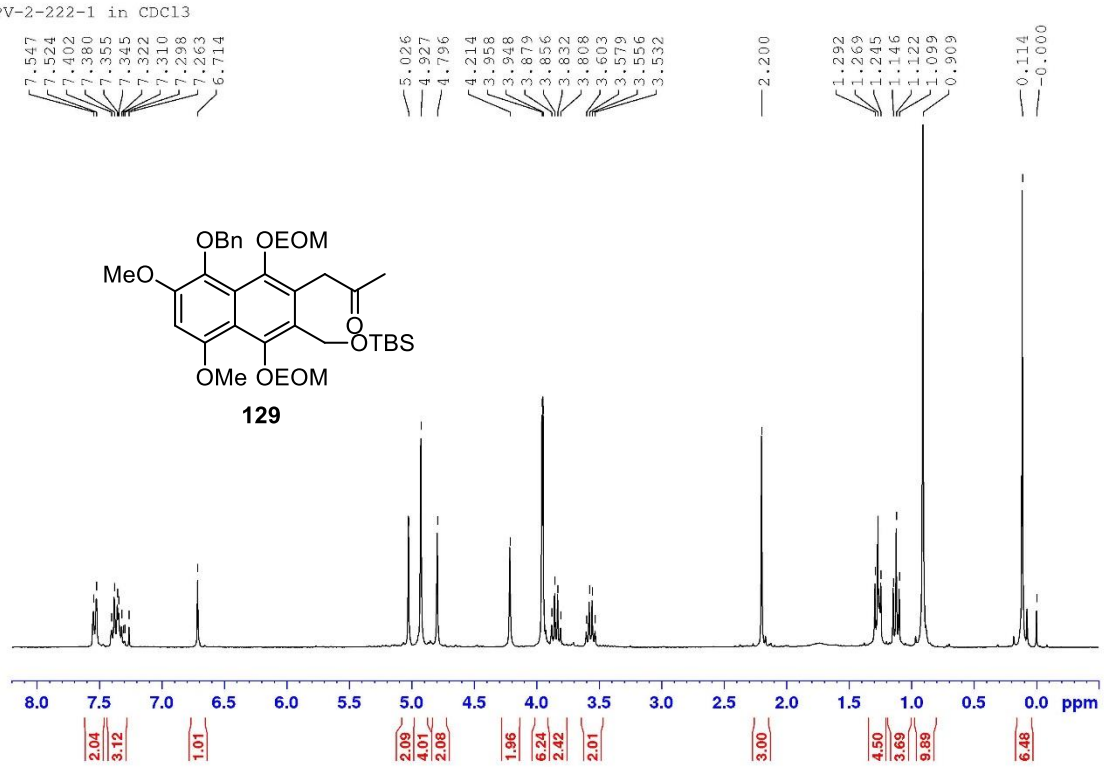

Figure 53 ^{13}C NMR (75 MHz, $CDCl_3$) spectrum of compound **129**

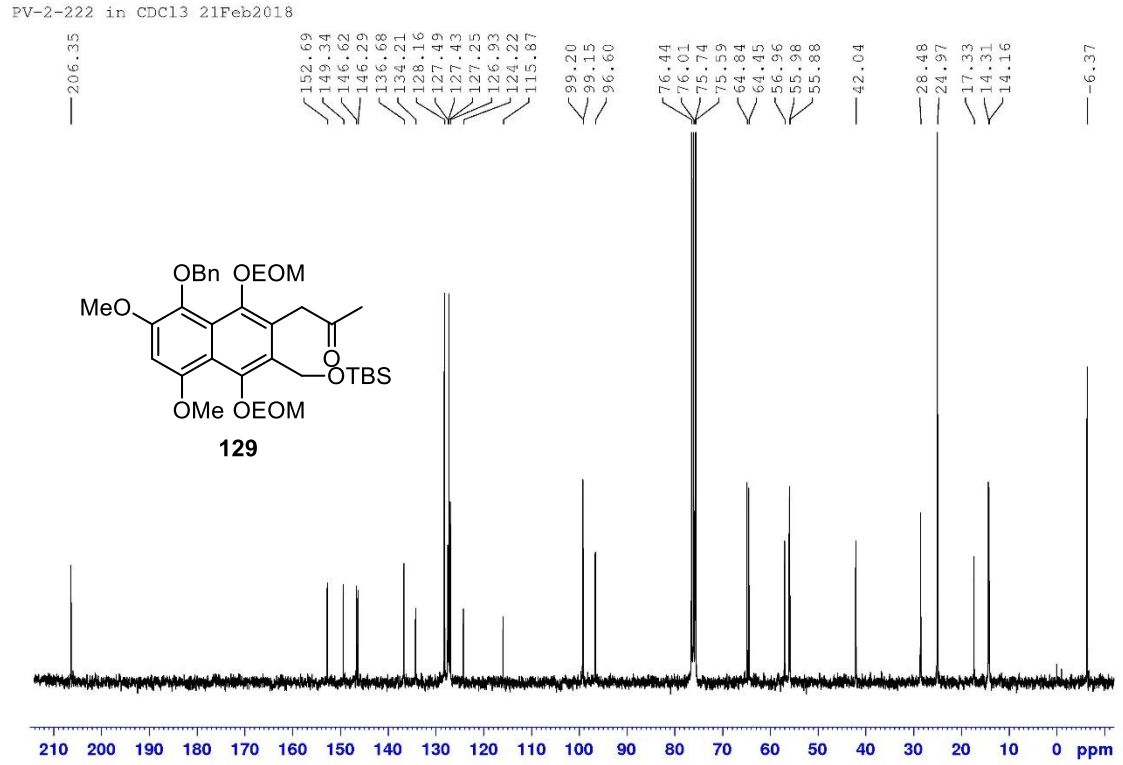

Figure 54 ^{1}H NMR (300 MHz, $CDCl_3$) spectrum of compound **130**

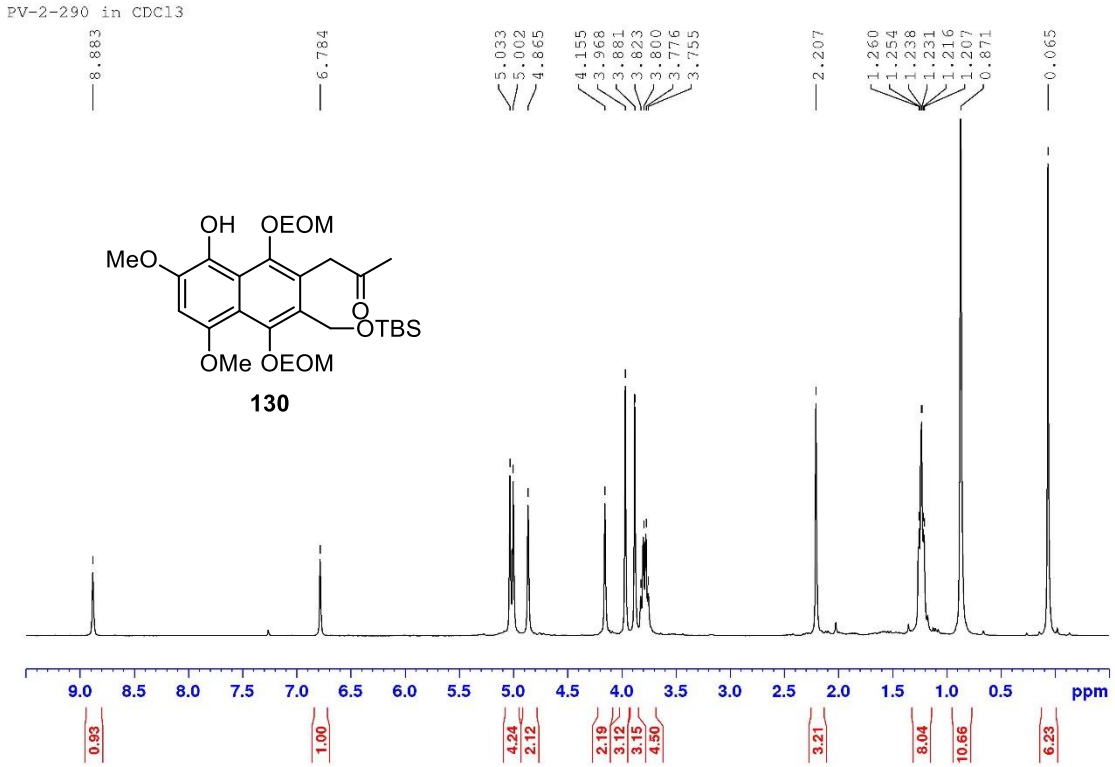

Figure 55 ^{13}C NMR (75 MHz, $CDCl_3$) spectrum of compound **130**

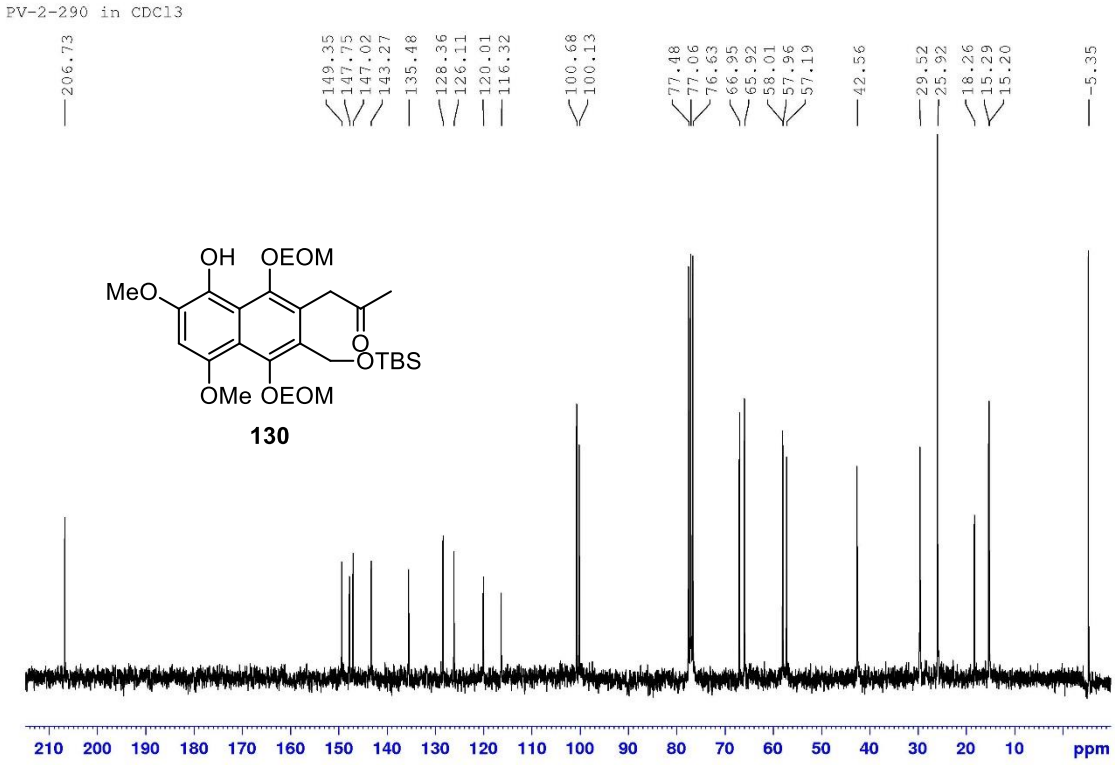

Figure 56 ^{1}H NMR (300 MHz, $CDCl_3$) spectrum of compound **131**

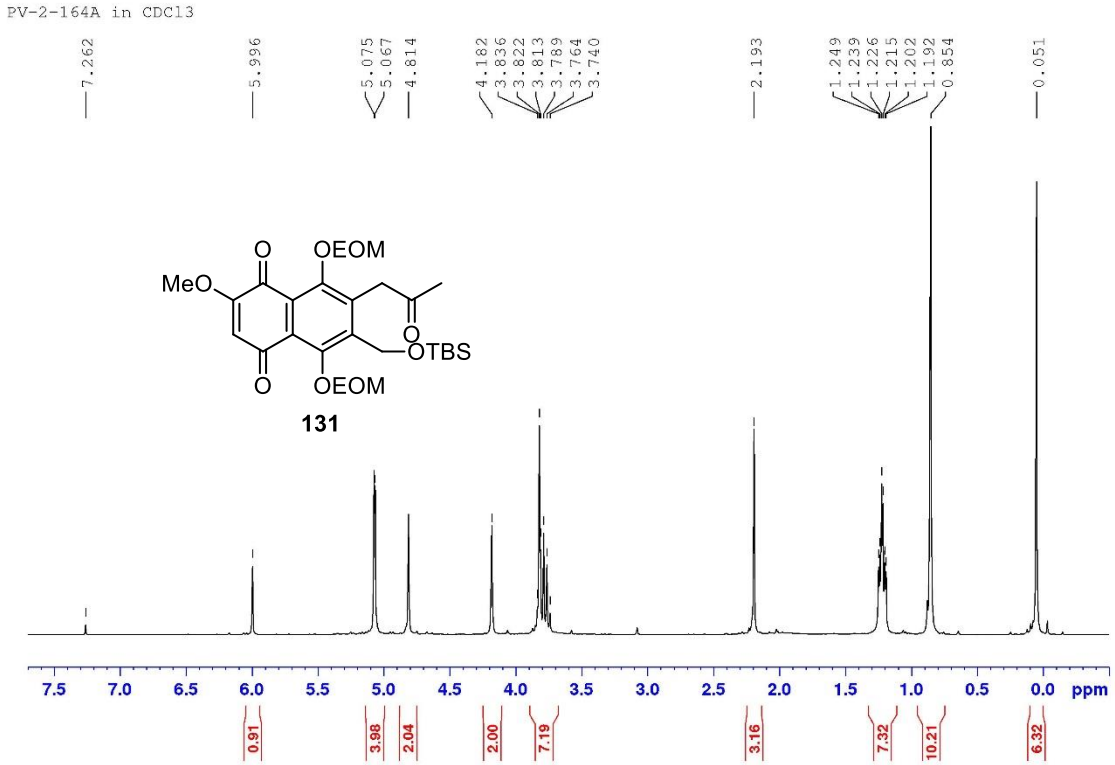

Figure 57 ^{13}C NMR (75 MHz, $CDCl_3$) spectrum of compound **131**

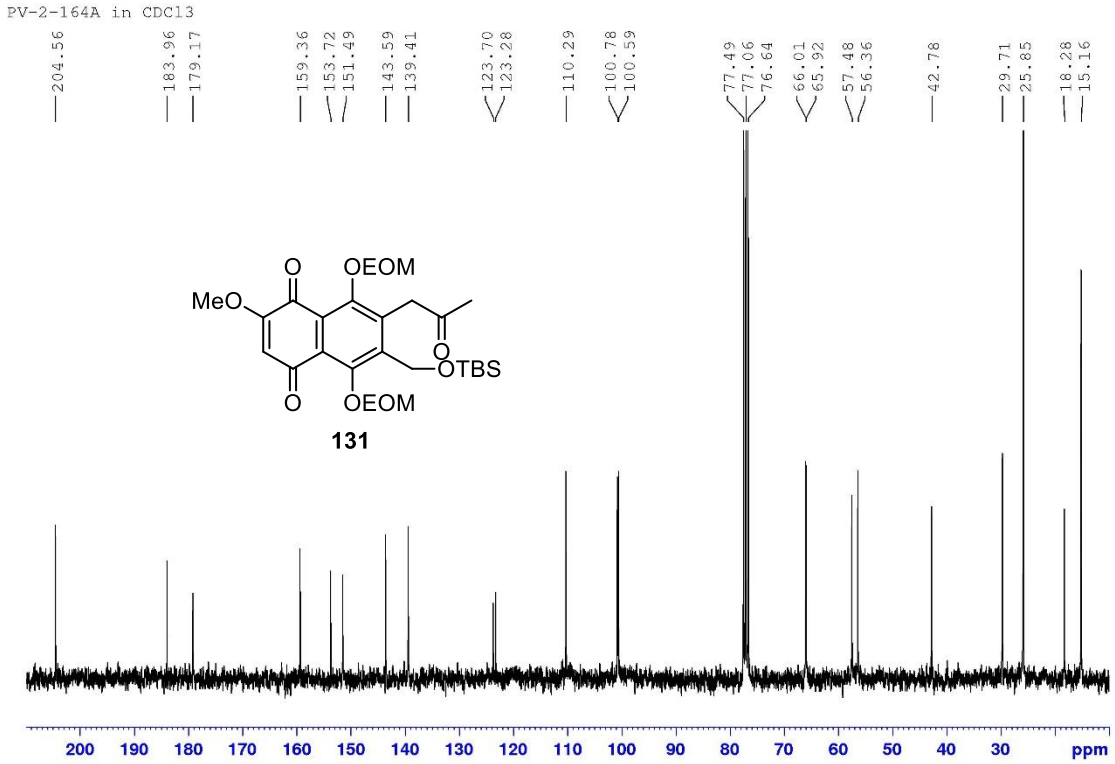

Figure 58 ^{1}H NMR (300 MHz, $CDCl_3$) spectrum of compound **132**

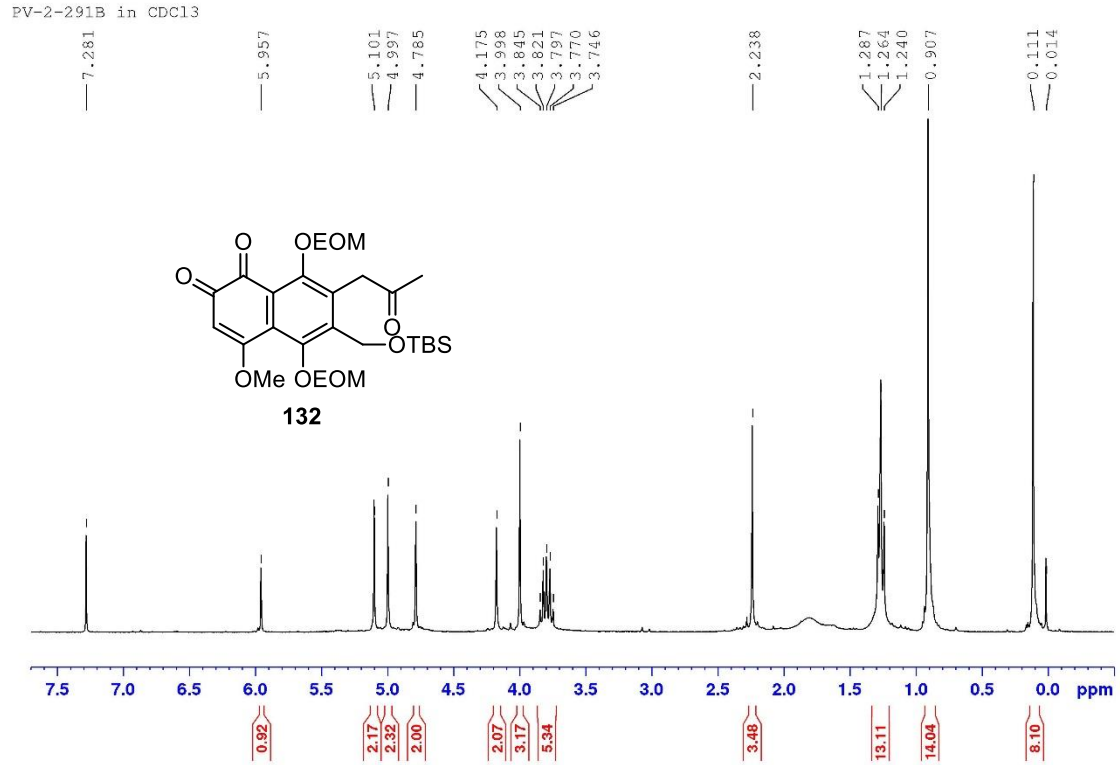

Figure 59 ^{13}C NMR (75 MHz, $CDCl_3$) spectrum of compound **132**

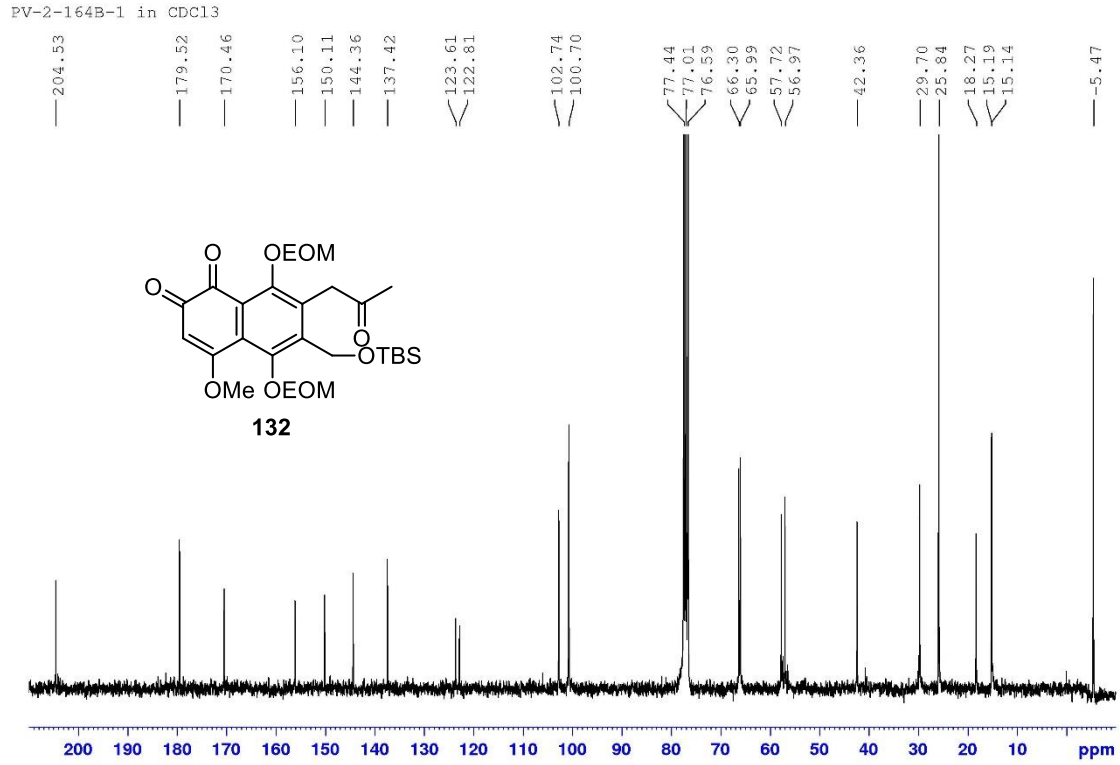

Figure 60 ^{1}H NMR (300 MHz, DMSO-d_6) spectrum of fusarubin (**17**)

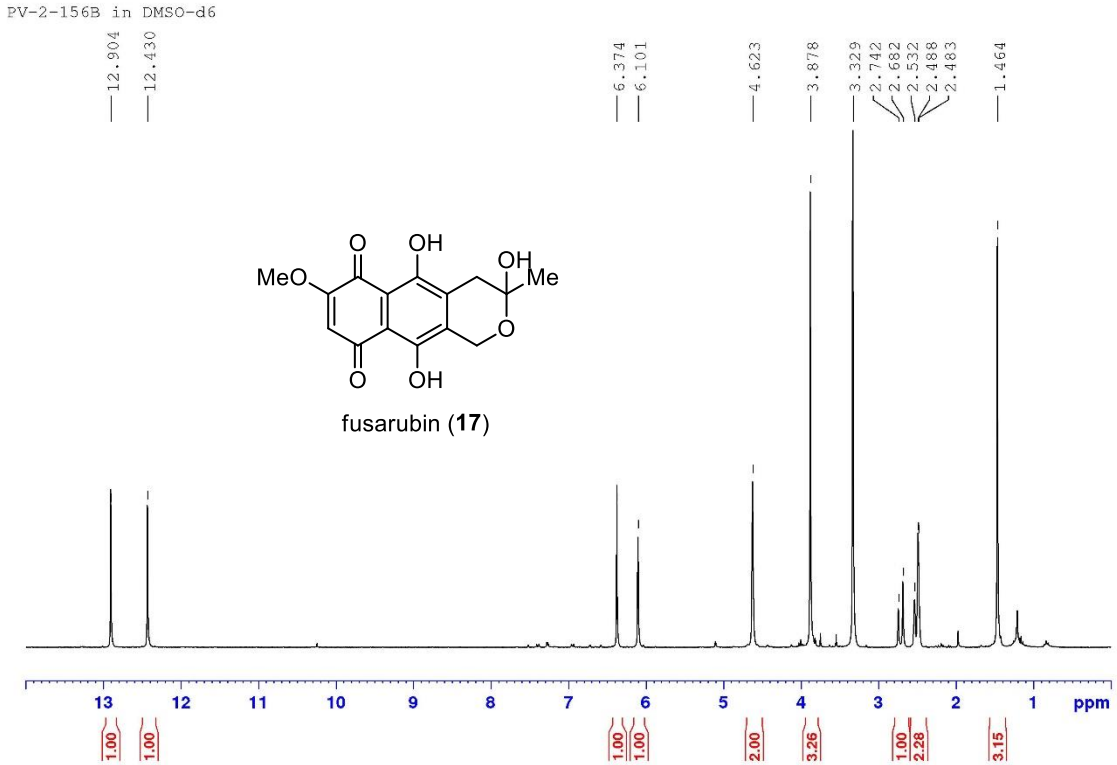

Figure 61 ^{13}C NMR (75 MHz, DMSO-d_6) spectrum of fusarubin (**17**)

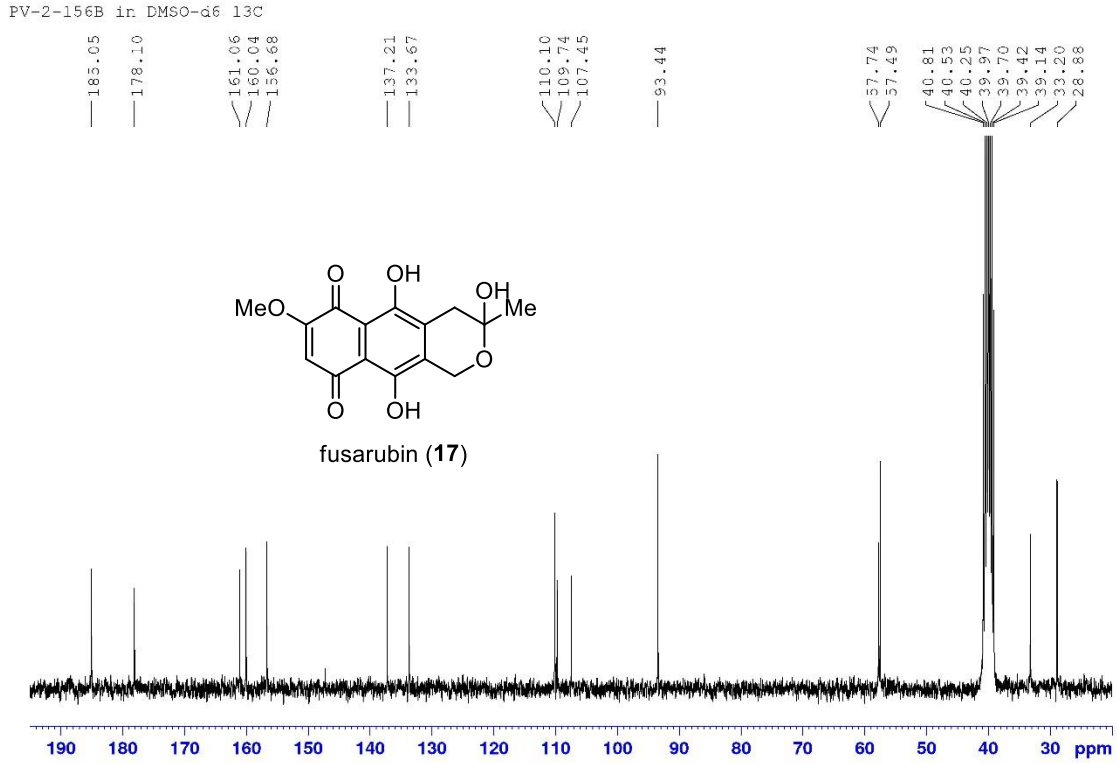

Figure 62 ^{1}H NMR (300 MHz, $CDCl_3$) spectrum of anhydrofusarubin (**18**)

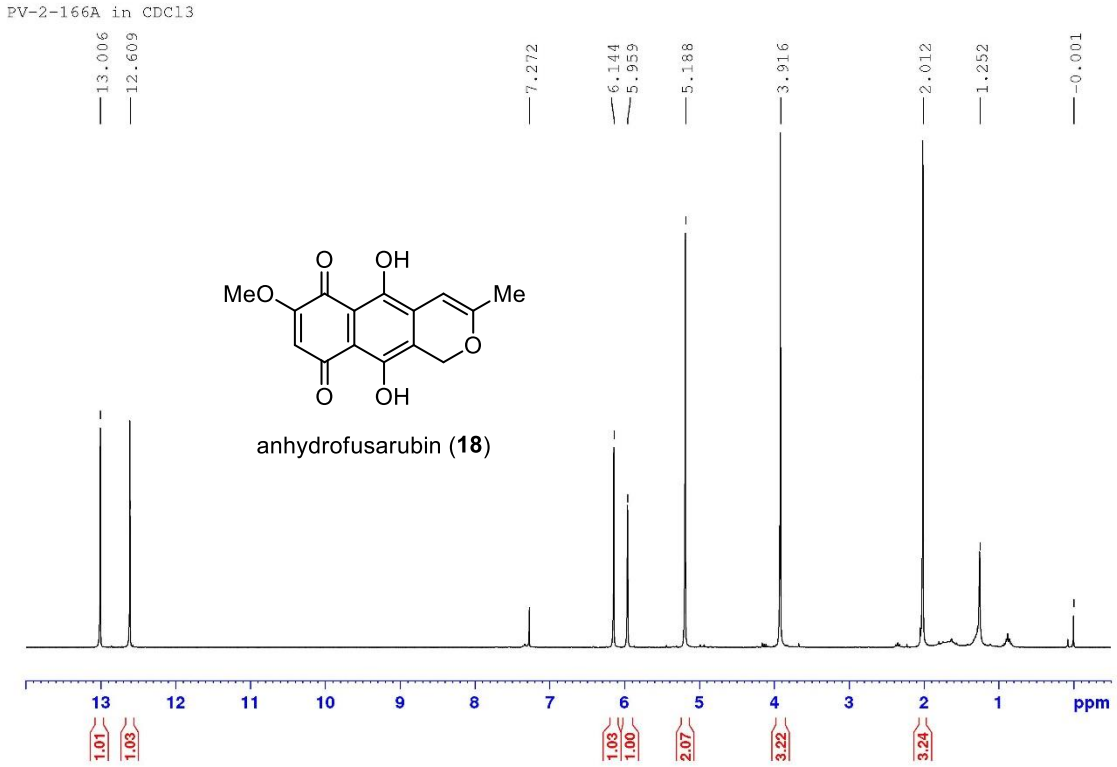

Figure 63 ^{13}C NMR (75 MHz, $CDCl_3$) spectrum of anhydrofusarubin (**18**)

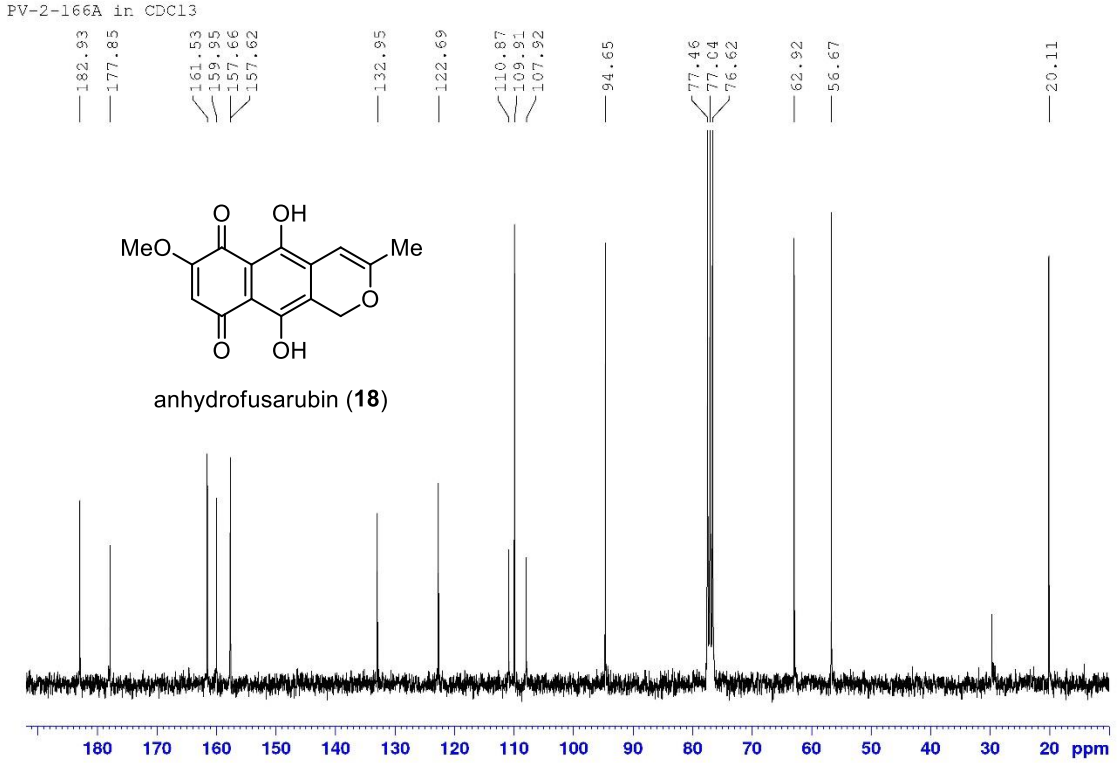

VITAE

Name Mr. Pongsit Vijitphan

Student ID 5910220045

Education Attainment

Degree	Name of Institution	Year of Graduation
Bachelor of Science (Chemistry)	Prince of Songkla University	2016

Scholarship Awards during Enrolment

Research Assistantship from Faculty of Science and Partial Scholarship from PERCH-CIC

List of Publication and Proceeding

Vijitphan, P.; Rukachaisirikul, V.; Muanprasat, C.; Iawsipo, P.; Panprasert, J.; Tadpetch, K. 2019. Unified synthesis and cytotoxic activity of 8-*O*-methylfusarubin and its analogues. Org. Biomol. Chem. 17, 7078–7087.